Green Energy and Technology

Stanislav Misak
Lukas Prokop

Operation Characteristics of Renewable Energy Sources

Springer

Green Energy and Technology

More information about this series at http://www.springer.com/series/8059

Stanislav Misak · Lukas Prokop

Operation Characteristics of Renewable Energy Sources

Springer

Stanislav Misak
VŠB-Technical University of Ostrava
Ostrava, Poruba
Czech Republic

Lukas Prokop
VŠB-Technical University of Ostrava
Ostrava, Poruba
Czech Republic

ISSN 1865-3529 ISSN 1865-3537 (electronic)
Green Energy and Technology
ISBN 978-3-319-43411-7 ISBN 978-3-319-43412-4 (eBook)
DOI 10.1007/978-3-319-43412-4

Library of Congress Control Number: 2016951973

Printed on acid-free paper

This Springer imprint is published by Springer Nature
The registered company is Springer International Publishing AG
The registered company address is: Gewerbestrasse 11, 6330 Cham, Switzerland

Foreword

The use of renewable energy sources has been known for many millennia; their importance, however, has not been fully appreciated until the present time. Although many of us do not like it, we are consuming increasingly more energy. The boom in industrial production and a high living standard of part of mankind brought along a vast expansion of equipment using electricity. Today, the electricity and energy industry is the most important sector of the global economy. Basically, it can be said that we already cannot imagine any current human activity without a reliable functioning of this sector. Energy self-sufficiency is discussed and addressed at both national and international levels, not only in our country. Today, the matter is rather political than technical or professional. It is often stated that the cheapest energy is the energy which is not produced (sorry, "law of conservation …"). However, the energy shortage is more expensive.

Increasingly higher demands of the society on energy consumption are reflected in our environment. Conventional sources of energy, particularly fossil fuel burning, have a very negative impact on the environment; moreover, reserves of these important raw materials are not inexhaustible. It is believed that drives using combustion engines will be limited or will completely disappear in the future but the electric drive will remain. Therefore, it is necessary to look for new primary sources for electricity production. These sources may also include renewable energy sources although they will probably never be dominant.

Renewable energy sources have a lower impact on the environment. With regard to the length of human life, the energy derived from these sources should be inexhaustible. The disadvantages of these sources include relatively small concentration of usable energy, reduced possibility of energy accumulation and especially the possibility of large power fluctuations at short time intervals. These drawbacks greatly increase the technological and consequently also economical production demands. In terms of the amount of energy supplied, these sources will always be rather complementary to traditional sources.

The motivation for compiling this publication was to present the experience with the previous operation of the two most topical renewable energy sources currently used in our country, the wind and photovoltaic power plants.

It becomes clear that building a significant amount of renewable energy sources has brought not only economic and political problems but also technical problems. When stating this, I mean the fluctuations in electricity production, unstable supply from renewable sources and the associated need for regulation of energy networks, and the construction of systems suitable for electric energy accumulation.

These plants, as any technical work, require operational reliability and safety. Therefore, it is necessary to ensure good maintenance and diagnostics of functional properties of the power plants. This will reduce the spread of negative reports on their aggressive impacts on the nature. It should be appreciated that the authors present the results of their long-standing work and experience gained in building research centers as well as in practical realization of the hybrid system.

Assoc. Prof. Karel Chmelík

Preface

Dear readers, dear colleagues, friends ☺. More than ten years ago, as a young team (then) under the guidance of our mentors, mostly Assoc. Prof. Karel Chmelík, we gained a unique and unrepeatable opportunity to participate in the development and evolution of technologies for renewable electricity sources, first wind and then photovoltaic power plants, which were among the most dynamically emerging representatives of renewable sources. Under the auspices of the research project of Prof. Hradílek, we had the opportunity to be at the beginning of this development; as part of working trips, we gained valuable experience in the operation of these sources and felt the atmosphere of different locations. However, the possibility to be in contact with people, adventurers and main implementers, can be considered as particularly invaluable. At that time, these people were not guided solely by the prospect of profit but attracted by the opportunity to be pioneers in the given field. They were not afraid to invest their valuable time and risk not only their investments but also their health in promoting the development to the extent which was unusual for the situation in the Czech Republic. Also thanks to these people who enabled us to perform many time-consuming experimental measurements, we have created an extensive database of characteristic values describing the operation of the mentioned representatives of renewable sources, which we further utilized in the optimization of individual components or renewable sources as a whole.

The main goal of our efforts was to find a balance between the requirements of the operators of these sources and requirements of the operators of the network receiving the power from these sources, all with a guaranteed minimum negative environmental impact. Over time, our team thus gained a lot of experience and knowledge, in both theoretical and mainly experimental area which can be identified as particularly beneficial for the given field.

We would like to share with you especially our experience in the area of practical experimental measurements. This is a book that does not aspire to replace professional textbooks or other literature describing the general principles of selected representatives of renewable sources; currently, there are a plethora of such publications in our country and elsewhere in the world. The aim of our efforts is to make available information (hopefully interesting for you) from experimental

measurements of operating conditions, mainly in wind and photovoltaic power plants or their combinations, within long-term measurements and analyses of transient phenomena which accompany the operation of those sources, and thus complement the mosaic of related literature. Individual chapters are arranged chronologically, just as the individual experimental measurements were carried out, i.e. from the analysis of operation of wind power installations for different power and voltage levels, through the analysis of operation of photovoltaic power plants, to their mutual symbiosis in off-grid operation which is addressed in the final part of the book.

To conclude this preface, we would like to thank again Assoc. Prof. Karel Chmelík for his leadership, his active participation in the measurements and the patience with which he shared with us his experience. Furthermore, we would like to thank Prof. Hradílek, within the research project, he provided us, with a technical and financial base for realizing experimental measurements as well as for building unique research testing sites. We thank all operators of renewable sources for access to their facilities where the experimental measurements were carried out. Last but not least, we appreciate our wives for their constant care and endless patience.

Ostrava, Czech Republic

Stanislav Misak
Lukas Prokop

Acknowledgment

This book was conducted within the framework of the project LO1404: Sustainable development of ENET Centre and Students Grant Competition project reg. No SP2016/177 and project reg. No SP2016/128.

Contents

Abbreviations

ASG	Asynchronous Generator
CTL	Centralized Telecontrol of Loads
DS	Distribution System
DSO	Distribution System Operator
DTS	Distribution Transformer Substation
EC	European Commission
EIA	Environmental Impact Assessment
EU	European Union
FR	Frequency Converter
LV	Low Voltage
MPP	Maximum Power Point
MPPT	Maximum Power Point Tracking
MV	Medium Voltage
NER	National Energy Regulator
PPP	Photovoltaic Power Plant
RES	Renewable Energy Sources
SG	Synchronous Generator
SOC	System Operation Code
THD	Total Harmonic Distortion
TS	Transmission System
WPP	Wind Power Plant

Chapter 1
Renewable Energy Sources—Overview

The main aim of this chapter is introduction of the proportion of electricity produced with the use of renewable energy sources (RES) in the total production of electricity in the individual EU Member States in comparison to traditional sources. The proportion of electricity produced from the most dynamically developed RES in the last decade—wind power plants (WPP) and mainly photovoltaic power plants (PPP), is described in a detail. The other part of this chapter belongs to the description of the condition for the connection of last mentioned sources WPP and PPP to the distribution system as an external grid.

Currently, the use of electricity is an integral need of human society. With the rising standard of living in developed countries, the dependence on electricity deepens. The bulk of electric energy production consists in burning coal, oil and natural gas, i.e., the use of fossil resources. The future of fossil fuels is given by their finite natural reserves and their non-renewability. We can take for granted that fossil fuels will be completely extracted in the future; the only questionable item is the time frame in which their depletion will occur [1].

On the Earth, the fossil fuel resources are distributed very unevenly. In many cases, a high consumption is in countries with low reserves of resources and vice versa. Developed countries with high consumption of fossil fuels are becoming increasingly dependent on imports of raw material base [2].

An alternative to fossil non-renewable are renewable energy sources (RES) which are currently often very controversial topic for discussion, whether among lay or professional community. Most RES—wind, solar, water, biomass and others—originate in the solar radiation that reaches the Earth. The exception is geothermal energy which originates through various processes within the Earth, together with ebb and flow energy which also does not come from the Sun but is generated by gravitation of the Moon and Earth.

The amount of incident solar radiation is enough. It has been reported that the solar energy reaching the Earth in 1 h equals the consumption of all primary sources on the whole planet for 1 year [2].

S. Misak and L. Prokop, *Operation Characteristics of Renewable Energy Sources*,
Green Energy and Technology, DOI 10.1007/978-3-319-43412-4_1

The consequences of climate change, increasing dependence on fossil fuels and rising energy prices are the reason why the area of RES is currently gaining ground. The contribution of RES lies primarily in their ability to reduce greenhouse gas emissions and the level of pollution, promote industrial development based on knowledge, create jobs and boost economic growth as well as competitiveness and regional development.

1.1 Development of RES in Europe

In 2015, according to data of the European statistic office Eurostat, the proportion of RES in gross final energy consumption in the European Union already reached 16 %. Since 2004, this proportion has almost doubled. Nine EU Member States are thus already reaching their national renewable energy targets in the area of RES, which were set for 2020 within the Europe 2020 strategy [3]. Part of this strategy dedicated to combating climate change and promoting sustainable energy sources imposes an obligation on EU Member States to reduce greenhouse emissions by 20 % compared with 1990, increase the proportion of energy produced from RES in gross final energy consumption to 20 % and increase energy efficiency by 20 % (Fig. 1.1).

Since 2004, the portion of RES in gross final energy consumption has increased significantly in all EU Member States [4]. Compared to 2013, the monitored proportion increased in 24 of the 28 Member States.

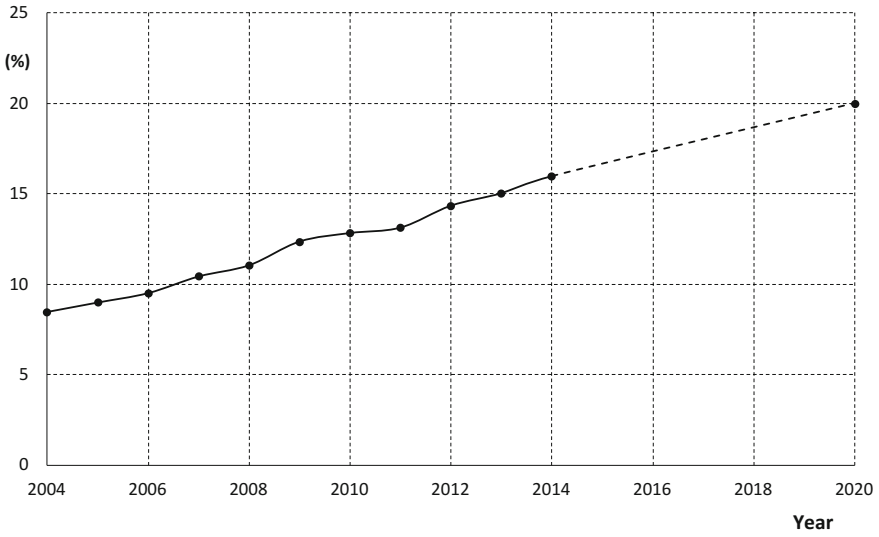

Fig. 1.1 The proportion of energy obtained from RES in gross final energy consumption in the entire European Union with a marked target for 2020

In 2014, by a large margin, the largest portion of RES in gross final energy consumption belonged to Sweden, which reached 52.6 %. Following countries were Latvia and Finland (38.7 %), Austria (33.1 %) and Denmark (29.2 %). On the other side; there are countries like Great Britain (7.0 %), Netherlands (5.5 %) and Malta (4.7 %), whereas the lowest proportion of RES in gross final energy consumption falls on Luxembourg where RES provide only 4.5 % of energy [4] (Fig. 1.2).

The growth of investment in RES reaches tens of percent a year in developing countries; in recent years, on the contrary, the investment in RES is declining in Europe. Here, the investment in 2015 reached the lowest values since 2006. Compared to 2015, investments decreased by 18 % to 58.5 billion USD. In 2015, the dominant European market was the UK where the investments increased by 24 % to a total of 23.4 billion USD. The second largest amount was invested in Germany where the investment in the construction of new facilities reached 10.6 billion USD; however, this represents an annual decline by a full 42 %, caused mainly by lower support of solar and wind energy as well as uncertainty about the future shape of the new auction system to be introduced in 2017. In France, the investment fell even more, by 53 % to 2.9 billion USD.

The Fig. 1.3 shows the total installed capacity of power plants of various types put into or out of operation in the individual EU countries in 2015 [4]. In 2015, the total newly installed capacity of all types of power plants in the EU was 29 GW. For 2015, the Fig. 1.3 shows that the largest installed capacity relates to wind (mostly in Germany and Poland) and photovoltaic power plants. The third largest

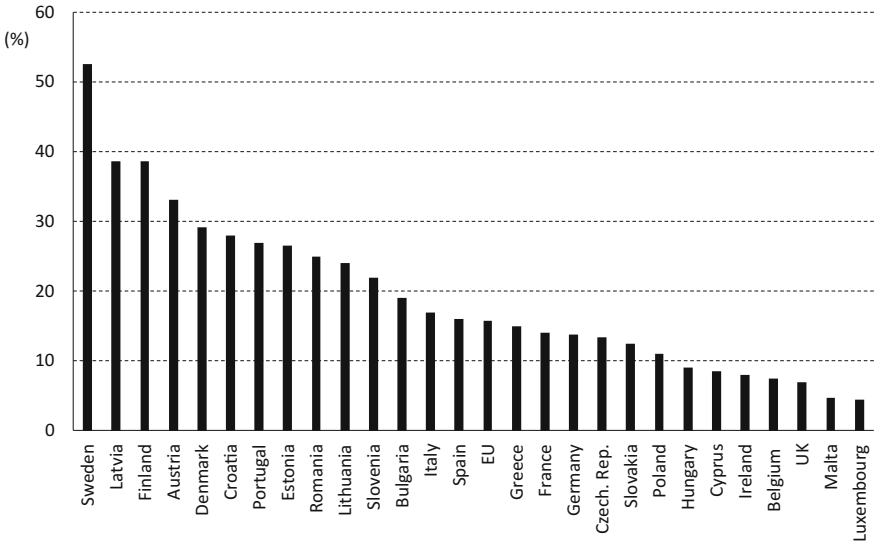

Fig. 1.2 The proportion of energy obtained from RES in gross final energy consumption in the individual EU Member States; the values are given in percentage

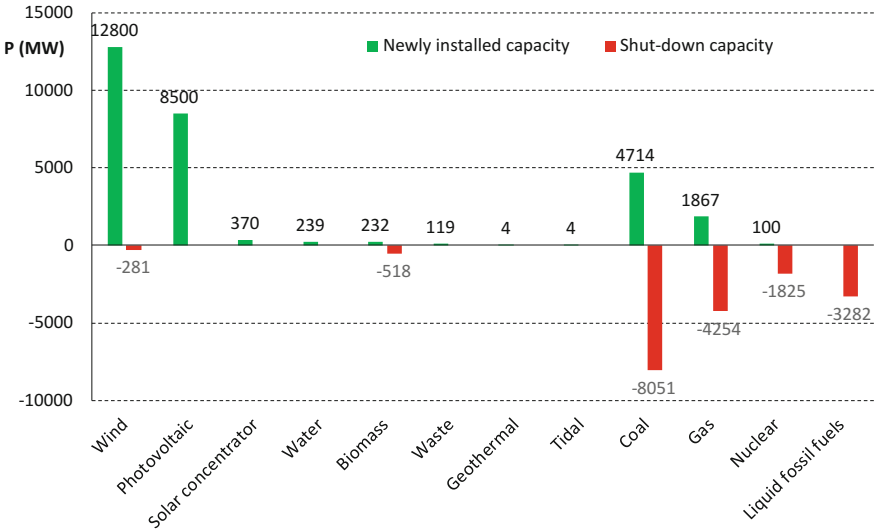

Fig. 1.3 Newly installed and shutdown capacity of various types of power plants in the individual EU countries in 2015

newly installed capacity relates to heat power plants which are also being built primarily in Germany and Poland.

In the European Union, during the last quarter-century, the installed capacity of all types of power plants has increased with the exception of nuclear plants whose period of greatest prosperity (the beginning of the 1980s) was terminated by the accident at the Chernobyl nuclear power plant, which greatly weakened public support for nuclear energy, especially in the Western countries. New projects of nuclear power stations were halted and only the more modern plants continued operation. In the 1990s and the early 21th century, the installed capacity of nuclear power plants was, therefore, almost constant. After the accident of another nuclear power plant, in Fukušima Daiichi, Japan, in 2011, the support of nuclear energy throughout the world further decreased and many nuclear plants (planned to be in operation for a long time) were shut down in the following years. Since 2011, the total installed capacity of nuclear power plants is, therefore declining. This decline will continue but a change in this trend is expected after 2020. At that time, all reactors to be put out of operation in response to the Fukushima disaster will already be shut down but, on the contrary, new reactors being built today or scheduled for a soon construction will be put into operation, mainly in developing countries.

In the last 25 years, the installed capacity of power plants burning fossil solid and liquid fuel was growing throughout Europe [4]. This growth was linked to a gradual modernization of old power plants whose installed capacity increased due to the replacement of old equipment. Nevertheless, the total installed capacity of these power plants in the European Union has already reached its peak and is decreasing from 2012. This decrease is caused by the decommissioning of old power plants in

connection with the transition to low-carbon energy. In Europe, however, new coal-fired power plants are put into operation even today, mainly in Poland.

Conversely, in the case of power plants burning gaseous fossil fuels, the installed capacity is gradually growing as these plants fit into the modern electrical energy sector more than power plants burning solid fossil fuels. Natural gas-fired power plants are able to flexibly regulate their output according to the needs of the power system; in the combustion of natural gas, the unit of energy produced is connected with roughly half-amount of carbon dioxide emissions. In the coming years, the size of newly installed capacity of these power plants will much depend on the price of natural gas in world markets.

The total installed capacity of hydroelectric power stations has not changed much during the past 25 years; the growth in this segment is slow but steady. In Europe, the potential of large dams with high-capacity hydroelectric power stations was achieved already in the 20th century. Today, mainly small hydropower plants with small installed capacity are built on smaller streams.

The installed capacity of wind power plants reached the value of 1 GW as late as in 1993. Over the last 10 years, however, the European wind energy production is prospering. At the beginning of the millennium, the growth of the total installed capacity was mainly driven by Spanish installations; in recent years, the growth has moved to Germany, Denmark and Great Britain.

Until 2004, photovoltaic power plants represented a marginal source with minimal installed capacity. Their huge development started later, both in terms of technical level and investments. After 2009, thanks to generous public funding, Europe is experiencing the so-called solar boom due to which the total installed capacity of photovoltaic power plants has approximated to the installed capacity of water and wind power plants. Due to the decline in state subsidies, however, the growth of the installed capacity of photovoltaic power plants has slowed in recent years (Fig. 1.4).

The development of the installed capacity of various power plants is then linked to the development of the amount of electricity produced in different power plants, as shown by the Fig. 1.5. The Fig. 1.5 especially presents the decline in the use of oil and its products. This decline was caused in the past, mainly by rising prices of oil in comparison with other fossil fuels. Currently, the role of oil is primarily reduced by the transition to low-carbon energy.

Natural gas consumption in the power generation was gradually increasing since the 1990s. It surprisingly achieved its interim peak already in 2008. The subsequent sharp drop in natural gas use was associated with changes in the European electricity market, when the wholesale price of electricity started to decline with the growing portion of subsidized electricity (produced from RES) in total energy produced. Electricity produced from expensive natural gas has proven not to be competitive against cheaper sources of electricity, which resulted in a gradual reduction in the production of gas power plants although they represented modern facilities with high efficiency and minimal environmental impact.

The decrease in the use of natural gas has slowed the decline in the use of power plants burning solid fossil fuels. The price of electricity produced from inexpensive brown coal is still able to compete with other sources in the market and the temporal

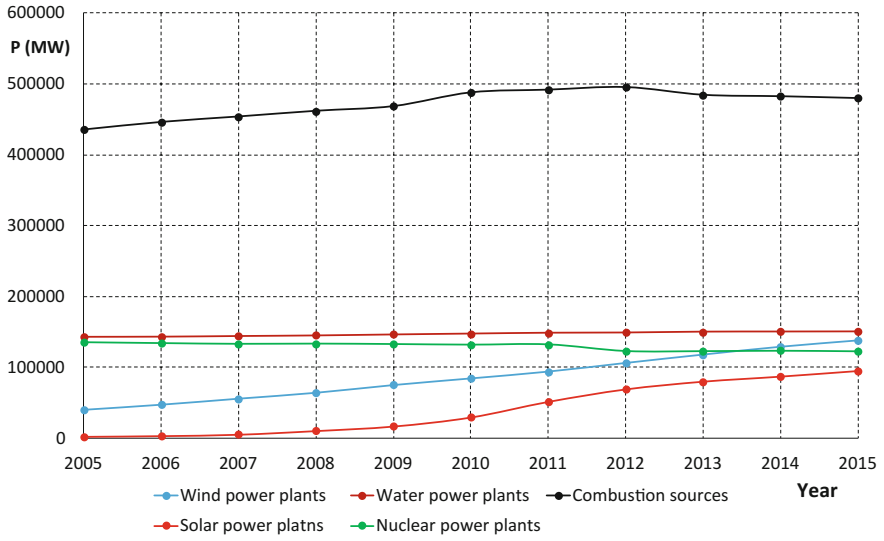

Fig. 1.4 Development of the total installed capacity of various types of power plants in the European Union in 2005–2015

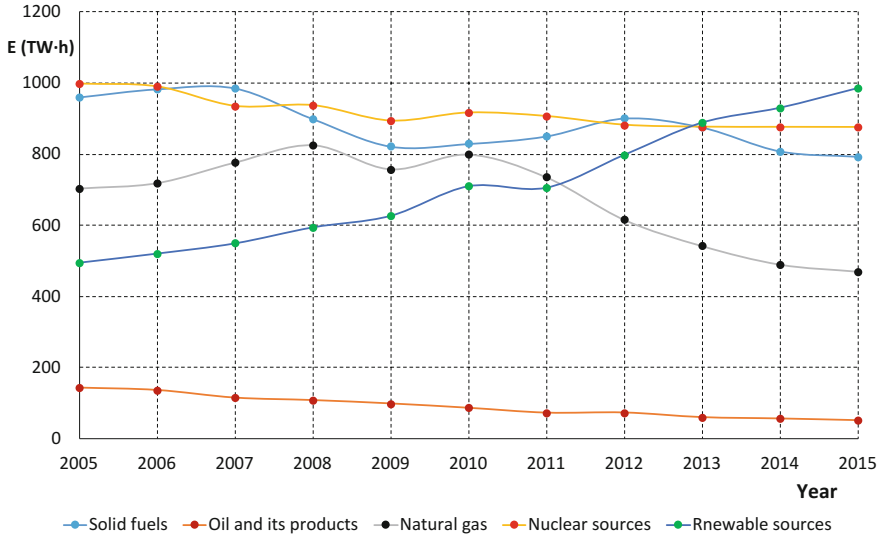

Fig. 1.5 Development of electricity production using different types of energy sources in the European Union during 2005–2015

variation in the production of electricity from RES enforced the continued operation of controllable power plants. The growth of electricity produced from RES thus paradoxically led to the increased utilization of coal power plants, including those that should have been already shut down according to the original plans.

The next graph (Fig. 1.6) describes the development of electricity production from various types of power plants using RES. Despite the large increase in the total installed capacity of these plants during the past 25 years, the growth in electricity production was slower. Power plants using RES usually face a lower coefficient of utilization of installed capacity than the conventional power plants, so that the portion of electricity produced by such plants in the total amount of electricity produced is lower than the portion of their installed capacity in the total installed capacity of all types of sources.

Nevertheless, the electricity generation from wind and photovoltaic power plants has already reached high levels; in 2014, wind power plants and photovoltaic power plants produced 253 TW·h and almost 98 TW·h, respectively.

The extent to which natural conditions affect the production of these power plants is clear from the development of hydroelectric power production. Despite the constant growth of their total installed capacity, their power generation considerably fluctuates during the past 25 years. In 2001, rich in rainfalls, their total production was 408 TW·h. Rainfalls in the subsequent period were lower and electricity generated in 2002, therefore, decreased to 353 TW·h. An even greater decline occurred between 2010 and 2011, when the energy produced decreased from 408 to 340 TW·h.

On the contrary, the electricity production in power plants burning biomass and waste constantly grows without fluctuations. Biomass production is not as dependent on the weather as the output of solar power and wind power plants; in addition, the power plants burning biomass do it gradually and can bridge the period of crop failure thanks to biomass reserves (Fig. 1.6).

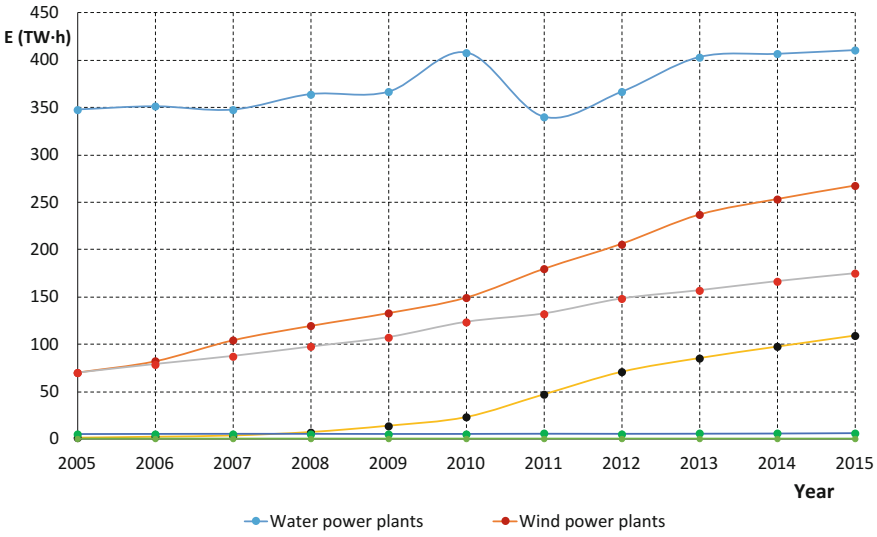

Fig. 1.6 Development of electricity production using different types of RES in the European Union during 2005–2015

1.2 Utilization of Different Sources of Electrical Energy in the Various Countries of the European Union

Energy mix of individual EU Member States is very diverse. Its composition is related to the local availability of fossil fuels, extraction of fuels on the territory of each state, economic level of the state or the support of the given energy sources by communities.

In the mid-20th century, thanks to rich deposits of coal and lignite, the coal power plants in Germany, Poland, Czech Republic and Great Britain became a basis of the local energy mix. As shown Fig. 1.7, these countries still produce large amounts of energy by burning solid fuels. Coal is an important source of energy also in Spain or Italy [4, 5].

Amount of electricity produced by combustion of oil and its products is small in comparison with the production from other sources. For the use in the electricity sector, fuels made from oil are too expensive in comparison with solid fuels and the utilization of RES further decreased the position of oil fuels in the electricity industry. The largest amount of oil and oil products is used in the production of electricity in Italy and Spain, i.e., in the two countries with high consumption and small deposits of solid fossil fuels. Today, even these two countries are switching to cheaper and more readily available energy sources, i.e., RES in combination with natural gas.

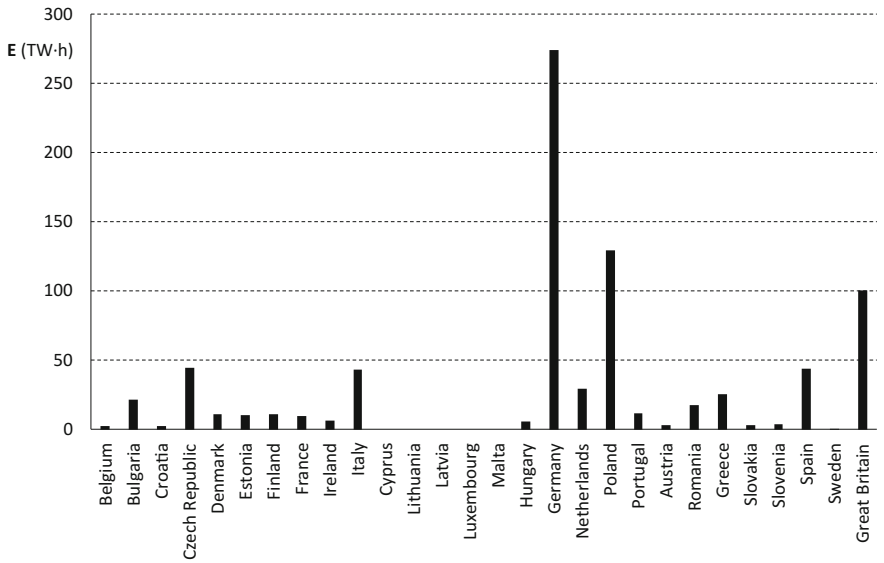

Fig. 1.7 The amount of electricity produced from fossil fuels in different countries of the European Union in 2015

Other European countries use power plants burning oil products only as back-up sources with high flexibility [4] (Fig. 1.8).

Consumption of natural gas in the European electricity sector has gradually increased; today, it is used for generating a great amount of energy. Although the amount of electricity produced from natural gas declines throughout the Europe since 2008, this type of production still maintains a significant position in some states. In addition to Italy and Spain mentioned in the previous paragraph, the natural gas is widely used in Germany, the Netherlands and Great Britain. In Germany, flexible gas-fired power plants are used to regulate the electricity system loaded with variable output of peak power sources. The Netherlands and Great Britain are the major miners of natural gas; thanks to the home exploitation, consumption of natural gas in the electricity sector of these states is economically more profitable than in other European countries [4] (Fig. 1.9).

Nuclear power plants are the dominant source of electricity in France or Sweden. These countries are among the largest European producers of nuclear power. Annually in France, nuclear power plants produce 4.5 times more electricity than nuclear power plants in Germany which is the Europe's second largest producer. Due to Germany's plans to close all nuclear power plants, the local production of nuclear power will decrease in future years, possibly to zero. Conversely, production increase can be expected in Sweden and Great Britain where the construction of new nuclear reactors is being planned (Fig. 1.10).

The amount of electricity produced from RES is gradually increasing in all the EU countries. Currently, the largest amount of electricity from RES is produced in

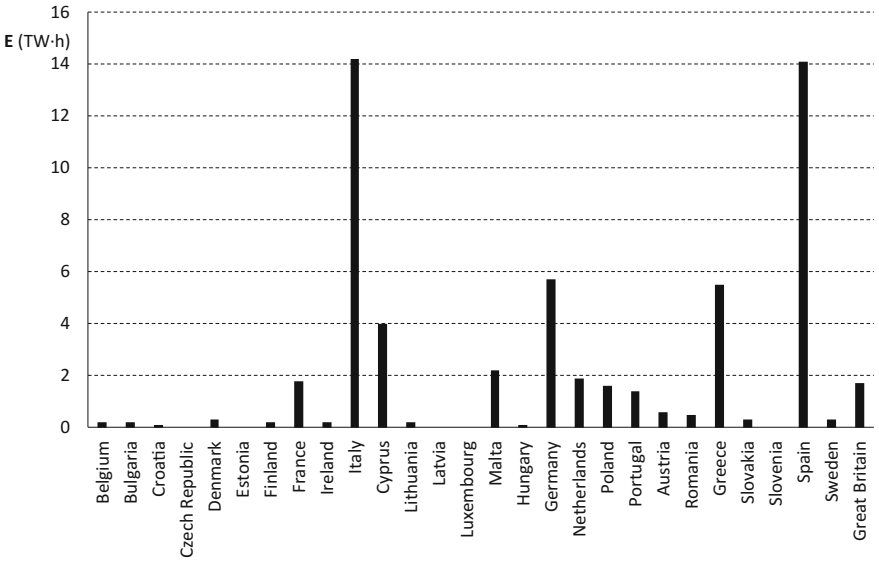

Fig. 1.8 The amount of electricity produced from oil and its products in different countries of the European Union in 2015

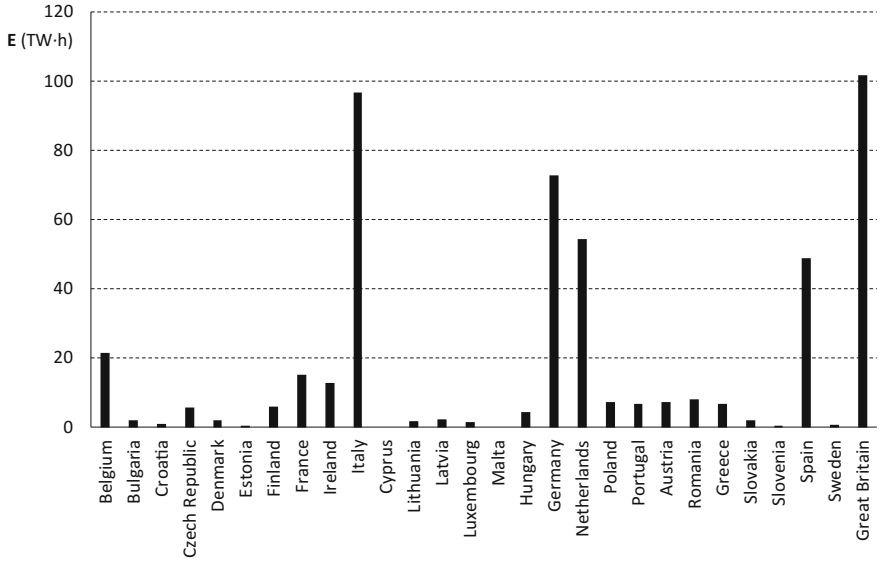

Fig. 1.9 The amount of electricity produced from natural gas in different countries of the European Union in 2015

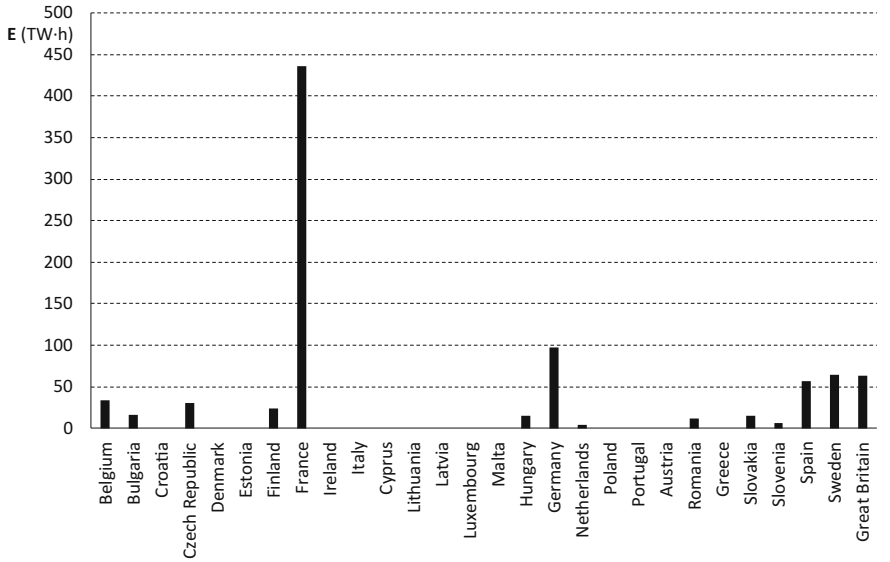

Fig. 1.10 The amount of electricity produced by nuclear power plants in different countries of the European Union in 2015

Germany where the total production of electricity from RES amounted to 168 TW·h in 2014. In recent years, the growth in local production is considerable, mainly due to new installations of wind and photovoltaic power plants.

The second largest European producer of electricity from RES is Italy. It has a large installed capacity of hydroelectric power plants in the Alps, which produce the majority of electricity from RES. Recently, the installed capacity of the Italian photovoltaic power plants has significantly increased; thanks to the Italian sunny climate, these power plants are currently the biggest contributor to the total amount of electricity produced from RES.

The third largest producer of electricity from RES is Spain. Here, the most dominant source using RES is represented by wind power plants; the Spanish installed capacity of wind power plants has already reached 23 GW. In 2015, these wind power plants produced 52 TW·h of electricity. Spain produced a large amount of electricity from RES already in the last century, through local water power plants located mainly on mountain rivers in the Pyrenees. The production of Spanish hydroelectric power plants, however, is very variable; years rich in rainfalls, when Spanish water power plants produce up to 45 TW·h of electricity, alternate with years poor in rainfalls, when the water power plants produce <30 TW·h. The biggest natural potential of Spain consists in solar energy. During recent years, the installed capacity of Spanish photovoltaic power plants is slowly growing as well as the electricity produced by them. Since 2009, the photovoltaic power plants represent the third largest producer of electricity from RES in Spain (Table 1.1; Fig. 1.11).

Table 1.1 The structure of energy production in TW·h (2015)

Country	Solid fuels	Oil and its products	Natural gas	Nuclear power plants	RES
Belgium	2.2	0.2	21.5	33.7	13.4
Bulgaria	21.3	0.2	2.1	15.9	8.0
Croatia	2.4	0.1	1.0	0.0	10.0
Czech Republic	44.4	0.0	5.7	30.3	10.2
Denmark	11.1	0.3	2.1	0.0	18.0
Estonia	10.4	0.0	0.6	0.0	1.4
Finland	11.3	0.2	6.0	23.6	26.3
France	9.5	1.8	15.2	436.5	97.1
Ireland	6.5	0.2	12.9	0.0	6.6
Italy	43.5	14.2	96.7	0.0	122.4
Cyprus	0.0	4.0	0.0	0.0	0.4
Lithuania	0.0	0.2	1.7	0.0	2.2
Latvia	0.0	0.0	2.3	0.0	2.8
Luxembourg	0.0	0.0	1.5	0.0	1.5

(continued)

Table 1.1 (continued)

Country	Solid fuels	Oil and its products	Natural gas	Nuclear power plants	RES
Malta	0.0	2.2	0.0	0.0	0.1
Hungary	6.0	0.1	4.3	15.6	3.2
Germany	274.4	5.7	72.8	97.1	168.4
Netherlands	29.5	1.9	54.5	4.1	11.7
Poland	129.5	1.6	7.4	0.0	20.4
Portugal	12.0	1.4	6.8	0.0	32.3
Austria	3.0	0.6	7.4	0.0	53.7
Romania	17.8	0.5	8.1	11.7	27.6
Greece	25.7	5.5	6.8	0.0	12.3
Slovakia	2.9	0.3	2.1	15.5	6.5
Slovenia	3.8	0.0	0.4	6.4	7.0
Spain	43.8	14.1	48.8	57.3	114.1
Sweden	0.5	0.3	0.8	64.9	85.9
Great Britain	100.8	1.7	101.8	63.7	67.5
European Union	808.7	57.4	490.07	876.3	931.0

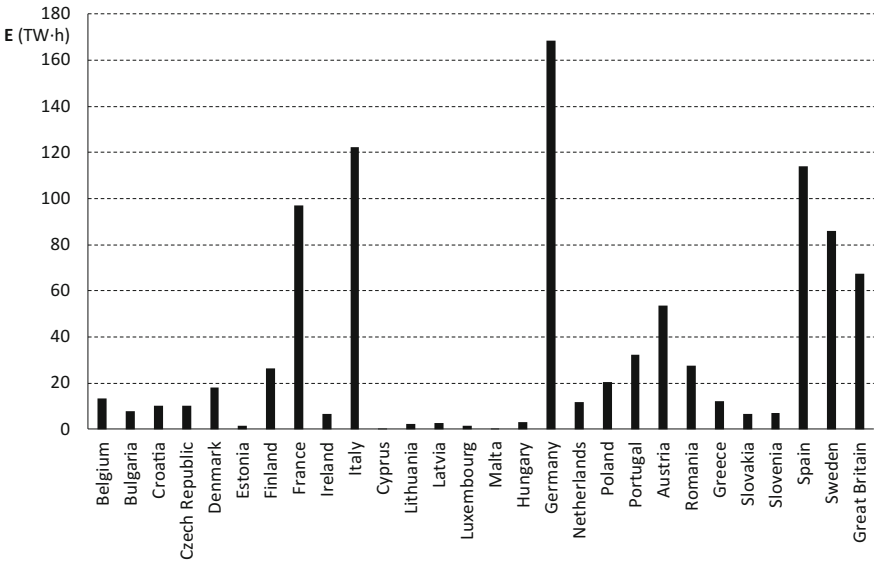

Fig. 1.11 The amount of electricity produced with the use of RES in different countries of the European Union in 2015

1.3 The Proportion of Energy Obtained with the Use of RES in the Consumption of Various Sectors

Utilization of RES is steadily growing in all European Union countries and in various industrial sectors. This growth is motivated not only by binding agreements within EU countries on supporting the development of renewable energy use but also by increasing economical popularity of RES compared to conventional sources of energy or the efforts to achieve sustainable development, both for private companies and public institutions.

The following three figures (Figs. 1.12, 1.13, 1.14) show the use of RES in individual Member States in the production of electricity, transport, and heating and cooling buildings [4–7].

The use of RES in electricity production reaches high values primarily in Austria and Sweden. For decades, the dominant source of electricity generation in Austria is represented by water power plants; thanks to their modernization and development, the amount of electricity produced by them is gradually increasing. Austria has learned to effectively use its great energy potential consisting in alpine rivers. Today, Austria thus produces 70 % of electricity using RES and the Austrian government plans to reach 100 % portion soon. To achieve this goal, it will be necessary to exploit the local potential as well as other RES; in Austria, therefore, we see investments in the development of the energy use of biomass or wind energy.

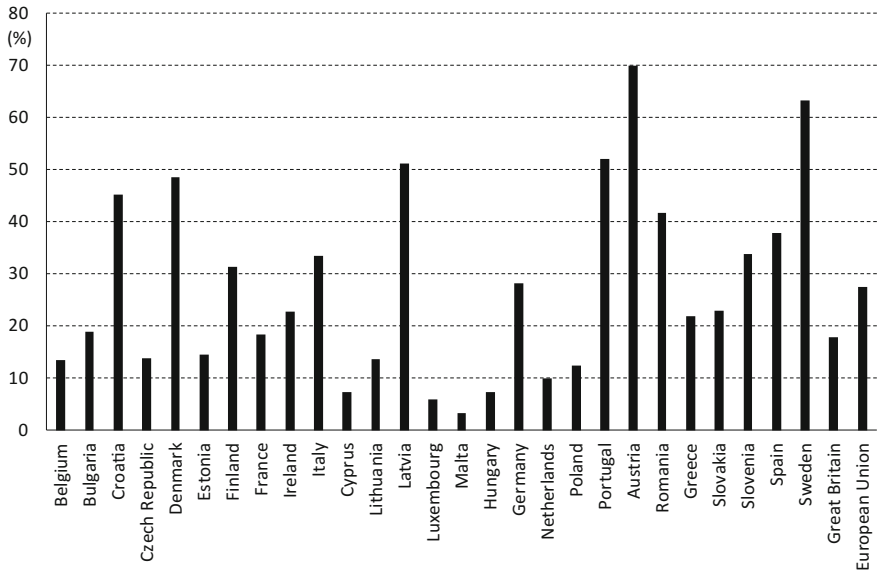

Fig. 1.12 The proportion of electricity produced with the use of RES in the total production of electricity in the individual EU Member States in 2015

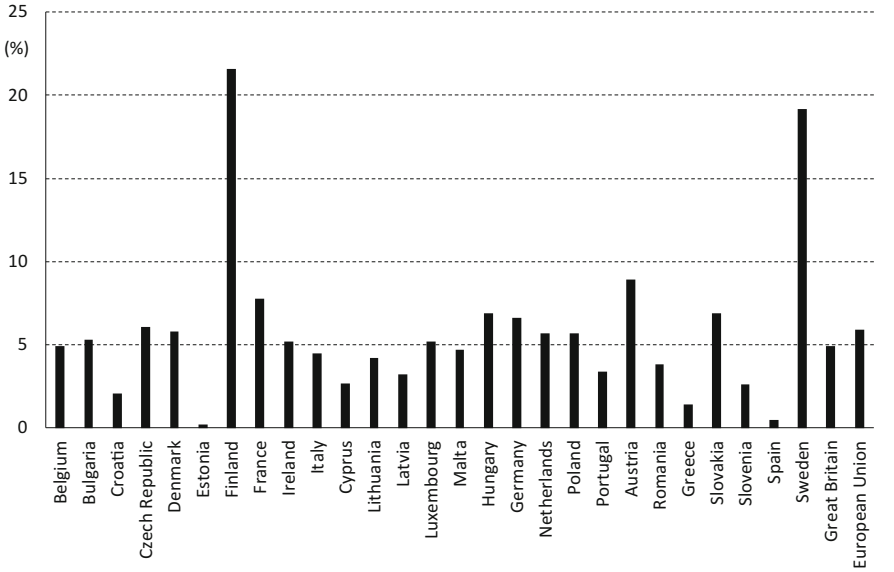

Fig. 1.13 The proportion of electricity obtained from RES in the total energy consumed in transport in the individual EU Member States in 2015

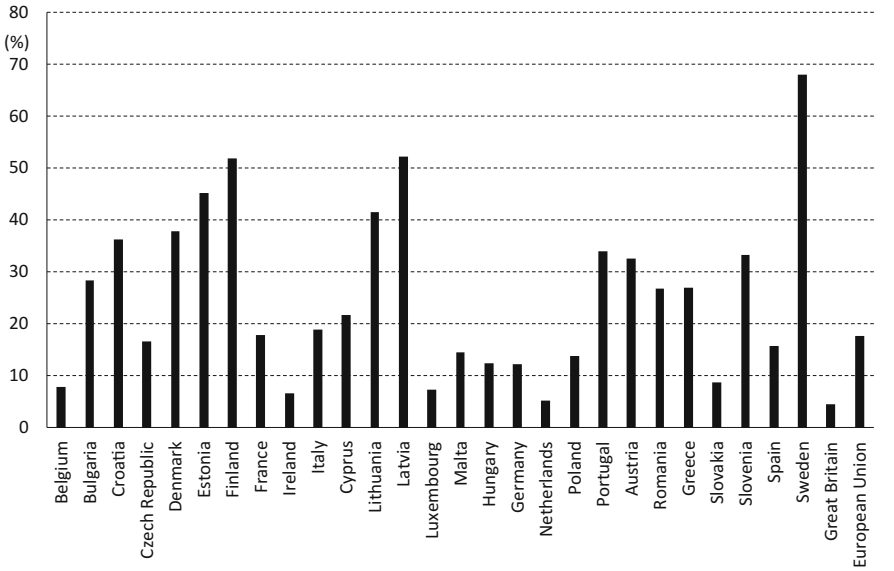

Fig. 1.14 The portion of renewable energy in heating and cooling buildings in the individual EU Member States in 2015

The second largest portion of energy obtained using RES in the total amount of electricity produced falls on Sweden. Sweden is going well with a long-term development of RES utilization and, conversely, with a reduction in the consumption of fossil fuels. In the case of Austria, RES play a very dominant role in the energy mix. Regarding the Swedish energy sector, an important position belongs to nuclear power plants which produced 42.5 % of electricity in this country in 2015. The biggest natural energy potential of Sweden lies in mountain streams which provide large amounts of electricity in hydroelectric power plants already for decades. As in other European countries, the local production of hydroelectric power plants also varies greatly with rainfalls, so that their annual electricity production fluctuates between 80 and 50 TW·h. Since most of the local energy-exploitable hydro potential has already been used, Sweden seeks to develop also other RES. An extraordinary potential is represented by large Swedish forests from which Sweden obtains large quantities of biomass. Increasing temperature of the Swedish climate accelerates the growth of local trees and the production of energy-usable biomass increases. Due to its location at the North Sea, Sweden also has a great potential of the wind. The development of technology for offshore wind power plants increases the economic feasibility of wind potential in Swedish shores; the local government is, therefore, investing heavily in new wind power plants. Thanks to the great heyday of the local wind energy sector in recent years, the wind power plants have become the second largest Swedish source of electricity generated using RES and thus pushed power plants burning biomass to the third place.

In 2014, two more countries exceeded the 50 % threshold for representation of RES in the total electricity production—Latvia and Portugal.

Latvia is a small country with a small population; this is also reflected in the local electricity consumption which is low in comparison with the energy potential of local RES. Its energy mix consists only of energy produced using RES and energy obtained by burning natural gas. The main Latvian gas supplier is Russia with which the Baltic States do not have good political and trade relations; Latvia, therefore, seeks to reduce dependence on Russian supplies through maximum utilization of local renewable energy potential. The main energy potential of local RES lies in water energy. Today, Latvia is already fully using its economically available potential of energy from water; therefore, Latvia must invest in other sources to further develop the use of RES. Due to the low performance of the local economy, Latvia does not have sufficient funds for large investments in wind energy generation at sea although the wind energy potential in the Baltic Sea is large. Instead of the wind potential, the Latvian government is trying to exploit the vegetable potential of large Latvian forests. In the future, electric power generated from local biomass could replace the energy produced from Russian natural gas.

Portugal now reaches a high proportion of electricity produced using RES in the total amount of electricity produced thanks to a great blow of its local wind power generation. In the beginning of the 21st century, like in the neighboring Spain, large

funds were invested in the construction of new wind power plants; in 2015, Portugal already had 4856 MW of installed capacity in wind power plants. Today, these wind power plants represent the second largest source of electricity in Portugal and help reduce fossil fuel consumption in the local energy sector. The largest Portuguese source in the electricity production is represented by local water power plants. Like in Spain, their production greatly varies from year to year depending on the amount of rainfall in the Pyrenees, between 5 and 17 TW·h; the portion of RES in the production of electricity in Portugal thus fluctuates considerably.

RES also have powerful applications in European transport. European directives prescribe minimum bio-component content in fuels used in road transport; bio-component portion in fuels is more closely specified by national legislations. In addition to traditional fuels with the added bio-component, European fuel filling stations offer a number of fuels produced purely from biomass grown directly for the purpose of use in transport. In most countries, the overall portion of energy fuels produced from RES in the total energy consumption in the transport sector is around 5 %; in Sweden and Finland, however, biofuels enjoy great interest and support of local governments for long years. In 2015, the portion of energy produced using RES and consumed in transport in Finland and Sweden was 21.6 and 19.2 %, respectively, i.e., much higher than in other European countries.

A traditional way of using energy from RES is its use for heating buildings. Especially in the Nordic countries, the local biomass is a popular fuel for heating local homes. Biomass, as a fuel for home boilers, is today often financially supported by various European governments due to the production of smaller quantities of pollution during its burning compared to combustion of solid fossil fuels.

Thermal solar collectors are greatly used in the countries of southern Europe where they can provide enough hot water to ensure home consumption for most of the year. Due to low prices of solar panels, this way of water heating is also successful in the states where home photovoltaic power plants have not yet found great application because of the high purchase price.

In 2015, the highest portion of energy produced from RES in the total consumption for heating and cooling buildings was achieved in Sweden. The local government strongly supports the use of biomass grown in Sweden in the energy sector; for many Swedish households, the wood from local forests is a traditional choice for heating the house.

Year by year, the usage portion of energy generated from RES is growing in all sectors of the economy. The greatest growth occurs in the electricity sector where the portion of electricity produced from RES increased from 14.4 to 27.5 % between 2005 and 2015, respectively. Because the electricity production process results in the formation of most greenhouse gas emissions in Europe, the efforts to considerably reduce the use of fossil fuels in the energy sector will continue also in the coming decades and the input energy for the electricity production process will

have to be covered by other sources instead of fuels. Given the public support for RES and the negative attitude towards nuclear energy in many European countries, the total proportion of electricity produced from RES will soon exceed 50 % of the total electricity produced.

The use of energy from RES is also growing in transport but considerably slower than in the electricity sector. This portion did not reach 1 % in 2005 while reaching almost 6 % in 2015. In future years, however, this portion will not grow significantly due to unfulfilled expectations connected with the application of biofuels, whether in terms of environmental, technological or public support. The greening of European transport is now moving towards the replacement of liquid fuels with natural gas which has lower carbon dioxide emissions compared to oil fuels, or towards the complete removal of combustion process from road transport and replacement of cars using internal combustion engines with electric vehicles.

In heating of buildings, the use of solar energy or the energy released by burning biomass is the simplest and cheapest option for many residents in the European Union. With the increasing price of fossil fuels and decreasing price of fuels produced from biomass, this portion will grow also in the coming years, whereas it increased from 10.2 to 17.7 % between 2005 and 2015, respectively. Heat generated from RES is used primarily outside urban areas. Regarding the future, it is expected that the use of heat generated in this way will grow even in cities, in district heat supply systems (Figs. 1.15, 1.16, 1.17).

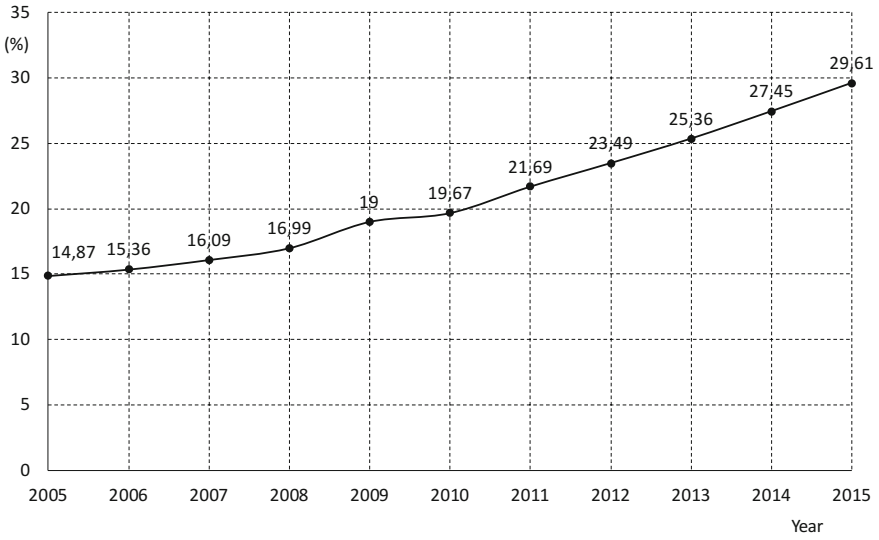

Fig. 1.15 Development of the portion of RES in the total electricity produced throughout the European Union in 2005–2015

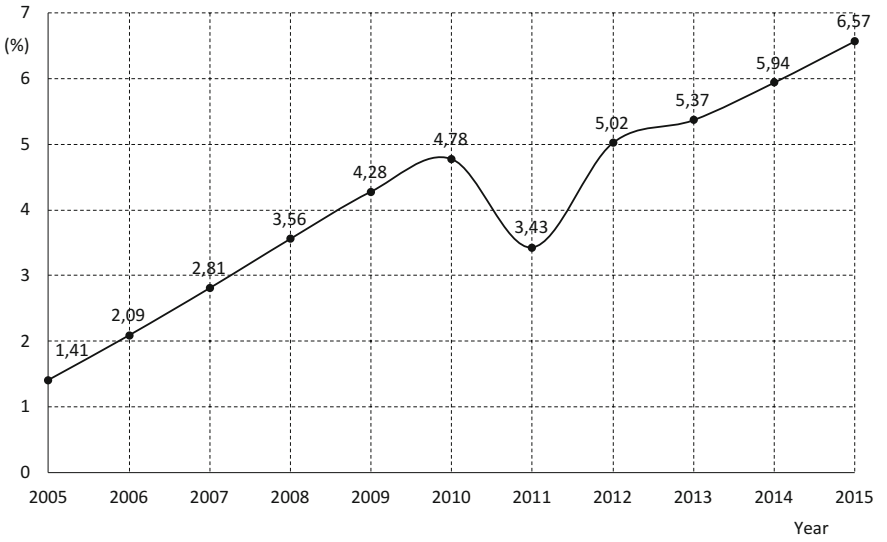

Fig. 1.16 Development of the portion of RES in the total energy consumption in transport throughout the European Union in 2005–2015

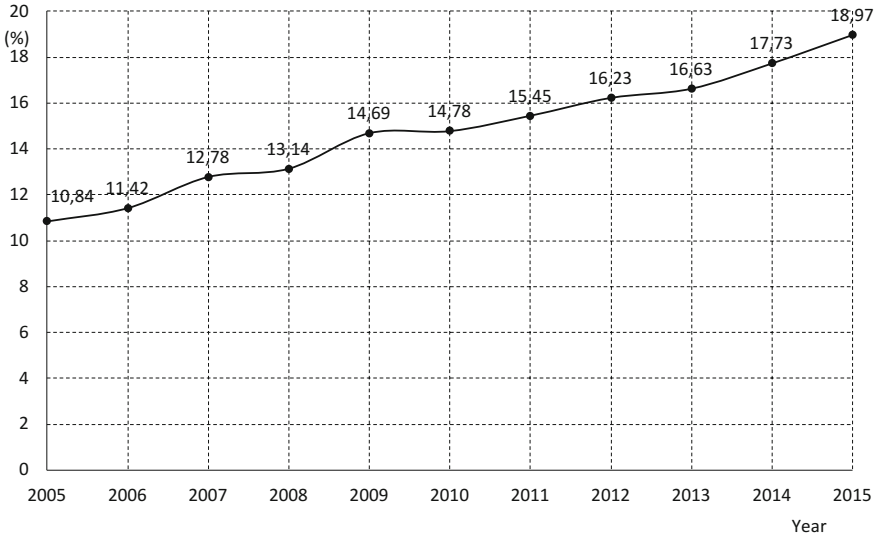

Fig. 1.17 Development of the portion of RES in the total energy consumption in heating and cooling buildings throughout the European Union in 2005–2015

1.4 Wind Power Plants

Utilization of wind energy is currently the fastest growing segment of all RES. European seaside countries dispose of great potential of RES thanks to the windy climate in their coastal areas. Due to the significant technical progress, new wind power plants are more efficient than those installed in the late 20th century when the wind energy began to be used for electricity generation. The most efficient currently manufactured wind power plant have an installed capacity of 8 MW. Propeller of these wind power plants describes a circle with a diameter of 164 m and its single blade has a length of 80 m. Further technological advancements will result in building even larger wind farms with larger installed capacity. Thanks to advancements in the technology of designing wind power plants, the wind power plants are today installed also at sea, whereas the underwater foundations of the plant can reach up to a depth of 60 m. Another innovative solution, that may further shift the possibilities of technology of offshore wind power plants, is represented by floating wind power plants that are not tightly connected to the seabed by means of concrete foundations; such wind power plants are anchored only by ropes. This technology allows the installation of wind power plants even in the seas where the concrete foundations could not be used because of the great depth. The floating wind power plants could thus considerably extend the range of energy-usable potential of wind. In terms of Europe's potential, these floating wind power plants would be interesting mainly for Mediterranean countries. Unlike the North Sea, where the majority of previously installed offshore wind power plants still occur, the seabed of the Mediterranean Sea quickly descends to great depths; therefore, the installation of offshore wind power plants is only possible near the coast where the wind potential is not yet high enough to pay for the installation of costly offshore wind power plants.

The European wind energy development began in the late 20th century in Denmark, Spain and Germany. In 2000, wind power plants with a total output power of more than 2 GW were installed in Denmark and Spain, and even 6 GW turbines were installed in Germany.

In the early 21st century, the Danish wind energy growth slowed down and renewed as lately as in the past few years with increased financial support for RES in the European Union after 2008. Today, Denmark has more than 5300 wind power plants with a total installed capacity of 5070 MW, including 1271 MW representing the output of offshore wind power plants.

In 2015, Danish wind power plants created a new world record as for their portion of produced electricity in the total consumption of the country; overall, the Danish wind power plants produced 42.1 % of total consumption in the country. Thus, they broke their own record from 2014 when they produced 39.1 % of the total electricity consumed. According to plans of the Danish government, this portion should achieve 50 % in 2020. Denmark has very suitable climatic

conditions for operating wind power plants as the average speed of wind blowing on the Danish territory is 7.6 m/s. Danish energy potential of solar and water energy is small compared to other European countries; the local government, is, therefore trying to maximally exploit the local production of biomass which is used in combined heat and power production.

In Spain, unlike Denmark, the development of wind energy usage continued to accelerate in the early 21st century. The total installed capacity of wind power plants in Spain reached nearly 10 GW in 2005 and almost 23 GW in 2012. In 2013, however, the state system for supporting the use of RES was changed; since that moment, the installed capacity of Spanish wind power plants has increased just by tens of megawatts. Despite, Spain has already reached the installed capacity of wind power plants which makes it the world's fourth country in terms of the total installed capacity in wind power plants. Today, Spanish wind power plants supply 19 % of the total electricity consumed.

In Germany, the use of wind energy is growing since 1998 at a constant rate of approximately 2 GW of newly installed wind power plants annually. In the past 3 years, technology advancements accelerated this growth and the total installed capacity of German wind power plants at the end of 2015 was 45 GW (including 3 GW attributable to the output of offshore wind power plants). Germany powerfully invests in systems using various forms of RES with a view to reduce consumption of fossil fuels in its energy mix and thus also reduce the amount of greenhouse gases released in the German industry. Germany is preparing its own national action plan for the environment in 2050. Climate Action Plan 2050 [8] should be adopted by the German government in mid-2016 and should open the way of Germany from fossil fuels to reduce carbon dioxide emissions by up to 95 % relative to 1990 levels, whereas this target is to be achieved just by 2050. As a time-closer objective, the document envisages to reduce CO_2 emissions by 2030 to half the amount of CO_2 emitted in 2014. Climate Action Plan 2050 [8] also describes a way of achieving the reduction in emissions at the given level. According to the document, 75 % of electricity should be produced from RES in 2030.

After 2005, the wind energy production began to be developed also in other European countries. Its great boom was seen in Portugal, inspired by neighboring Spain, which decided to develop RES based on wind. Compared to Spain, Portugal has much better conditions for wind power plants as the wind blowing along the Atlantic Ocean is much stronger and more enduring than the wind in the interior of the peninsula. In 2015, the installed capacity of wind power plants in Portugal reached 5 GW and this capacity is steadily growing. Thanks to the large installed capacity of local hydroelectric power plants, the power plants using RES produce most of the electricity already today. Due to the large potential of solar energy, Portugal may soon become energy-independent on fuel imports for energy sector.

Along with Portugal, after 2005, also Great Britain started to invest in wind sources. By 2010, the installed capacity in Great Britain reached 5.4 GW. Later, the

governments support for wind energy even increased. In 2015, thanks to massive investments, the total installed capacity of British wind power plants reached 13.6 GW. This rapid growth is likely to continue also in the coming years. Private companies are keen to invest in British wind farms despite declining financial support of the British government. Current investments are shifting from the British mainland to the adjacent seas. The current total installed capacity of British offshore wind power plants is about 5 GW, representing 45 % of the overall output of this type of power plants in the world. According to the wind power plans of the British Department of Energy and Climate Change [9], the total installed capacity of coastal wind power plants on the British territory should nearly double until 2020. Currently, several projects are started to further increase the installed capacity of offshore wind power plants by a third; e.g., this includes the project Neart na Gaoithe of the company Mainstream Renewable Power Ltd [10] with investment costs of 1.9 billion EUR, project Beatrice Offshore Wind Farm of the company Scottish Power Ltd. with investment costs of 2.5 billion EUR or project East Anglia One of the company SSE Plc with investment costs of 3.1 billion EUR. However, an important project is mainly the Hornsea wind farm [11] being built by the company Dong Energy. In 2020, when the project should be completed, it will offer a total installed capacity of 1.2 GW provided by 240 wind power plants and should be the largest offshore wind park in the world. According to the analyses of the company Dong Energy, the total costs of building the park should make six billion GBP.

The windiest part of the British territory is represented by the islands north of Scotland. Especially the Outer Hebrides, Orkney Islands and Shetland Islands have the potential to cover up to 5 % of the total electricity consumption in Great Britain by 2030.

In France, the wind energy sector is being slowly developed since 2005. Approximately 800 MW of new wind power plants are installed each year; in 2015, the total installed capacity of French wind power plants reached 10.3 GW. Due to the high consumption of electricity, France will have to accelerate the installations in the coming years to meet the targets prescribed by the Europe 2020 strategy. According to estimates, France would have to install at least 1600 MW in wind power plants annually during the coming years.

A similar situation is in Italy which installed almost 9 GW in wind power plants by 2015. In recent years, however, the interest of investors is shifting from wind energy to solar energy whose potential in Italy is greater. Nevertheless, the development of Italian wind energy sector may renew with the development of floating wind power plants.

In Europe, the biggest potential for the growth of wind energy utilization now exists in the areas of the North Sea and Baltic Sea. In the past, its strong usage in the energy sector began in Denmark and then in Germany. Currently, also neighboring countries are starting to exploit this potential, the Netherlands with Belgium in the west, Norway and Sweden in the north, and Finland and the Baltic States in the east.

In 2015, the largest capacity of wind power plants was installed in Germany and then in Poland which installed 1266 MW. This great newly installed capacity suggested that the Polish wind energy industry could grow with similar dynamics as in neighboring Germany; instead, however, the Polish wind power sector is facing a downturn. The current Polish government is not keen on further construction of new wind power plants, especially on the Polish mainland; therefore, it came up with restrictive laws and measures which should discourage investors from the construction of new power plants and which encumber the operation of already existing plants with high taxes.

From the all European countries point of view, the wind power plants experienced a large increase in both installed capacity and energy produced. In 1990, in all countries that are now EU members, the total installed capacity of wind power plants was only 454 MW but reached 12.7 GW in 2010 and 129 GW in 2015. Between 1990 and 2015, the installed capacity of European wind power plants thus increased 286 times. Between 2005 and 2014, the amount of electricity produced by wind power plants increased from 70 to 253 TW·h. In 2015, therefore, the European wind power plants represented 13.2 % of the installed capacity of all European power plants and generated 7.9 % of the total electricity produced [6] (Figs. 1.18, 1.19, 1.20, 1.21, 1.22, 1.23).

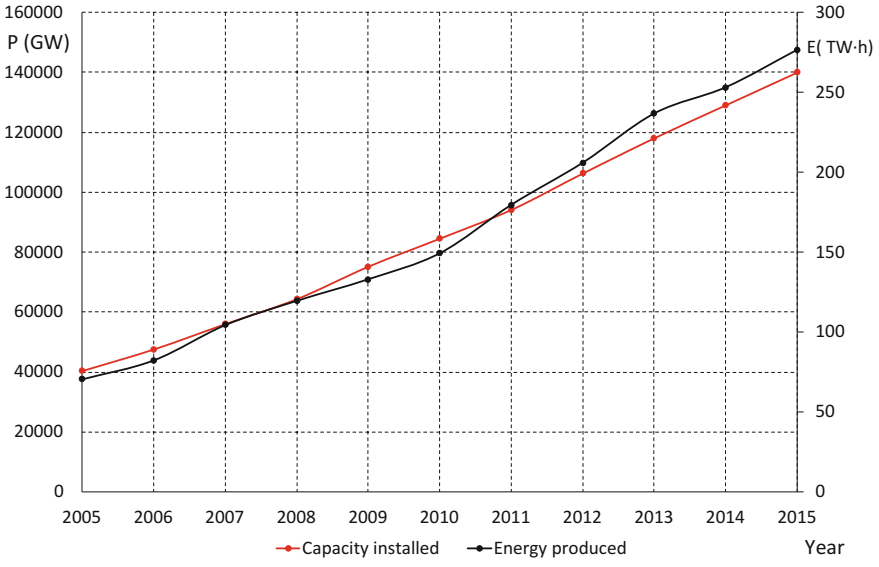

Fig. 1.18 Development of the installed capacity of wind power plants and their electricity production in the European Union in 2005–2015

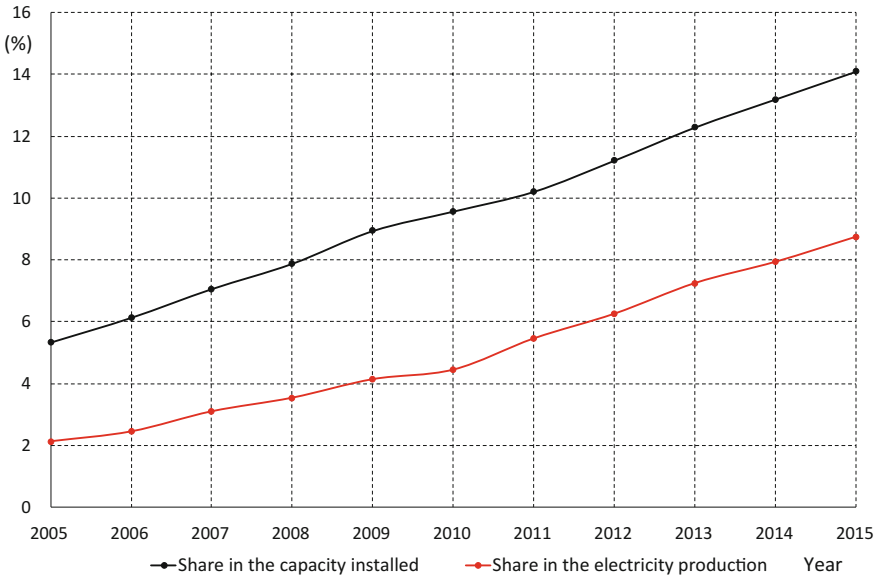

Fig. 1.19 Development of the average utilization ratio of the installed capacity of wind power plants in the European Union in 2005–2015

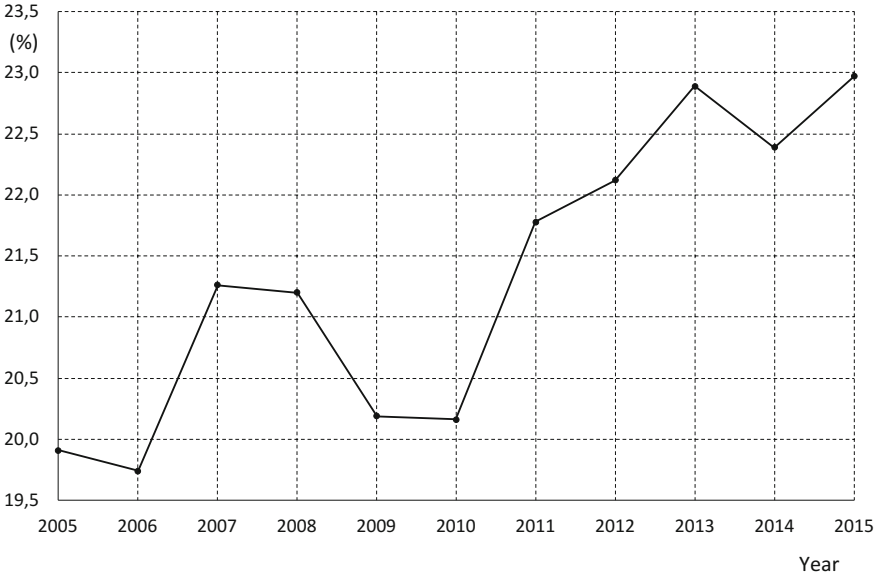

Fig. 1.20 Development of the average utilization ratio of the installed capacity of wind power plants in the European Union in 2005–2015

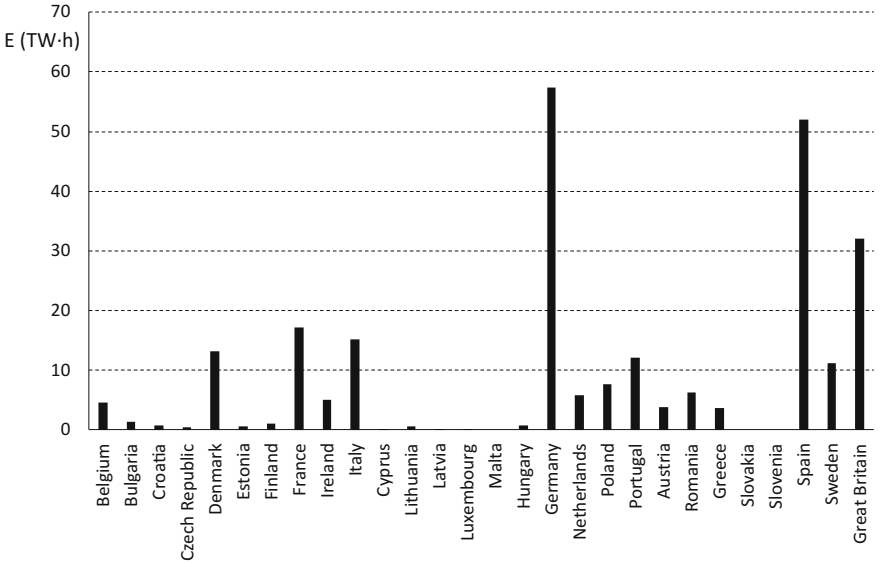

Fig. 1.21 Amount of electricity produced by wind power plants in the individual EU Member States in 2015

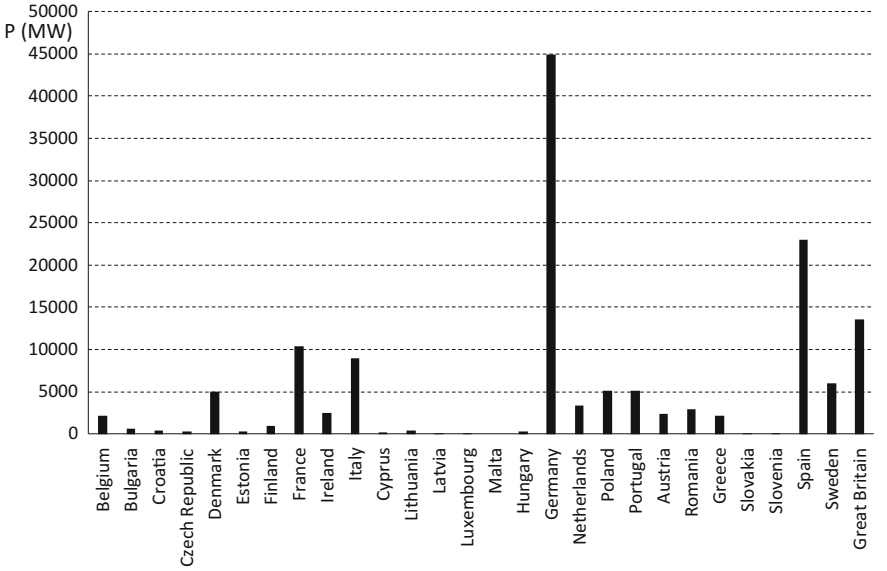

Fig. 1.22 Total installed capacity of wind power plants in the individual EU Member States on January 1, 2016

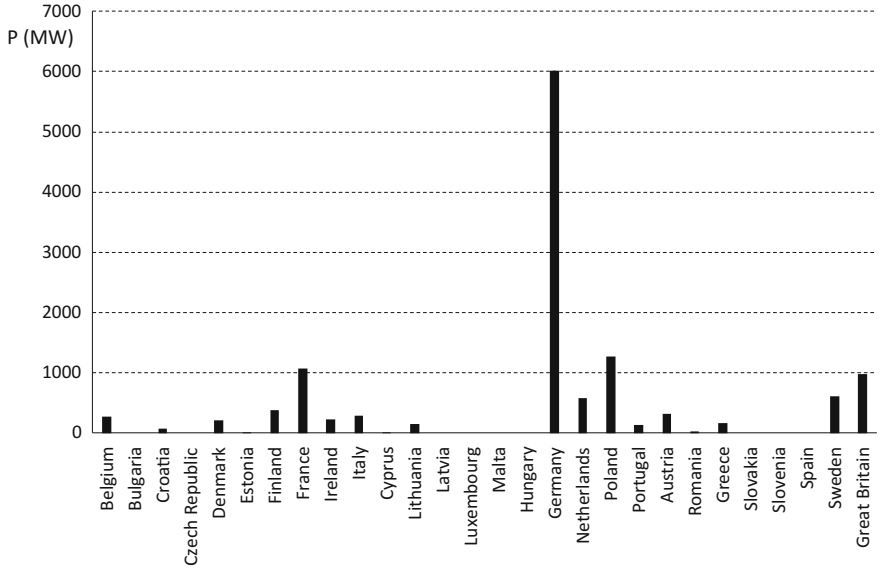

Fig. 1.23 Newly installed capacity of wind power plants in the individual EU Member States in 2015

1.5 Photovoltaic Power Plants

Even at the end of the 20th century, the commercial use of solar radiation in the energy sector was virtually zero. However, significant technological advances in the production of photovoltaic panels and massive financial support for solar energy from the European Union and individual European governments that crossed each other in the first decade of the 21st century caused a rapid rise in the use of solar energy in the electricity industry. Yet in 1990, the total installed capacity of European photovoltaic power plants was only 10 MW and was made up of several experimental installations with small capacities. Until 2003, the total installed capacity did not exceed 1 GW; the first sharp increase was recorded between 2006 and 2007 when the European installed capacity grew from 3.3 to 5.2 GW. In the following years, the growth continued to accelerate, reaching the highest year-on-year increase between 2010 and 2011 when it rose from 30.1 to 52.5 GW. With the falling price of photovoltaic panels and thanks to guaranteed purchase prices, the new installations became very profitable. Return on investment shortened to units of years and photovoltaic power plants turned into a very profitable business. In many countries, the total state funding of photovoltaic power plants escalated to such an extent that it significantly increased the price of electricity for large and small customers. To limit further growth in electricity prices for end customers, individual states have introduced measures which sharply reduced profits from the solar business. This was reflected in deceleration of the

development of photovoltaic power plants in Europe. Nevertheless, between 2013 and 2014, the total European installed capacity increased by 7.1–89.1 GW which already represents a big production of electricity. In 2014, photovoltaic power plants in the European Union produced 97.8 TW·h of electricity [4–7].

Due to the continued decline in prices of photovoltaic panels on world markets, however, the photovoltaic power plants again become an economically interesting solution to increase the use of energy obtained from RES even at reduced financial support from the state. Photovoltaic power plants are now successful, especially in the form of small and medium-sized installations for houses and apartment buildings or at the roofs of office buildings and industrial halls. With the increasing popularity of small off-grid networks, for which small photovoltaic plants are preferred source of energy, it is thus expected that the total European installed capacity of photovoltaic power plants will grow at a fast pace in the coming years.

With the growth of the installed capacity of photovoltaic power plants and the gradual shutdown of old classic power plants, the portion of photovoltaic power plant will further grow, both in the total installed capacity of European power stations and the total amount of electricity produced. In 2015, the portion of installed capacity of photovoltaic power plants reached 8.9 % of the total installed capacity and the portion of electricity produced by them was 3.1 %. Due to fluctuations in their immediate output with changing weather, the photovoltaic power plants have considerably lower utilization ratio of the capacity installed compared to power plants burning fossil fuels or nuclear power plants; however, thanks to the improving technology of photovoltaic panels, the annual utilization ratio of the capacity installed in photovoltaic power plants increased from 7.3 % in 2005 to 12.5 % in 2014. In 2014, the total area of photovoltaic panels installed in the European Union reached 47.7 km^2.

The current European leader in the installation of photovoltaic panels is Germany, as in the case of wind power plants. In 2014, the total installed capacity of German photovoltaic power plants is 38.2 GW. In that year, the amount of electricity produced by photovoltaic panels reached 36.1 TW·h. According to the national plan, the installed capacity of German photovoltaic power plants should grow to 51.8 GW by 2020 to cover a large part of the electricity consumption of German households. In southern Germany, the electricity produced by local photovoltaic power plants covers 10 % of local electricity consumption already today. In the future, the total installed capacity of photovoltaic panels in Germany could grow to 150 GW, as estimated by current studies.

The growth of installed German photovoltaic power plants began after 2003 when the total installed capacity was only 435 MW. It increased to 1105 MW in the following year and then accelerated from year to year. Period of the highest growth then came between 2009 and 2012 when the installed capacity of photovoltaic power plants rose from 10.6 to 32.6 GW. In Germany, small photovoltaic power plants enjoy great popularity and appear at the roofs of German homes more and more often.

The second largest producer of electricity in photovoltaic power plants is Italy. Regarding the energy of solar radiation, this country has much larger potential than Germany; however, in 2014, despite this fact, Italian photovoltaic power plants produced only 62 % of the amount of electricity produced by photovoltaic power plants in Germany. In 2014, the total installed capacity of Italian photovoltaic power plants reached 18.6 GW. In Italy, the rapid development of the utilization of solar energy started a few years later than in Germany. Yet in 2007, the local installed capacity was only 87 MW. In the next year, however, this capacity was 432 MW, and then rapidly increased with new installations. The highest jump in installed capacity occurred between 2010 and 2011 when the capacity increased from 3.5 to 12.7 GW. In 2014, the total installed capacity of Italian photovoltaic power plants reached 18.6 GW. In that year, the Italian photovoltaic power plants produced 22.3 TW·h.

The third largest producer of electricity from the energy of sunlight is Spain which have the best climatic conditions for solar energy production from all European countries. In 2014, Spain produced 13.7 TW·h of electricity, i.e., only 38 % of the amount of electricity produced by photovoltaic panels in the same year in Germany. To produce this amount of electricity, however, the Spanish photovoltaic power plants needed only 7.1 GW of installed capacity, i.e., only 18.6 % of the total installed capacity of German photovoltaic power plants. These figures indicate that the Spanish photovoltaic power plants achieve much higher utilization ratio of capacity installed. In Spain, the development of solar energy sector began in 2006 when the solar installed capacity was only 180 MW. This capacity increased to 750 MW in the following year and even to 3450 MW in 2008. Rapid growth continued until 2012 when it slowed down slightly.

To greater or lesser extent, the installations of photovoltaic power plants also grow in other EU Member States. By 2014, more than 3 GW were installed also in photovoltaic power plants in France, Great Britain and Greece. For France and Great Britain, the solar energy utilization is one of the ways to get closer to meeting European targets for reducing greenhouse gas emissions. Nevertheless, Great Britain, famous for its weather with frequent rain, does not have climatic conditions much suitable for solar energy utilization; it will, therefore, focus on other RES (Figs. 1.24, 1.25, 1.26, 1.27, 1.28).

The Fig. 1.29 demonstrates the fact that electricity production in European photovoltaic power plants is heavily dependent on the geographical location of the respective installation. While the countries of southern Europe gain more than 1 TW·h of electricity from 1 GW of installed capacity in photovoltaic power plants per year, Germany, Great Britain or Belgium gain <1 TW·h. A comparison of columns clearly shows that the Spanish photovoltaic power plants reach the highest utilization ratio of installed capacity, being able to produce almost 3 TW·h of electricity from 1 GW of installed capacity in photovoltaic power plants.

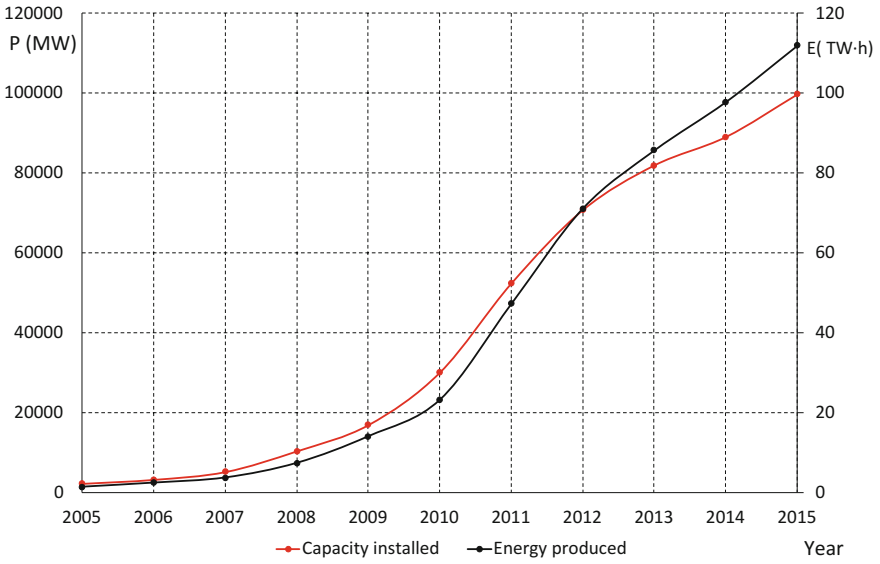

Fig. 1.24 Development of the installed capacity of photovoltaic power plants and their electricity production in the European Union in 2005–2015

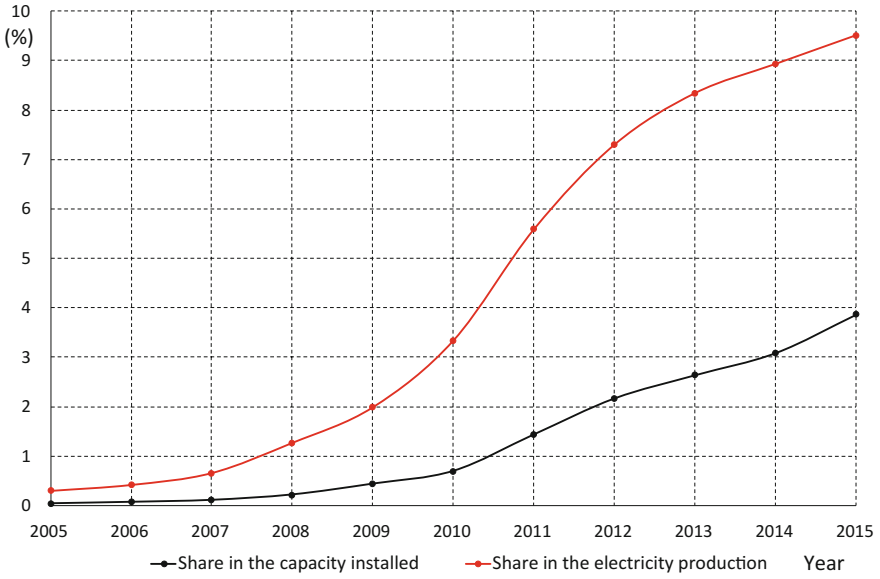

Fig. 1.25 Development of the portion of photovoltaic power plants in the electricity production and the total installed capacity in the European Union in 2005–2015

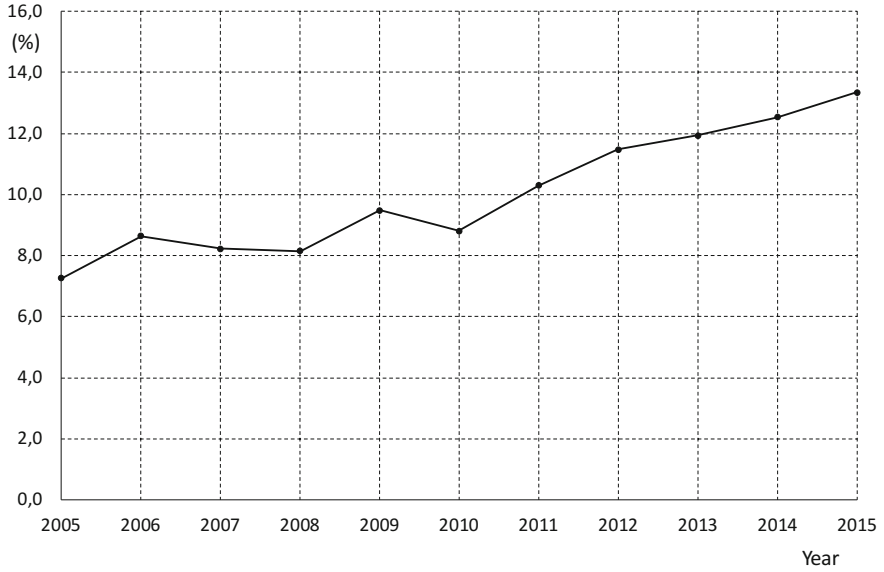

Fig. 1.26 Development of the average utilization ratio of the installed capacity of photovoltaic power plants in the European Union in 2005–2015

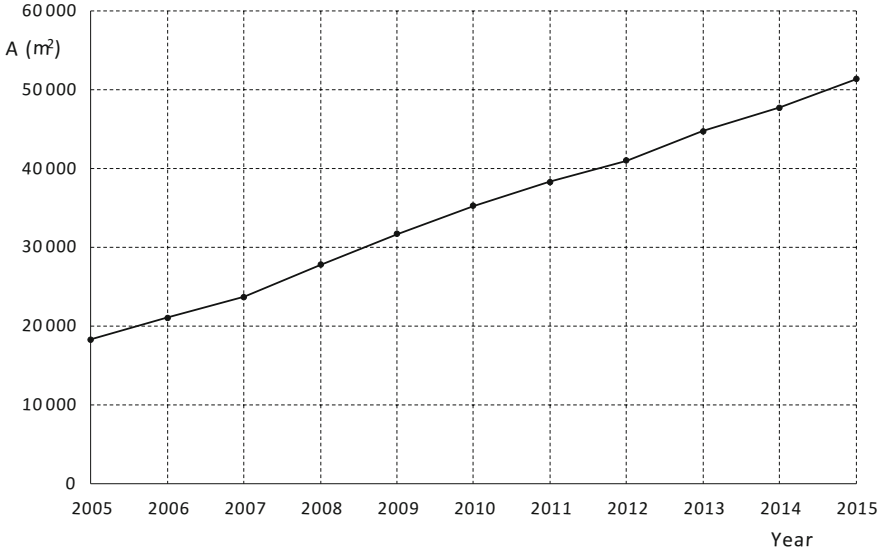

Fig. 1.27 Development of the total area of installed photovoltaic panels in the European Union in 2005–2015

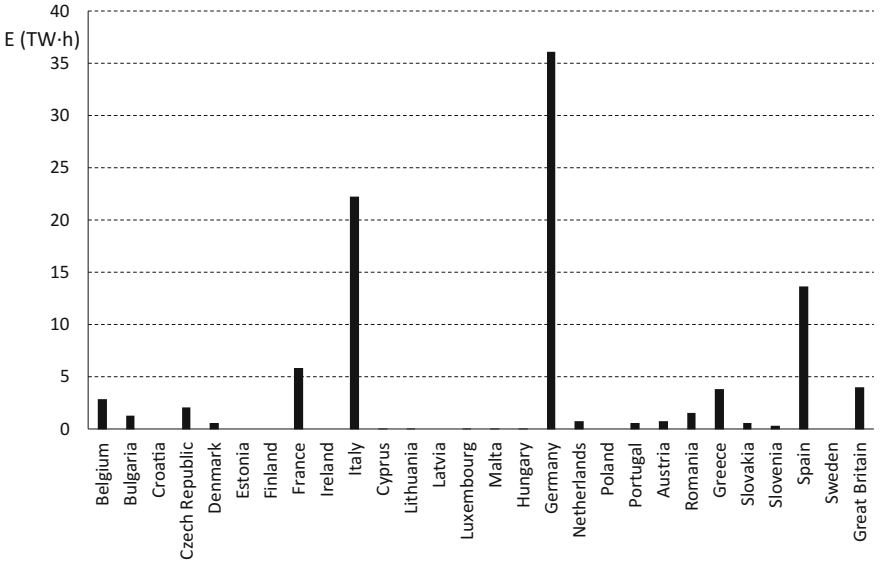

Fig. 1.28 Amount of electricity produced by photovoltaic power plants in the individual EU Member States in 2015

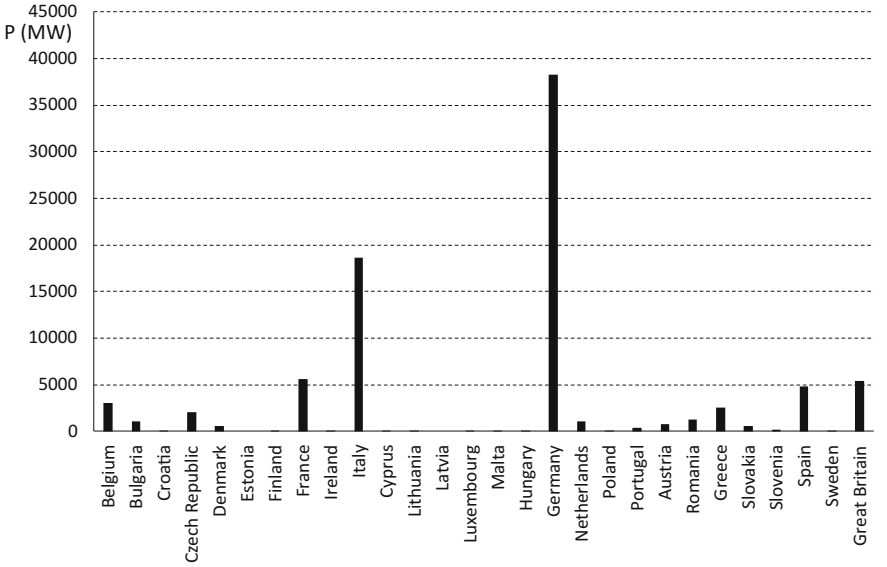

Fig. 1.29 A comparison of the installed capacity of photovoltaic power plants in the individual EU Member States in 2015

1.6 Conditions for Connecting RESs (Wind, Solar)

Conditions for connecting RESs are mainly regulated by acts, decrees and price decisions of the National Energy Regulators (hereinafter referred to only as NER) or other national authorities by the System Operation Code (SOC) with all Annexes. The relevant directive is the Directive of the European Parliament and Council 2001/77/EC of September 27, 2001, on the promotion of electricity produced from RES in the internal electricity market, which came into force on October 27, 2001 [12]. The following rules summarize key terms which need to be considered when connecting the power plants to medium-voltage and low-voltage or 110 kV networks of the Distribution System Operator (hereinafter referred to only as DSO). Therefore, these rules serve equally for the distribution systems operators as well as for producers of electricity and operators of local distribution systems with embedded resources, as a basis for planning and decision aid.

These documents discuss in detail the aspects of the application procedures (e.g., applications for connection, the assessment of the applications for connection, the extent of connectivity study and project documentation), connection of plants to the network, measurements, issues of protection, reverse effects on the network, etc. Unless given the reasons set out in the Energy Act for which the applicant's RES cannot be connected to the transmission or distribution system, the applicant receives a draft agreement on a decision on the plant connection from the operator of distribution system within 30 days or within 60 days, in case of the facility connected to medium or high voltage levels, from the submission of a complete application for connection or connectivity study if the connectivity study was required.

After implementing the plant, wind power plant (WPP) and/or photovoltaic power plant (PPP) in detail, and submitting the necessary documentation (according to the SOC), the DSO permits the test operation of the plant at the producer's request. This operation is time-limited for the purpose of putting the plant into service, performing the necessary measurements and tests. The test operation runs without any installed commercial metering of the supply to the DS.

Implementation procedures for setting up PPPs, WPPs vary depending on whether the owners of PPPs and WPPs use the produced electricity only for their own purposes or are connected to the distribution network. For the second case, it is necessary to summarize the essential steps:

- obtaining an opinion from one of the energy companies, the operator of the distribution system,
- obtaining land-use planning approval, depending on the construction type; in larger constructions, it is necessary to ensure the respective environmental impact assessment (EIA),
- obtaining a license from the NER,
- making contracts with the DSO,
- registration of the participant in the energy market.

In recent years, one of the fastest growing sources of electricity from RESs were PPPs. The increasing number of PPPs implicates an increasing number of problems related not only to their connection but also to the operation of the distribution system when respecting all relevant rules and regulations, and company standards, and DSO guidelines.

Connectivity study is a part of the so-called application procedure at the moment when the capacity of the desired source reaches the limit for a possible request rejection, at which it is necessary to submit specified DSO documents (SOC). The basic document is the so-called application for connection which is submitted to the operator of the distribution system (DSO). With regard to this application, the operator must declare whether it is necessary to verify the connection by a connectivity study or not. Necessity of the study depends on the character of production and the proposed connection point. Requirements for the connectivity study extent are different, even among various DSOs. According to the SOC, the study extent in sources to be connected to low-voltage (LV) and medium-voltage (MV) networks is given by the station with power transformer and the power line containing the recommended connection point determined by the relevant DSO's opinion. If required by the situation, the applicant is obliged to consider other stations and lines in the study, sources already operated or planned. Today, the sources to be connected to voltage levels higher than MV levels must be also assessed in terms of potential overflows to transmission and superior systems.

The connectivity study mainly addresses the voltage changes caused by continuous operation of the plant, the voltage changes during switching, rapid voltage changes (flicker), the contribution to the level of higher harmonic currents and more. Source materials for preparing the study are provided by the DSO to the respective preparer of the study, paid by the applicant. The study must stem from the fact that it is necessary to comply with the agreed power factor at the connection point ($\cos \varphi = 0.95$, inductive to neutral; $\cos \varphi = 0.95$, capacitive to neutral). For smaller sources, such as PPPs with smaller capacity connected to the LV network, the connectivity study is not required.

The power factor is a physical quantity that expresses the ratio of active and apparent electric power. It expresses how much of the apparent power can be converted into useful energy. Low values of the power factor in a circuit mean greater energy losses. Under normal steady state operating conditions at the permissible tolerance range of the nominal voltage, the source power factor shall be at the limit of 0.95 (capacitive) and 0.95 (inductive), assuming that the active power component exceeds 20 % of the rated power of the source. Active power of RES production units must be controllable according to instructions of TSO and DSO to counteract the balance threat or disturbance in the DS and TS. At the same time, the output power in any operating condition and from any operating point must be reducible to a pre-set value specified by the network operator. This pre-set value for the connection point is prescribed by the DSO; it corresponds to the percentage

value related to the connection output of the source. Reduction in the supplied output to the signaled value must be at least 10 % of the connection power per minute, without disconnecting the facility from the network.

Figure 1.30 presents example of PPP and WPP operating states. Most often, WPPs and PPPs work in the third generator operating state. The third operating state means the supply of active and reactive energy into the network (capacitive power factor). In this operating condition, the PPP supplies the majority of electricity to the network. Another operating state is the second operating state with inductive power factor (the supply of active energy with inductive power factor). Under this condition, the PPP supplies energy with power factor of 0.95 to neutral.

Figure 1.31 shows the amount of electricity supplied by the PPP with rated capacity of 2 MWp. The PPP capacity (output) is brought to 22 kV network. During 1 year of operation, the PPP supplied 1295 MW h of electricity to the network. The PPP supplied the largest percentage of energy (57 %) with capacitive power factor of 0.95–0.99 (the supply of reactive power to the network), 42 % of electricity with neutral power factor and 1 % of electricity outside the specified limit of the power factor, i.e., under 0.95. The PPP operation fulfilled the conditions set out in the SOC, because 1 % of the energy was supplied outside the set limit but the active output component did not exceed 20 % of the source rated power [13].

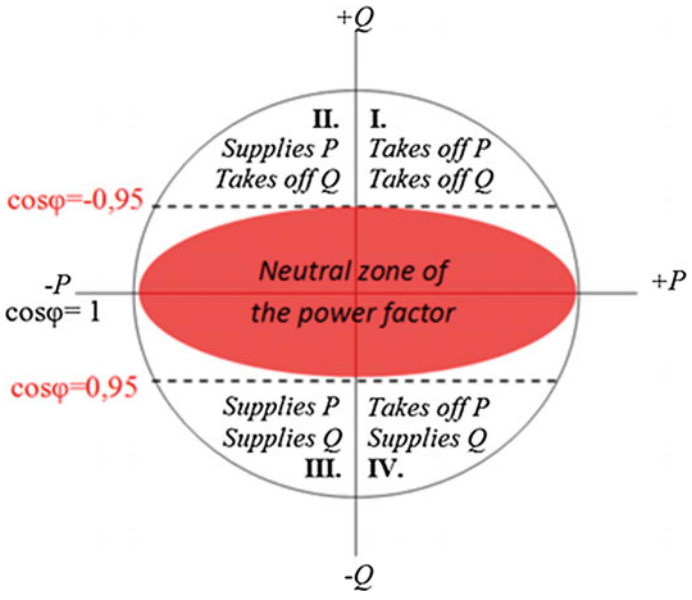

Fig. 1.30 PPP and WPP operating states (take-off Q-capacitive power factor, supply Q-inductive power factor

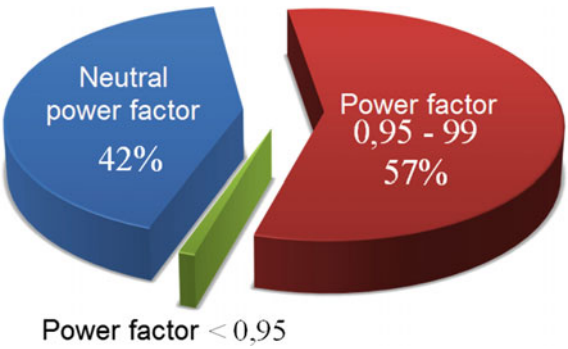

Fig. 1.31 Quality of electricity supplied by the PPP with rated capacity of 2 MWp

1.6.1 Voltage Increase

Voltage changes in the distribution network are due to changes in the flows of outputs of the connected sources or loads. A voltage change in one node influences voltage changes in other network nodes. Recently in practice, it is assumed that number of decentralized sources in MV and LV networks will be increased. In these networks, it is usually difficult to keep voltage changes in required limit. According to the SOC, the voltage increase caused by the operation of connected plants, in the worst-case scenario in the connection point, must not exceed Δu_{MV}, $110 \leq 2$ % and $\Delta u_{\mathrm{LV}} \leq 3$ % compared to the voltage without their connections. The limit value refers to the effective value of the operating voltage at the plant connection point. The voltage level must be assessed with regard to the magnitude of the voltage actual value at the connection point. When assessing the connectivity of plants in terms of voltage increase, we consider neutral power factor at the connection point to the DS unless provided otherwise by the DSO because of local conditions (balance of reactive energy, network voltage). Adherence to the prescribed condition prevents the introduction of significant voltage deviations in the network and thus helps to control and stabilize voltage at all points of the network.

For assessing the connectivity of PPPs and WPPs into the DS, the operator of the electricity supply system has a variety of simulation tools. Calculations of the steady state of the electrical network commonly involve many supportive and computational software tools which provide the user with relatively high user comfort and allow the user to easily calculate the steady state even of relatively large electrical networks. These sophisticated simulation programs allow the user to build integrated networks in accordance with all relevant parameters describing the network operation in the steady state. These computational tools also allow the calculation of parameters (e.g., voltage changes at the connection point, output overflows to higher voltage levels, the calculation of short-circuit conditions) affecting the operation and stability of the given network due to the dynamic variability of PPP and WPP operations [14].

Figure 1.32, using measured data, shows the voltage changes at the connection point during 1 day with variable cloudiness, in the PPP with installed capacity of

70 kWp. This PPP is connected at the end of a radial network with a nominal line-to-line voltage of 400 V AC and external grid with a rated voltage of 22 kV AC.

The given limit of 3 % for voltage increase at the PPP connection point to the DS is exceeded at 8:45, at 27 % PPP output and 33 % network load. Excess of the limit lasts until 17:40, whereas the maximum change occurs at 93 % PPP output and 60 % network load. Figure 1.33 clearly shows the voltage change in the network before and after the PPP connection.

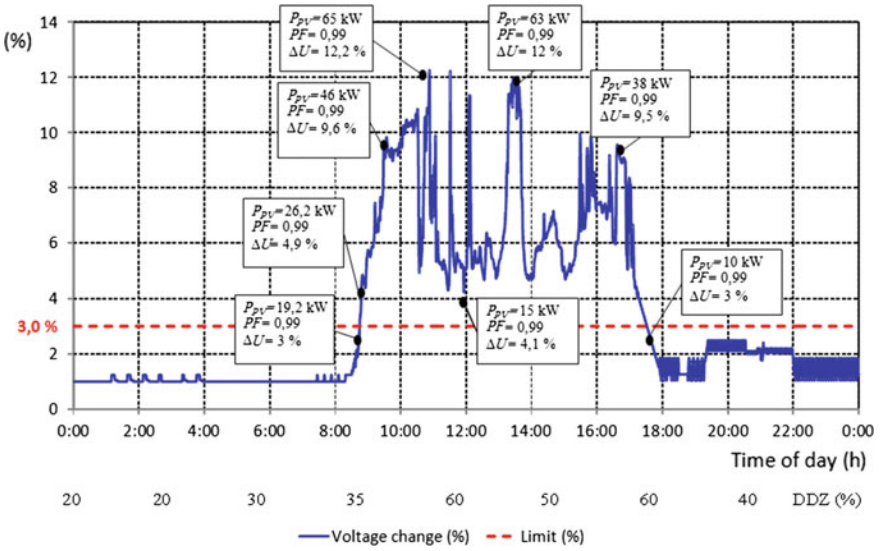

Fig. 1.32 Voltage changes at the PPP connection point

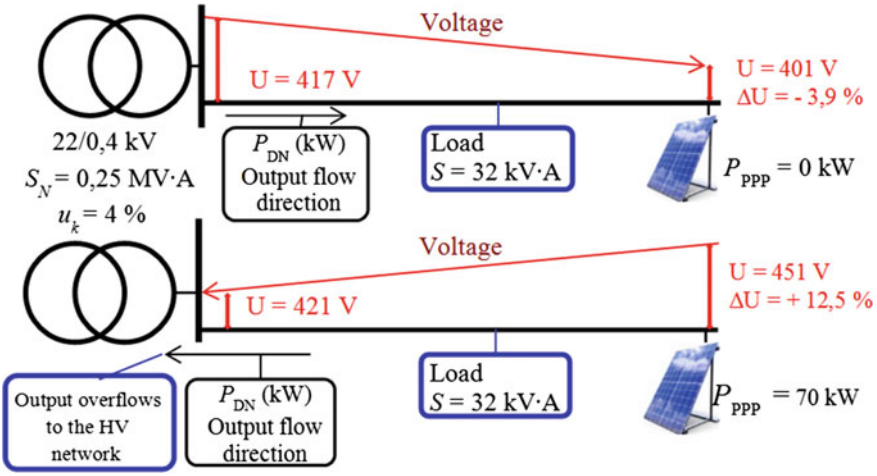

Fig. 1.33 Voltage change at the connection point before and after the PPP connection

The most important reverse effects on the network caused by the operation of PPPs include fast voltage changes due to switching, load changes and changes in the supplied power. According to the SOC, the rapid voltage changes must not exceed ±10 % of the rated voltage under normal operating conditions. Voltage fluctuation is defined as a series of changes in the voltage effective value. The subsequent effect of voltage changes is associated with interference (e.g., flicker). Figure 1.34 shows an example of rapid voltage change in the LV network at the connection point of a PPP with rated capacity of 70 kWp. Due to the large output supplied by the PPP to the network, the rapid voltage changes exceed ±10 % of the rated voltage in all three phases of the LV network.

There are several possible solutions to limit the voltage change at the PPP connection point. In some cases, one of the best but economically expensive solutions is to increase the network short-circuit power, i.e., the source transformer, in this case. In the network containing the analyzed PPP with such great output, we can often suppose with the following situation: the PPP performs the function of source for the given network arm instead of 22/0.4 kV transformer, which leads to output overflow to higher voltage levels and changes in the network short-circuit power. Another option is to reduce the PPP-supplied output to the DS using accumulation. The accumulation serves for capturing short-term power peaks during low production output and, vice versa, for covering output declines during normal supply, e.g., in the case of cloudiness over the PPP.

1.6.2 Voltage Changes Due to Switching

The condition for stabilizing the network voltage is the voltage change in the connection point induced by connecting or disconnecting the plant or during

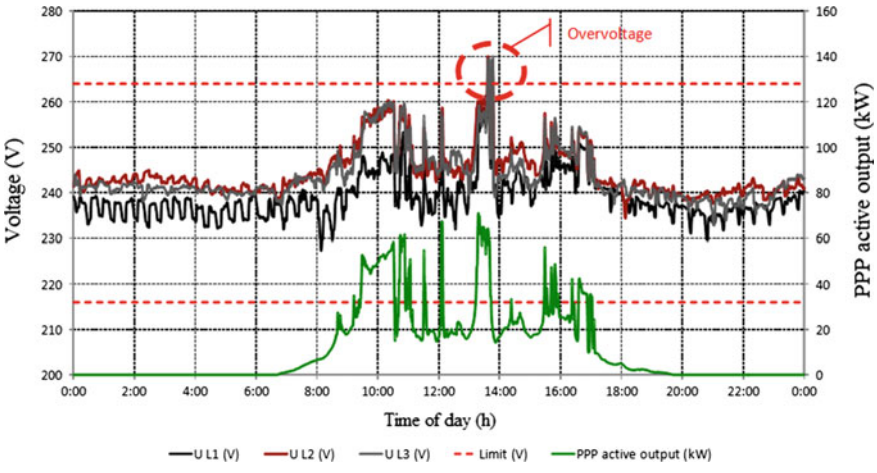

Fig. 1.34 Rapid voltage changes at the connection point caused by the PPP operation

intermittent loads ($\Delta u_{\max MV} \leq 2$ %, $\Delta u_{\max LV} \leq 3$ %). These limit values are valid provided that the switching frequency of the production unit is less than once per 90 s. With very little switching frequency and when it is allowed by the network conditions, the operator of the distribution system may tolerate switching with larger voltage changes. For the plants in 110 kV network and for limiting the voltage changes, ($\Delta u_{\max 110} \leq 0.5$ %) applies to switching one production unit under normal operating conditions, and ($\Delta u_{\max 110} \leq 2$ %) applies to switching a larger number of production units, such as a wind park. ($\Delta u_{\max 110} \leq 5$ %) applies to fault operating conditions.

A special "switching factor dependent on the network" applies to WPPs. This factor must be proven by the manufacturer; it is used to evaluate WPP switching and also respects the ultra-short transient phenomena. This factor respects not only the amount but also the waveform of the current during transients and is expressed as a function of the angle of the network impedance for each device in the test report. WPPs with asynchronous generators connected with approximately synchronous speed may cause very brief voltage drops due to their internal transients. Such a decline may reach a double of otherwise admissible value. With a view to minimize the voltage changes in the network during switching, it is necessary to prevent simultaneous switching of multiple generators in one connection point. The technical solution consists in time grading of the individual switching operations, depending on the induced voltage changes.

According to the SOC, the step voltage changes caused by PPP/WPP connecting and disconnecting, can be determined using the following simplified calculation.

$$\Delta u_{\max} = ki_{\max} \cdot \frac{S_{nE}}{S''_{kV}} \tag{1.1}$$

S_{nE} is the apparent output of the RES, S''_{kV} is the short-circuit output at the RES connection point, $ki_{\max}$ is the factor of the highest switching pulse—according to the SOC, it is equal to 1 PPP inverters; a special "switching factor dependent on the network" applies to wind power plants, which must be proven by the manufacturer, is used to evaluate WPP switching and also respects the ultra-short transients.

1.6.3 Connection of Plants with Inverters or Frequency Convertors

In plants with inverters, or frequency convertors, it is necessary to keep switching conditions applicable for synchronous generators. i.e., it is necessary to use a synchronization device which must meet the following conditions for synchronization:

- Voltage difference $\Delta U < \pm 10$ % U_N.
- Frequency difference $\Delta f < \pm 0.5$ Hz.
- Phase difference $<\pm 10°$.

Depending on the ratio of the network impedance to the generator output, it may be necessary to provide narrower switching limits to prevent unacceptable reverse effects on the network.

Figure 1.35 shows the time course of connecting the inverter of a small photovoltaic power plant (4 kW) to the network. For a better idea, the *y*-axis on the figure above is given in relative units. The process of synchronizing the inverter with the network can be divided into several sections. During the time until 37 s, the inverter occurs in the so-called stand-by mode. At the time of 38 s, we observe a transient phenomenon caused by relay contact which allows the inverter to start initialization with sufficient voltage on the DC side. At the time from 38 s till 47 s, the inverter parameters are synchronized with the network parameters. At the time of 48 s, the inverter starts to supply electricity to the network, whereas a visible growth in power supply is seen at the time of about 70 s. This phenomenon is caused by finding the so-called maximum power point tracking (MPPT) point which expresses the ideal relationship between voltage and current on the PPP DC side and ensures maximum efficiency of the systems.

Figure 1.36 illustrates the same process as in the previous case, but for a WPP. It is a small WPP with a synchronous generator with permanent magnets and installed capacity of 12 kW, whose power is led to the DS via inverters for WPPs. To the *y*-axis, the same rule applies as in the previous case. The stand-by mode is characterized by a higher take-off than in the case of PPP inverter, which is caused by a higher amount of semiconductor technology within the inverter itself. The second part of synchronizing the inverter with the network is more time-consuming, also because the inverter initialization begins to occur from a certain voltage value in the

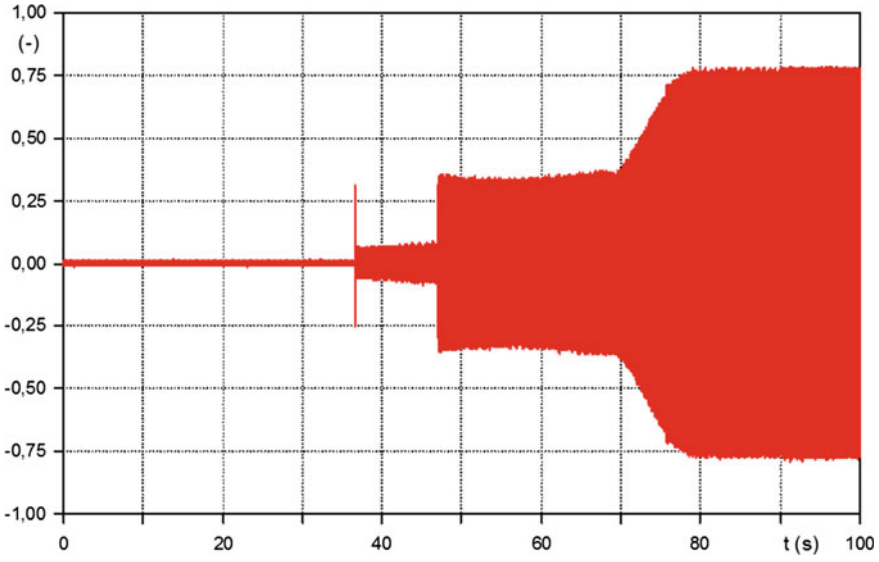

Fig. 1.35 Synchronizing of the PPP inverter with the network

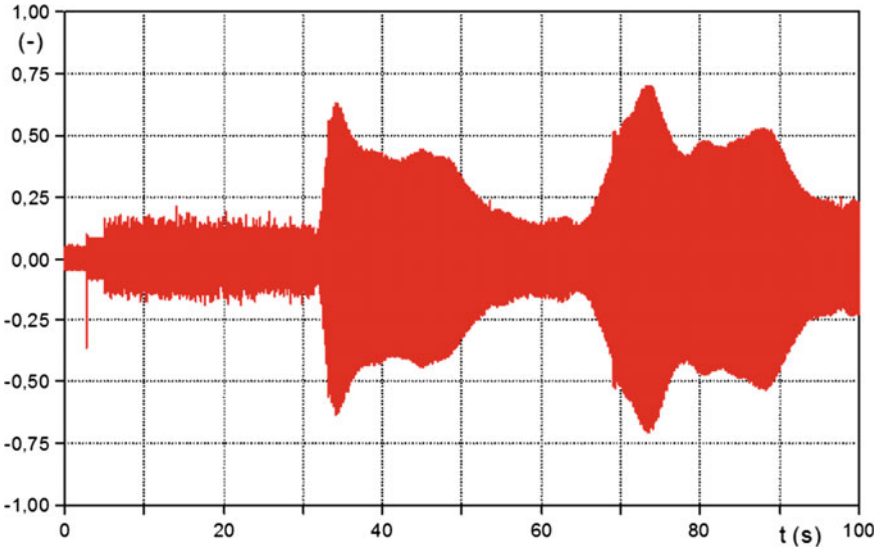

Fig. 1.36 Synchronizing of the WPP inverter with the network

DC bus of the WPP, which changes dynamically. After finishing the synchronization of the WPP inverter with the network, at the time of 37 s, we observe a very sharp increase in the supplied power which consists of mass inertia of the unloaded turbine of the WPP. This is followed by a course of active power supply, depending on wind speed and direction.

1.6.4 Special Requirements for the Plants with RESs

Special requirements for the plants with RESs with a capacity above 15 MW are based on the German VDN Transmission Code 2007 [15] which deals with conditions for the continued operation of sources connected to 110 kV networks and networks with higher voltage during network breakdowns beyond their own internal network.

The aim of these requirements is not only to avoid outages of the sources during voltage drops but rather support the voltage in a certain way as it is in the case of conventional synchronous generators. Another aim is to respond to frequency increases by reducing the supplied active power before their disconnection due to over-frequency.

Determination of the Rated Power

In this sense, the rated output power of the plant is determined by the sum of individual production units in one network connection point. Accordingly, e.g., in WPPs, the installed capacity of the entire park is considered as the rated power

(eventually, this summarization must be applied to galvanic-separately operated groups of 110 kV networks).

Active Power Supply

Active power of production units with RES must be controllable according to instructions of the operator of the transmission and distribution network to counteract the balance threats or disturbances in the system. Simultaneously, the power output in any operating condition and from any operating point must be reducible to the maximum power value (setpoint) specified by the network operator. This value for the connection point corresponds to the percentage value related to the source connection output. Reduction in the supplied output to the requested value must be at least 10 % of the connection output per minute, without disconnecting the facility from the network. Under working arrangements at a frequency higher than 50.2 Hz, all plants with RES must reduce the instantaneous active power with a gradient of 40 %/Hz from the currently available output of the generator—see Fig. 1.26.

The power reduction can be determined according to the following relationship:

$$\Delta P = 20\, P_m \frac{50.2 - f_s}{50} \tag{1.2}$$

ΔP is the required active power reduction; P_m is the instantaneous available power; f_s is the network frequency. No limitation is necessary in the range $47.5 < f_s < 50.2$; however, sources must be disconnected from the network when $f_s < 47.5$ and $f_s \geq 51.5$ Hz.

After the frequency returns to a value ≤ 50.05 Hz, the active power may grow again if the actual frequency does not exceed 50.2 Hz. Dead band must be <10 MHz. Currently, a conceptual design of resynchronization with the network is being prepared for WPPs which are disconnected from the network due to over-frequency (Fig. 1.37).

Reactive Power Supply

In the exchange of reactive power, all plants with RES must behave as follows:

Within a few minutes, the supply of reactive power must correspond to the value specified by the network operator.

Operating point for exchanging reactive power in steady state is determined by the requirements of the network.

The setting can be given:

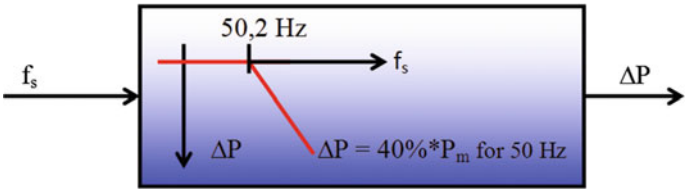

Fig. 1.37 Graphic representation of the reduction in the active power at the frequency

- by an agreed value or the course
- by a characteristic depending on the operating point of the plant
- online by entering the required value.

If the required value is entered online, the transition to the new operating point for exchanging reactive power at the connection point must occur no later than within 1 min.

Behavior in the Case of Faults in the Network

In the case of automated RESs in the network of the DS operator, the operators of such sources must take measures to prevent damage to their own production facilities, and must be able to safely detect and cope with a possible unit off-grid operation, although voltage and frequency does not exceed/decrease under the defined permissible limits.

Besides system functions such as under-voltage and overvoltage, under-frequency and over-frequency, which are already capable to recognize the off-grid operation (autonomous mode without connection of power plant to the external grid) in most cases, it is required that the auxiliary switch contacts on the side of lower or higher voltage of the network transformer give signal for output limitation and shutdown of all individual generators of the plant so that the off-grid operation is ended at least within 3 s. Also other ways of detecting the off-grid operation are allowed provided that they do not cause excessive activity in systematic faults. The issue of behavior in the case of faults is discussed in detail in SOC.

The issue of quality of electricity supplied by RES is also described in detail in the SOC.

References

1. Nalezeno.cz (2016) Fuels dictionary. http://www.nazeleno.cz/fosilni-paliva.dic. Accessed 15 Mar 2016
2. Hadjsaïd N, Sabonnadière J-C (2012) SmartGrids. Wiley, New Jersey
3. European Commission (2010) Energy 2020: a strategy for competitive, sustainable and secure energy. http://eur-lex.europa.eu/legal-content/EN/TXT/PDF/?uri=CELEX:52010DC0639&from=EN. Accessed 21 Apr 2016
4. Eurostat (2016) Energy statistics. http://ec.europa.eu/eurostat/web/energy/data/main-tables. Accessed 5 May 2016
5. European Commission (2006) European energy and transport, scenarios on energy efficiency and renewables. https://ec.europa.eu/energy/sites/ener/files/documents/ee_and_res_scenarios.pdf. Accessed 8 May 2016
6. European Commission (2015) EU energy in figures, statistical pocketbook 2015. https://ec.europa.eu/energy/sites/ener/files/documents/PocketBook_ENERGY_2015%20PDF%20final.pdf. Accessed 17 May 2016
7. European Commission (2014) EU energy markets in 2014. https://ec.europa.eu/energy/sites/ener/files/documents/2014_energy_market_en_0.pdf. Accessed 21 May 2016
8. Federal Ministry for the Environment, Nature Conservation, Building and Nuclear Safety (2015) German climate action plan 2050. http://www.bmub.bund.de/fileadmin/Daten_BMU/

Download_PDF/Klimaschutz/klimaschutzplan_2050_impulspapier_en_bf.pdf. Accessed 25 May 2016
9. British Department of Energy and Climate Change (2016) https://www.gov.uk/government/organisations/department-of-energy-climate-change. Accessed 30 May 2016
10. Neart na Gaoithe Offshore Wind Farm (2016) http://www.neartnagaoithe.com/. Accessed 15 May 2016
11. Hornsea Project One (2016) http://www.hornseaprojectone.co.uk/en. Accessed 16 May 2016
12. Directive 2001/77/EC of the European Parliament and of the Council of 27 September 2001 on the promotion of electricity produced from renewable energy sources in the internal electricity market (2001) http://eur-lex.europa.eu/legal-content/EN/TXT/PDF/?uri=CELEX:32001L0077&from=CS. Accessed 17 Mar 2016
13. Requirements for the connection of micro-generators in parallel with public low-voltage distribution networks (2007) EN 50438:2007
14. Vramba J, Stuchly J, Kosmak J (2013) Verification of simulation software for the stable operation of distribution network with photovoltaic power plant. Paper presented at 14th international scientific conference on electric power engineering, VSB—Technical University of Ostrava, Kouty nad Desnou 28. Accessed 30 May 2013
15. Verband der Netzbetreiber—VDN—e.V. beim VDEW (2007) TransmissionCode 2007. https://www.vde.com/de/fnn/dokumente/documents/transmissioncode%202007_engl.pdf. Accessed 24 Feb 2016

Chapter 2
Systems and Equipment of Wind Power Plants

As already mentioned in the previous chapter, wind power plants can be classified according to various aspects and criteria. One of the criteria, for example, is the design of the wind turbine according to which the wind power plants can be divided into plants with horizontal or vertical axis of rotation. Another aspect can be the method of swivelling the wind turbine or blades—accordingly, the wind power plants are divided into active or passive pitch control. However, more often we meet with the division of wind turbines according to their capacity of the wind power plant generator because this capacity subsequently determines the type of generator, actual adaptation of the wind power plant control system and power flow, including current type and the respective voltage levels to which the wind power plant output is brought. According to this major capacity viewpoint, the community dealing with the operation of wind power plants currently divides them as follows:

- micro wind power plants (up to 1 kV·A),
- small wind power plants (about 1–30 kV·A),
- medium wind power plants (30–300 kV·A),
- large wind power plants (300 kV·A and above).

Of course, the mentioned output power levels are just indicative and their determination is very subjective; nevertheless, if we perform a search of the currently operated wind power plants in the EU, we would come to a similar division. Capacity values are deliberately expressed in units of apparent output power, with regard to the possible regulation of active as well as reactive power using appropriate types of generators and modern control systems.

The following chapters will analyse the operating states of individual representatives of the output power levels of wind power plants using the results from long-term experimental measurements carried out by the expert group at the VSB-Technical University of Ostrava.

S. Misak and L. Prokop, *Operation Characteristics of Renewable Energy Sources*,
Green Energy and Technology, DOI 10.1007/978-3-319-43412-4_2

2.1 Micro and Small Wind Power Plants

According to the generated output power, the micro and small wind power plants are defined among small power sources scattered in different locations. When thinking of the implementation of such plants, it is necessary to consider the economic and technical aspects. Electric energy generated in this way can be consumed by the producer alone—e.g., for lighting, heating of buildings, for water heating. Regarding larger installations, it is also possible to supply the produced electricity into the public supply external grid on the basis of a contract with the distribution company. The use of small wind power plant is preferred for power generation in areas without electrical connection from the distribution external grid (e.g., recreational facilities). In most cases, the small wind power plants are designed with the passive swivelling system which is realized in the form of a wind rudder, and with the horizontal rotation axis of the wind turbine and the height of the mast for placing the wind turbine up to about 10 m above the ground (Fig. 2.1).

Energy of the wind flow is transferred from the shaft of the wind turbine to the shaft of the generator using a gear unit with fixed conversion ratio (Fig. 2.2). In older types of small wind power plants, the electrical output is subsequently brought from the plant nacelle through a current-collection gear and ring head. In more modern small power plants, the electrical output is brought out directly through a cable line with electronic anti-twist control.

Fig. 2.1 Example of low low-capacity wind power plant

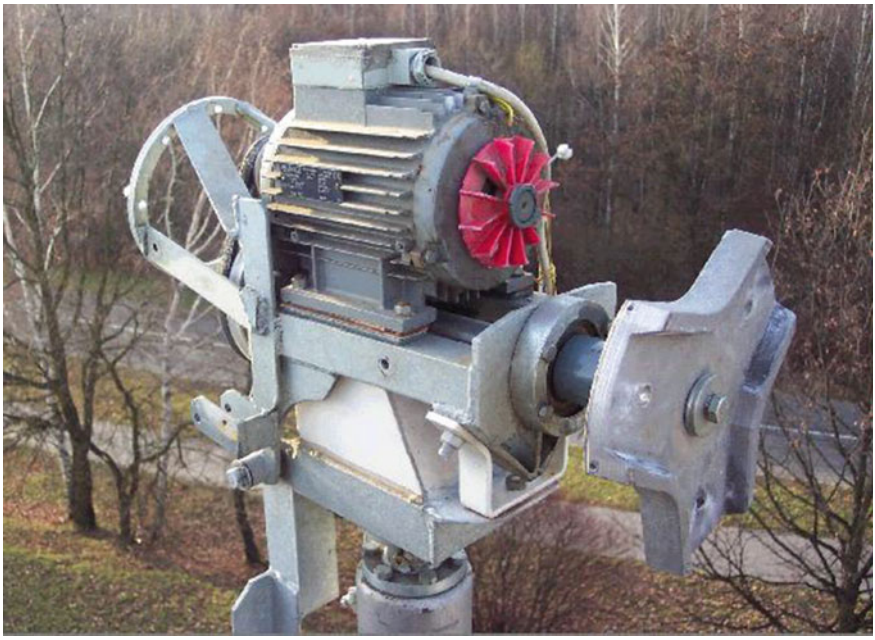

Fig. 2.2 A detail of the generator and gear mechanism placement

The control systems are relatively simple and can be divided by the type of operating the small wind power plant into the system for a autonomous mode (off-grid mode) without connection to the external grid and system for parallel generator cooperation with the external grid into which the generator output is brought. In the first case, the generator output power is directly brought into the load or is converted using the conversion elements to the desired voltage level, type of voltage and current (AC or DC), whereas the load may be constituted by general impedance, or the energy from the wind power plant can be directly accumulated in a storage facility. The control system thus only monitors the voltage limits for the connected load and overload current limits. The autonomous mode small wind power plants will be discussed in the following subchapters. In the second case, when the generator output is brought out to the distribution external grid, the control system mostly monitors the generator speed (n in Fig. 2.3) and provides connection of the generator with oversynchronous speed, reduces the current surge at the moment of connection, and switches the compensation device for compensating the power factor (C in Fig. 2.3) at the connection point. In modern small power plants, the wind speed is also measured and the plant is electronically or mechanically braked when the wind speed exceeds the limit at which the wind turbine could be mechanically damaged (v in Fig. 2.3).

In these plants, it is possible to use asynchronous or synchronous generators, less often dynamos as well as synchronous generators with permanent magnets (in

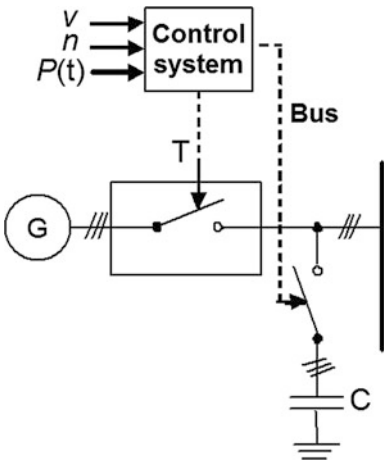

Fig. 2.3 Control system of low-capacity wind power plant

recent years). Static frequency converter is usually inserted between the asynchronous or synchronous generator and the external grid in order to better use wind energy. In such a system, the voltage is first rectified and then adjusted to the desired frequency. With regard to the simple design and the resulting operational reliability, the low-capacity power wind power plants commonly use induction machines.

From the design point of view, there is no difference between the induction motor and the induction generator; it is therefore normal that wind power plants (WPPs) are equipped with serially produced induction motors operating in generator mode. Installed wind power plants equipped with mass-produced induction motors reach low values of power factor; at rated power, the machine is therefore highly current-overloaded.

The following chapter presents an analysis of this operating state. The analysis is based on changes in electric power flow, i.e., the replacement of the motor electrical input and mechanical output by the mechanical input and electrical output of the generator.

Induction motor output P_{OUT} is the mechanical output P_{H} on the machine shaft according to the following relation (2.1).

$$P_{\mathrm{H}} = \omega \cdot M = \frac{\pi \cdot n \cdot M}{30} \tag{2.1}$$

where P_{H} is the mechanical output of the motor, ω is the angular velocity of the shaft and M is the torque on the shaft. Motor input is given by the electrical input P_{EL} on machine terminals according to the following relation (2.2)

$$P_{\mathrm{EL}} = 3 \cdot U \cdot I \cdot \cos \varphi \tag{2.2}$$

where P_{EL} is the motor input, U is the voltage, I is the current and cos φ is the power factor. Machine losses P_Z are given by the difference between the machine input P_{INP} and output P_{OUT} according to the relation below (2.3).

$$P_Z = P_{\mathrm{INP}} - P_{\mathrm{OUT}} \tag{2.3}$$

Total losses in the machine are not concentrated but unevenly distributed across individual parts, such as electrical losses in the winding, magnetic losses in iron, losses due to magnetic leakage, mechanical losses in the bearings, windage losses, etc.

The output of induction generator P_{OUT} means the electrical output P_{EL} on the machine terminals according to relation (2.2); the input P_{INP} means the mechanical output P_{H} according to relation (2.1). This change in the energy flow changes the way of recovering losses as well as their value. The change in the power flow is also reflected in the change of replacement machine diagram. Figure 2.4 shows an equivalent diagram of (a) the induction motor and (b) the induction generator. A fundamental change is reflected in the magnitude of the inner induced voltage U_i.

For induction motors, the magnitude of induced voltage is calculated according to the formula (2.4):

$$U_i = U_1 - Z_1 \cdot I_1 \tag{2.4}$$

and the induced voltage of the generator is calculated according to the following formula:

$$U_i = U_1 + Z_1 \cdot I_1 \tag{2.5}$$

where U_1 is the machine terminal voltage and $Z_1 I_1$ is the voltage drop across the stator winding. Therefore, if we operate the induction generator at the identical terminal voltage as the induction motor, then the magnitude of the internal induced voltage of the machine is greater by the double of the voltage drop across the stator winding. This is particularly reflected in the increased magnetic flux of the machine, higher induction in the air gap, the increase in total losses and, therefore, in the

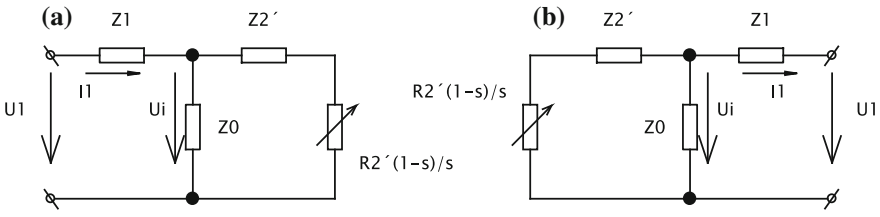

Fig. 2.4 Equivalent diagram of **a** the induction motor, **b** the induction generator

danger of overheating and reduced machine power factor. Reduced power factor of the machine leads to lower quality of the supplied electricity and the increased losses mean lower maximum machine utilization. A machine operated in this way is able to supply 50–70 % of the rated power to the external grid.

In practice, it is much better to use an induction machine designed for a higher voltage than the rated voltage of the external grid to which the generator is connected, or at least use a machine designed for D-connection operation in Y-connection operation.

To operate an induction machine as a generator, at least the following conditions must be satisfied:

- its speed must be oversynchronous,
- a source of reactive power must be at disposal.

Depending on operating conditions, the source of inductive reactive power may be, for example, a capacitor battery in case of independently working induction generator, or the generator can take inductive reactive power from the external grid into which the active power of the generator is supplied.

The generator reactive power can be determined from the following relation:

$$Q = m_1 X_{1\sigma} I_1^2 + m_1 U_i I_0 \cos \partial + m_1 U_i I_2 \sin \psi_2 \tag{2.6}$$

containing the following reactive inputs:

$m_1 X_{1\sigma} I_1^2$ on the stray magnetic field of the stator
$m_1 U_1 I_0 \cos \partial$ on magnetizing the magnetic circuit of the machine
$m_1 U_1 I_2 \sin \psi_2$ on the stray field of the rotor.

The minimum capacitance value of the capacitor battery can be determined from no-load (no-load) measurements. Because the power factor of no-load machine achieves very low values and high-output rolled capacitors are produced with tolerances ±20 %, the no-load current can be regarded as magnetizing. Then, the entire measurement can be simplified. The induction machine is connected to the external grid and the monitored variable is only the no-load current. The machine must be disconnected from the drive. Furthermore, this is based on the assumption of equality of the machine reactance and equality of the capacitor battery reactance.

$$x_C = x_L \tag{2.7}$$

According to the above described simplification, the current I_0 can be considered as magnetizing; therefore, the magnitude of the required capacitive reactance will be:

$$x_C = \frac{U_{1f}}{I_0} \tag{2.8}$$

where U_{1f} is the phase voltage of the generator; the value of the capacitance sought then will be

$$C = \frac{1}{2 \cdot \pi \cdot f \cdot X_C} \tag{2.9}$$

If a capacitor battery with this capacitance is connected to the generator, then the terminal voltage at speeds approaching synchronous speed (no-load speed) will be U_{1f}, at frequency f.

2.1.1 Start of the Excited Generator

If the capacitor battery is connected to the generator, then the voltage increases proportionally to the speed, as evident from the measured excitation characteristic of low-output generator in Fig. 2.5.

After starting up the generator (at low speeds), a voltage caused by remanent magnetism appears at the terminals. This remanent voltage varies in the range of 5–10 % of nominal voltage. The speed increases and a step voltage change is observed at a certain speed value (breakthrough speed—see Fig. 2.5). This voltage becomes stabilized at value U_0. Voltage U_0 and excitation speed are given by capacitance of the capacitors and reactances of the machine. Figure 2.5 shows the voltage magnitude depending on the machine speed whereas the parameter is the capacitance of the capacitor battery. The current flowing through the capacitors and the stator winding of the machine is shifted behind voltage by 90°; therefore, it is a reactive current ensuring the formation of the machine magnetic field.

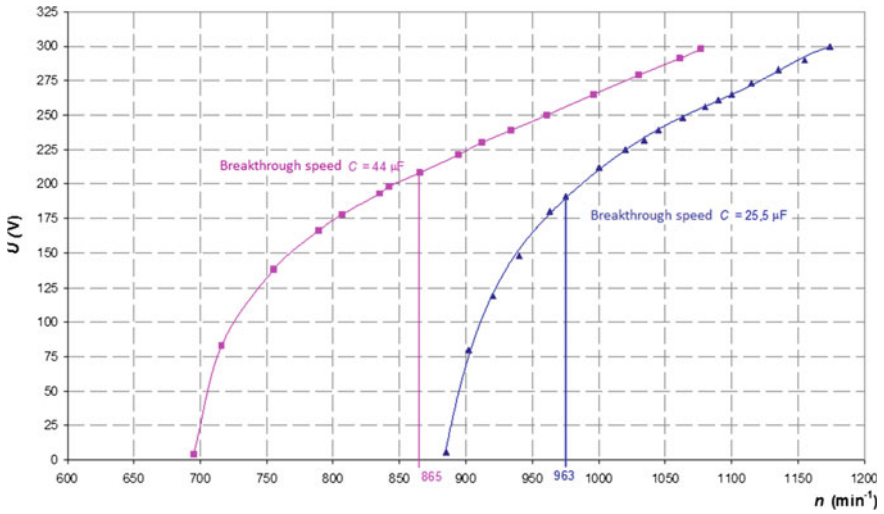

Fig. 2.5 Exciting characteristic of induction generator; C = 25 µF (*blue*), C = 44 µF (*pink*) (color figure online)

Excited generator is loaded by no-load losses and losses in the capacitors. This load causes a slip (we measured about 2 % at a 6 poles machine with output of 1.1 kW; this means that the generator frequency for the calculated capacitance of the capacitor battery was 50 Hz at 1020 min^{-1})—at this speed, therefore, the excited voltage corresponds to the external grid rated voltage.

2.1.2 *Connecting of the Induction Generator to the Distribution External Grid*

In the case of differences between instantaneous values of voltage, frequency and phase shift of the external grid and the generator, the actual connection to the external grid is accompanied by a current surge with magnitude being 10 times greater than the rated current and an overvoltage peak of large steepness and amplitude (see Fig. 2.6).

This current surge can be reduced by connecting the induction generator to the external grid via resistors connected in series to the generator winding. After a defined time delay, these resistors are bypassed. In this case, therefore, there are two smaller current surges. It has been measured that amplitudes of these current surges are less than half of the rated current if the resistance values are optimal.

Connection of the induction generator to the external grid through resistors is shown in Fig. 2.7. The optimal resistance value for the induction generator (P_n = 1.1 kW, U_n = 400 V, I_n = 3 A, cos φ = 0.75, 6p) was determined by

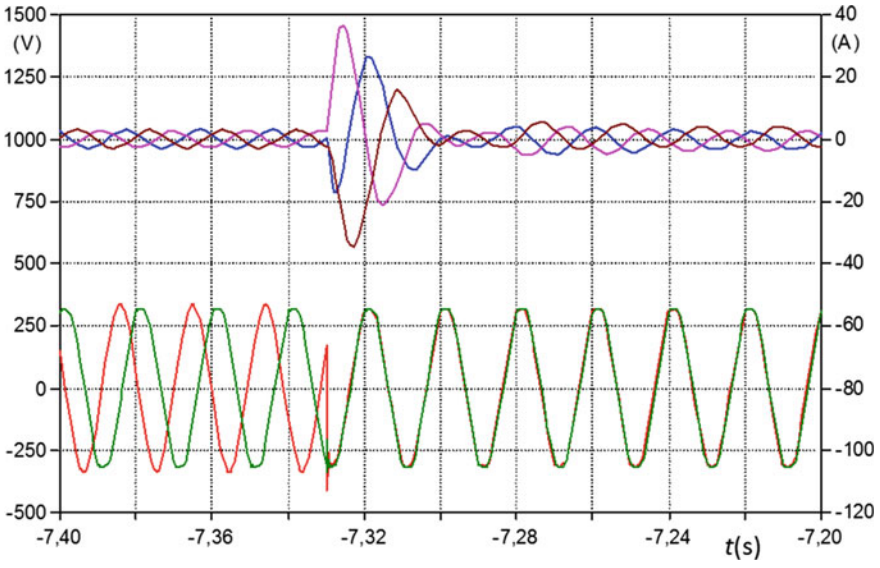

Fig. 2.6 Voltage curve when connecting the induction generator to the external grid. Generator voltage U_g (*red*) (V), external grid voltage U_s (*green*) (V), phase currents I_1 (*blue*), I_2 (*pink*), I_3 (*brown*) (A) (color figure online)

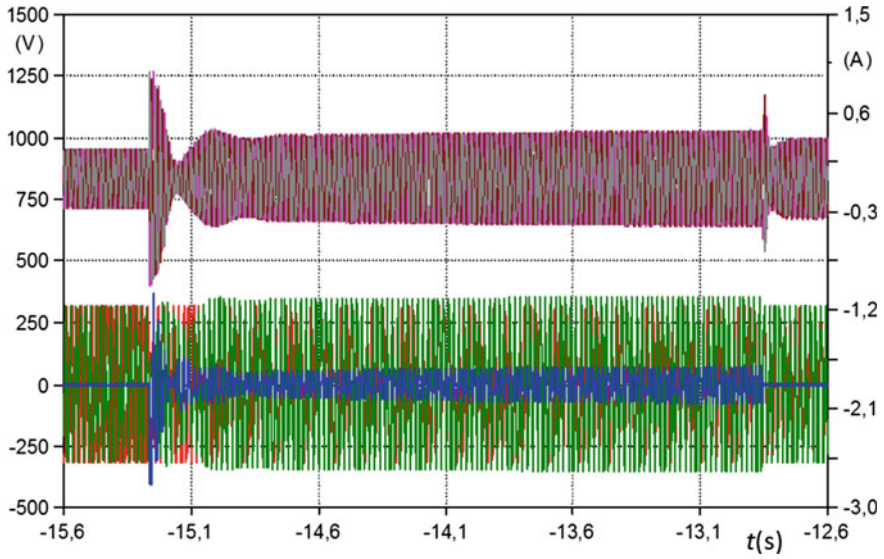

Fig. 2.7 Connecting the induction generator to the external grid in an optimal way—via 50 Ω resistors. External grid voltage U_s (*red*) (V), generator voltage U_g (*green*) (V), voltage across the resistor U_r (V), phase currents I_1 (*blue*), I_2 (*pink*), I_3 (*brown*) (A) (color figure online)

measurements as 50 Ω at a speed of 1022 min^{-1} [1–3]. Before connection, magnetizing current from the capacitor battery flows through the winding. The connection was carried out at the moment when the generator voltage was in phase opposition with regard to the external grid voltage. The connection to the external grid via resistors resulted in a current surge whose magnitude was 0.23-multiple of the machine rated current. Generator voltage was phase-delayed behind the external grid voltage. After about 2 s, the resistors were bypassed and the voltage across them dropped to zero. Generator voltage adapted to the external grid voltage. Magnitude of the respective current surge was 0.18-multiple of the rated current. Similarly, the current surge can be limited using soft start.

2.1.3 Connecting the Non-excited Generator to the External Grid

Connection of non-excited generators to the external grid is also accompanied by transients. However, the amplitude of the current surge is smaller than in the case of excited generator. This is because the worst case for this method of connecting the generator to the external grid can occur at the moment when the voltage on the generator is zero and the external grid voltage is maximal (see Fig. 2.8).

In the case of excited generator, the current surge is largest when the generator voltage is in the opposite phase (antiphase).

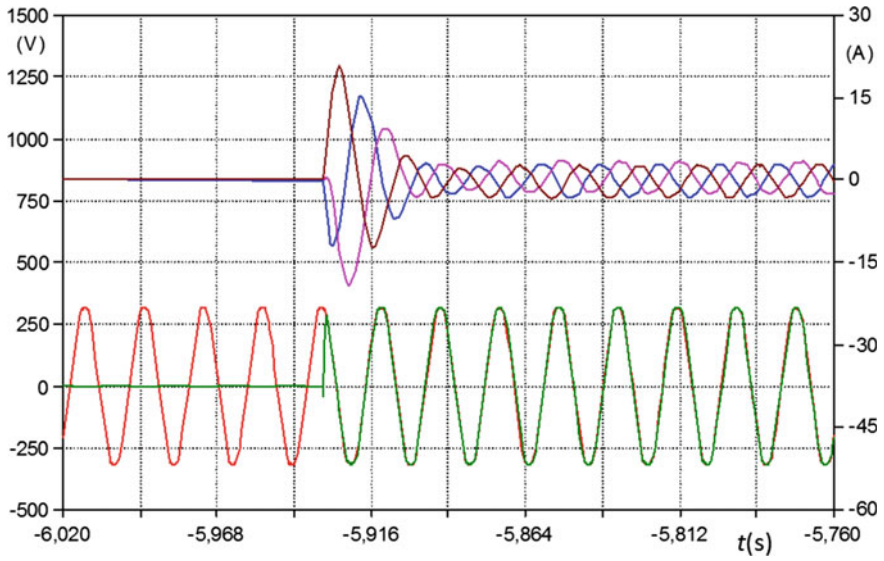

Fig. 2.8 Connecting the non-excited generator to the external grid External grid voltage U_s (*red*) (V), generator voltage U_g (*green*) (V), phase currents I_1 (*blue*), I_2 (*pink*), I_3 (*brown*) (A) (color figure online)

As in the previous case, the current surge can be limited by appropriately chosen resistance. When the non-excited generator was connected to the external grid via resistors, the current surges reached 0.4–0.55-multiple of the rated current of the machine at speed of 1022 min^{-1} [4].

In cases of connecting the generator to the external grid via resistors connected in series to its winding, no overvoltage was observed.

2.1.4 *Instantaneous Disconnection of the Generator from the External Grid*

Instantaneous disconnection from the external grid is associated with overvoltage that occurs due to sudden change of the generator power factor. All current becomes magnetizing and the total energy of the generator only covers its no-load losses and losses of the capacitor battery. The generator torque decreases and speed increases at constant output of the driving device.

The terminal voltage of the non-loaded generator increases with increasing speed (see Fig. 2.9) according to the excitation characteristic (see Fig. 2.5). When disconnecting the generator, it is therefore necessary to limit mechanical energy in the rotor in order to avoid damage to the machine insulation.

Overvoltage magnitude is proportional to the speed. If the generator is disconnected at the moment when it is not excited from the capacitor battery (not

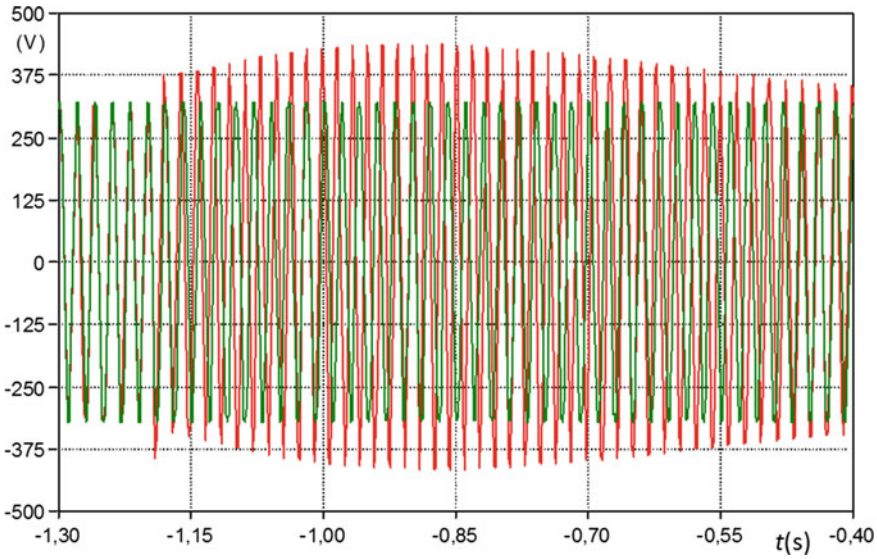

Fig. 2.9 Disconnecting the generator from the external grid. Generator voltage U_g (*red*) (V), external grid voltage U_s (*green*) (V) (color figure online)

connected in the circuit) but from the external grid, no overvoltage arises and the generator current ceases in a few periods.

2.1.5 Connecting Capacitors to the Running Generator

At the moment of connecting the capacitor battery to the running induction generator, the capacitor battery current excites the generator. Steady-state values of measured electric variables are presented in Table 2.1 and the course of connecting the capacitor battery to the running induction generator is shown in Fig. 2.10.

As evidenced by Table 2.1, increasing capacitance of the capacitor battery is associated with increasing current and voltage as well as with sharply rising machine losses.

Table 2.1 Steady-state values of electric variables at connecting the capacitor battery to the running induction generator

Capacitance	n (min^{-1})	I_0 (A)	U_0 (V)	f (Hz)	M (N m)	P_0 (W)
D 44 μF	1000	3.27	268.7	47.94	3.9	408
Y 25 μF	1000	1.43	181.6	48.26	1.1	115
D 44 μF	1022	3.77	292	50.55	4.5	482
Y 25 μF	1022	1.87	223	50.87	1.5	160
D 44 μF	1058	4.04	304.3	52.09	5.7	631
Y 25 μF	1058	2.07	239.32	52.57	1.8	199

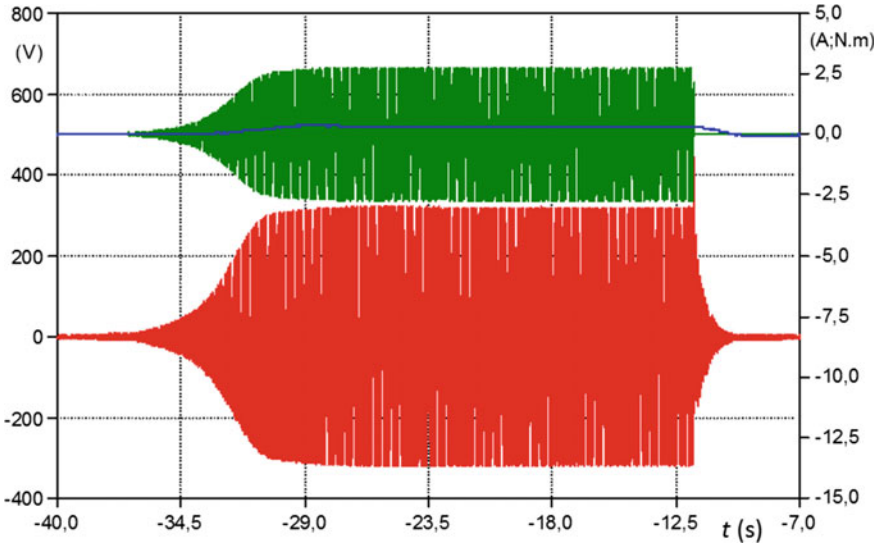

Fig. 2.10 Connecting the capacitor battery. Generator voltage U_g (*red*) (V), capacitor current I_c (*green*) (A), moment M (*blue*) (N·m) (color figure online)

2.1.6 Load Changes

If the generator at oversynchronous speed is connected to the external grid which has incomparably higher short-circuit power in comparison with the induction generator, it supplies active energy to this external grid. Increasing the torque on the shaft results in increased speed and thereby increased current of the generator; conversely, at the moment when its speed decreases below synchronous speed, the induction machine breaks into motor operation, as evidenced by Fig. 2.11.

2.1.7 The Effect of Terminal Voltage Changes During Cooperation with the External Grid

In operation condition, the distribution external grid voltage sometimes differs from its rated value, which may have a serious impact on the operation of induction generator in parallel cooperation with this external grid. Induction generator can operate in parallel with the distribution external grid whose rated voltage can fluctuate within ±5 % (according to standard EN 341610). Changes in the terminal voltage of the induction generator are associated with changes in the moment (torque) characteristic of the induction generator according to the following relation:

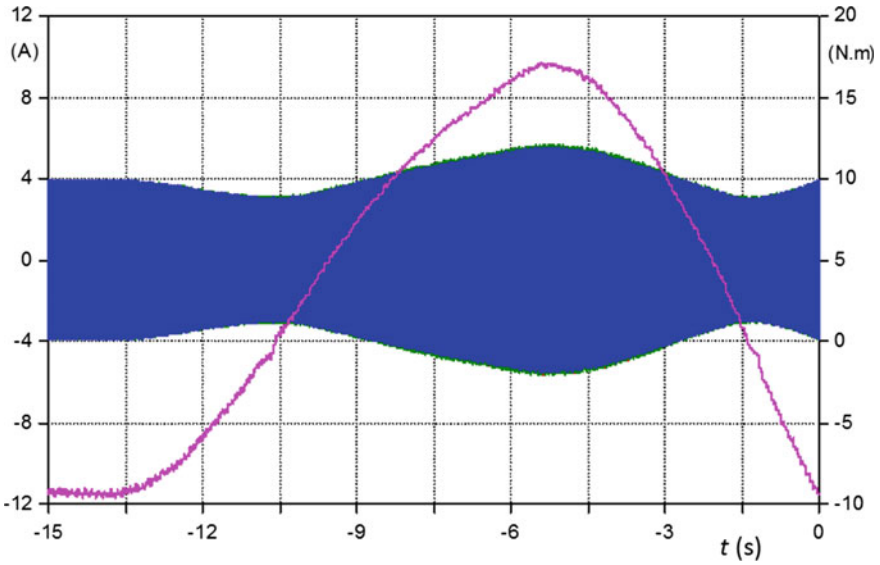

Fig. 2.11 Continuous speed change. Phase current I_1 (*black*), I_2 (*red*), I_3 (*green*) (A), moment M (*blue*) (N·m) (color figure online)

$$M = \frac{m_1 R_2' U_1^2}{s\omega_1 \left[\left(R_1 + c_1 \frac{R_2'}{s} \right)^2 + \left(x_{1\sigma} + c_1 x_{2\sigma}' \right)^2 \right]} \tag{2.10}$$

The torque is dependent on the square of the terminal voltage. The torque characteristic of the induction generator thus changes, especially the gradient of its linear part within the slip range $\pm s_{\max}$. Changes in the terminal voltage of the induction generator lead to changes in the value of maximum torque. Assuming that the external grid voltage U_{1n} changes to αU_{1n} at constant torque on the shaft of the generator, where $\alpha = < > 1$, then the generator slip will be given the relation 2.11:

$$s' \approx \frac{s}{\alpha^2} \tag{2.11}$$

Changes in the slip are associated with changes in the frequency in the rotor winding

$$f_2 = s \cdot f_1 \tag{2.12}$$

Increased frequency results in an increase in the rotor winding reactance

$$x_{2\sigma} = \omega_2 \cdot L_{2\sigma} \tag{2.13}$$

and decrease of the reactive component of the generator current. Reduction of the reactive current component is associated with an increase in the machine power factor.

The behaviour of the induction generator with changes in the terminal voltage was verified by measurements using an induction machine with the following parameters: P_n = 1.1 kW, U_n = 400 V, I_n = 3 A, cos φ = 0.75, 6p, 930 min^{-1}. Measurements were carried out on this induction machine in generator operation, changes in the terminal voltage were realized through an autotransformer within the range of 65–110 % U_{1n}. The measurement results for the constant speed of 1040 min^{-1} are shown in Fig. 2.12 [5–7].

Declining terminal voltage results in the reduction of machine torque and its output. At constant torque, the current decreases according to the following relation:

$$I'_{1a} \approx \frac{I_{1a}}{\alpha} \tag{2.14}$$

As mentioned above, the terminal voltage drop is also accompanied by a decrease of the current reactive component, resulting in the increase of the power factor. For this reason, also the induction generator efficiency slightly increases. When operating the induction generator with reduced terminal voltage, the working area of the machine becomes limited in terms of maximum torque reduction.

2.1.8 *Induction Generator of the Wind Power Plant in the Autonomous Mode*

Separately working induction generator has a soft shunt load characteristic. When the load changes, the machine slip as well as frequency changes according to the relation below:

$$f = \frac{n \cdot p}{60 \cdot (1 - s)} \tag{2.15}$$

The change in frequency leads to changes in capacitance X_C and reactance X_L. Increasing load further reduces the terminal voltage and also changes the machine power flow. Therefore, the magnitude of the calculated capacity is minimal. For loading the generator, this capacity must be increased. As regards a practical use of the generator in the area of rated power, the resulting magnitude of the capacity may be even double.

After starting, the machine becomes excited and its terminals show voltage given by the speed and magnitude of the capacity connected to the generator. After energizing the generator, it is possible to start its loading. The terminal voltage drops with decreasing load impedance. After reaching the minimum voltage (30–50 % of U_N) when the capacitor battery is no longer able to excite the machine, the voltage and current drops to zero. Load characteristic shows the so-called "knee"; in this area, the generator supplies the load with output of maximum efficiency—see Fig. 2.13.

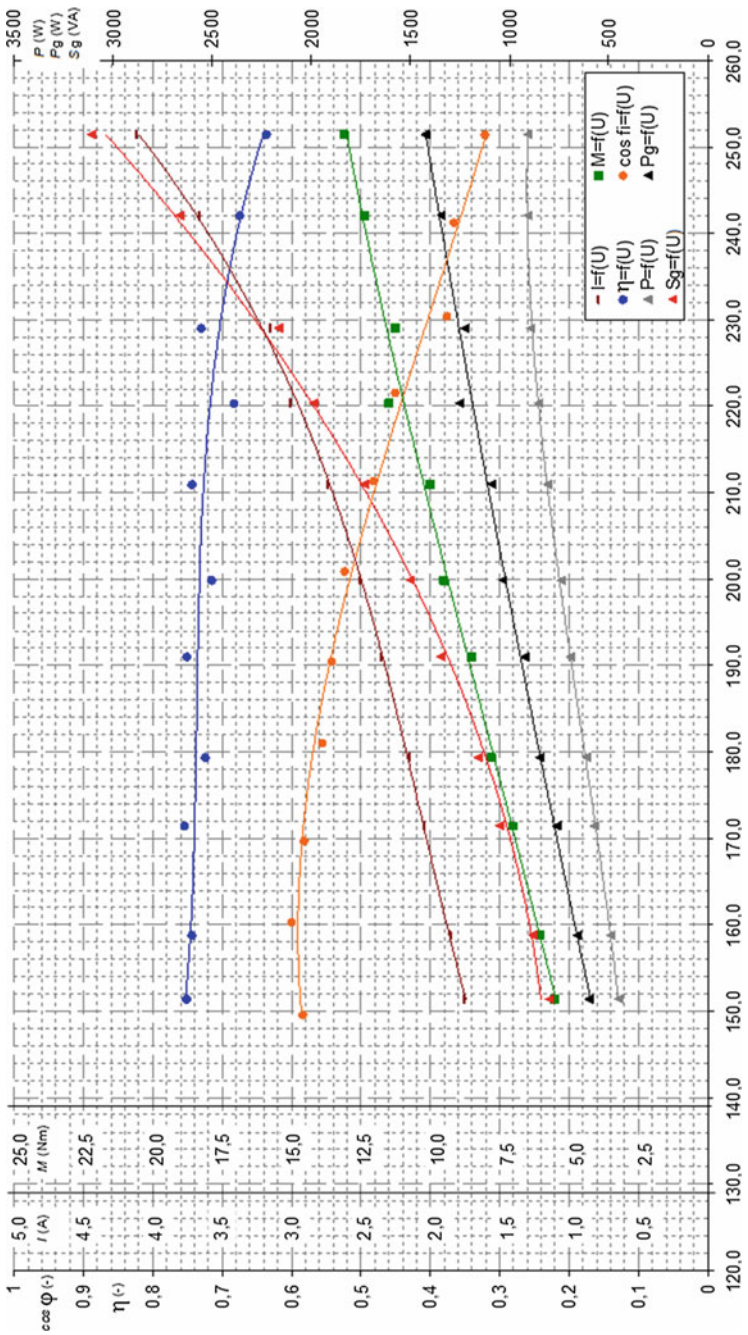

Fig. 2.12 Behaviour of the induction generator during terminal voltage changes

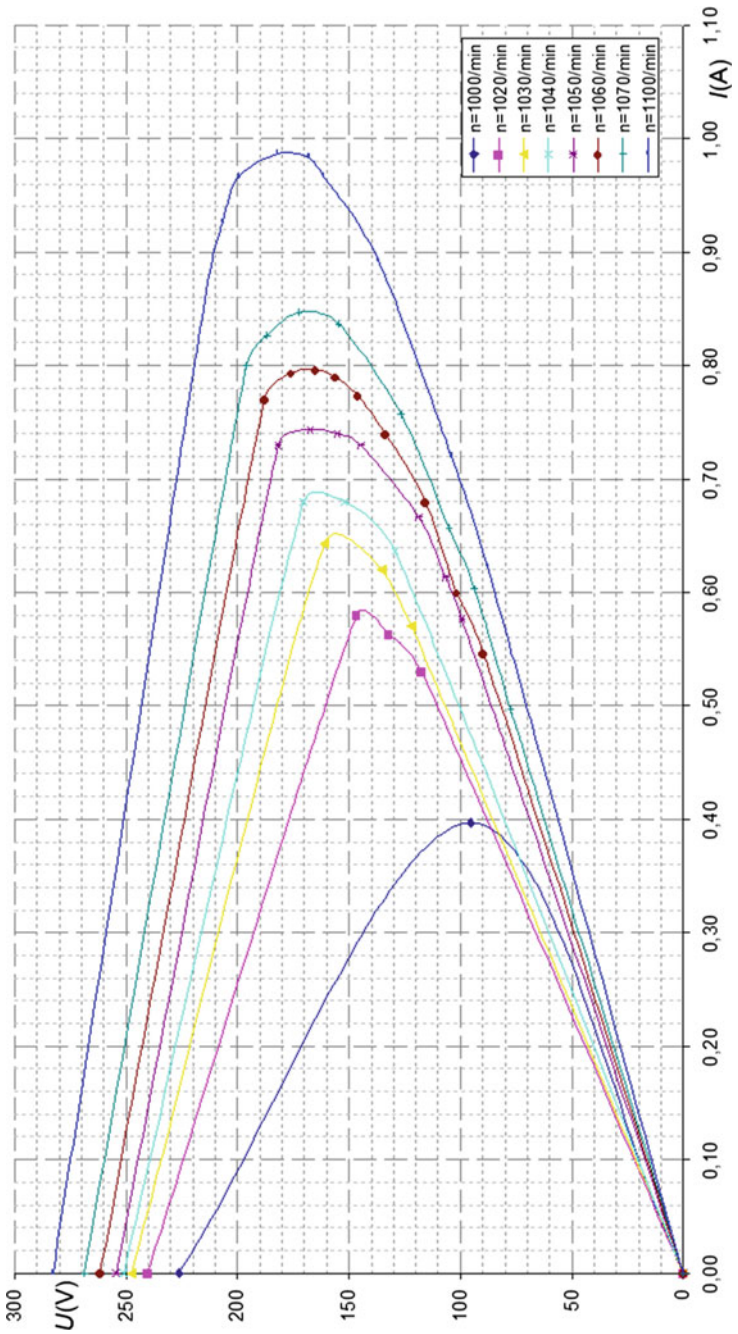

Fig. 2.13 Load characteristics of the separately working generator, for different speeds

Loading the generator with inductive load reduces the reactive energy supplied to the generator for excitation; the load characteristic is steeper and is therefore softer. Load characteristics for inductive loads are shown in Fig. 2.13. If the inductive power factor is compensated, the load characteristics are the same as for cases of loading with resistors. Increasing capacitive load, however, leads to considerable decreases in the machine efficiency (Fig. 2.14).

In the "knee" area of the shunt characteristic, the generator supplies the load with output of maximum efficiency, as shown in Fig. 2.15. This figure presents individual monitored variables (apparent generator output S_G, generator active input P_G, output on the resistive load P_R, generator current I_G, torque on the generator shaft M, efficiency η and power factor cos φ) depending on the terminal voltage U_R of the machine, at constant speed $n = 1070\ \text{min}^{-1}$. As shown in Fig. 2.15, the knee peak occurs at the terminal voltage $U_R = 190$ V. The maximum generator output is reached in the area before the knee of the load characteristic, at about $U_R = 210$ V. Optimum generator operation at constant shaft speed $n = 1070\ \text{min}^{-1}$ is achieved at the terminal voltage of 220–160 V when the efficiency of using the output on the shaft is maximal ($\eta = 68$ %) [7, 8].

2.2 Medium Wind Power Plants

Development of medium wind power plants was accelerated by the options of bringing the output from these plants into the external grid, i.e., mainly the medium-voltage system, with regard to their capacity. Therefore, these facilities included wind power plants and their control systems enabling parallel cooperation with the external grid whereas the respective output was brought out through a power transformer. Block connection of this power transformer and the wind generator then formed the so-called plant up to the transfer point, i.e., the place in which the output from this plant is transferred to the external grid.

From the viewpoint of the design of medium wind power plants, these were mostly systems with active vane swivelling (pitch) (Fig. 2.16) and generator placed in the nacelle (Fig. 2.17) which was located on the wind power plant tube at a height of about 30–50 m above the ground.

Entire equipment (Fig. 2.18) was placed in the base of the wind power plant tube, consisting of a simple control system, the compensation device and power outlet to a LV/MV transformer station through a low-voltage cable; the LV/MV transformer station is usually positioned close to the wind power plant and MV overhead lines.

The dominant element of the nacelle was "solely" the generator and hydraulic systems for swivelling the wind turbine and its vanes in order to optimally use the wind power, or (in older models) for swivelling the tips of vanes (blades) of the wind turbine during its braking (Fig. 2.19).

At the end of the last century, in terms of usability and return on investment, the installations in the Czech Republic were especially old refurbished machines

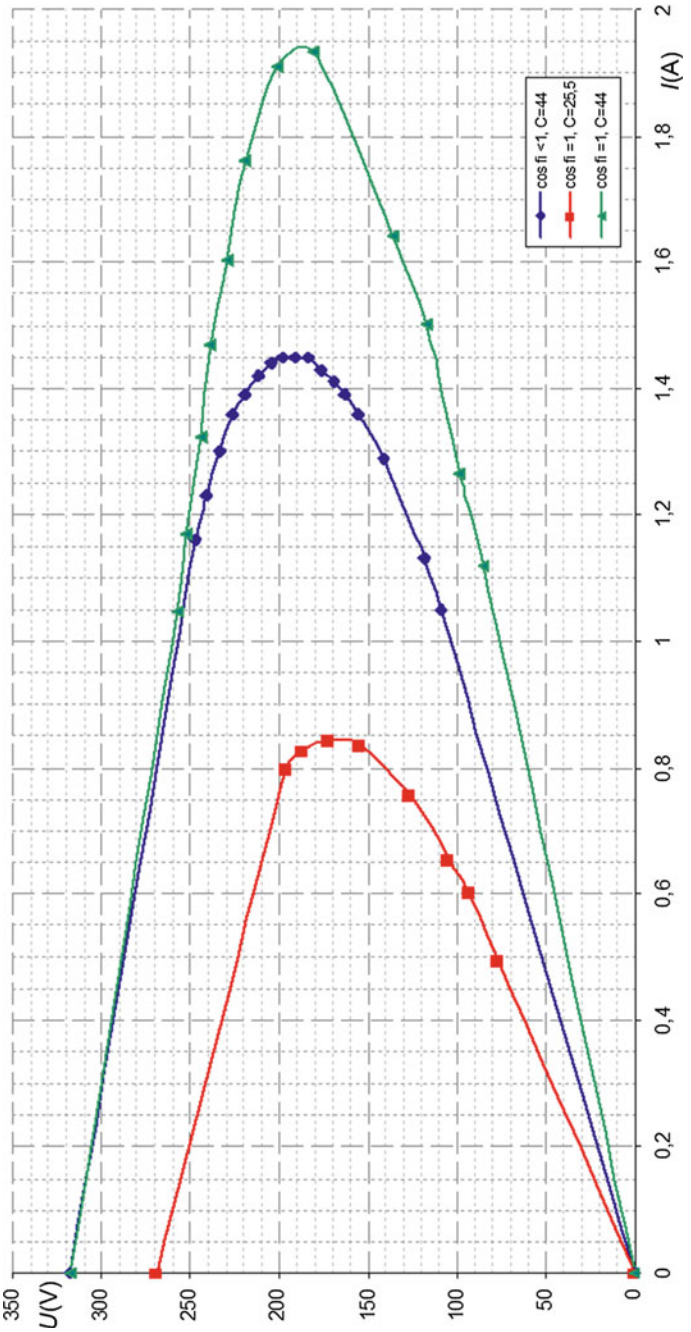

Fig. 2.14 Load characteristics for various connections, at constant speed

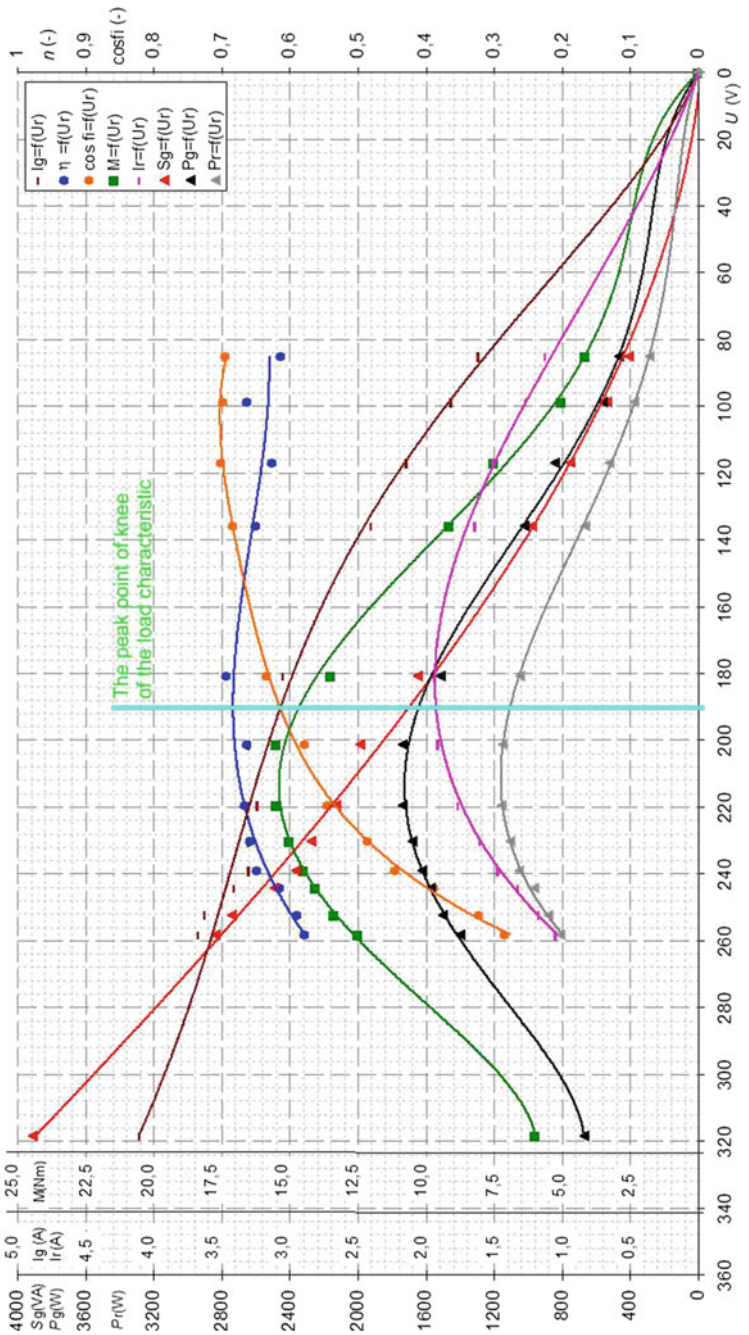

Fig. 2.15 Load characteristic of the induction generator at constant speed $n = 1070\ \text{min}^{-1}$ with attachable capacitor battery C2

Fig. 2.16 Active system of swivelling the vanes

Fig. 2.17 A generator placed in the nacelle of the wind motor

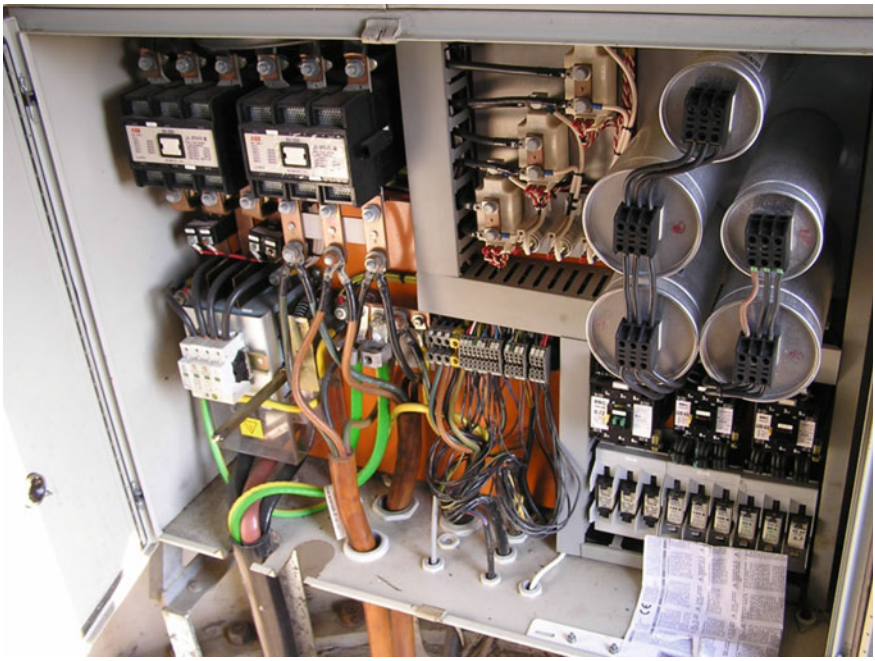

Fig. 2.18 Equipment of the medium wind power plant (a detail of the compensation device)

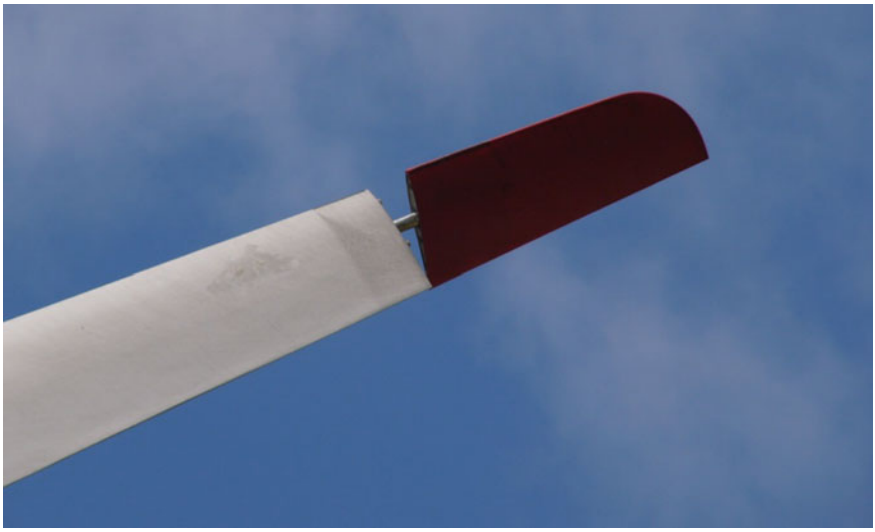

Fig. 2.19 Braking the wind turbine by deflecting tips of the blades

imported from Western Europe. They are used in areas with limited connectivity to the distribution external grid. Many times, they did not meet the conditions for connection to the external grid; their owners, therefore, gradually modernized the control algorithm and equipment of these wind power plants.

Common features of these power plants are firmly seated rotor blades with STAHL regulation; in order to block the power plant, the blade tips are extended and rotated so that the countermoment slacks up the rotor of the wind turbine. Then final braking is ensured by a hydraulic brake. For optimum conversion and the corresponding better use of wind energy, the medium power plants use a planetary gear that mostly propels an induction generator.

2.2.1 Generators of Medium Wind Power Plants

In addition to selecting a suitable site for the construction of wind power plants and optimum features of the wind turbine, the maximum use of wind energy is substantially influenced by the choice of the type and characteristics of the power generator. If looking into the catalogue of manufacturers of electric machines, we find that many machine parameters significantly vary with the magnitude of the machine output, speed, type, etc. When choosing the type and method of operation of any generators, we often have to decide whether we should use the drive with or without a gearbox, whether to choose a machine with more or less poles, etc. Besides the technical possibilities, investment costs and other conditions, we should take into account the efficiency, power factor and weight of the machine.

Apparent output power of electric machines is given by the so-called power equation:

$$S_i \approx D \cdot l \cdot n \cdot N_{S1} \cdot I_1 \cdot B_{\vartheta} \cdot k_V \cdot m \tag{2.16}$$

where: D and l are the internal diameter and length of the stator, respectively, n is the machine speed, B_{υ} is the induction in the air gap, I_1 is the stator current (it can be replaced by the product $\sigma_1 \cdot S_1$ where σ_1 is the load current and S_1 is the cross-section of stator winding conductors), k_V is the winding factor, k_B is the curve shape factor, N_{S1} is the number of conductors of one phase in series, and m is the number of phases).

The Eq. (2.16) shows the dependence of dimensions and hence the weight of the turbine on its output power. Therefore:

- To have a machine of the same output but with lower speed, we have to increase the amount of active iron; conversely, at the same volume, the output decreases with the increasing number of poles.
- The specific weight decreases with the output power.
- Multipole machines are massive (for the same output and lower speed, the turbine must have larger volume of the magnetic circuit).
- The better the winding (with higher k_v), the more we can reduce the magnetic circuit saturation or current density in the conductors at the same output.
- Energy indicators and thus the efficiency of the machine can be easily increased by increasing dimensions of the active parts of the machine, i.e., by increasing the volume of the magnetic circuit (through reducing its saturation) and increasing the cross-section of the winding conductors, while maintaining the rated power (this will reduce overall losses of the machine).
- contains a relationship indicating that the k-multiple increase in each dimension of the motor results in the increase of its efficiency η as follows:

$$\eta_k = \frac{k \cdot \eta_0}{1 + \eta_0(k-1)} \tag{2.17}$$

  where η_0 is efficiency of the motor with original dimensions. This is due to the fact that the machine output increase is proportional to k^4 while losses are proportional to k^3. The machine surface increases with k^2; therefore, the following should apply: the larger machine dimensions, the better thermal utilization of the machine.

The overall energy efficiency of machines in operation is affected mainly by the below-mentioned factors:

- Load magnitude.
- Time utilization.
- Number of starts.
- Magnitude of the machine rated voltage and deviations from the rated voltage.
- Harmonic content in voltage or current.
- Maintenance and repairs.

Medium wind power plants most often used induction generators primarily due to their simple design and the corresponding higher operating reliability, especially squirrel-cage induction generators.

Among other things, induction machines must have oversynchronous speed to work as generators. Furthermore, induction machines (motors as well as generators) need reactive power from the external grid (or other sources) to create the rotating magnetic field. Besides numerous advantages, this is a significant disadvantage of these machines. The required reactive energy for the motor will depend on:

- Design concept of the machine (the size of the air gap, the shape of the grooves, magnetizing current, stray, etc.).
- The number of poles.
- The type of the rotor used.
- Load magnitude.
- Terminal voltage.

Induction machines can have a rotor with squirrel-cage winding or wound rotor. Other used machines can switch the number of poles. Currently, often used induction generators are those with wound rotor. Their advantage is the possibility of dual feeding.

As seen from the relationship (2.16), induction machines with more poles, i.e., lower speed, must have greater capacity of the magnetic circuit at the same rated output. As the magnetic circuit saturation usually also remains the same, the excitation of the needed magnetic field will require greater reactive power. This means that machines of the same type size but with different number of poles will have a different power factor. The smaller the number of poles, the higher the power factor.

Compared to the slip-ring rotor, the machines with squirrel-cage rotor have higher power factor. This results from the magnitude of stray flux which is smaller in the cage rotor.

Magnitude of the reactive energy under load is determined from the relationship

$$Q_M = Q_o + Q_Z \tag{2.18}$$

where

$$Q_0 = I_0 \cdot U_N \cdot \sin \varphi_0 \tag{2.19}$$

is the no-load reactive input—independent of load, and

$$Q_Z = m \cdot X_\sigma \cdot I_2^2 \tag{2.20}$$

is the magnitude of the reactive input varying with load magnitude (X_σ is the total leakage reactance of the stator and rotor winding, and I_2' is the converted value of the rotor current to the stator).

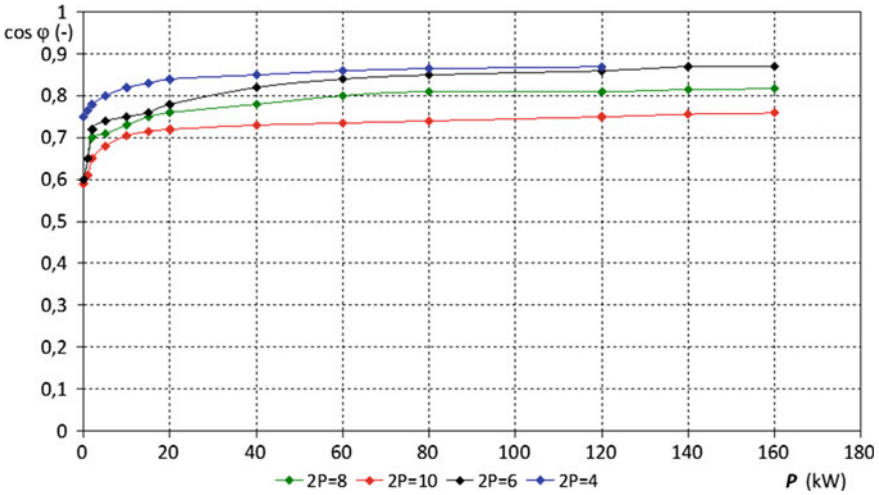

Fig. 2.20 Dependence of the power factor on the active output of asynchronous machine

The power factor of induction machine is significantly reduced with decreasing the load as the magnetizing current component becomes more significant. Figure 2.20 shows that the power factor increases with the machine output and decreases with the number of poles.

When assessing the consumption of electricity, we must also consider active losses caused by the reactive component of the current. The lower the power factor of the motor (at constant load), the higher the losses and thus lower drive efficiency. Furthermore, it holds that:

(a) The reactive power is consumed to excite the magnetic field. The size of the air gap in relation to the rated output of the machine is reduced and the consumption of reactive power in large machines is therefore less.
(b) At the same rated power, multi-pole machines have greater weight; the generation of the magnetic field of the same magnitude therefore requires greater reactive power.
(c) Variations in voltage cause a change in reactive power.
(d) Power factor of the machine decreases when the load is less than rated. This also reduces its effectiveness. Furthermore, it is equally important that losses in the supply external grid increase as well.

When selecting the induction generator, particularly for outputs up to 100 kW, we usually choose an available induction motor. In this respect, it is necessary to realize a few basic facts:

- The induction motor operating in the generator mode will have different output because the nominal motor output is the output on the shaft; in generators, it is the output on machine terminals,

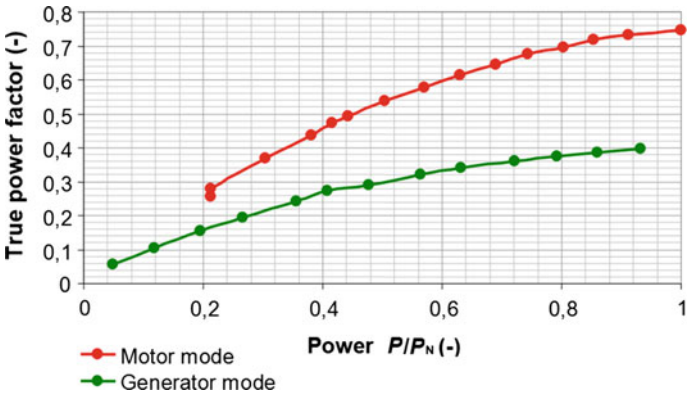

Fig. 2.21 The course of true power factor in induction machine 50 kW

- in generator operation, the machine will have a lower power factor because the internal induced voltage must compensate for voltage drop across the impedance of the stator to reach the rated voltage,
- efficiency in generator operation with maintaining the rated output on the shaft may be even higher because the mechanical losses are covered by the drive device.

These facts are evident from Fig. 2.21 which also shows the course of power factor subtracted by a circle diagram for 50 kW motor.

In machines with higher outputs, the difference for the motor area and generator area is not so large, as shown in Fig. 2.22 for 150 kW motor. Efficiency curves of the same machines are presented in Fig. 2.23 (Fig. 2.24).

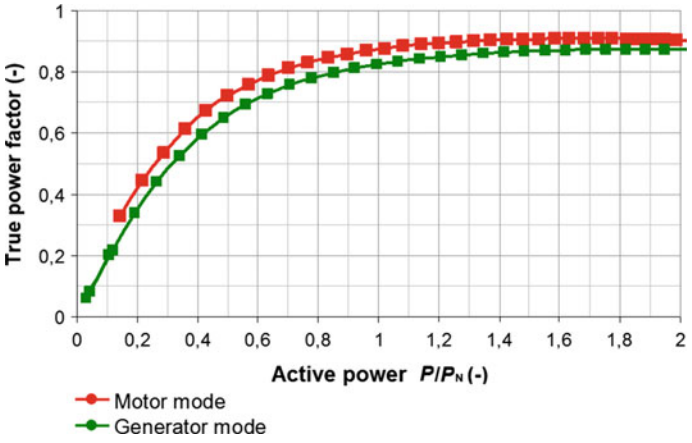

Fig. 2.22 The course of true power factor in induction machine 150 kW

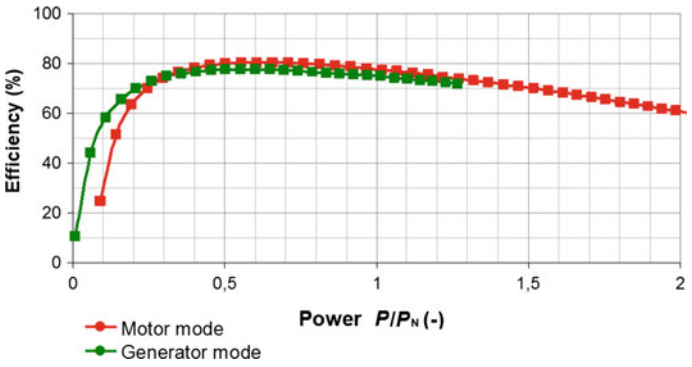

Fig. 2.23 Efficiency curve of induction machine 50 kW

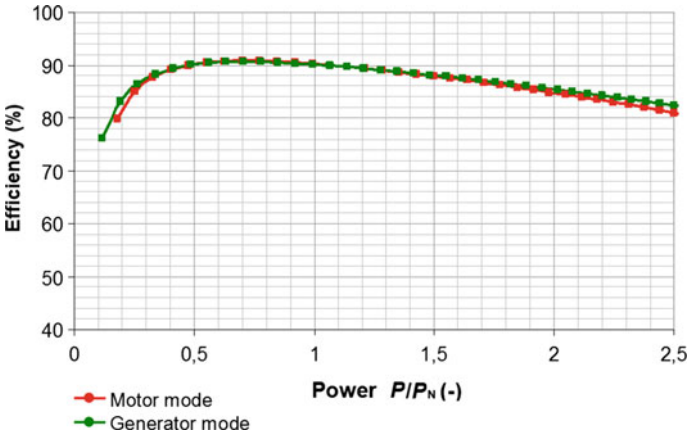

Fig. 2.24 Efficiency curve of induction machine 150 kW

The power factor differs in machines with different number of poles and different output within the same type range as already graphically shown in Fig. 2.20.

It is widely envisaged that the efficiency of the synchronous machines is usually higher than in induction machines. Comparison in Fig. 2.25 shows that this is not valid in general. Even this may be a criterion in deciding what kind of generator will be used. The same applies to the weight of these kinds of machines as evidenced by Fig. 2.26 [10].

Initially, the medium wind power plants were fitted with induction generators with a single squirrel-cage. Subsequently, modern wind power plants were using pole-changing induction generators (employing the method of changing the number of poles) or generators having a stator with a greater number of separate windings, eventually a combination of both. The reason for the expansion of the later solution is very prosaic and relates to the principle of conversion of the wind energy into

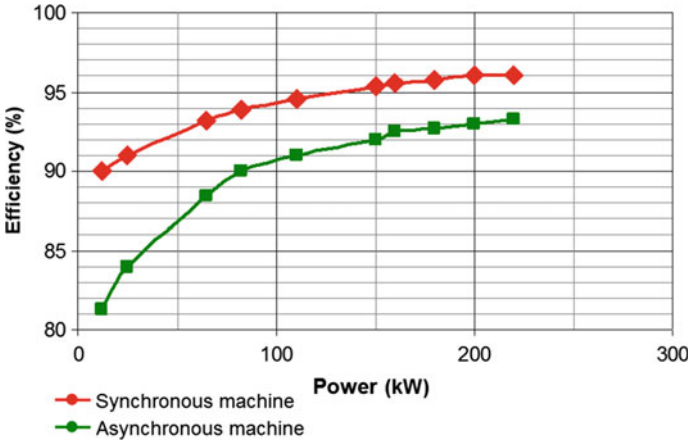

Fig. 2.25 Efficiency of synchronous and induction machines

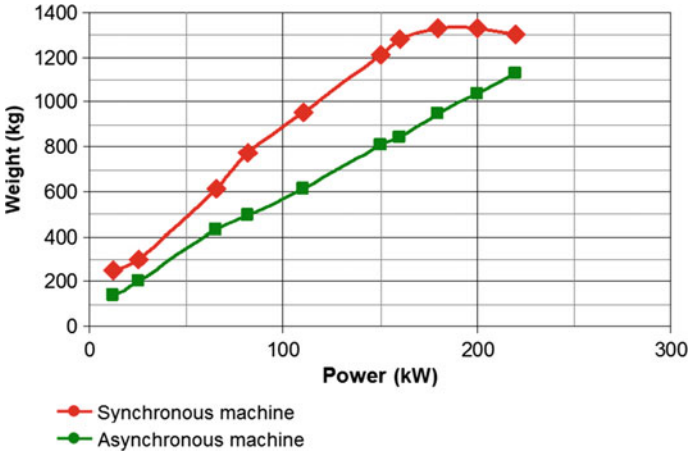

Fig. 2.26 Comparison of weights of synchronous and induction machines

electricity by wind power plants, which takes place according to the so-called power curve of the wind turbine, as already mentioned in previous chapters. Induction generators changing the number of poles better utilize wind flow energy for a wide range of wind velocities. At the start and lower torque and speed values on the wind motor shaft, they use the winding with higher number of poles; if the wind velocity and the corresponding mechanical output on the shaft of the wind turbine increases, the winding with lower number of poles is subsequently connected.

The steps of changing the speed correspond to synchronous speed at different number of poles. The stator has either a number of separate windings with different

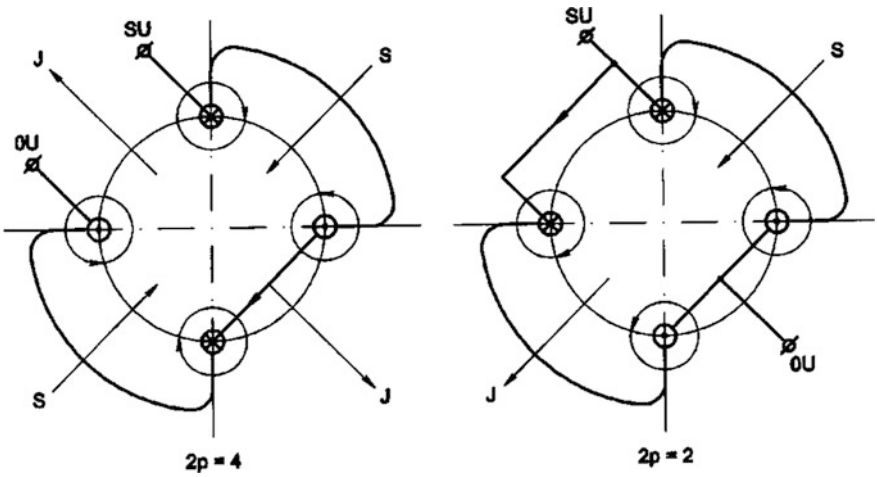

Fig. 2.27 The principle of Dahlander connection

number of poles or one switchable winding, or both methods are combined. Such a solution leads to an increase in the machine size and weight but provides the possibility of any speed ratio, e.g., 1/3 as well as 1/12 [8, 9].

When changing the number of poles, the windings must meet many requirements. The machine must mainly have the same sense of rotation within the entire speed range; the machine rated output power output must be determined for each speed, etc.

Creating a switchable winding meeting all the requirements is not easy and the solutions are usually patented. For switching a motor with one winding in ratio 1/2, the most frequently used system is the so-called Dahlander connection. Its principle is shown in Fig. 2.27.

In one phase, two coils of 4 poles winding are connected in series with brought-out neutral point. If both coils are connected in series, they form a 4 poles magnetic field. When connected in parallel, the magnetic field between the coils ceases and 2 poles magnetic field is formed. For 2 poles, the winding is less utilized because the winding step is reduced to 1/2 of the pole pitch (Figs. 2.28 and 2.29).

Induction motors usually use two ways of changing the number of poles:

- Wye (Y)—double wye switching.
- Delta (D)—double wye (YY) switching.

Y—YY Switching

Output power at Y connection is

$$P_y = 3\,\frac{U_N}{\sqrt{3}} I_f \eta_y \cos\varphi_y \tag{2.21}$$

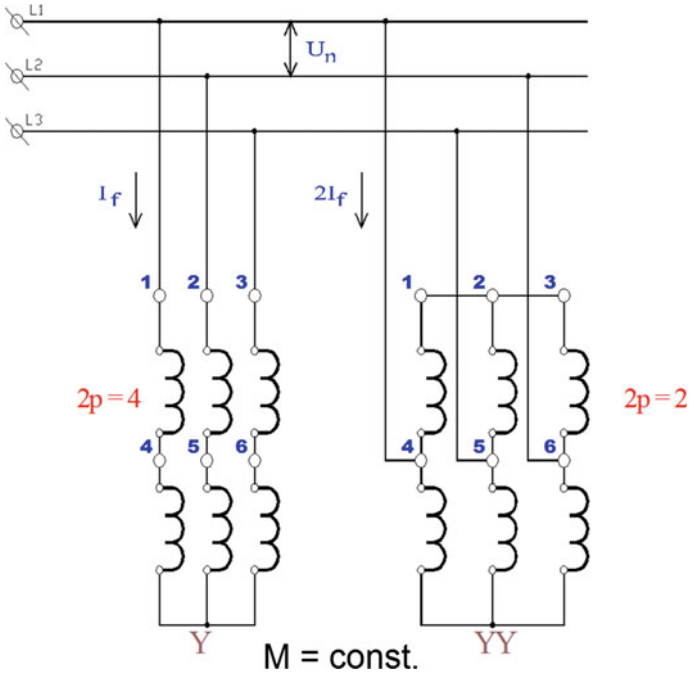

Fig. 2.28 Dahlander connection, wye—double star switching (Y–YY)

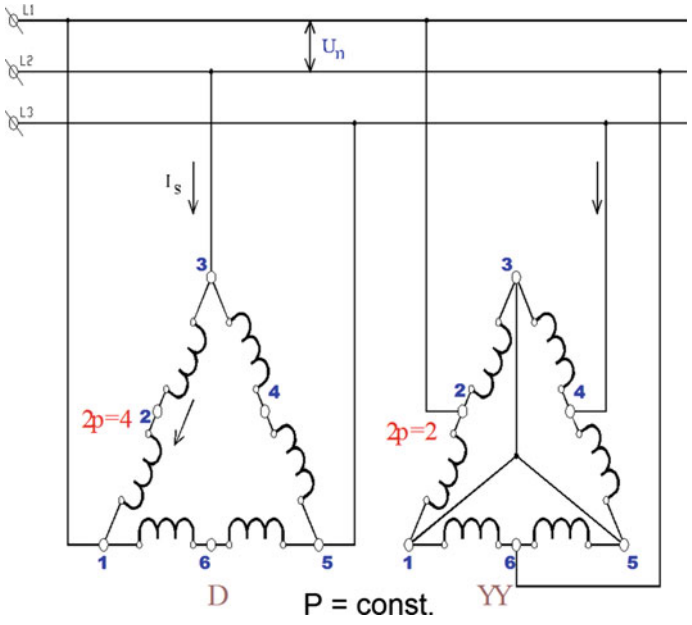

Fig. 2.29 Dahlander connection, delta—double star switching (D–YY)

where P is the active output, U_N is the rated voltage of the machine, I is the winding current, η efficiency and cos φ is the power factor of the machine.

At YY connection:

$$P_{yy} = 3 \cdot \frac{U_n}{\sqrt{3}} \cdot 2 \cdot I_f \cdot \eta_{yy} \cdot \cos \varphi_{yy} \tag{2.22}$$

For approximate assumption that the power factors and efficiencies are the same ($\eta_y \cdot \cos \varphi_y = \eta_{yy} \cdot \cos \varphi_{yy}$), it holds that

$$P_{yy} = 2 \cdot P_y \tag{2.23}$$

Because the turbine moment (torque) $T \approx \frac{P}{n}$ and because $n_{yy} = 2n_y$, the moment will be the same in both cases, i.e., $T_{yy} = T_y$.

D—YY switching

Phase voltage at the delta connection will be $U_{fd} = U_n$,

$$P_y = 3 \cdot \frac{U_n}{\sqrt{3}} \cdot I_s \cdot \eta_y \cdot \cos \varphi_y \tag{2.24}$$

At YY connection:

$$P_{yy} = 3 \cdot \frac{U_n}{\sqrt{3}} \cdot 2 \cdot \frac{I_s}{\sqrt{3}} \cdot \eta_{yy} \cdot \cos \varphi_{yy} \tag{2.25}$$

Again, assuming the same power factors and efficiencies, the following applies

$$P_{yy} = \frac{2}{\sqrt{3}} P_d = 1.16 P_d \tag{2.26}$$

The output is therefore constant (almost); Torque T_d then will approximately $2T_{yy}$. Machine output or torque at certain speed is given by load torque of the driven machine. Therefore, the term "switching at constant output or moment" characterizes the fact that the motor can operate with the respective output or torque without the danger of thermal overload.

However, when changing the number of poles, there are switching transients causing the emergence of switching surges (overvoltages). Switching overvoltages strain the winding insulation; it is therefore essential to choose an appropriate control system to limit these surges. Obviously, the magnitude of these surges is affected by the moment of the transient inception, the magnitude of the instantaneous generator load (RLC parameters of the generator) and the moment at which individual contacts are closed. Figure 2.30 shows the voltage of the Y and YY winding terminals during one switching cycle of the test induction machine 0.65/2.5 kW, 700/1400 min^{-1}. At 0–Y–YY–Y–0 switching cycle, the largest overvoltage was measured when disconnecting the wye connection [see Fig. 2.30,

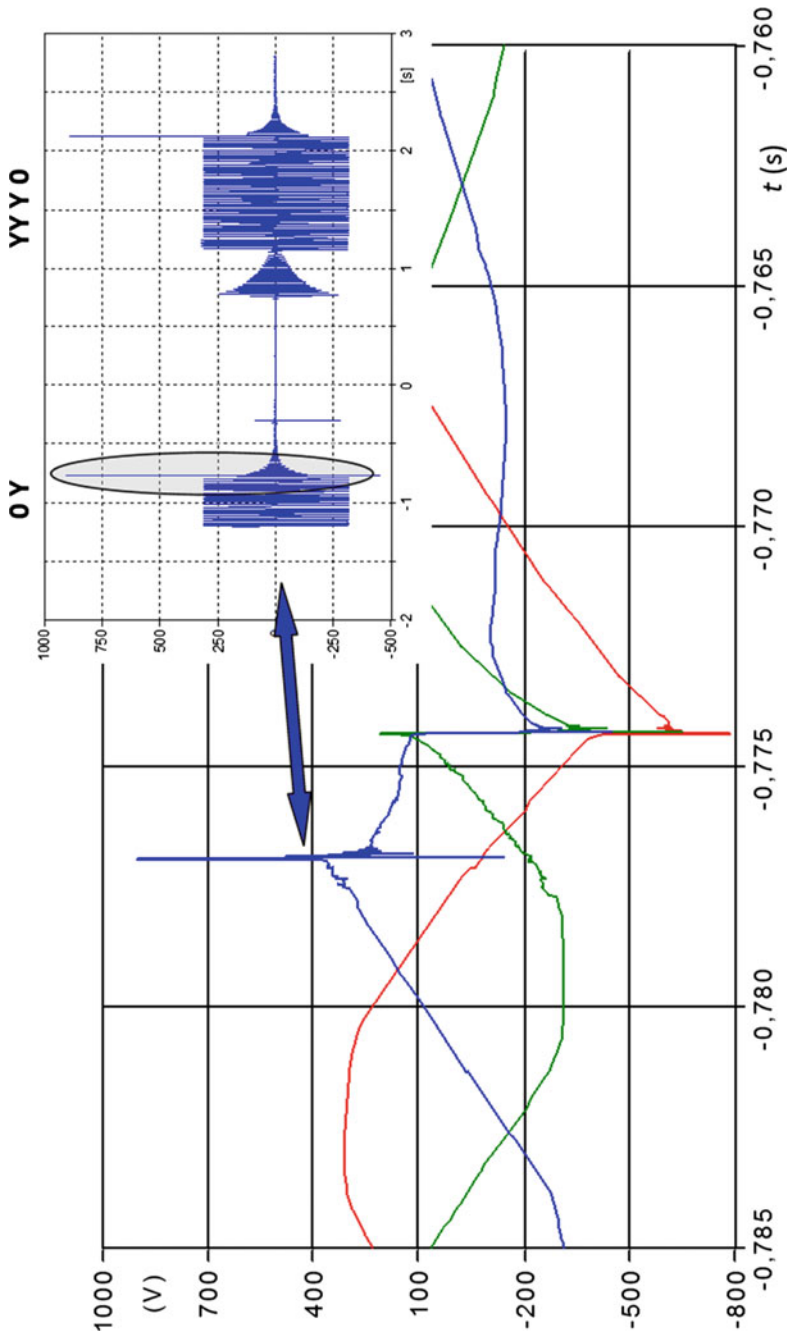

Fig. 2.30 Overvoltage formation when switching the number of poles

voltages U_1, U_2, U_3 (V)]. Magnitude of the first amplitude of the transient is 900 V for time of 20 μs; steepness of the voltage rise is therefore 45 kV m s^{-1}.

Magnitude of overvoltage amplitudes is limited due to increasing load of the generator. With a suitable control system, these peaks can be reduced. The mentioned conclusion was confirmed by practical measurements in the wind power plant; this wind power plant uses an induction generator changing the number of poles to 6/8 and measurements did not find overvoltage peaks in the range presented in Fig. 2.30.

Figure 2.31 shows the already mentioned output curve of the wind power plant, which is the main characteristic of each wind power plant, necessary for determining the overall efficiency of the wind power plant operation, e.g., through utilization ratio as defined in the preceding chapters, as well as for determining its appropriate location. Figure 2.31 explains the process of changing the number of poles: 8 poles active winding is used for the area specified by speeds of 4–6 m s^{-1} (the so-called starting phase) while 6 poles active winding is used for the area defined by speeds of 6 m s^{-1} and above (the so-called operational phase). The output curve was constructed for a wind power plant with double squirrel cage induction generator, rated output of 150/30 kW, with the corresponding system for changing the number of poles to 8/6 and speed of 758/1012 min^{-1}.

A simplified block diagram of the control system of this wind power plant equipped with the induction generator with a double squirrel cage and the system

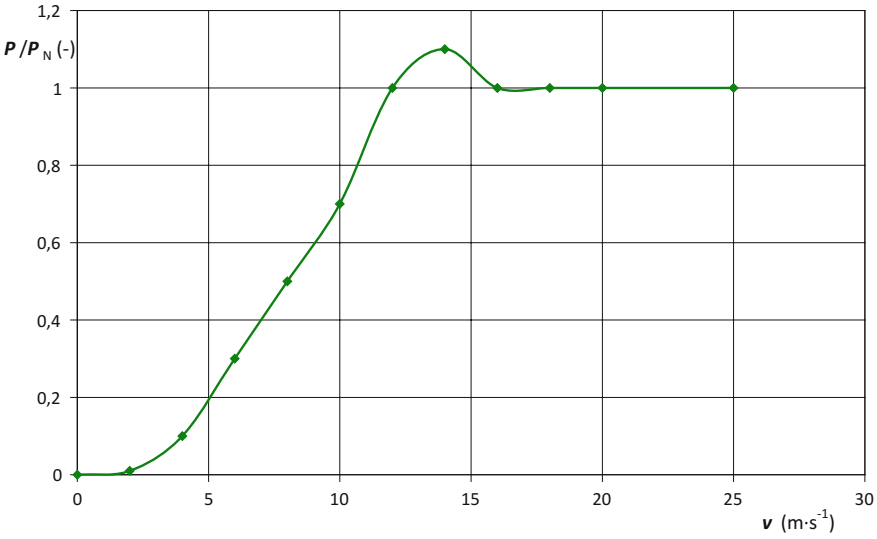

Fig. 2.31 Output curve of the WPP fitted with induction generator 150/30 kW with short-circuit armature and the system for changing the number of poles

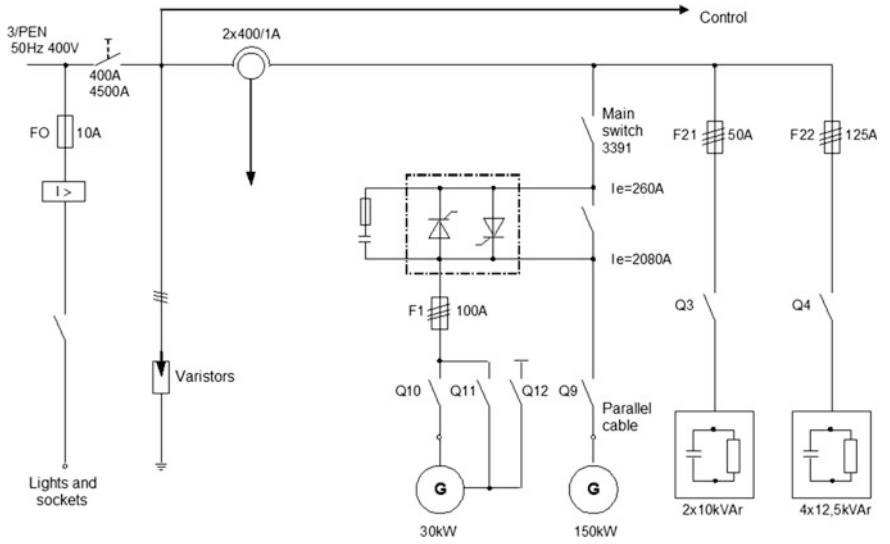

Fig. 2.32 Simplified block diagram of the control system of WPP equipped with the squirrel-cage induction generator and the system for changing the number of poles

for changing the number of poles is shown in Fig. 2.32. The algorithm for connecting and operating the analyzed wind power plant is very simple.

The control system monitors the wind speed; if the speed exceeds the first level W1, the WPP is unbraked and the vanes of the wind turbine are swivelled in breakaway angle. Faster rotation of the aggregate is ensured by operation in the machine motor range.

Upon exceeding the second wind speed level W2, the system breaks into standby mode; the motor drive is disconnected when the wind speed excess persists. After reaching the synchronous speed for the respective winding, the WPP is connected to the parent electricity external grid via a soft starter (motor controller) whereas the connected stator winding is that with a higher number of poles.

The soft starter limits the current surge and torque on the shaft of the WPP generator which subsequently reduces mechanical shocks as well as voltage drops in the power system at the connection point. Through controlling the phase angle of the thyristor in antiparallel connection, the voltage on the generator terminals is reduced to the set initial value and smoothly increases to full voltage value within the set interval using a ramp function. Comparison of the direct connection of the wind turbine to the external grid and the connection via the soft starter is presented in Figs. 2.33 and 2.34.

If the wind speed (i.e., WPP speed) falls below a specified level, the WPP is disconnected and waits until the condition for exceeding the limit W2 is met again. If the limit W2 excess persists for a set period (usually about 5 s), the winding with a lower number of poles is connected directly outside of the soft starter.

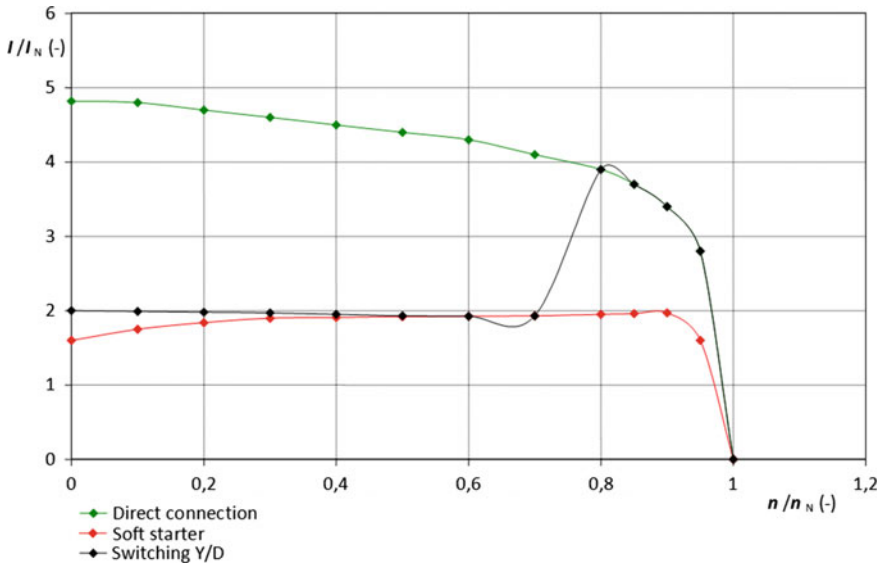

Fig. 2.33 The course of current effective values

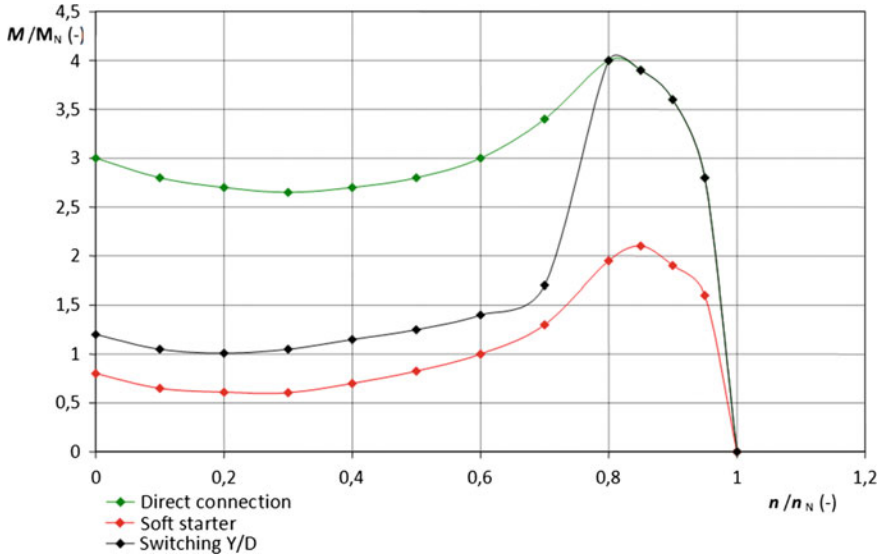

Fig. 2.34 The machine torque characteristic

Once the generator operates in parallel with the distribution external grid, the WPP system involves a compensation unit to compensate for the low power factor of the generator. Courses of electrical quantities when connecting the wind power plant to the distribution external grid are shown in detail in Figs. 2.35 and 2.36.

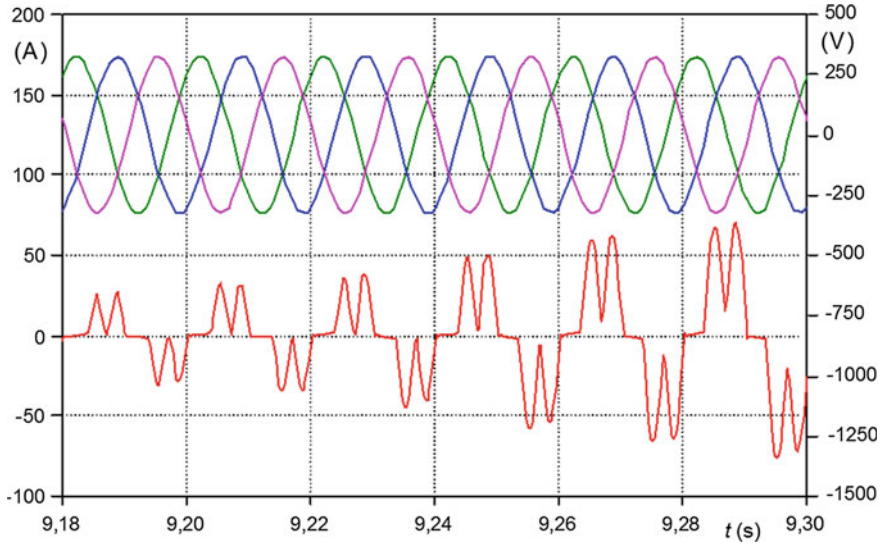

Fig. 2.35 The cycle of connecting the generator to the external grid, soft start detail, course of voltages U_1 (*green*), U_2 (*blue*), U_3 (*pink*) (V) (*right axis*) and current I_1 (*red*) (A) (*left axis*) (color figure online)

In area 1, the wind turbine is run by the generator which operates in the motor mode and is connected to the external grid via soft-start. When the wind turbine rotates, the generator is disconnected from the external grid; if the aggregate speed rises above the synchronous speed, the device is reconnected to the external grid using the soft-start, as seen from area 2—see Fig. 2.36.

Although using the soft start, there are transient phenomena associated with the current and torque strain of the device, which is reflected especially voltage fluctuations at the connection point, etc.

After determining the appropriate generator, the other basic factors include the way of connection to the distribution external grid and the selection of measuring and control equipment. The way of connecting the wind power plant to the external grid (external grid) is provided by the competent operator of the external grid on the basis of the given external grid conditions, power and the method of wind power plant operation mode. It is important to choose an appropriate switching device. During switching, there can be short-term changes in voltage; for wind power plants with the connection point in the low-voltage external grid the allowable tolerance is ≤ 3 % of the rated voltage unless the switching occurs more frequently than once every 1.5 min. In wind power plants with induction generators, short-term declines may occur during the connection at approximately asynchronous speed due to internal transients. Such a decline may reach a double of otherwise allowable value (approximately 6 % for low-voltage external grid) unless in interval longer than 2 periods. For wind power plants, it is necessary to

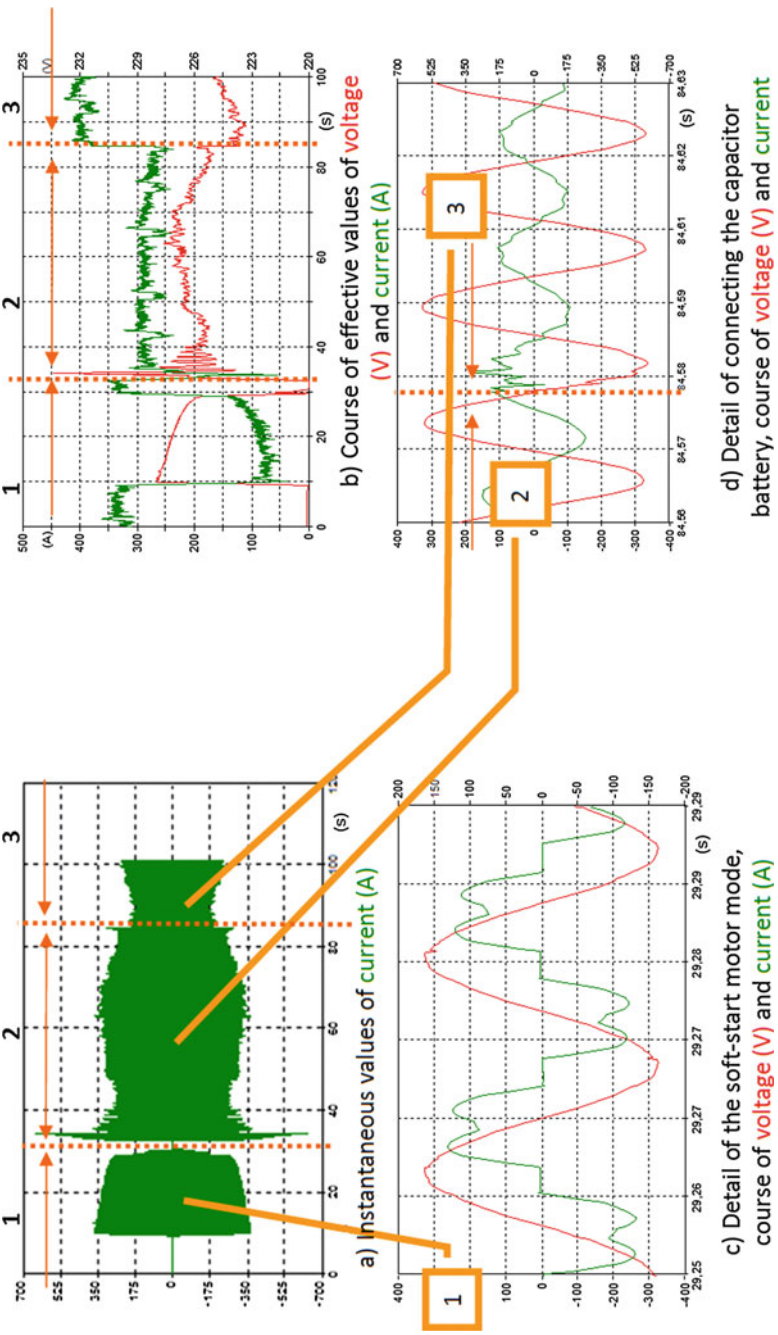

Fig. 2.36 The process of connecting the wind power plant to the external grid

consider a special switching factor dependent on the control system conditions, which is used to evaluate their switching and which also respects the mentioned ultra-short transients.

Figure 2.36b shows the mentioned voltage drop at the time of connecting the wind power plant to the value of about 221 V—this is associated with a percentage change of 4.3 % which is not in accordance with the prescribed value for low-voltage connections. At the moment of direct connection (process 2) at approximately synchronous speed, there is again a short-term decline of about 4.2 % which meets the limit of 6 % for WPPs; nevertheless, the decline is outside of the range of 2 periods.

For switching, i.e., connecting the wind power plant to the external grid, the so-called current surge factor is defined. This factor is given by the ratio of the inrush current surge to the rated current of the generator and is equal to 4 for induction generators connected with 95–105 % of synchronous speed.

Reactive power control applies to sources of 5 MW and above. These sources must be equipped for some of the following modes of reactive power control: maintaining the specified power factor, maintaining the desired value of reactive power (take-off/supply) within the operating machine diagram, maintaining the voltage in the transfer point (block connection of a generator and the block transformer). The generator must be able to supply power in the range of power factors of 0.85 (supply of the reactive power of inductive nature) to 0.95 (generator running in an underexcited state) at the permitted range of voltage on the generator terminals and at frequency in the range of 48.5–50.5 Hz. In the compensating device of sources, it is necessary to consider the manner of production operation and the resulting reverse effects on the system voltage. When the drive of wind power plants heavily fluctuates, the reactive power compensation must be automatically and sufficiently quickly regulated.

Figure 2.37a shows the course of power factor at the switching process of connecting the wind power plant to the external grid. The figure clearly presents the variance of a power factor, from 0.56 for the inductive character to 0.98 for the capacitive character. For 2-step compensation device connected to the analyzed wind power plant according to the block diagram in Fig. 2.32, it is clear that the compensation is insufficient, mainly in the area of motor starting. Inadequacy of the compensation is also enhanced by the difference in output ratios when operating the pole-changing generator (changing the number of poles to 6/8) which corresponds to the rated power of 150/30 kW. The course of connecting the capacitor battery is shown in detail in Fig. 2.37b.

Figure 2.37 demonstrates the distortion due to parallel resonance between the stray reactance of the transformer, the reactance of the generator and the sum of all external grid capacitances including the compensating device, which is evident from the course of currents. Connection of the capacitor battery is also accompanied by the formation of overvoltage (up to 1.5)—see Fig. 2.37.

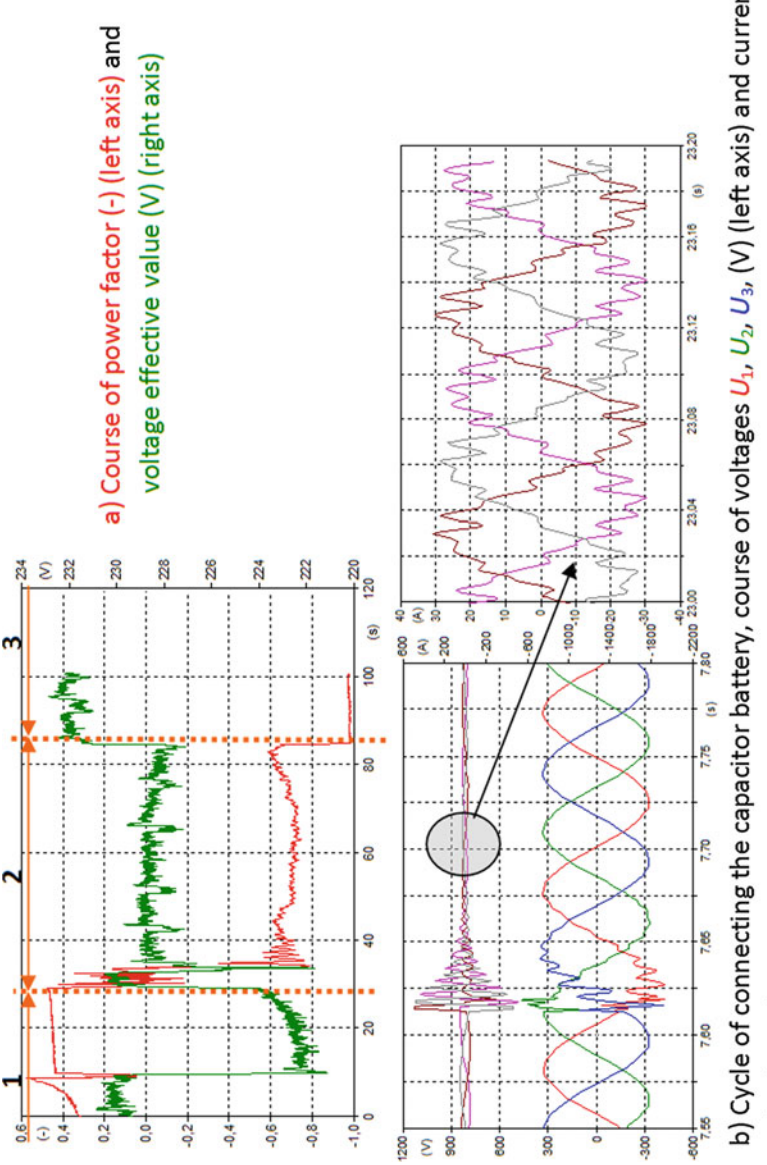

Fig. 2.37 Analysis of the process of connecting the wind power plant to the external grid—detail the compensation device connection

2.3 Large Wind Power Plants

In recent years of the development of wind power plants (WPPs) in the Czech Republic, the investors therefore mainly preferred construction of high-capacity wind power plants (large wind power plants); with regard to a substantial increase in the height of the wind power plant tube, the priority for their construction was not high altitude as they can also be used in lowland sites. In the case of building modern high-capacity power plants, mainly the following fundamental trends of development were respected:

- increase in the WPP unit output associated with the increased size of the wind turbine rotor,
- increase in the WPP tube height,
- improvement in the quality of WPP technology and the consequent reduction in fault rate, noise and other negative impacts,
- reduction in the unit costs of WPP construction and operation, etc.

Unlike medium and low-capacity WPPs, the high-capacity WPPs use of wind turbines with swivelling propeller blades, i.e., the pitch type regulation, which allows adjustment of the blades according to the current wind speed through their swivelling. A further substantial difference from the medium and low-capacity WPPs is the location of the transformer (typically with the ratio of transformation of 0.69/22 kV) directly in the WPP nacelle where it also balances the relatively large masses of the turbine, generator and semiconductor technology. A typical arrangement for high-capacity WPPs, together with a basic description, is presented in Fig. 2.38.

The wind turbine blades are usually made of plastics reinforced with glass fibres whereas the reinforcement can also be made using carbon fibres or laminates. Some blades are fitted with technologies for protection against lightning strikes. In cold areas, the blades are equipped with a heating device to prevent icing. Angle of the blades is controlled by a control system and is usually adjusted by a hydraulic system or electric motors. The pitch type regulation also allows for a more even start of the turbine when the wind speed rises (Table 2.2).

To achieve an optimal gear ratio, the high-capacity WPPs are fitted with a planetary gearbox with variable transmission ratio. The planetary gear consists of a sun gear (central gear), satellites, the satellite carrier and the ring gear. The sun gear, ring gear and the satellite carrier have a common axis. The satellites are placed on the carrier and are engaged in the central as well as ring gear. The basic advantages of the planetary gearbox include:

- smaller dimensions compared to conventional gearboxes,
- simpler shifting due to gears in constant engagement,
- longer lifespan of gears than in conventional gear units,

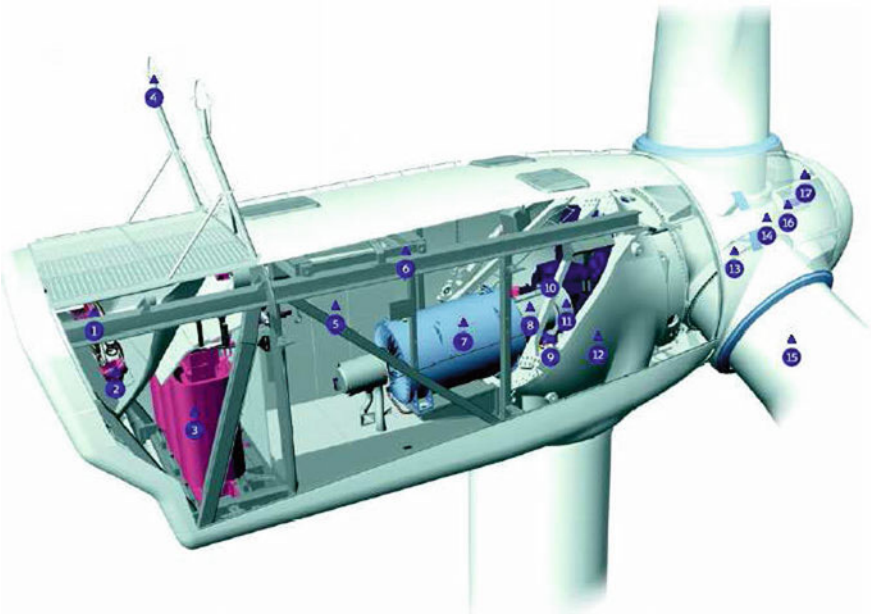

Fig. 2.38 Structural division in the nacelle of a large WPP (VESTAS V90)

Table 2.2 Components of large wind power plants

1	Oil cooler	10	Gear unit (gearbox)
2	Cooler of water for the generator	11	Mechanical clutch
3	Transformer	12	Machine frame
4	Ultrasonic wind sensor	13	Bearing of the rotor blades
5	Inverter control panel	14	Rotor head
6	Service crain	15	Turbine blade
7	Generator	16	Cylinder for adjusting the angle of inclination
8	Composite clutch	17	Controller for adjusting the angle of inclination
9	System for swivelling the nacelle		

- easy achievement of large gear ratios with respect to the dimensions,
- torque reaction only, symmetric distribution of the load, more gear combinations.

Its drawbacks may include higher bearing loads, more complex design and higher cost compared to conventional transmissions. The operating principle is illustratively shown in Fig. 2.39.

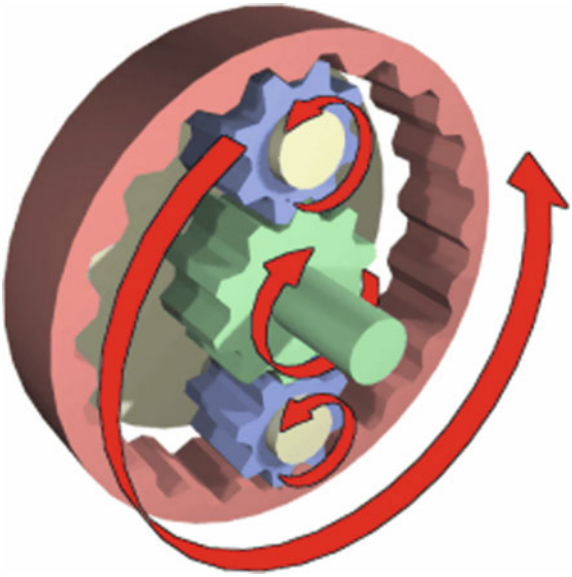

Fig. 2.39 The operating principle of planetary gearboxes

2.3.1 Control Systems for High-Capacity Wind Power Plants

High-capacity WPPs, i.e., wind power plants with their capacities in the range of hundreds of kV·A up to units or tens of MV·A, are characterized by bringing the output on the generator terminals to the external grid through power electronics which helps to optimize the plant operation including the connection process, regulation for maximum wind energy utilization within a wide range of wind speeds and provision of qualitative elements of the electric energy. After various prototype solutions, the control systems for high-capacity wind power plants have settled on two essential solutions that differ from each other by the type of generator used and the method of connecting the power electronics-converter through which the output from wind power plants is brought into the external grid.

2.3.2 WPP Control System Cooperating with Frequency Converters

Currently, the high-capacity (usually 850 kW) wind power plants mostly use control systems with induction generators with wound rotors utilizing cooperation with a frequency converter with recuperative unit. It is a system in the so-called "cascade connection". When works the WPP control system with frequency

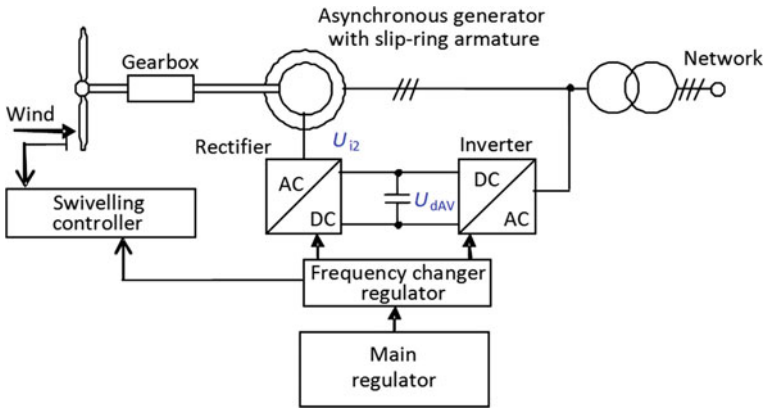

Fig. 2.40 The system of wind power plant with frequency converter in the cascade connection

converter, it is possible to better use the wind energy flow and ensure a more stable supply of electricity to the external grid.

If the system works in cascade, the generator stator is directly connected to the electricity supply system (through a low voltage/medium voltage transformer) and the wound rotor of the generator is powered from the frequency converter.

It is a special connection of indirect frequency converter consisting of two thyristor bridges. The converter is connected between the rotor of the slip-ring induction motor with a slip frequency and the external grid (Fig. 2.40).

The control principle is as follows: Voltage u_{i2} is induced in the rotor of induction machine and the control voltage is brought against from the converter. This control voltage is actually the voltage of the DC intermediate circuit, $U_{d\mathrm{AV}}$, that is set using the control angles of the inverter consisting of a 3 phase thyristor bridge operating in an inverter mode. When the control voltage is changed, u_{i2} changes in the same way; e.g., if increased, u_{i2} grows—therefore, the slip must increase and the speed falls accordingly. If the control voltage is zero, i.e., for the control the angle $\alpha = 90°$, the speed is approximately synchronous. Speed control through the slip when using control voltage is also utilized in classical loss control by rotor resistors where its function is represented by voltage drop across these resistors. This drop, however, is dependent on the load and the torque characteristic therefore becomes softer. In the cascade control, the control voltage is independent of the load and torque characteristics are the same as in the frequency control [11].

To determine the power balance when operating the system in subsynchronous cascade, it is possible to rely on general relations for output ratios of induction machines.

The following holds for the machine moment (torque):

$$M = \frac{P}{\omega} = \frac{P_\delta(1-s)}{\omega_1(1-s)} = \frac{P_\delta}{\omega_1} \tag{2.27}$$

where P_δ is the output in the air gap, ω is the angular velocity of the rotor and ω_1 is the angular velocity of the stator field, i.e., synchronous angular speed.

On small slips, almost entire P_δ is consumed for the mechanical output according to the following relation

$$P = P_\delta(1 - s) \tag{2.28}$$

Oh higher slips, however, the remaining, the so-called slip output $s \cdot P_\delta$, is redundant. The synchronous cascade transfers it back to the external grid; under resistance control, it is converted into heat output, i.e., power dissipation.

The cascade is therefore advantageous, both in terms of control and economy.

2.3.3 Switching the Wind Power Plant in the External Grid

Operation of the WPP control system in cooperation with the frequency converter is mostly ensured by multiprocessors. The control system evaluates the wind velocity and wind turbine speed; the torque characteristic of the machine is adapted accordingly. The course of voltage and current on the generator rotor is therefore controlled in order to maximally utilize the wind energy assuming minimal negative impacts on the external grid. The output power controlled by the frequency converter is fractional compared to the generator output; therefore, its effects on the distribution external grid can be negligible. The control system also ensures connecting to the external grid with minimal current surges in generator operation and without significant overvoltage events.

Figure 2.41 shows a detail of the connection of a WPP system with induction generator with wound rotor in the so-called cascade connection (2 MW, 690 V, D connection). Figure 2.41 demonstrates the optimization of the WPP connection to the external grid without high-frequency transients, with current surges corresponding maximally to 1/3 of the rated current of the generator. In modern WPPs, these current surges are further limited by switching the Y–D stator winding.

Special rotor winding is energized through rings from the four-quadrant frequency converter. A choke and sinusoidal filter are placed between the converter and the rotor winding in order to smooth the voltage and current waveforms.

For switching, i.e., for connecting the wind power plant to the external grid, the so-called current surge factor is defined by [5]. This factor is given by the ratio of the inrush current surge to the rated current of the generator is equal to 4 for induction generators connected with 95–105 % of synchronous speed.

A priority for the operator of the external grid is maximum elimination of adverse effects of the WPP operation on the external grid. These effects are primarily caused by the way of connecting the wind power plant generator to the external grid, parameters of the external grid connection point (short-circuit capacity) and the choice of the measuring and control equipment. The way of

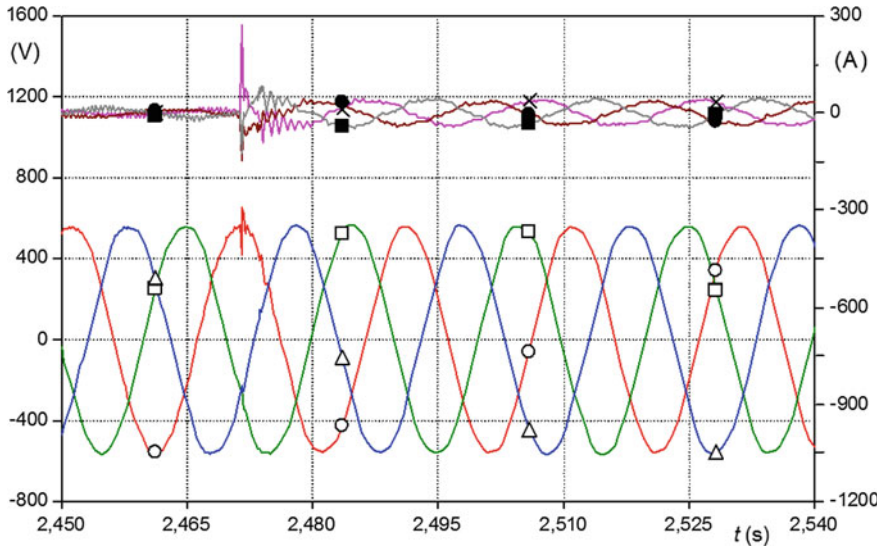

Fig. 2.41 A detail of the connection of the system with induction generator with wound rotor in the cascade connection, the course of phase voltage U_1 (*red*), U_2 (*green*), U_3 (*blue*) (V) (*left axis*) and stator winding currents I_1 (*pink*), I_2 (*brown*), I_3 (*grey*) (A) (*right axis*) (color figure online)

connection to the distribution external grid is provided by the competent operator of the external grid on the basis of the given external grid conditions, power and the method of production operation. It is important to choose an appropriate switching device. During switching, there can be short-term changes in voltage; according to [5], for power plants with the connection point in the LV external grid, the allowable tolerance is ≤ 3 % of the rated voltage unless the switching occurs more frequently than once every 90 s. In wind power plants with induction generators, short-term declines may occur during the connection due to internal transients. Such a decline may reach a double of otherwise allowable value (approximately 6 % for low voltage) unless lasting longer than 2 periods [5]. For wind power plants, it is necessary to consider a special switching factor dependent on the system conditions, which is used to evaluate their switching and which also respects the mentioned ultra-short transients.

For comparison, Fig. 2.42 shows the course of instantaneous values of the phase voltage at the connection point for the WPP for the system with squirrel-cage induction generator (150 kW, 400 V, D connection) and the system with induction generator with the wound rotor in the cascade connection (2 MW, 690 V, D connection) at the moment of connecting the WPP to the power supply system (time 12 ms in Fig. 2.42). Figure 2.42 again clearly demonstrates the following: if the process of connecting the WPP to the external grid is optimized using the control by recuperative frequency converter (U_{1f} in Fig. 2.42), there is no significant transient affecting the steady course of the system voltage. If the wind power

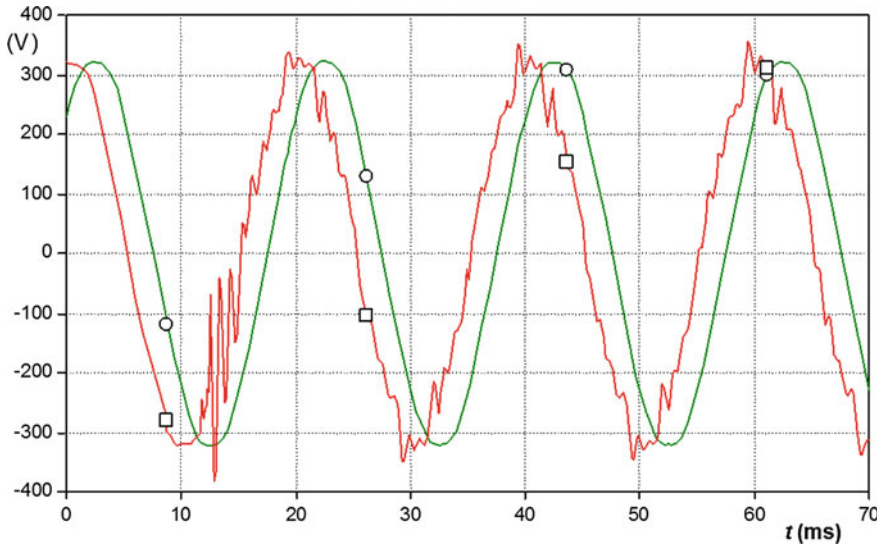

Fig. 2.42 The course of instantaneous values of phase voltage at the WPP connection point for the system with squirrel-cage induction generator (*red*) and the system with induction generator with wound rotor in the cascade connection (*green*) (color figure online)

plant is connected to the external grid via a thyristor starter, the current surge is limited but overvoltage may be present (U_{1f} in Fig. 2.42) [12].

2.3.4 *Comparison of Different Systems of Wind Power Plants*

Using the results of experimental measurements on wind power plants with various capacities and control systems, we analyzed switching processes in three systems used in WPPs with rated capacity of about 1.5 MV·A for a synchronous machine, and 1.4 in the range of 1–1.6 MW for an induction machine.

Particularly, the following systems were involved:

- Control system with a synchronous generator with separate excitation and direct connection to the external grid.
- System with an squirrel-cage induction generator and direct connection to the distribution external grid.
- Control system with an induction generator with wound rotor and frequency converter in the cascade connection.
- Analysis of reverse effects of switching processes was carried out for the same conditions of the actual load setup, the same power system topology and identical conditions of the mechanical input on the shafts of individual generators.

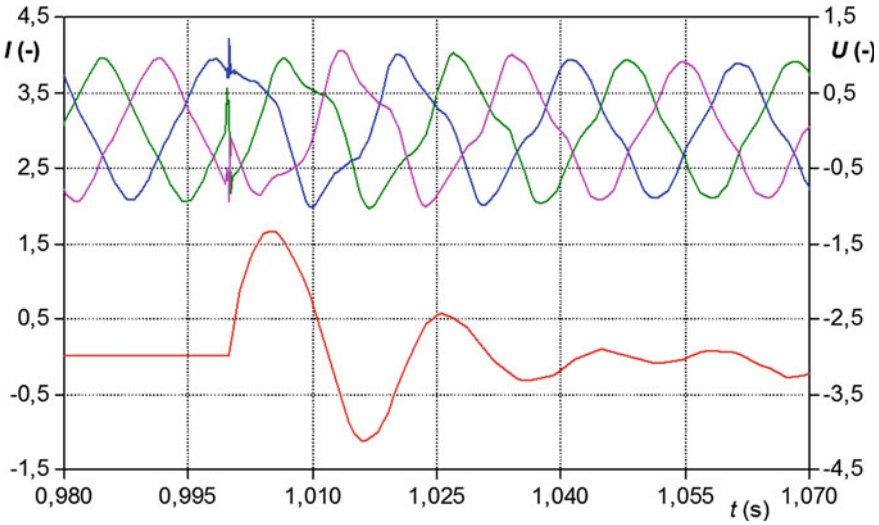

Fig. 2.43 The course of instantaneous voltage values at the connection point U_1 (*blue*), U_2 (*green*), U_3 (*pink*) (–) and one phase current I_1 (*red*) (–); a detail of the WPP connection—synchronous generator (color figure online)

Specifically, the switching processes were evaluated according to the following parameters:

- relative current surge at the moment of connection I/I_N,
- relative voltage change at the connection point at the moment of connection U/U_N,
- THD voltage at the moment of connection and in the steady-state of the generator operation of the analyzed machine.

Figure 2.43 shows a detail of the connection of the WPP with synchronous generator and the system of direct connection to the distribution external grid. At the moment of connection, we simulated the conditions for connecting the synchronous generator excited to the rated value at the connection point and the difference in frequencies up to about 15 % of the system frequency while respecting the direction of rotation and the phase sequence. The figure demonstrates the current surge with the relative value of 1.58, subsequently causing a percentage change in voltage at the connection point up to the relative value of 1.02. The resulting values are always relative to the rated current of the given generator and the rated voltage value at the connection point of the WPP. The figure also shows the voltage waveform distortion; this distortion disappears in the steady state and THD settles at the value of 1.1 %.

Connection of an squirrel-cage induction generator and the system of direct connection to the distribution external grid is shown in Fig. 2.44. The induction

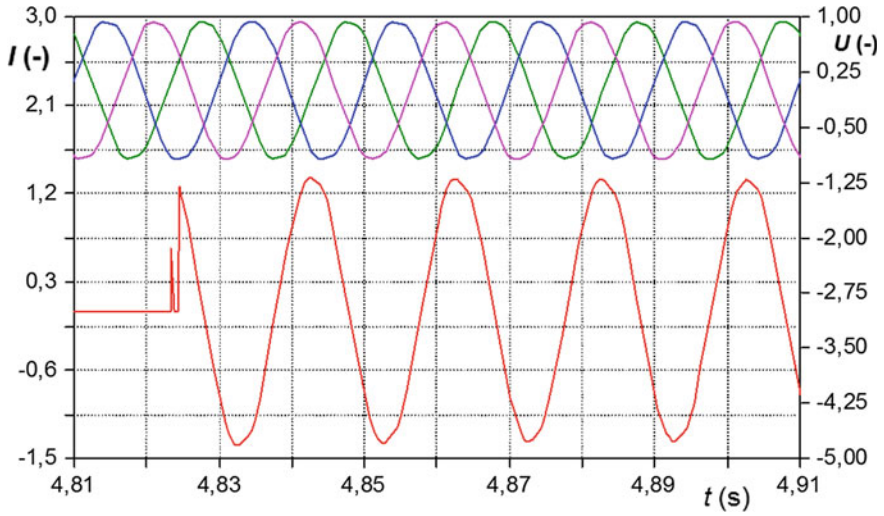

Fig. 2.44 The course of instantaneous voltage values at the connection point U_1 (*blue*), U_2 (*green*), U_3 (*pink*) (–) and one phase current I_1 (*red*) (–); a detail of the WPP connection—induction generator (color figure online)

generator was connected as non-excited; for the graphic demonstration, we have chosen the state of connection at generator speed approaching the synchronous speed (−2 %). This resulted in a current surge with amplitude having a relative value of 1.2 (Fig. 2.45).

At the moment of connecting the compensation, we observe a similar surge, but reactive in its nature, and the corresponding voltage waveform distortion at the connection point with amplitude of about 1.2 which disappears after about 2 waveform periods.

Figures 2.46 and 2.47 show the voltage and current waveforms for the last analyzed system, i.e., the system with induction generator with a wound rotor and frequency converter in the cascade connection. It is the most commonly used system in the Europe; in terms of the observed parameters, it exhibits lower values of the current surge and percentage changes in voltage as evidenced by Fig. 2.46 where the resultant value of the current surge does not exceed 50 % of the rated current. Figure 2.46 further demonstrates the course of voltage at the connection point and the course of one current phase in the steady state of the generator operation (Table 2.3).

Furthermore, a comprehensive evaluation of the systems was performed on the basis of:

- the results obtained from experimental measurements of the team of authors,
- the analysis of the database of faults for selected types of control systems (criterion—reliability),
- offering sheets (criterion—price).

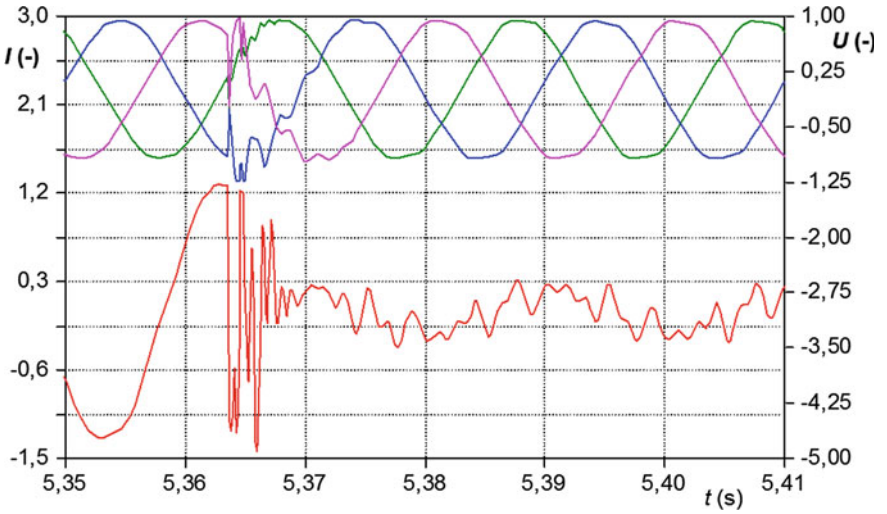

Fig. 2.45 The course of instantaneous voltage values at the connection point U_1 (*blue*), U_2 (*green*), U_3 (*pink*) (–) and one phase current I_1 (*red*) (–); a detail of the WPP compensation connection—induction generator (color figure online)

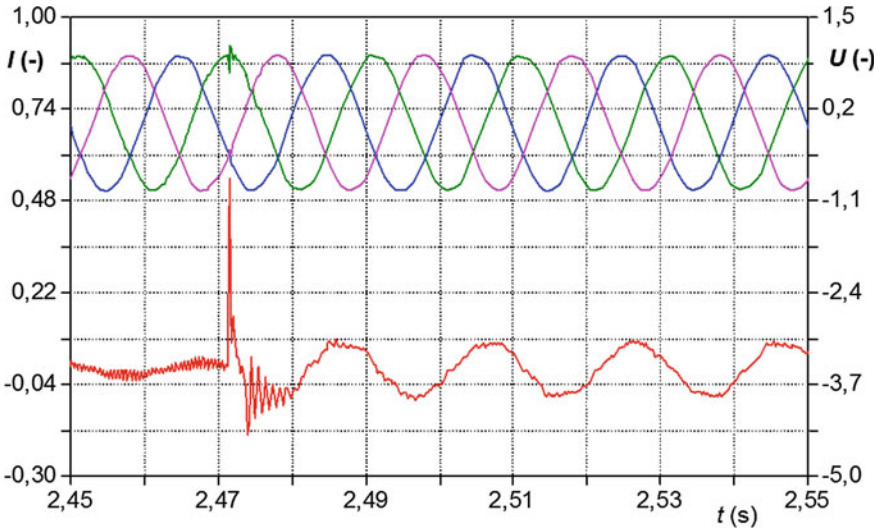

Fig. 2.46 The course of instantaneous voltage values at the connection point U_1 (*blue*), U_2 (*green*), U_3 (*pink*) (–) and one phase current I_1 (*red*) (–); a detail of the WPP connection—induction generator with frequency converter in the cascade connection (color figure online)

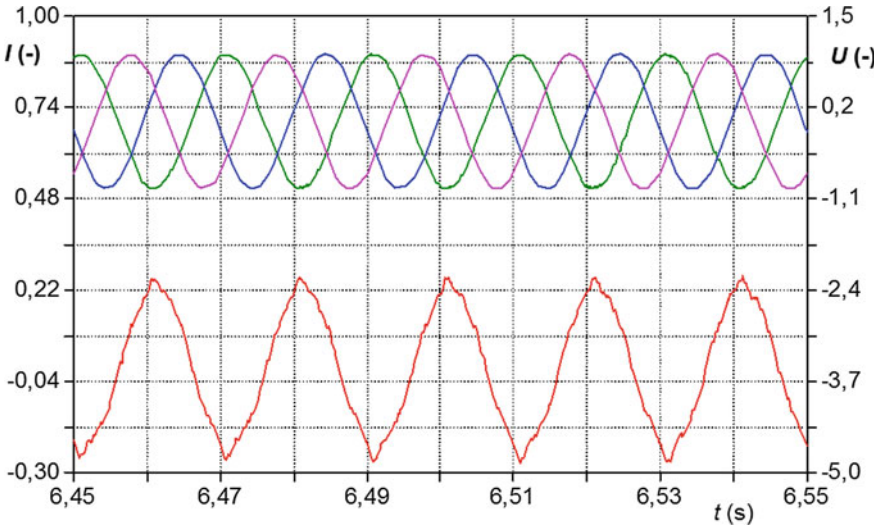

Fig. 2.47 The course of instantaneous voltage values at the connection point U_1 (*blue*), U_2 (*green*), U_3 (*pink*) (–) and one phase current I_1 (*red*) (–); a detail of the WPP operation in the generator mode—induction generator with frequency converter in the cascade connection (color figure online)

Table 2.3 The final evaluation of the WPP control systems

Source	Connection status	I/I_N	U/U_N	THD
SG	Optimal	1.12	1.03	1.1
	Speed +1 %	1.46	1.02	1.1
	Voltage +1 %	1.12	1.02	1.1
	Voltage −1 %	1.07	1.02	1.1
	Dephasing 5°	1.17	1.02	1.1
	Dephasing 15°	1.58	1.02	1.1
	Dephasing 30°	2.37	1.02	1.1
	Dephasing 45°	2.39	1.02	1.1
	Output outage 50 %	0.63	1.01	1.1
	Optimal	1.2	0.95	1.8
ASG	Speed +10 %	2.5	0.90	1.8
	Speed −10 %	2.5	0.90	1.8
ASG + FR-ME	Independent	By setting (<1)	RMS—no effect (<1)	3.2

The resulting evaluation is shown in Table 2.4 where the scores of 1 and 5 correspond to the best and the worst rating, respectively.

For an optimum process of connecting to the external grid, the synchronous generator with separate excitation and direct connection needs a phasing device ensuring the synchronization of waveforms of the machine output voltage and the voltage at the connection point. However, even in the case of optimum connecting

Table 2.4 Overall evaluation of the WPP control systems

	Synchronous generator with separate excitation	Induction generator with direct connection	Induction generator in the cascade connection with frequency converter
Steady-state THD voltage	2	2[a]	3
Current surge at the moment of connection	3[b]	3	1
Voltage change at the moment of connection	3	2[c]	1
Utilization of torque on the wind turbine shaft for the given wind velocity	4	4	1
Possibility of regulating the reactive power	1	5	1
Price	3	1	2
System reliability	3	1	3

1—best, *5*—worst

[a]Valid for a steady state after connecting the compensation battery

[b]Valid in the case of ensuring optimal phasing conditions

[c]Valid in the case of connecting a non-excited machine (without the capacitor battery)

process, there is a current surge having mainly active character—with regard to the accuracy of measuring the phase shift of voltage signals and the corresponding change in the frequency of connected source systems (score 3). The dynamic current surge then causes a short-term voltage drop about 2 periods of the voltage signal (score 3). The quality of the supplied power and the corresponding THD value of the voltage signal is primarily derived from using semiconductor elements in the control system of the WPP with the induction machine and also from the value of the harmonic modulation of the excitation system (score 2). In the case of a synchronous machine with separate excitation, it is possible to control the reactive power in both quadrants of the Gaussian plane; therefore, the inductive reactive power can be supplied and also consumed (score 1). In the case of a synchronous generator with a direct connection through the synchronization unit, it is difficult to utilize the wind speed in its wide range; the generator is connected at the speed near synchronous speeds and the wind energy is not utilized optimally, even when assuming that the wind turbine is fitted with the planetary gearbox (score 4 and the planetary gear and score 5 for a transmission with a constant speed ratio). With reference to the necessity of the excitation system and the corresponding control system, this system can be included among the less reliable systems in comparison with induction generators, for example (score 3). The requirement for excitation system in a relatively high price (Grade 3). The requirement for excitation system is also reflected in a relatively high price (score 3).

When connecting a non-excited squirrel-cage induction generator to the external grid, we observe a current surge of mainly active character because this system is usually connected at subsynchronous speed (score 3). If considering the connection

process for an induction machine in non-excited state, there is usually no voltage drop at the connection point (score 2). The quality of electricity is determined by the machine design and the characteristic of the compensating device. If the compensation device is designed optimally for the entire range of machine speeds, there is no significant distortion of the output current and the corresponding distortion of the output voltage (score 2). Although it is possible to use a pole-changing induction machine or machine with double winding, the machine does not utilize the wide speed range optimally (score 4). From the design point of view, the squirrel-cage induction machine represents the simplest system which is also reflected in the price (score 1) and the overall reliability (score 1).

Systems with an induction generator with wound rotor in cascade connection with a frequency converter are the most widely used WPP control systems in the Europe. Using the frequency converter and control system optimizes the process of connection without current surges (score 1) and consequent voltage changes (score 1). The frequency converter control system subsequently adapts the torque characteristic of induction machines for the entire range of wind velocities; the system is therefore capable of supplying electricity continuously within the entire range of available wind speeds and torque on the shaft of the wind motor (score 1). However, the frequency converter affects the overall quality of supplied electricity; the values of current (as well as voltage) distortion factor may be higher, especially in the lower output range (score 3). When considering the cooperation between induction machines with wound armature and frequency converter in the cascade connection, the converter output is designed only for approximately 30 % of the overall machine output; this also affects the total price which is comparable with the price of synchronous generators (score 3).

2.4 Reactive Power Regulation

At present, the most widely used systems are those with frequency converter, operating in the cascade connection with the frequency converter. Nevertheless, the power factor regulation is another problem associated with bringing the output of WPPs with induction generator to the external grid. As results from the principle of induction machine operation, the power factor is not constant. This machine needs reactive energy for its magnetization and therefore acts as a consumer of inductive reactive power. The inductive current component, taken by induction machines from the distribution external grid, is proportional to the rotor field frequency and the slip value. However, if the induction machine output is brought to the external grid via a frequency converter with a recuperation unit with voltage or current DC bus, the power factor/true power factor value at the outlet from the WPP can be regulated within the desired range using the reactive power control, through the elements in the voltage intermediate circuit, and such a system (induction machine + frequency converter) can thus operate in all four quadrants of the PQ diagram (active power P vs reactive inductive power Q).

Generally, according to [5], the electrical power sources are subject to the following set rules for any of the below-mentioned modes of reactive power control:

- maintaining the specified power factor,
- maintaining the set value of reactive power (take-off/supply) within the operating machine diagram,
- maintaining voltage at the transfer point (generator outlet, behind the block transformer).

The generator must be able to supply power in the power factor range of 0.85 (the supply of reactive power of inductive character) up to 0.95 (the supply of reactive power of capacitive character) at the allowed range of voltage on the generator terminals and at the frequency range of 48.5–50.5 Hz. Regarding the compensating device of sources, it is necessary to consider the manner of production operation and the resulting reverse effects on the external grid voltage. In case of heavily fluctuating outputs of WPP drives, the reactive power compensation must be regulated automatically and sufficiently quickly. As already mentioned in the introductory part of the text, the lack of compensation at fluctuating power is a disadvantage mainly in systems utilizing squirrel-cage induction generators designed as step-switched. The mentioned disadvantage is solved by using frequency converters allowing 4-quadrant operation; power factor of the control system is then usually in the range of 0.96 (inductive character) up to 0.98 (capacitive character). In machines fed by frequency converters with vector-oriented control, it is therefore possible to achieve an optimum magnetic flux control and reductions in the required reactive energy.

Figure 2.48 shows a PQ diagram of the system of WPP with frequency converter (2 MW, 690 V, D connection). Figure 2.48 clearly demonstrates the following: when using the system with frequency converter in the cascade connection, it is possible to regulate the supply of active power with constant power factor in the mode of supplying reactive power of inductive nature (red curve in Fig. 2.48) or reactive power of capacitive nature (green curve in Fig. 2.48). Based on an agreement with the operator of the external grid to which the WPP is connected, the WPP control system defines the operation area according to the PQ diagram.

2.4.1 Selected Reverse Effects on the External Grid

The next chapter analyzes the selected qualitative parameters of electricity supply for the control system of a WPP using an induction generator (2 MW, 690 V, D connection) with wound rotor in the cascade connection with a voltage-type frequency converter according to the block diagram in Fig. 2.40.

As mentioned above, it can be expected that the operation of a wind power plant will affect the parameters of the external grid. Interaction between the external grid and the analyzed WPP is defined in the so-called connection point.

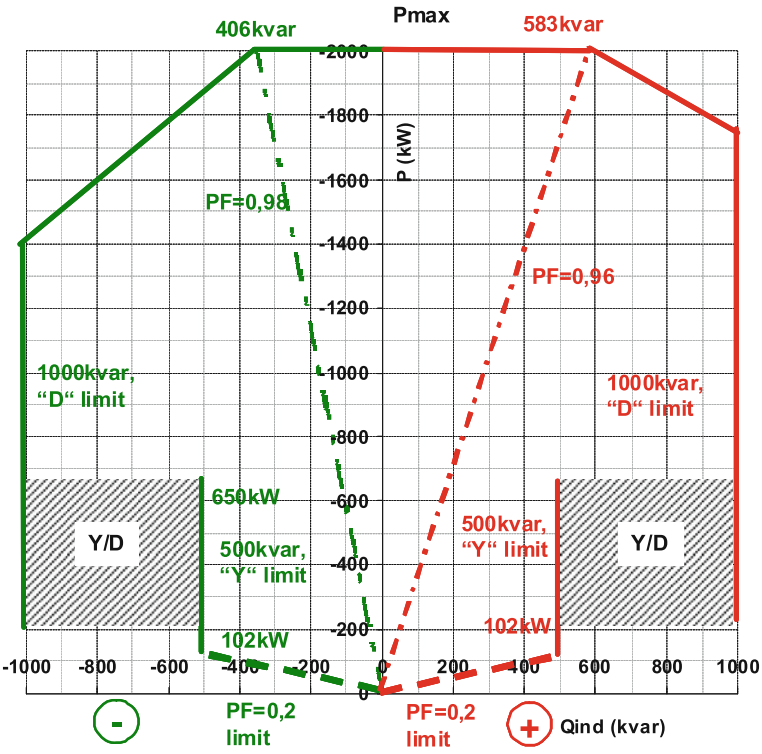

Fig. 2.48 Operating diagram of the system with frequency converter in the cascade connection (2 MW, 690 V, D connection)

For the operator of the distribution external grid, the priority is to ensure a stable supply of electricity, preferably with constant system parameters.

In terms of quality of the supplied energy, it is necessary to particularly monitor:

1. Changes in voltage.
2. Flicker—voltage fluctuations.
3. Effects on the devices of mass remote control.

Changes in Voltage

Annex no. 4 [5] stipulates that the changes in voltage caused by the power supply from connected sources, i.e., wind power plants in our case, must not exceed 2 % of the nominal voltage U_N for WPPs connected to the medium-voltage external grid.

$$\Delta u_{vn} \leq 2\,\% \tag{2.29}$$

In our case, the wind power plants are connected to 22 kV external grid, i.e., the phase voltage is about 12.7 kV; the maximum allowable increase in voltage is then about 254 V. As shown graphically in Fig. 2.49, the voltage change ΔU copies the

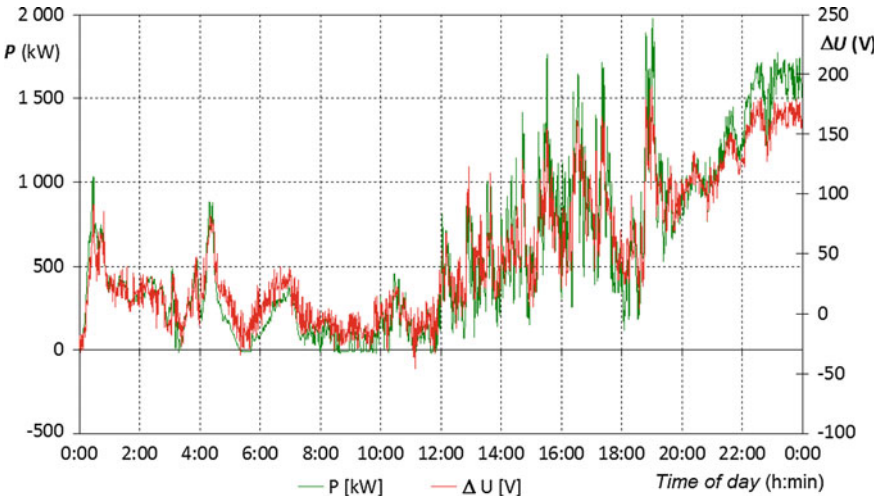

Fig. 2.49 Effect of power supplied from WPPs on changes in voltage at the connection point

change in power supplied. At the maximum supplied power (2 MW), at the time around 19:12, the voltage increased maximally by 200 V, which meets the condition defined by the rules for operating distribution external grids [13, 14].

Flicker—Voltage Fluctuations

Flicker is defined as a fluctuation in the light flux of light sources due to periodic voltage drops in the area of subharmonic frequencies, perceptible by human eye. These voltage variations are generally caused by changes of load in consumers or changes in power generation.

If analyzing the theoretical possibility of flicker which accompanies the operation of wind power plants, we may identify two basic causes of its origin: the influence of wind gusts and the influence of the wind power plant tube.

At short-term deviations of the wind velocity from its mean value, the influence of wind gusts is eliminated by the inherent inertia of rotating parts of the wind power plant; the influence of stronger gusts is more or less eliminated by the turbine power control.

Effect of the tower (mast) can be suppressed much harder. The tower represents an obstacle for wind flow and slows it down. At the moment when the turbine blade coincides with the tower, the turbine output is also naturally reduced. This is also one of the reasons why large wind power plants are always built with the turbine located before the tower (upwind placement). In the construction with the turbine located behind the tower (downwind placement), the blade would get to a complete wind shadow of the tower. Due to such resulting periodic power drop, both active and reactive, the following voltage drop arises across the external grid impedance:

$$\Delta U = \frac{\Delta PR + \Delta QX}{\sqrt{3}U_N} \tag{2.30}$$

where ΔU is the voltage drop across the external grid impedance (V); ΔP, ΔQ are active and reactive variations in the WPP output (W, var); R, X are external grid resistance and reactance (Ω); and U_N is the external grid rated voltage (V).

The relation (2.30) clearly indicates that changes in voltage causing the flicker do not virtually exist in external grids with significantly inductive character. Changes in active power, which tend to be greater than the changes in reactive power, are negligible at low-resistance external grids [15].

When respecting the external grid short-circuit power at the common feed point, it is possible to obtain the below-mentioned relationship for the proportional voltage drop:

$$\frac{\Delta U}{U_N} = \frac{\Delta S}{S_k''}\cos\left(\psi + \varphi_f\right) \tag{2.31}$$

where $\psi = arctg\frac{X}{R}\,\psi$ is the angle of external grid impedance, $\varphi_f = arctg\frac{\Delta Q}{\Delta P}$ is the relevant flicker angle, S_{kV} is the external grid short-circuit power at the common feed point.

However, the voltage drop caused by flicker is not directly used as a parameter determining the flicker; for this purpose, we use the quantity called the flicker emission or the level of flicker perception. We distinguish between the short-term flicker emission P_{st}, measured or counted in a time interval of 10 min, and the long-term flicker emission P_{lt} determined for the interval of 2 h. The flicker emission is proportional to the relative voltage drop:

$$P_{\mathrm{st,lt}} = \mathrm{d}u = \frac{\Delta u}{U_N} \tag{2.32}$$

Generally, the more blades of the wind turbine, the less the flicker emission. In most cases, the systems with frequency converter have less emissions than the systems with induction generator connected directly [16].

Magnitude of Voltage Drops

The total torque of the turbine is given by the sum of partial moments per individual blades; a third or half of the total torque falls on one blade in the case of 3-blade or 2-blade turbine, respectively. At the moments when the blade occurs in the area of the tower influence, the generator connected to the 3-blade turbine loses a third of its active output provided that the speed is constant. If connected to the 2-blade turbine, it loses a half of its output. If knowing also the change in reactive power, we can use the above relation (2.32) to calculate the relative voltage drops at the common feed point of the local external grid. Except the magnitude of the voltage drops, it is also essential to know the time of their duration and their frequency.

The latter two parameters are independent of the external grid and the generator; they are determined only by the equipment design.

Frequency of Voltage Drops

Repetition frequency of voltage drops in the external grid is derived from the turbine speed and number of blades. The frequency of blade passages along the tower is given by the following relation

$$f_f = a \cdot \frac{n_t}{60} \tag{2.33}$$

where f_f is the frequency of the voltage drop (Hz), a is the number of turbine blades, and n_t is the turbine speed (min^{-1}).

Therefore, it is a simple linear relationship where we additionally assume a direct proportionality between the changes in voltage and luminous flux of the light sources.

Human eye is capable of perceiving changes in the luminous flux from the frequency of 0.5 Hz up to 25 Hz and is most sensitive to frequencies around 9 Hz; with respect to the flicker phenomenon, the working speed of the wind turbine should therefore avoid this frequency band. However, this is impossible. The speeds of wind turbines typically achieve 30–50 revolutions per minute and this is reflected in the frequency of external grid voltage drops of 2–3 Hz.

Any design efforts may therefore result only in minimizing the emergence of flicker as the consequence of WPP operation but they can never completely remove it for physical reasons.

Duration of Voltage Drops

If the frequency of voltage drops is given only by the turbine design, their duration is also directly influenced by the size (diameter) of the tower—see Fig. 2.50.

If the turbine is characterized by its radius R, then the tower can be characterized by its radius r. Because of the conical shape of towers, the simplified calculation uses a mean diameter or mean radius. The time t, for which the blade passes along the tower, is determined by the circumferential speed of the blade tip v_R and the tower diameter $2r$. The circumferential speed is given by the following relation

$$v_R = \omega \cdot R \tag{2.34}$$

where R is the turbine radius, $\omega = \frac{2 \cdot \pi \cdot n_t}{60}$ is the angular velocity, and n_t is the turbine speed (min^{-1}).

The distance, that the blade must overcome, equals to the tower diameter. The time required is therefore given as

$$t = \frac{1}{\omega} \cdot \frac{2r}{R} \tag{2.35}$$

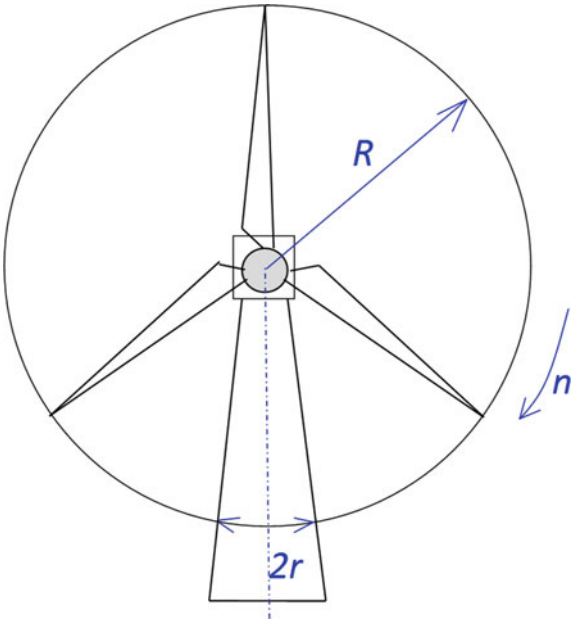

Fig. 2.50 A scheme for determining the duration of voltage drops

The ratio $R/2r$ (or its reciprocal value) is a characteristic number which, together with the turbine speed, ultimately determines the duration of voltage drops in the external grid caused by the wind power plant.

With the turbine radius $R = 40$ m and the average tower diameter of 3 m, which corresponds to the real situation, the voltage drop takes a full period of the external grid frequency, i.e., 0.02 s.

The flicker emergence is therefore given by three variables—the magnitude, frequency and duration of voltage drops; however, it is impossible to clearly determine which of them has greater impact. It is true that restrictions of any of these variables are positively reflected in the flicker reduction. Therefore, it is possible to establish the following general principles:

- Wind power plants should not be connected to local distribution external grids with low surge short-circuit output.
- Wind power plants with induction generators connected directly to the external grid should be connected in places where the value of the external grid impedance angle is close to 70°.
- Operating turbine speed should be lower rather than higher. The higher the turbine speed, the more sensitive reaction of human eyes.
- The ratio of the turbine radius to the mean tower radius $R/2r$ should be maximized.

However, the voltage drop caused by flicker is not directly used as a parameter determining the flicker; for this purpose, we use the quantity called the flicker

emission or the level of flicker perception. We distinguish between the short-term flicker emission P_{st}, measured or counted in a time interval of 10 min, and the long-term flicker emission P_{lt} determined for the interval of 2 h.

Generally, the more blades of the wind turbine, the less flicker emission. In most cases, the systems with frequency converters exhibit less emissions than systems with induction generators connected directly.

The rules for operating the external grid again define the maximum permissible values of the long-term level of flicker perception P_{lt}: it must not exceed the level of 0.46.

This value (0.46) indicates the contribution to the total P_{lt} caused by the source, i.e., the wind power plant. Figure 2.51 shows an example of the analysis of the wind power plant contribution to the increase in the value of long-term flicker perception at the connection point. 95 % value, $P_{lt} = 0.587$ (average of three phases: 0.581, 0.604, 0.577), was detected for the connection point. Given the fact that the standard specifies the permissible value, $P_{lt} = 1$, we can conclude that the connection point meets the requirements of the standard.

As demonstrated by the performed measurement whose results are shown in the graph in Fig. 2.51, it is impossible to prove the influence of the magnitude of the power supplied on the level of flicker perception P_{lt}. In Fig. 2.51, we can see the course of P_{lt} during the period of one week where P_{lt} values range from 0.338 to 0.631.

With respect to the permitted value ($P_{lt} = 1$) and the highest found 95 % value ($P_{lt} = 0.604$), it can be concluded that the wind power plant does not exceed the allowable contribution of 0.46 of the total P_{lt} value, and that our found value of 0.604 should be taken rather as a external grid background.

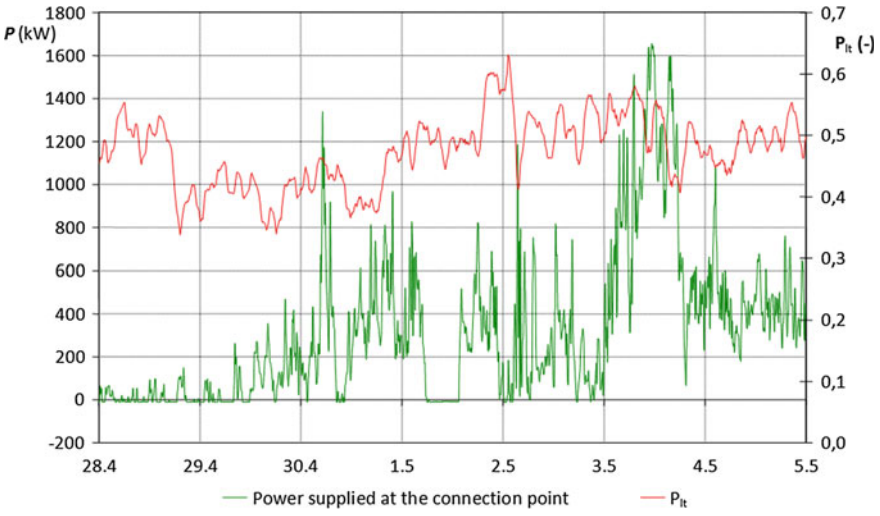

Fig. 2.51 Influence of the power supplied from the WPP on P_{lt}

Effects on the Devices of Centralized Telecontrol of Loads
Plants affect centralized telecontrol of loads (CTL) due to additional load of CTL transmitters:

- By the WPP equipment.
- Or by increased load of the part of the external grid into which the source supplies.

This influence can cause unacceptable changes in the levels of CTL signal at the common feed point. More detailed conditions and information about this reverse effect are available in [5].

2.4.2 *Influence of the WPP Operation on the Substation Supply Systems*

From previous chapters, it is clear that the WPP operation can affect the parameters of the external grid at the connection point and that this impact is primarily dependent on the ratio of the short-circuit power of the system into which the WPP capacity (output) is brought to the short-circuit power of the WPP generator, as well as on the WPP control system. If the high-capacity WPP output is brought to a external grid primarily with radial arrangement, whereas the WPP connection point is a position at the end of a branch, it is also necessary to respect the possibility of influencing the system parameters directly at the outlet from the substation of the given branch.

The following chapter analyses such a case. To identify the reverse effects of the connected wind power plants, we measured power balance of a distribution external grid branch to which two high-capacity WPPs are connected, each with an induction generator with wound rotor (2 MW, 690 V), working in the cascade connection with a frequency converter with recuperation. A simplified scheme of the connection of wind power plants is shown in Fig. 2.52.

Measuring point no. 1 was at the outlet of the monitored distribution external grid branch in a 110/22 kV substation. Measuring point no. 2 was in a distribution

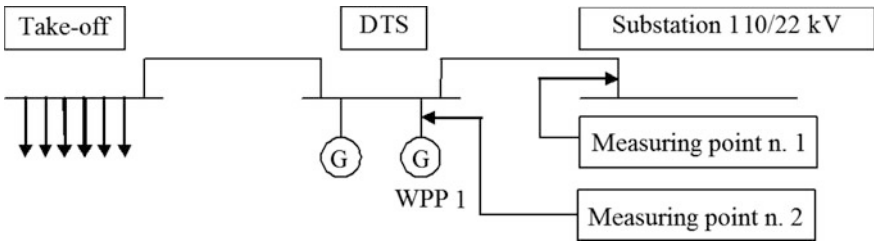

Fig. 2.52 A simplified scheme of the connection of wind power plants to a branch of the external grid

transformer station (DTS), i.e., at the connection point of the WPPs to the external grid. Measurements were carried out only for one wind power plant. Both instruments (meters) were time-synchronized; the electrical parameters were measured in all three phases.

When evaluating the measured data, the following three states of power balance were identified:

State 1—the connected wind power plants cover the consumption of customers connected to the monitored branch; in addition, the WPPs supply excess power to the distribution external grid through the parent 110/22 kV substation.
State 2—the connected wind power plants exactly cover the consumption of customers connected to the monitored branch (it is a balanced power balance, no active power is supplied to/from the parent substation).
State 3—the connected wind power plants do not cover the consumption of customers connected to the monitored branch; it is therefore necessary to supply the missing active power from the substation to which the monitored branch is connected.

If U_1 is the voltage at the connection point and U_2 is the voltage in the substation, the voltage deviation ΔU can be mathematically defined as the following difference

$$\Delta U = U_1 - U_2 \tag{2.36}$$

The dependence of the output supplied by the wind power plant on the voltage deviation ΔU can be seen in Fig. 2.53; if the WPP supplies power in the range of 0–100 kW (about 5 % of the installed capacity) to the external grid, the voltage in the substation is higher than at the connection point which is caused by voltage drop across the line. If the WPP supplies power higher than 100 kW, the voltage at the connection point increases to such a degree that the voltage deviation ΔU is getting from negative values, and the voltage U_1 at the connection point of WPPs therefore gradually increases with increasing power supply. This increase has a linear character. Deviations from the linear trend of growth are most likely caused by a small number of measured values for the monitored magnitude of the power supplied.

The evaluation of the measured data further shows that the operation of the wind power plant does not appreciably affect the long-term level of flicker perception, both at the connection point and in the parent substation. For each phase, the 95 % values of P_{lt} interval are shown in Table 2.5 [13].

The graph in Fig. 2.54 compares the courses of P_{lt} during the monitored period; the course of P_{lt} in the parent substation—in green, the course of P_{lt} at the connection point—in red. As evidenced by the graph, P_{lt} in the parent substation is higher which confirms the correctness of reasoning that the WPP contribution to the total P_{lt} value is almost negligible compared to the external grid background.

When analyzing the voltage total harmonic distortion (THDu), we also did not find any correlation with changes in the output supplied from the WPP and the total

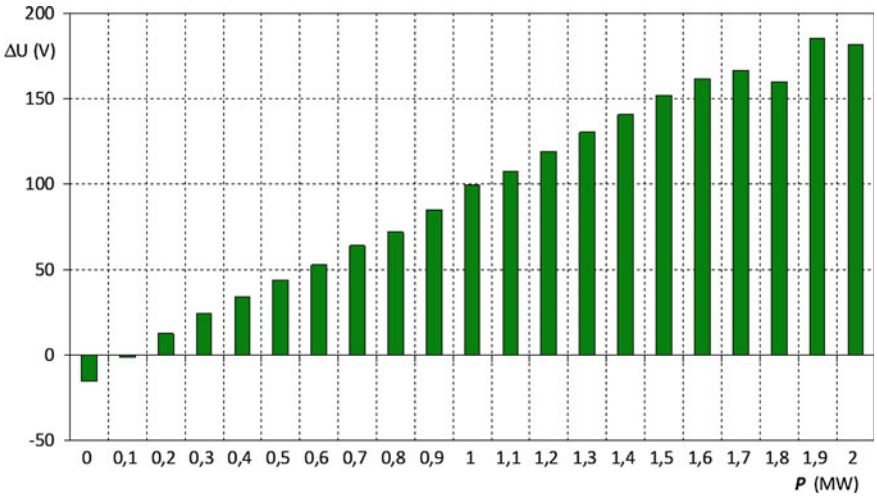

Fig. 2.53 Dependence of the voltage deviation on the output

Table 2.5 P_{lt} values for individual phases at the WPP connection point and in the parent substation

	Phase 1	Phase 2	Phase 3
Connection point (1)	0.581	0.604	0.577
Parent substation (2)	0.603	0.631	0.598

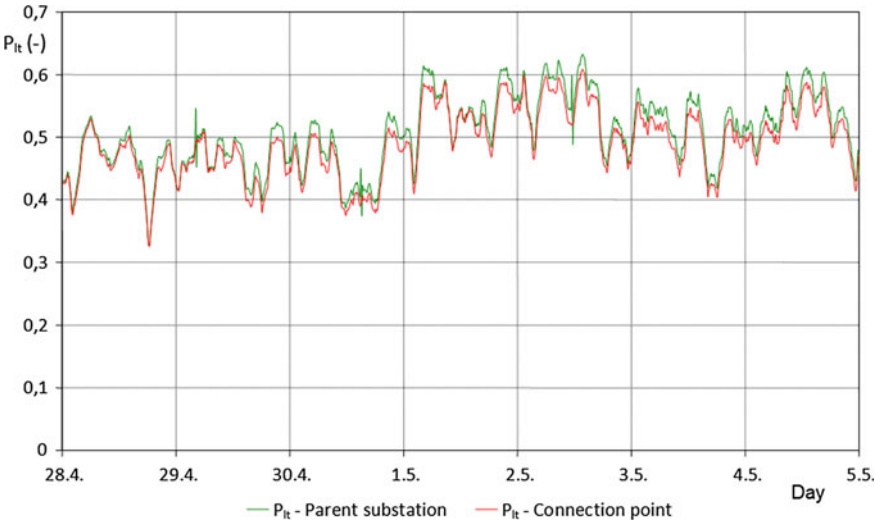

Fig. 2.54 Comparison of P_{lt} in the parent substation and at the WPP connection point

harmonic distortion factor varied around the value of 0.6 % with occasional deviations up to 1.8 % at the WPP connection point. The measured average value of the voltage total harmonic distortion (THDu) in the parent substation reached 0.7 % with occasional increases up to 2.2 %. Nevertheless, no timing between THDu increases at the connection point of wind power plants and in the parent substation has been proven.

References

1. Mišák S, Nevřala J (2008) Operation of small wind power plants with induction generators. Adv Electr Electron Eng 7:179–183
2. Mišák S, Nevřala J (2008) Asynchronní generátor v malé větrné elektrárně—část 1. Časopis pre elektroniku a energetiku 2:25–26
3. Mišák S, Nevřala J (2008) Asynchronní generátor v malé větrné elektrárně—část 2. Časopis pre elektroniku a energetiku 3:25–26
4. Mišák S, Chmelík K (2009) Generator for wind power plant of small and medium power. EPE 2009
5. System operation code (2010)
6. Mišák S (2010) Vybrané typy zdrojů elektrické energie. VŠB—TUO. Ostrava
7. Mišák S, Chmelík K (2007) Analýza provozu větrných elektráren s asynchronními generátory. Časopis pre elektrotechniku a energetiku 3:38–43
8. Mišák S, Chmelík K (2007) Analysis of wind power plant running with induction generators. Branzoly Odrodem Badawczo-Rozwojowy Maszyn Elektrycznych KOMEL, Katowice
9. Kačor P, Mišák S (2010) Zvýšení účinnosti synchronního generátoru s permanentními magnety pro větrnou elektrárnu. EPE 2010
10. Mlčák T, Mišák S (2010) Vyhodnocení provozních účinností větrné elektrárny. EPE 2010
11. Mišák S, Prokop L, Sikora T (2008) Provoz větných elektráren s frekvenčními měniči. ELEKTRO 10:4–6
12. Mišák S, Prokop L, Sikora T, Krejčí P (2008) Větrné elektrárny s asynchronními generátory v sítích VN. Elektrorevue 47:1–11
13. Mišák S, Prokop L, Sikora T, Krejčí P (2008) Zpětné vlivy provozu větrných elektráren na distribuční síť. Energetika
14. Mišák S, Prokop L (2009) Problem of wind power plant turbineering in the Czech Republic. POWERENG 2009
15. Mišák S, Chmelík K (2009) Characteristics parameters and operational states of generators for wind power plants. ISEM 2009
16. Mišák S, Nevřala J (2007) Using frequency converter at wind-power plants with induction generator. EPE 2007. Ostrava

Chapter 3
Operating Characteristics of Photovoltaic Power Plants

The aim of this chapter is not to repeat the well-known definitions of the physical principles and characteristics, such as the photoelectric effect, but mainly to share the experiences of a large number of measurements and analyses carried out during last two decades, since the time when the photovoltaics started its expansion until now when the installed capacity reaches about hundreds megawatts.

3.1 Development of PPP Components

Division of photovoltaic cells into separate generations can be sometimes subjective; therefore, it represents only the opinion of the authors. This division may differ in other publications.

3.1.1 The First Generation

The first generation includes photovoltaic cells based on silicon wafers. Today, it is the most common technology in the market (approximately 90 %) reaching relatively high conversion efficiency (16–19 % in cells produced on a mass scale, up to 24 % in special structures). These photovoltaic cells were launched into the market in the 1970s. Although their production is relatively expensive (particularly because of the expensive input material—crystalline silicon), they will continue to dominate the market during the next few years.

S. Misak and L. Prokop, *Operation Characteristics of Renewable Energy Sources*,
Green Energy and Technology, DOI 10.1007/978-3-319-43412-4_3

3.1.2 The Second Generation

The impetus for developing the cells of the second generation was mainly an effort to reduce the manufacturing costs through savings in the expensive base material—silicon. Cells of the second generation are characterized by 100 times to 1000 times thinner active absorbing semiconductor layer (thin film); they are represented, for example, by the cells made out of amorphous and microcrystalline silicon (eventually silicon-germanium or silicon-carbide, but also the so-called mixed semiconductors from materials, such as Cu, In, Ga, S, and Se, generally referred to as the CIS structures). In comparison with cells of the first generation, the material saving led to a decrease in production costs (i.e., also to price declines, assuming mass production); the achieved efficiency, however, is usually lower (generally below 10 % in series production). An indisputable advantage of thin-film cells is the possibility to choose the substrate (on which the thin-film structures are deposited) as well as a considerably wider application sphere in the case of using flexible materials (organic, metallic or textile foils). Photovoltaic cells of the second generation were placed on the market in the mid-1980s.

3.1.3 The Third Generation

Solar cells of the third generation represent an attempt to start "photovoltaic revolution." In this case, the primary goal is not only an effort to maximize the number of absorbed photons and subsequently generated electron–hole pairs ("current" gain) but also to maximize the utilization of energy of incident photons ("voltage" gain of photovoltaic cells). There are a number of directions addressed by the research:

- multilayer solar cells (from thin films);
- cells with multiple bands;
- cells that would use "hot" charge carriers to generate more electron–hole pairs;
- thermophotovoltaic conversion where the absorber is also the radiator emitting selectively at one energy level;
- thermophoton conversion where the absorber is replaced by electroluminescence;
- the cells utilizing quantum phenomena in quantum dots or quantum wells;
- spatially structured cells emerging through a self-organization during the growth of the active layer;
- organic cells (e.g., based on volume heterojunctions).

So far, the only commercial examples of well-functioning cells of the third generation (directly linked to photovoltaic cells of the second generation), known to authors, are multilayer structures (two layer cells, the so-called tandems, and three layer cells); each sub-structure (p–i–n) absorbs a certain part of the spectrum and

thus maximizes the energetic usability of photons. An example of a tandem solar cell is the structure consisting of p–i–n junction of amorphous (hydrogenated) silicon (a-Si:H) and p–i–n junction of microcrystalline (hydrogenated) silicon (μc-Si:H). Amorphous silicon has a high absorption in the blue, green, and yellow part of the spectrum, while microcrystalline silicon well absorbs also in the red and infrared part of the spectrum. Microcrystalline silicon can be replaced by a silicon-germanium "alloy"; according to the selected ratio of the two materials, it is possible to adjust their optical (as well as electrical) properties. For example, this material is commercially used for the three layer solar cells where the two lower cells are made with different concentrations of Si and Ge. The basic condition for the good function of multilayer cells is that each of them generates the same current. Otherwise, the worse (or the worst) cell limits the achievable efficiency. The resulting voltage is then the sum of the two (or all) cells.

3.2 Basic Operating Characteristics of PPPs

3.2.1 PPP Power Curve

The basic parameters specifying the operation of the plant include its power curve. In the case of photovoltaic power plant, this curve represents the dependence of the output electric power (W) on the total solar energy ($W \cdot m^{-2}$).

Figure 3.1 shows a power curve of the analyzed PPP which was obtained by processing statistical data for about five months of its operation; the figure demonstrates the availability of power output for different weather conditions resulting from differences in the time interval in the given calendar month. The following fact is obvious: Due to the specific weather conditions of the Czech Republic, the PPP does not reach its maximum installed capacity (1100 kW) even during the summer season, and the maximum disposable output converges to the value of 600 kW (which is 54 % of the installed capacity) and decreases with decreasing intensity of solar radiation up to 300 kW (around 28 % of the installed capacity) in the autumn and winter months. For completeness, it should be noted that the individual points of the power curve were obtained from the average values of 10-min intervals. To correct irrelevant values and construct the power curve, it is possible to use data that were obtained from calculating the median of 10-min intervals (see Fig. 3.2); this provides the basic advantage of the median as a statistical indicator allowing us to exclude the influence of extreme values. In the case of the median expression of the power curve, the maximum disposable power approaches the value of 800 kW (73 % of the installed capacity) in the time interval with prevailing total solar radiation of 700 $W \cdot m^{-2}$ and the value of 250 kW (23 % of the installed capacity) for the solar energy of about 300 $W \cdot m^{-2}$.

Another view on the analysis of the PPP basic specification is provided by the graphic representation of the variability of power flow within one-day cycle for

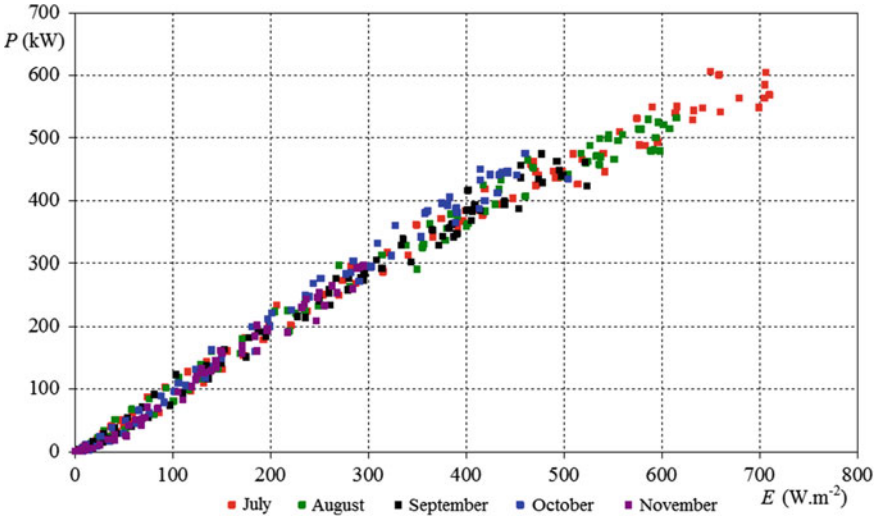

Fig. 3.1 Power curve—average

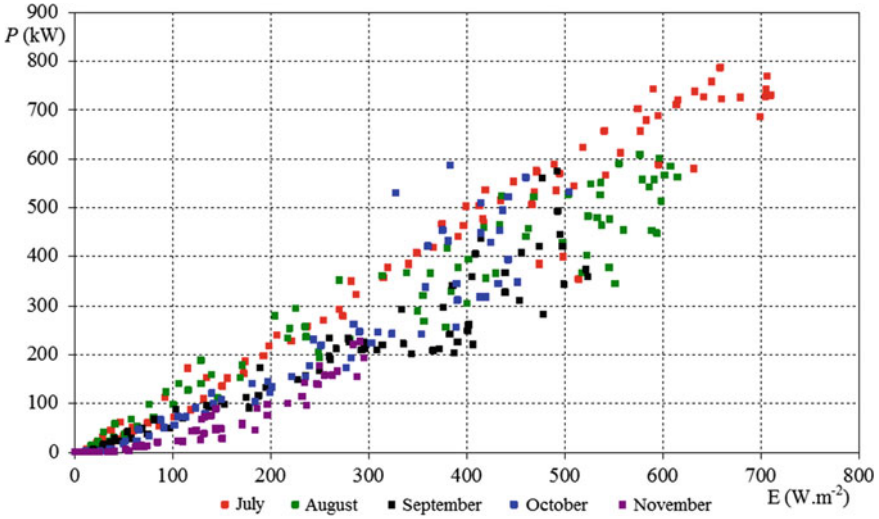

Fig. 3.2 Power curve—median

various specific meteorological conditions given by the month of operation. The respective results are shown in Fig. 3.3 for the average values of 10-min intervals and in Fig. 3.4 for the median values of 10-min intervals. The figures clearly show that both variants (averages as well as medians) demonstrate not only changes in the maximum disposable power for time intervals with different values of the total solar

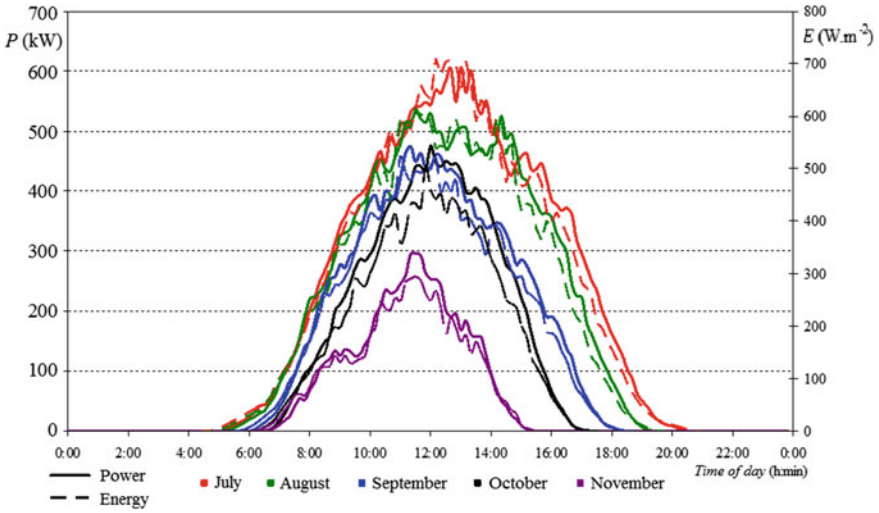

Fig. 3.3 Comparison of the PPP output and solar energy—average

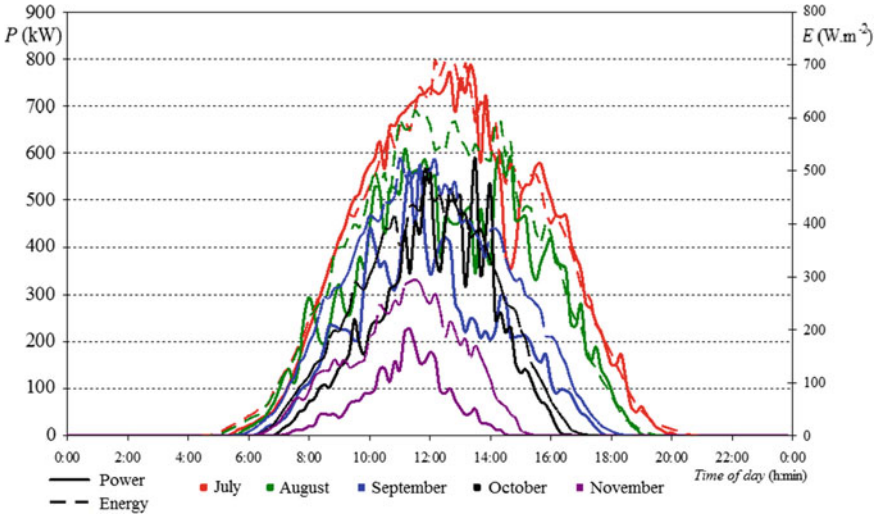

Fig. 3.4 Comparison of the PPP output and solar energy—median

radiation, but also shifts of the maximum during the day cycle. This maximum of disposable power shifts from the daytime of 11:00 for the month of November through the value of 11:30 for the month of September to the value of 13:00 for the month of July. This dependence is clearly given by the trajectory of the Sun, which is different for each month within the daily cycle. This argument can be generalized

for the graphic expression of variability of power flow during the daily cycle while respecting the results of the average values as well as median values; when correcting for outliers using the median calculation, the maximum power output increases in line with the above comments on the PPP output curve.

3.2.2 Production, Utilization Ratio, Efficiency, and Power Flows

Other PPP parameters include utilization ratio and the value of estimated or actual electricity production. The next chapter compares the anticipated and actual productions of electric energy and stipulates the value of utilization ratio.

To estimate the PPP production, we used the photovoltaic geographic information system PVGIS [1]. Accuracy of this system is given by statistical data collection that took place during 1985–1995 in all of Europe. Using interactive maps and computer simulations, we can estimate the potential production of the photovoltaic system during individual months. The calculation includes total system losses, such as estimated losses due to temperature, angular reflectance, losses caused by cables or converters. The calculation is done according to the following formula:

$$E = 365 \cdot P_{\mathrm{PEAK}} \cdot r_{\mathrm{P}}, \tag{3.1}$$

where P_{PEAK} is the installed maximum capacity (kWp) and r_{P} is the estimated performance ratio.

The results of the measured and estimated values of energy supplied are visible in Table 3.1 and Fig. 3.5. Table 3.1 shows that the most productive months are June, July, and August.

Figures 3.5 and 3.7 demonstrate the PPP production efficiency. The highest values of monthly utilization ratio, in the range 16–18 %, are achieved during summer months. The total annual utilization ratio is about 11 %. Clear instability of electricity supply (see Fig. 3.6) results from the dependence of the output power on the solar energy as well as on the position of the Sun with regard to the inclination and orientation of photovoltaic panels. Using polycrystalline or microcrystalline panels, it is possible to partially stabilize power flows and thus also limit the influence of cloudiness on the performance.

Real efficiency η_{eff} and performance ratio (PR) describe the PPP behavior under conditions of the given location for the given time period, i.e., half-year in this case:

$$\eta_{\mathrm{eff}} = \frac{E_{\mathrm{FVE}}}{E_{\mathrm{SOL}}} = \frac{618{,}239}{5{,}321{,}190} = 0.1161 \Rightarrow 11.61\,\%, \tag{3.2}$$

Table 3.1 Energy produced in each month

Month	$E_{\text{m-ACT}}$ (kW·h/month)	$E_{\text{m-PVGIS}}$ (kW·h/month)
January		39,200
February		56,800
March		87,900
April		108,000
May		130,000
June	138,062	122,000
July	145,756	134,000
August	128,949	121,000
September	92,994	92,100
October	73,893	79,700
November	33,676	39,000
December	4909	27,800
E_{FVE} (kW·h)	618,239	1,037,500
Total annual consumption per operation (kW·h)	4560 of which taken from the network 2300	

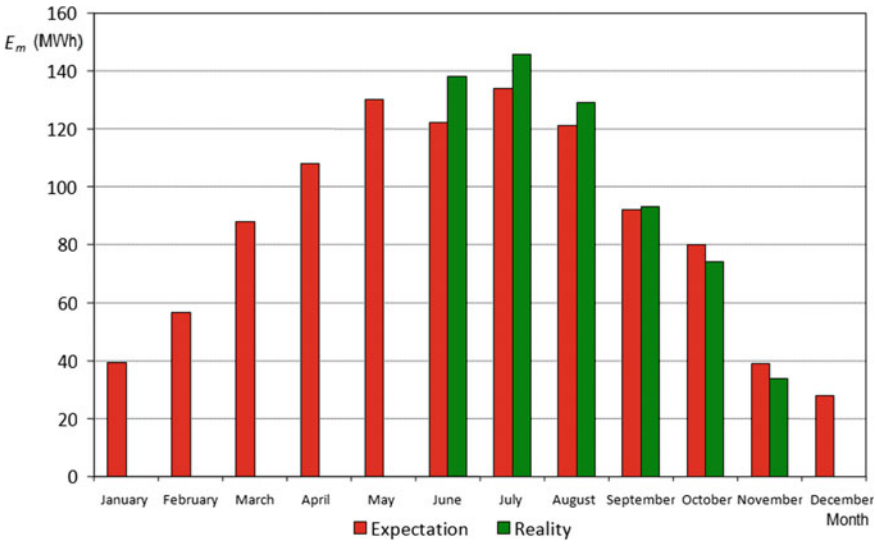

Fig. 3.5 Comparison of estimated and actual production

where η_{eff} is the efficiency of conversion into electric power (%), E_{FVE} is the actually produced electrical energy (kW·h), and E_{SOL} is the amount of solar energy incident on the panels (kW·h)—its values were taken from [1] and are valid for the respective surface of panels used by the analyzed PPP.

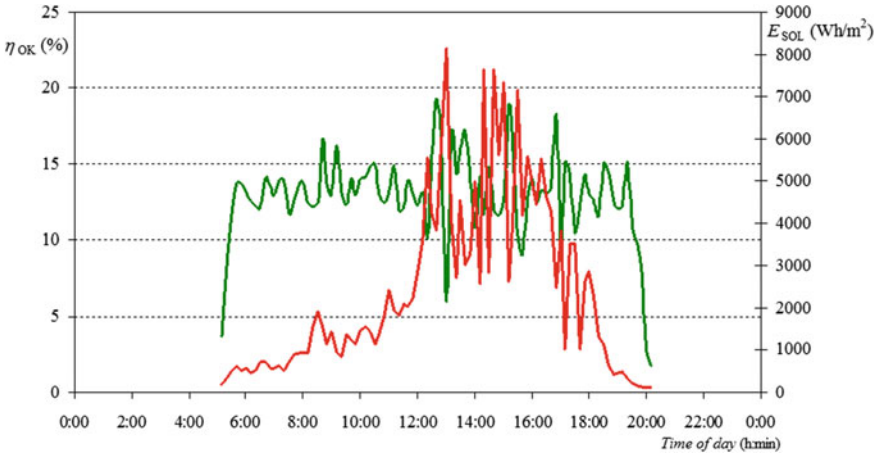

Fig. 3.6 Instantaneous efficiency of the PPP and the solar energy incident on the PPP area. In *red*—the course of ESOL; in *green*—the course of efficiency η_{OK} (color figure online)

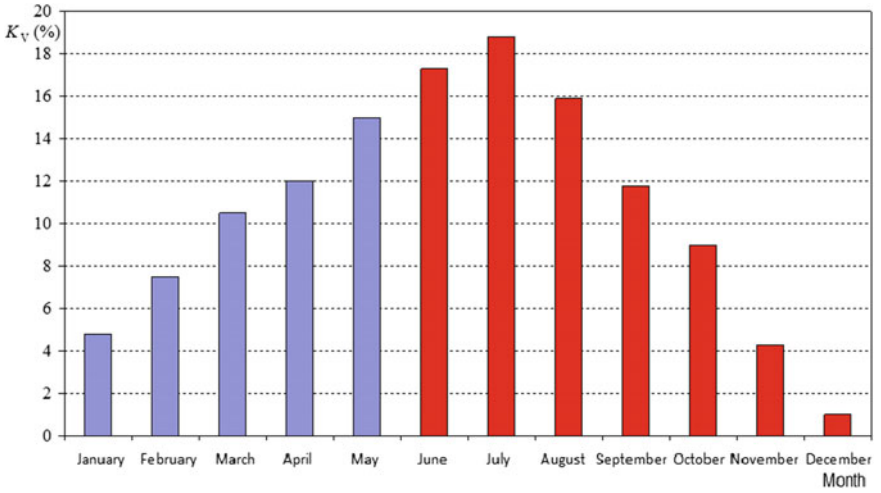

Fig. 3.7 PPP utilization ratio (in *blue*—expected values from [1]; in *red*—actual values calculated from the measured data; the month of December is calculated from incomplete data) (color figure online)

To calculate the real efficiency, we can determine the coefficient of actual and long-term achievable efficiency—PR (%):

$$\mathrm{PR} = \frac{\eta_{\mathrm{eff}}}{\eta_{\mathrm{STC}}} = \frac{11.61}{17.7} = 0.65 \Rightarrow 65\,\%, \tag{3.3}$$

where η_{STC} is the efficiency under standard test conditions.

Instantaneous efficiency of a PPP can be calculated using the formula:

$$\eta_{OK} = \frac{P_{OK}}{G \cdot S_{FVE}}, \tag{3.4}$$

where η_{OK} is the instantaneous efficiency of the PPP, P_{OK} (W) is the instantaneous output of the PPP, G is the intensity of solar radiation incident on m^2 in the given location ($W \cdot m^{-2}$), and S_{FVE} is the PPP area (m^2), i.e., 7551 m^2 in this case.

The course of PPP instantaneous efficiency for a model day in July is shown in Fig. 3.6.

3.3 PPP Operating States

3.3.1 PQ Diagram

To evaluate the operation of a photovoltaic power plant and the corresponding reverse effects on the distribution system into which its output is brought, it is necessary to know the parameters of the photovoltaic plant for different operating states. As already mentioned in the introductory part of the text, the output of individual panels of the PPP is routed into the distribution system (grid) through frequency converters, whereas the total output of individual outlets of photovoltaic arrays is subsequently transformed into the grid via a power transformer. With the use of power electronics of the frequency converters, it is, therefore, possible to operate the photovoltaic power plant in the so-called 4-quadrant mode, i.e., it is possible to expect consumption and supply of active power as well as consumption and supply of inductive reactive power. For the plants, the basic expression of the said 4-quadrant operation is the so-called PQ diagram where the individual operating states are displayed on a scale of individual outputs. The PQ diagram of a photovoltaic power plant will be discussed in detail in the text below. First, in the following paragraph, we will deal with the analysis of PPP power factor and the corresponding balance of inductive reactive power.

The power factor is defined as the cosine of the angle between the voltage and current waveforms for the first harmonic; however, if the phase shift is determined generally for voltage and current waveforms considering also harmonics of higher orders, the term “true power factor” is used. For mapping the operation of photovoltaic power plants, we employed a measuring system allowing us to analyze waveforms with respecting higher harmonics; therefore, the following analysis only considers the value of true power factor. The value of true power factor is important in determining the magnitude of supply or consumption of inductive reactive power; the SOC stipulate limits for the value of true power factor—from 0.95 (the supply of inductive reactive power) up to 0.98 (the supply of capacitive reactive power). If the measured value of true power factor is out of this permitted range, the respective plant operator is sanctioned by a price surcharge in accordance with the

rules laid down by the operator of the distribution system into which the plant output is brought. Figures 3.8 and 3.9 show the evaluation of the production of electricity in the given range of true power factor for 2 months with different meteorological conditions and the corresponding total solar radiation. These figures clearly demonstrate the supply of active power even outside the permissible range of true power factor; this results from the nature of the photovoltaic power plant which is connected to the grid even during hours with a minimum supply of active

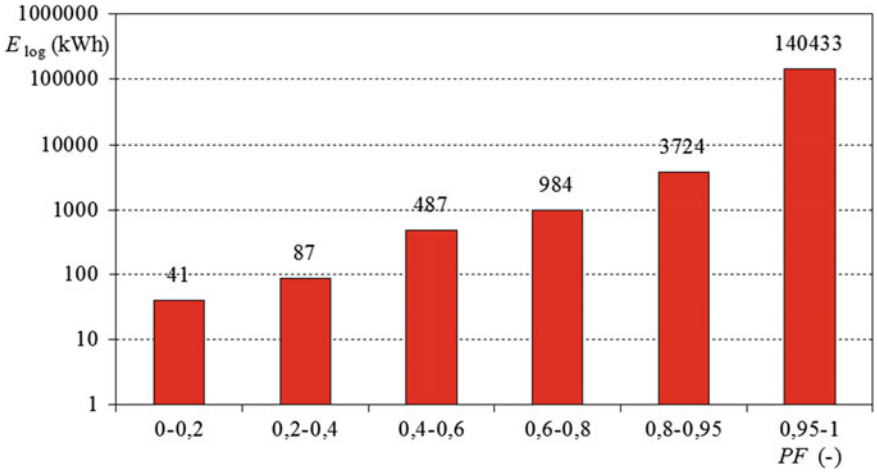

Fig. 3.8 The amount of energy supplied in July with the respective true power factor. Due to the disproportion between various PF intervals, logarithmic *y*-axis is used

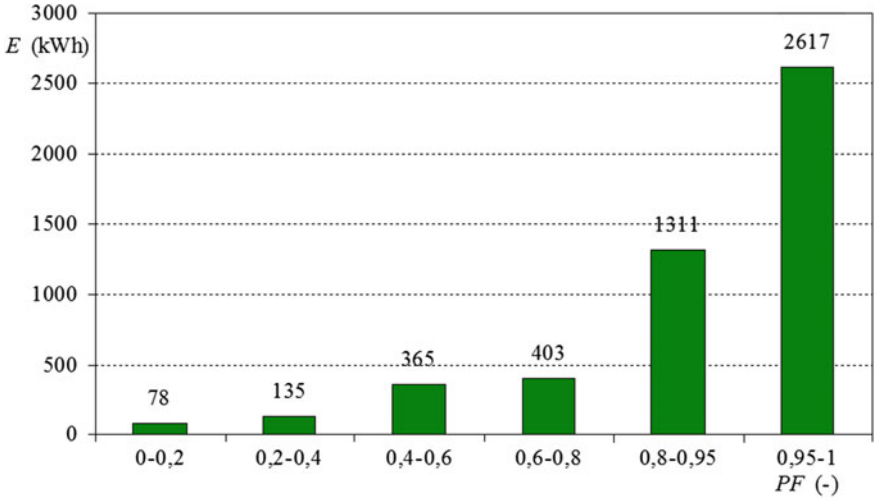

Fig. 3.9 The amount of energy supplied in December with the respective true power factor

power (night hours), and the power electronics of frequency converters is unable to perform compensations within the required tolerance.

One of the main conditions for the supply of electricity to the grid is to keep the neutral zone of power factor. Any PPP connected to the high-voltage network is required to observe the so-called neutral zone of power factor. The plant must be able to supply rated active power with inductive power factor in the range of 0.95–1.00 unless provided otherwise in a contract with the operator of the distribution system (according to local grid conditions, the supply of reactive power with power factor of 0.85–1).

Balance of inductive reactive power is an individual matter of each facility with regard to the plant configuration and network parameters of the distribution system at the connection point, whereas the elements affecting the overall balance of inductive reactive power can include frequency converters, cables, and distribution transformer.

Regarding the electric lines, it is necessary to respect the high-voltage 22-kV line from transformer stations to the connection point to the DS and low-voltage lines from the inverter to the transformer, whereas the charging current (for keeping the cables under voltage) causes the capacitive nature of this load, i.e., a positive contribution to the supply of inductive reactive power.

Note: The charging current for 1 km of cable 3 × 1 × AXEKVCE 240 mm^2 is about 1.3 A, which means capacitive power of 50 kvar at the given voltage. Capacitive charging power for cable 3 × 1 × AXEKVCE 120 mm^2 is roughly half.

In the case of transformer, in terms of the reactive power, it is a consumption of inductive reactive power.

As a precaution against supply/takeoff of inductive reactive power outside the permitted range of true power factor, the operator can install different (de)compensation elements. Currently, however, the distribution systems will require a dispatch control of the power factor in the range of 0.95 (inductive) up to 1.00. This implicates a necessity to install compensation and decompensation switchboards with output of about one-third of the maximum PPP capacity. For 1 MWp, this represents 350 kvar of reactors or conventional capacitor compensation.

PPP enables the supply of active power to the distribution grid already in the early morning as well as evening hours, with regard to weather conditions. In Fig. 3.10, it can be seen that the PPP supplies already at 6:30 or even sooner (depending on the sunrise and generally on weather conditions), but the neutral zone of true power factor is not kept. In the neutral zone of power factor 0.95–1, the plant starts to supply at 7:30 at the corresponding value of active power of about 100 kW, and ends with the supply after 18:00.

Figure 3.11 shows the total balance of the flow of reactive as well as active power in the so-called PQ diagram. From this figure, it is clear that the PPP operation is defined for three basic states: the mode of the supply of active power ($-P$) and the supply of inductive reactive power ($-Q$); the mode of the supply of active power ($-P$) and the consumption (takeoff) of inductive reactive power ($+Q$); and finally, the mode of the consumption of active power ($+P$) and the consumption

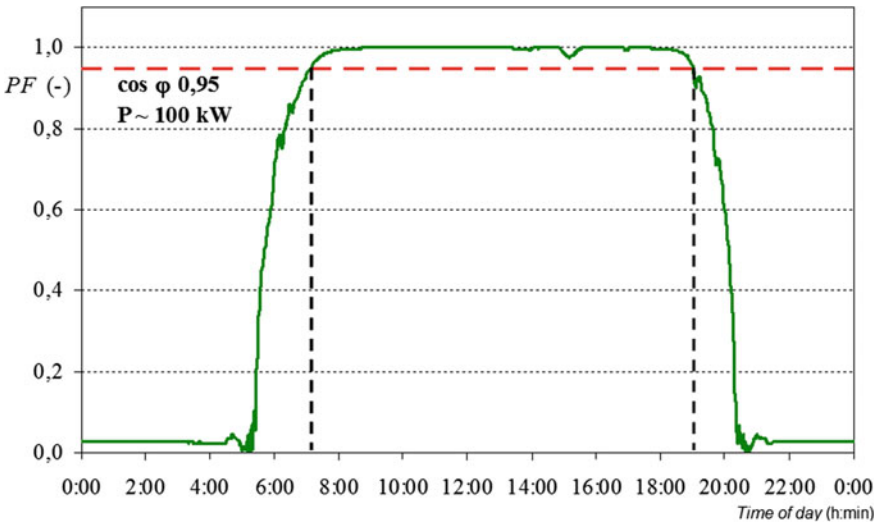

Fig. 3.10 Values of true power factor during a sunny day

of inductive reactive power (+Q). Given the nature of inductive reactive power, it is, therefore, necessary to envisage the possibility of increased voltage at the connection point for the supply of inductive reactive power or, conversely, the possibility of reduced voltage at the connection point for the consumption of inductive reactive power, always with respect to the value of active power. To determine the amount of reactive power or energy for the individual operating states in compliance with the PQ diagram, it is possible to perform an evaluation according to the frequency of individual values of mentioned energies for the given intervals of true power factor. Results of the analysis are presented in the following Table 3.2.

Table 3.2 allows us to make some interesting conclusions. First, it is possible to define the most common operating state of the photovoltaic power plant with prevailing supply of active power (i.e., energy) but also with consumption of inductive reactive power (i.e., energy), even outside the specified neutral zone of power factor/true power factor. The overall percentage frequency of the supply of active power (i.e., energy) in the neutral zone of true power factor is 51 % of the total supply of active energy; however, the supply of inductive reactive power is represented only by 19 %. The PQ diagram and data of Table 3.2 further clearly show the following: When the value of supplied active power exceed about 150 kW, the true power factor is fully compensated in the permitted range of the neutral zone and also the balance changes from the supply to the consumption of inductive reactive power, which is reflected in the frequency of 100 % of the total reactive energy consumed and 43.5 % of the total active energy supplied. That conclusion is further confirmed by the graphical representation in Fig. 3.12.

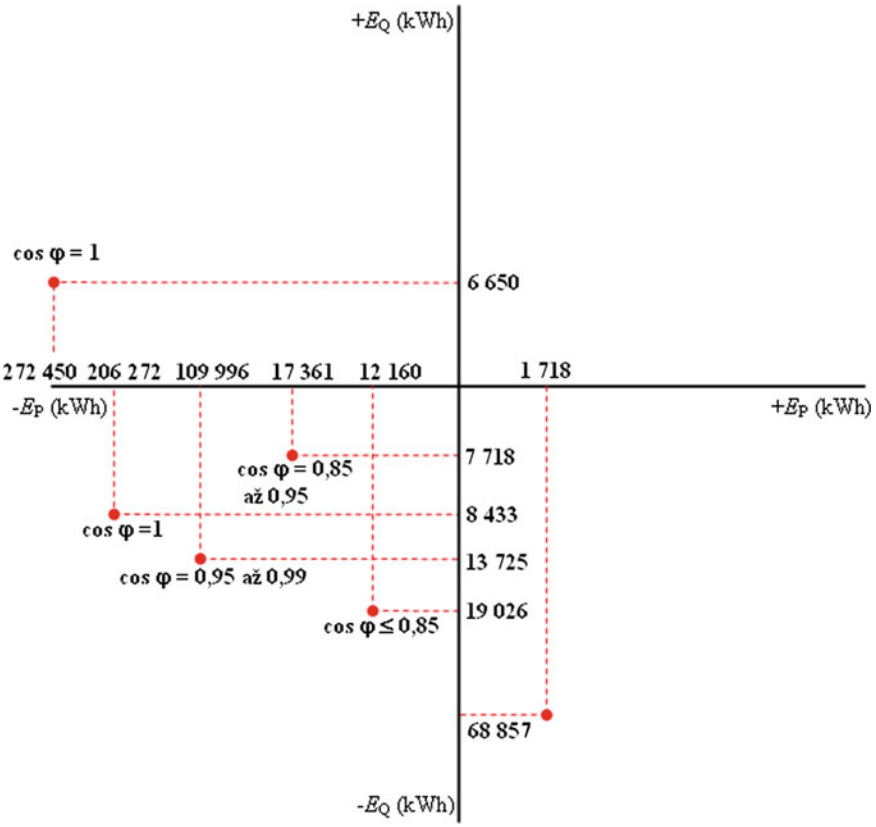

Fig. 3.11 PQ diagram of a PPP

In the case of "motor" mode of the photovoltaic power plant, i.e., in the mode of the consumption of active power (+*P*), the entire system from the PPP to the transfer point operates in the mode of inductive reactive power.

3.4 Power Flow Variability and Its Impact on the System

Other important characteristics of photovoltaic power plants include the time change of power flow, the so-called dynamic variability of power flow. This characteristic is important for the operator of the electrical power system into which the power from the respective plant is brought. It serves for optimal planning of power reserves in the event of large changes in outputs 0 supply outages; it is also important as a basis for analyzing the system stability or developing the concept of protection. To depict the mentioned characteristic, it is necessary to have sufficient set of data from long-term measurements covering a period of time with varying

Table 3.2 Analysis of the PPP operating states for 6 months of operation

cos ϕ (–)	$+Q$ (consumption) (kvar·h)	$-P$ (supply) (kW·h)	n of the total consumed reactive energy (%)	n of the total supplied active energy (%)
1	+6156	−272,450	100	43.5
cos ϕ (–)	$-Q$ (supply) (kvar·h)	$-P$ (supply) (kW·h)	n of the total consumed reactive energy (%)	n of the total supplied active energy (%)
1	−8433.2	−206,272	7	33
0.95–0.99	−13,725	−109,996	12	18
0.85–0.95	−7718	−17,361	7	3
0.5–0.85	−10,014	−10,116	9	2
<0.5	−9012.8	−2044	8	0.5
cos ϕ (–)	$-Q$ (supply) (kvar·h)	$+P$ (consumption) (kW·h)	n of the total supplied reactive energy (%)	n of the total consumed active energy (%)
0.023	−68,857	1718.2	57	100

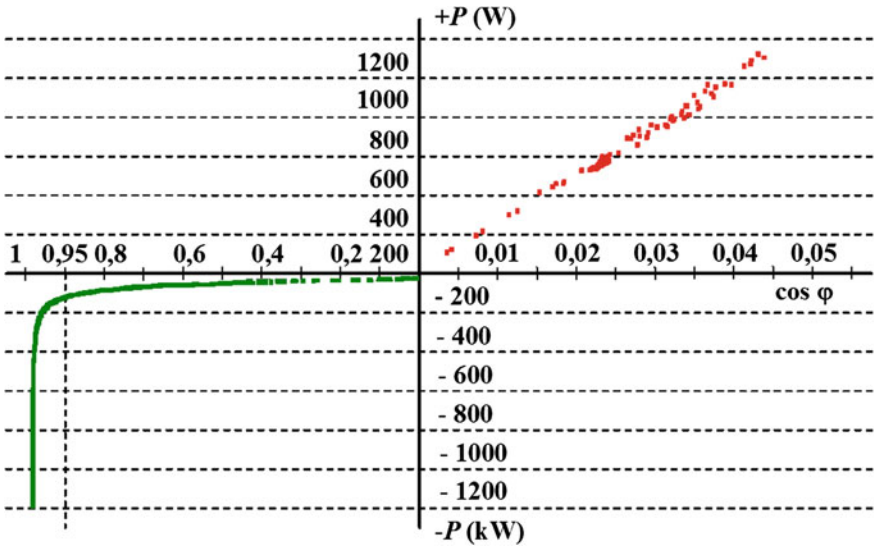

Fig. 3.12 Dependence of the active power and power factor

specifications meteorological conditions. Figure 3.13 shows the result of the dynamic variability of active power based on comparing changes in active power with the rated (installed) capacity and on monitoring the absolute (see Fig. 3.13) and relative (see Fig. 3.14) frequency of the magnitudes of individual changes (differences in outputs) in minute intervals. This analysis was performed for the

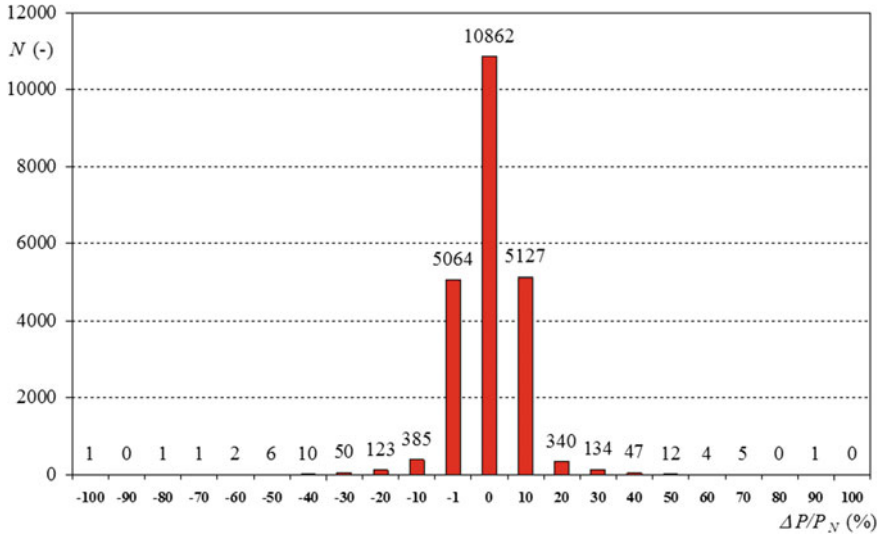

Fig. 3.13 The number of power changes

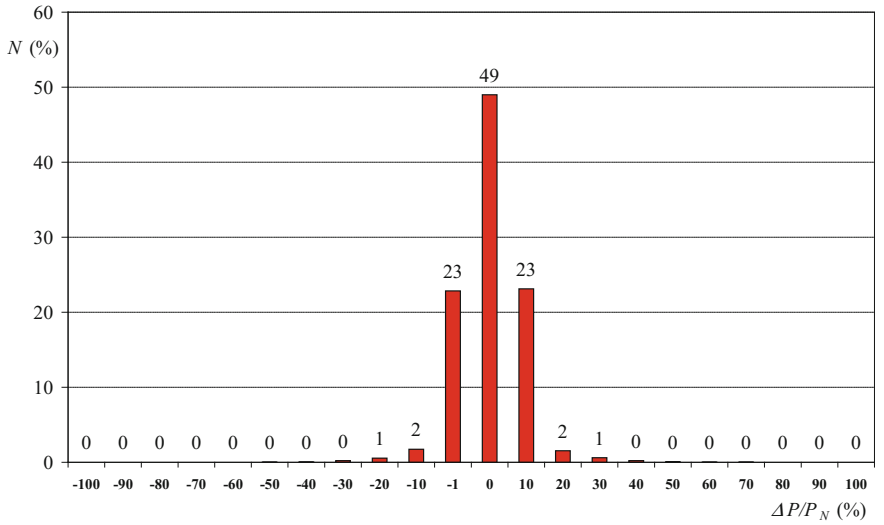

Fig. 3.14 Percentage representation of the number of changes

entire monitored period of the PPP operation (5 months) with different weather conditions and the corresponding different characteristics of output curves; therefore, the initial data set can be regarded as sufficient for processing. Both figures, for the absolute as well as relative frequencies, clearly show that the minimum power change converging to the value of 0 has a maximum frequency representation with

a number of 10,862 events, which corresponds to 49 % of the total number of events. This representation decreases with increasing power change—for example, for a power change of 10 %, the frequency of such events is about 23 %; for a power change of 20 %, however, the frequency is in the order of a few percent.

The graphical frequency representation includes both operating states of the photovoltaic plant where the (−) sign earmarks the area of active power supply and the (+) sign earmarks the area of active power consumption (takeoff). The actual values of absolute and relative frequency are not affected by the PPP operation in the mode of active power supply/consumption; the distribution of the individual values is symmetrical along the frequency axis and approaches the normal Gaussian distribution. Nevertheless, it should be noted that the dynamic variability of power flow also includes values of power change which approach 80 %; however, these occur only rarely and are determined by the nature of the technology used in the production of photovoltaic panels. Regarding the technology used in the analyzed PPP, this incidence is due to a reduced efficiency of monocrystalline panels in the case of reduced direct solar radiation (movement of clouds in the sky), which causes a decrease in the output power. When using technologies (polycrystalline panels) which can process diffuse solar radiation with higher efficiency, the incidence of such isolated points will be lower.

In Figs. 3.13 and 3.14, the analysis of the dynamic variability of power flow was performed for the entire monitored time interval. When concretizing the above analysis for each month, the frequency distribution for individual months and the active power supply/consumption mode again approaches the normal Gaussian distribution. Figure 3.15 demonstrates a higher dynamic variability of power flow in the summer months compared to the autumn months, which is caused by weather

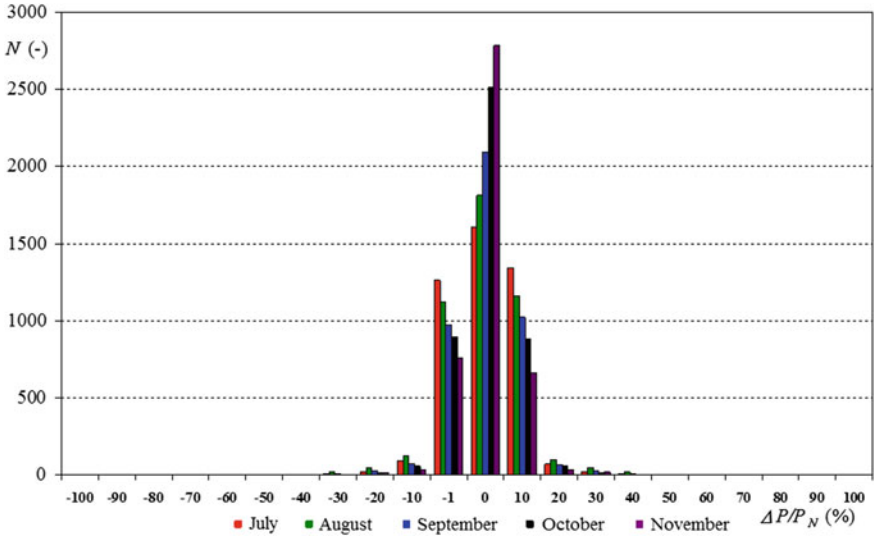

Fig. 3.15 The number of power changes in each month

instability during the summer season due to changes in the atmospheric pressure and the corresponding increased storm activity and changes in cloud cover. In the autumn, the dynamic variability of power flow is conversely lower, with respect to more uniform nature of the weather. It should be again noted that this dependence, in addition to weather conditions in individual months, is also given by the ability of the used technology of photovoltaic panels to process direct as well as diffuse components of the solar radiation.

3.5 PPP Negative Effect on the Distribution System

The rule for parallel operation of sources with the network of the operator of the distribution system included in [2] says that the increase in voltage at the connection point caused by the operation of plants connected in the HV and 110 kV network, in the worst case, must not exceed ΔU_{MV}, $110 \leq 2$ %. For production plants with the transfer point in an LV network, the increase in voltage must not exceed $\Delta U_{\mathrm{LV}} \leq 3$ % compared to the voltage without their connection. Variation in voltage in distribution networks is due to changes in the output of connected sources but also due to changes in power consumption (takeoff) by customers. A voltage change on one node translates into voltage changes in other network nodes.

In practice, we can meet with networks with a weak load (low-power consumption) and large number of scattered sources. In these networks, it is often difficult to observe the prescribed voltage tolerances. Compliance with the prescribed voltage tolerances reduces the impact of significant voltage deviations in the network and thus helps to control and stabilize voltage at all points of the network.

A condition for stabilizing the network voltage is as follows: the voltage change at the common feed point, induced by a connection or disconnection of the production facility, must be $\Delta U_{\mathrm{max\ MV}} \leq 2$ %, $\Delta U_{\mathrm{max\ LV}} \leq 3$ %. These limits apply unless the switching of the production facility is more frequent than once every 1.5 min, which is met in PPPs. With very little switching frequency and if allowed by the network conditions, the operator of the distribution system may approve switching with larger voltage changes.

Regarding plants connected in 110-kV networks, the limit for voltage changes when switching one production facility under normal operation is as follows: $\Delta U_{\mathrm{max}}\ 110 \leq 0.5$ % [2].

Nevertheless, the aforementioned outcomes apply to the definition of voltage at the transfer point of the photovoltaic power plant, and the results of this analysis were already presented in earlier stages of project development. In addition to the analysis of voltage at the PPP transfer point, however, it is also necessary to analyze the effect of the plant operation on the voltage of the line outlet in the substation to which the PPP power is brought. This analysis is very important because of the following situation: under conditions of reduced electricity consumption in the network in which the PPP operates and together with a simultaneous substantial

increase in the power supply from the respective PPP, the total consumption at the given outlet of the distribution system can be covered only from the PPP. This would result in a reverse flow of active power of the power transformer, causing a voltage increase at the connection point. Since the system control is implemented on the secondary side of the power transformer, the voltage regulation is very difficult in the case of the reverse flow of active power of the power transformer, and the voltage increase on the primary side of the power transformer can lead to a voltage change on the transmission system. The increase in voltage can be reduced by changing the reactive power, but this increases the total loss in the transmission path. This study was also conducted for the analyzed photovoltaic power plant 1100 kW, whereas it was necessary to install a new measurement technique to the outlet of the line into which the plant operates. Using this measurement technique, it was possible to analyze power flows, current load, and voltage magnitude. The result of the analysis is shown in Fig. 3.16 which presents the dependence of the line voltage on the magnitude of supplied active power; the red line indicates the allowable 2 % voltage range for the level of 22 kV. In conclusion, it can be said that the voltage is within the permissible tolerance in about 90 % range of the active power balance. When the active power supply approaches the value of installed capacity, the reactive power balance changes from the consumption mode into the mode of the supply of inductive reactive power according to the PQ diagram in Fig. 3.11, which corresponds to the change in voltage with short-term varying character. However, this claim cannot be unambiguously generalized, because, in the case of voltage, it is a systemic parameter depending on the parameters of all components of the mentioned voltage level.

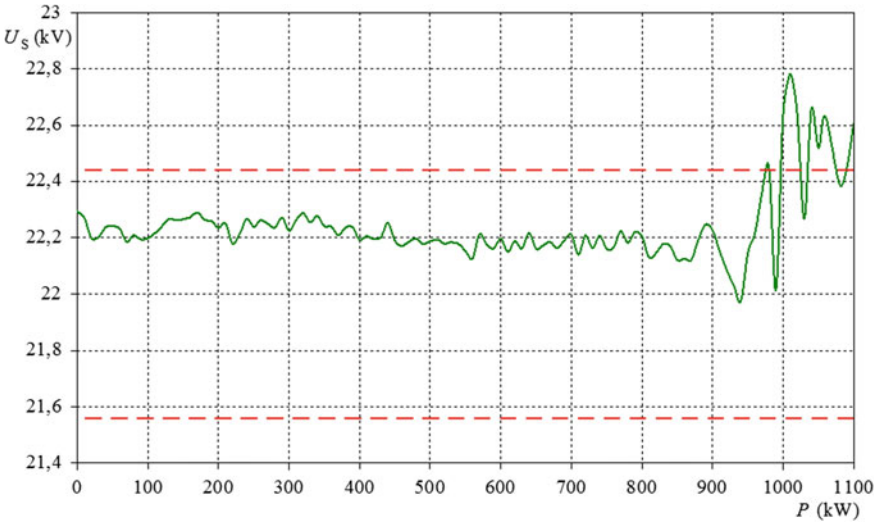

Fig. 3.16 Voltage changes on the line outlet in 22 kV substation to which the PPP power is brought

3.6 Prediction Methods for PPP Power Output Prediction

3.6.1 The General Principle for Predicting the Production of Electricity from PPPs

For clearness, the description of methods for predicting the production of electricity should address the source of solar radiation, the passage of solar radiation through the atmosphere, and the incidence of solar radiation on the surface of the photovoltaic panel. Subsequently, it is necessary to determine how much electricity is produced from the solar radiation incident on the panel surface.

3.6.2 The Source of Solar Radiation

The source of solar radiation consists in thermonuclear processes inside the Sun which produces vast amounts of energy that is emitted into the space in the form of electromagnetic radiation. After passage through the atmosphere, this flow of energy strikes upon the Earth's surface.

Electromagnetic radiation of the Sun covers a broad spectrum, from the ultraviolet region to near-infrared region. Wavelengths of the radiation reaching the Earth's surface are mostly (approximately 99 %) in the range from 0.3 to 4 μm with a maximum of about 0.5 μm in the visible region of the spectrum. Of this, approximately one half of the radiation is emitted in the infrared region, approximately 40 % in the visible region and approximately 10 % in the ultraviolet and X-ray region.

After passage through the atmosphere, the solar radiation undergoes a number of changes which are often referred to as the extinction (absorption and scattering) of radiation. Most of the radiant energy at wavelengths below 0.3 μm is absorbed by the atmosphere.

The amount of radiant energy from the Sun that reaches the unit area of a plane perpendicular to the Sun's rays outside the Earth's atmosphere at a mean Earth–Sun distance is called the solar constant. Its value is approximately 1370 $W \cdot m^{-2}$. Due to changes in the Earth–Sun distance throughout the year, the value of the solar constant (irradiance) also changes, from about 1410 $W \cdot m^{-2}$ in January to about 1320 $W \cdot m^{-2}$ in July (Fig. 3.17).

3.6.3 A Decrease in Radiation Energy Due to Passage Through the Atmosphere

Figure 3.18 shows a successive passage (transmission) of solar radiation of certain energy ES through the atmosphere where the radiation energy loses its

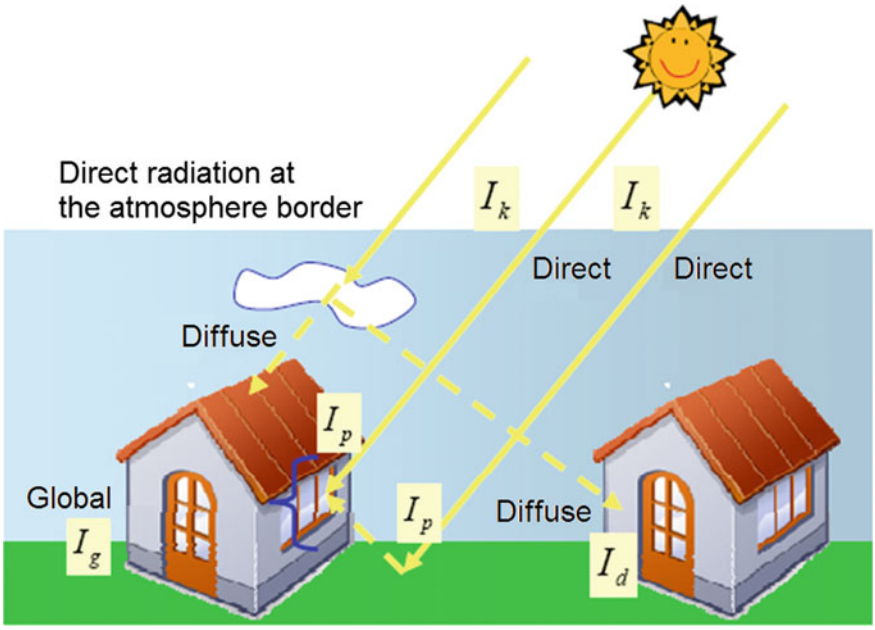

Fig. 3.17 Direct and diffuse solar radiation [3]

subcomponents due to effects acting on the solar radiation in the atmosphere. When passing through the atmosphere, the solar energy is absorbed and scattered. It is very difficult to define these losses with mathematical precision; this requires a lot of information, both meteorological and physical. As an illustration, however, it is sufficient to present a brief overview of influences and dependencies which affect the passage of solar radiation through the atmosphere.

If proceeding according to Fig. 3.18, the first loss of solar energy is caused by passage of sunlight through the ozone layer of the Earth. The magnitude of this loss is, therefore, dependent on the width of the ozone layer.

Another loss is caused by the so-called Rayleigh scattering which is the scattering of light on gas molecules in the atmosphere or other particles smaller than the wavelength of the solar radiation.

Other losses of solar energy are caused by aerosols contained in the atmosphere and water vapor dispersed in the atmosphere.

The last of losses with a substantial influence on the reduction of solar energy during the passage of solar radiation through the atmosphere is the loss of solar energy caused by the atmospheric cloudiness.

Most of the radiant energy at wavelengths below 0.3 mm is absorbed by the atmosphere. Scattering of direct solar radiation in the atmosphere is the cause of diffuse sky radiation—see Fig. 3.17. Radiant energy at a given time and at a specific location of the Earth's surface is, therefore, the sum of direct and diffuse solar radiation.

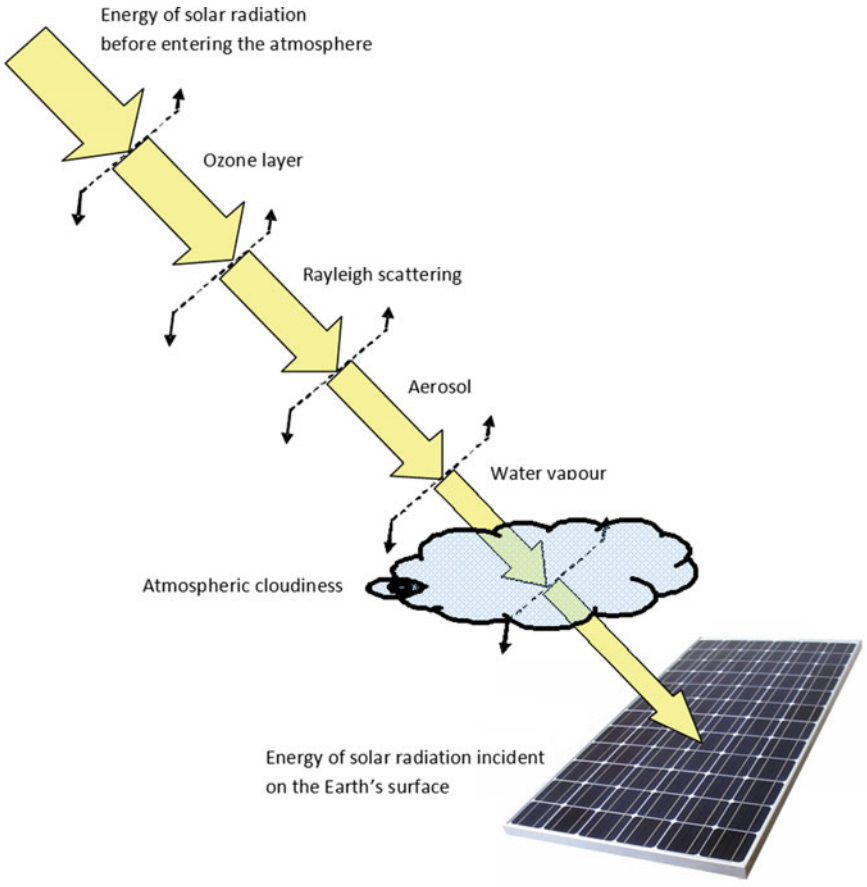

Fig. 3.18 The passage of solar radiation through the atmosphere

The results of measurements of the spectral composition of solar radiation under given conditions (time and place) are, therefore, valid only for these conditions and include, besides the above-mentioned and hardly definable atmospheric conditions, also the effect of season and daytime (the Sun's azimuth and the height of the Sun above the horizon, i.e., the solar zenith angle).

At accurate physical measurements, the water vapor content or ozone content in a vertical column of the atmosphere is measured as the height of the column of the corresponding condensed water or ozone, e.g., in centimeters. Scattering on the aerosol particles and absorption is expressed by the so-called Angström turbidity factor.

In practice, the evaluation of changes in solar radiation during its passage through the atmosphere uses the so-called airmass coefficient (airmass influence coefficient) which serves for expressing the path length of sunrays in the Earth's

atmosphere. This factor is considered to be equal to 1 if the Sun is at its zenith and is denoted as M. In another height of the Sun above the horizon, the airmass coefficient approximately indicates the cosecant of this height, i.e., the secant of the solar zenith angle. The airmass coefficient $M = 1$ (unit thickness of the atmosphere) is characterized as a notionally compressed column of perfectly clean atmosphere with height of 8000 m, which is perpendicular to the plane of the sea surface. The notional thickness of the atmosphere for the passage of sunrays is 216 km.

The amount of radiation that passes through the atmosphere is indicated by the following relationship Eq. (3.5):

$$R_g = R_S \cdot k^{\cos ec\,\alpha} \cdot \sin \alpha, \tag{3.5}$$

where R_g is the global radiation incident on a horizontal surface of the Earth at sea level, R_s is the solar constant (adjusted to a current distance between the Earth and the Sun), k is the atmosphere permeability coefficient (dependent on the atmospheric pollution) ranging between 0.7 and 0.9, α is the angle of the Sun's height above the horizon, and cosec α is the cosecant of angle α, i.e., 1/sin α.

3.6.4 Losses Due to Conversion in the Photovoltaic Cell

Under the climatic and meteorological conditions, the energy of solar radiation incident on the surface of the photovoltaic panel fluctuate during the year. Before conversion of this energy into electrical energy, there are losses of various physical causes, as shown in Fig. 3.19. The values shown in Fig. 3.19 are merely indicative and are different for different types of photovoltaic panels.

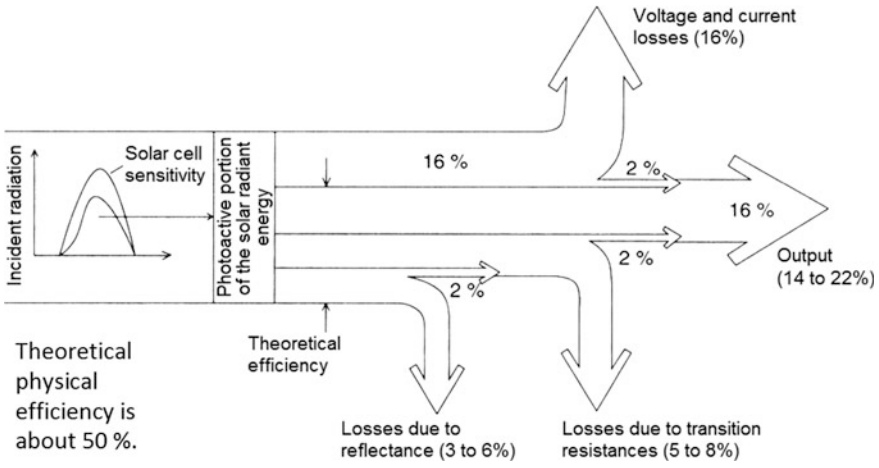

Fig. 3.19 Losses in converting the solar radiation into electrical energy

The amount of energy which can be absorbed by the photoactive part of the photovoltaic panel is dependent on the panel type; monocrystalline panels only absorb direct solar radiation while polycrystalline panels are able to absorb also a part of the diffuse radiation.

3.6.5 Methods for Predicting the Production of Electricity from PPPs

As well as for predicting the production of electricity from wind power plants, there are currently several different approaches to predicting the production of electricity from photovoltaic power plants.

The most commonly used method is based on a forecast for climatological and meteorological variables that have a significant effect (cloud cover, temperature, wind speed, etc.) on the resulting amount of electricity produced. Together with data from local devices for measuring the current climatological variables and data from local solar databases, these data are used as input data for the prediction system; based on these input data and after performing a large amount of corrections, this system predicts the expected energy produced from the respective photovoltaic plant.

Another possibility of predicting the production of electricity from photovoltaic power plants is to use highly sophisticated mathematical methods based on time series; using a database of real measurements, these methods are able to predict the amount of produced electricity with some accuracy.

At present, also the use of the so-called neural networks for predicting the electricity production is gaining importance. These are networks which utilize sets of input and output data and create logical links between these data; based on these links, they are able to independently generate output data for the given input data. A general example of the prediction procedure using a neural network is shown in Fig. 3.20.

However, the modern prediction systems for photovoltaic power plants mostly use of a combination of the above procedures to minimize prediction errors [4, 5].

3.6.6 Solar Databases

In Europe, there are hundreds of weather stations; in addition to many other meteorological variables, they also measure solar radiation, whether directly or indirectly.

To obtain a comprehensive database of solar radiation data for the entire European territory, the measured values must be used for deriving solar radiation values for locations where no meteorological measurements are performed. The most commonly used mathematical procedures are different interpolation methods,

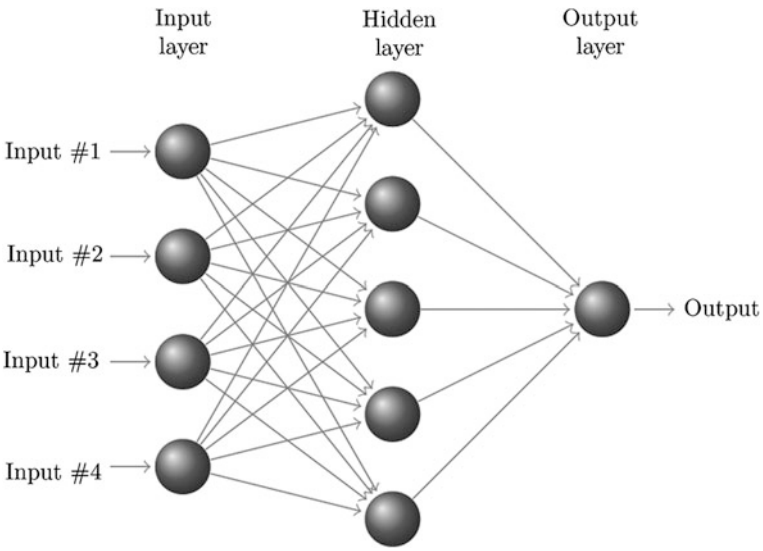

Fig. 3.20 The general principle of the use of neural networks

such as "spline" functions, the methods of weighted average or kriging (geostatistic techniques used to interpolate parameter values in neighborhood of a known value of the monitored parameter).

Especially, values of territorially continuous variables, such as radiation energy, can be obtained directly using the images from geostationary and orbiting satellites. The data obtained from satellites are compared with data from ground-based measurements.

New satellites, such as Meteosat 8, and new models, such as Heliostats-3, provide data of high-spatial (grid 1 × 1 km) and temporal (1 image every 15 min) resolution.

GIS systems are often integrated into the models of solar radiation to eliminate the influence of rugged terrains. The following chapters briefly mention some of the global solar databases.

3.6.7 The European Solar Radiation Atlas (ESRA)

This atlas [6] is a unique tool for obtaining information about solar energy in the area from the Ural Mountains to the Azores islands and from the African coast to the Arctic Circle. The basis of this database consists of measured data from 1981 to 1990. The database contains information about the total solar energy (direct and diffuse), duration of sunshine, air temperature, precipitation, water vapor pressure, and atmospheric pressure.

Using a suitable software, it is possible to display maps with meteorological data as well as specific graphs for each measurement site.

3.6.8 HelioClim

Databases HelioClim [7] consist of data obtained from satellite observations. They include three databases containing information about the solar energy and cover the area of Europe, Africa, the Mediterranean Sea, the Atlantic Ocean, and the Indian Ocean (Table 3.3).

Currently, a new database HelioClim-4 with a higher geographic resolution and 15-min time resolution is going to be started.

3.6.9 Satel-Light

Satel-Light database contains data from 1996 and 1997. These data are based on satellite images from the satellite Meteosat for a half-hour interval. Using meteorological models, the data from the satellite are transformed into values valid for the surface of the Earth. The database covers the whole of Europe [8].

3.6.10 Nasa SSE

Over 200 satellites measure meteorological data and various parameters of the solar radiation. These data are used already for 22 years to calculate monthly average values by means of mathematical models. Likewise, NASA has established a network of 1195 ground weather stations that measure meteorological variables since 1964 [9].

Table 3.3 Specification of HelioClim databases

	HC1	HC2	HC3
Status	Version 4	Version 1.0.1	Version beta
Spatial resolution	About 20 km	About 10 km	About 5 km
Period	1985–2005	2004–2010	2004–2010
Time resolution	Day	Hour	15 min
Updating	None	Daily	Daily
Data availability after obtaining the satellite image	None	Within 1 day	Within 1 day

3.6.11 SWERA

SWERA [9] provides information on solar energy in selected localities. Databases are created based on information from satellites and measurements of ground meteorological stations. These databases are specifically designed for operators of photovoltaic power plants and allow a simplified planning of photovoltaic plants using maps with data on the average energy of solar radiation throughout the year.

3.6.12 SOLEMI

SOLEMI [10] is an acronym for Solar Energy Mining. It is a new source of data on solar energy based on processing images from satellites which operate with high resolution; the grid side is 2.5 km. Images are taken at 30-min intervals. Maps with data on solar energy cover more than half of the Earth's surface (Europe, Africa, South America and part of Asia).

Two satellites, Meteosat 7 and Meteosat 5, are used for monitoring and measuring. A simplified procedure for processing the data is shown in Fig. 3.21.

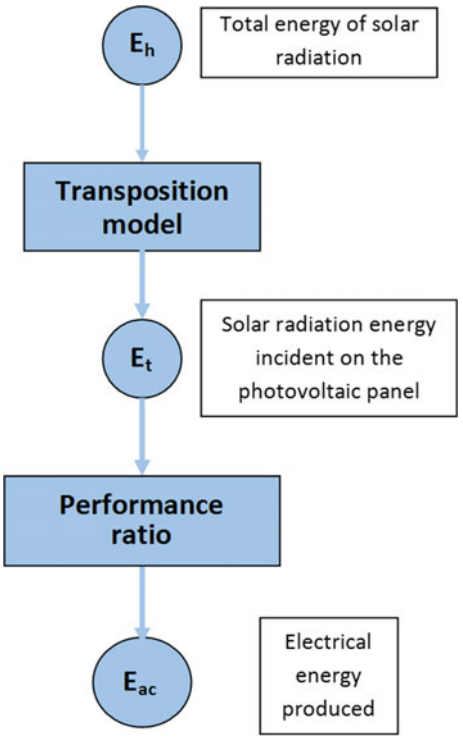

Fig. 3.21 The sequence for estimating the electricity production by a PPP connected to the network

3.6.13 METEONORM

METEONORM is a comprehensive meteorological instrument containing the catalog of meteorological data and mathematical computational tools for applications in the photovoltaic industry. It includes several databases of various meteorological parameters; the database containing data of the total energy of the incident radiation comprises data since 1981 and is constantly replenished [11].

3.6.14 SolarGis

It is a database obtained from satellite images from Meteosat satellites of the second generation and atmospheric parameters using high-performance algorithms. These data are available for Europe, North Africa, and the Middle East. The default resolution is 5 km; when involving mathematical models, however, it is possible to obtain data with a resolution of about 80 m [12].

3.7 Influence of Factors on Changes in the Predicted Power Output

After putting a photovoltaic power plant into operation, the return on investment depends on the volume of annual production of electrical energy which can be obtained by the PPP operation. The amount of electricity produced is dependent on the availability of solar radiation in the given area and the operability of the entire PPP system. To describe the procedure for estimating the electricity production from photovoltaic power plants, the best way is to follow the flow diagram in Fig. 3.21.

A key problem is the description of the behavior of the solar radiation source. In general, it is considered an amount of energy E_h (kW·h/m^2/day) incident on a horizontal surface, unit area of 1 m^2, during the day. Photovoltaic panels are usually not placed horizontally; in the vast majority of cases, they are directed to the south at a certain angle according to the position of the respective photovoltaic power plant.

The total amount of solar radiation incident on the surface of the photovoltaic panel (E_t) is calculated from the total energy of solar radiation E_h incident on the horizontal surface using the so-called transposition model.

Subsequently, the energy of solar radiation incident on the surface of the photovoltaic panel is converted into DC voltage and current which are then converted into AC voltage and current through inverters. The efficiencies of these

transformations can be classified separately, but they are usually evaluated together as a performance ratio:

$$\mathrm{PR} = \frac{(E_{\mathrm{AC}} \cdot G^*)}{(E_{\mathrm{t}} \cdot P^*)}, \tag{3.6}$$

where P^* (kW) is the system performance under standard test conditions, G^* (kW/m^2) is the reference radiation corresponding to 1 kW/m^2, E_{AC} (kW·h) is the amount of electricity produced, and E_{t} (kW·h/m^2) is the amount of solar energy incident on the photovoltaic panel.

Basically, the performance ratio expresses how much of the total solar energy incident on the photovoltaic panel is converted into electrical energy. The performance ratio respects all possible losses that accompany the conversion of solar energy into electrical energy. These losses mostly include the following sub-items:

- losses due to the efficiency of inverters;
- wiring losses;
- losses caused by incorrect connections;
- losses caused by the temperature dependence of panels;
- losses due to non-use of the complete spectrum of solar radiation;
- losses caused by pollution of the surface of photovoltaic panels;
- losses due to covers on the surface of the panels, e.g., snow;
- losses due to a reduced performance of individual cells;
- losses caused by system failures;
- losses caused by defects of individual components.

According to the procedure indicated in Fig. 3.21, the inaccuracies associated with the estimates of the amount of electricity produced can be divided into three categories:

- Inaccuracy of determining the amount of solar energy incident on the horizontal surface, which can be divided into inaccuracy in estimating the amount of incident energy and inaccuracy associated with the year-on-year variability in the amount of solar radiation in different months of the year.
- Inaccuracies associated with the use of the transposition model.
- Inaccuracies associated with the performance of the entire system defined by the performance ratio.

The following section describes the influences of various relevant factors on the accuracy of predicting the electricity production by photovoltaic plants. The following section only applies to photovoltaic panels based on crystalline silicon.

3.7.1 Estimation of the Average Values of Solar Radiation

The amount of solar radiation can be predicted using multiple usable sources, as indicated previously. Most commonly, the prediction uses large databases of measured values of solar radiation energy for a relatively long period (tens of years). Another option is to use mathematical models, interpolation of values of the amount of sunlight or estimation of values using models derived from satellite images.

These methods of predicting solar radiation energy differ from each other, not only in their techniques but also in the volume and extent of necessary annual data as well as spatial and time resolution.

3.7.2 Databases of Measured Values

Around the world, there are many reputable academic institutions as well as private companies that deal with measurements of the energy of incident solar radiation and evaluations of these measurements to create maps that display the average values of the energy of incident solar radiation.

The accuracy of these maps, as mentioned earlier, is determined by two main factors. The first crucial factor with a significant influence is the length of measurements and the associated volumes of data for the creation of such maps. The most accurate maps are created from databases of measured values for the last 40 years of continuous measurements; these databases are continuously improved in accordance with the growing robustness of individual databases.

The second factor that influences the final accuracy of such maps is the amount of ground stations where the above-mentioned continuous measurement takes place. The number of such stations reaches tens up to hundreds of measurement points in the observed area.

According to scientific resources, the errors in predicting the energy of global solar radiation generally vary in the order of several percent, about 3–6 % of the monthly basis.

3.7.3 Mathematical Models

These network models are based on mathematical modeling of global solar radiation values using meteorological models. The models respect the geometry of the Earth's position toward the Sun, information on cloudiness and other necessary parameters. Mathematical models are used for calculations in the areas where no

data are available from the databases of measured values. The models generate hourly estimated values of global solar radiation.

Inaccuracy of these models also varies in the range of several percent, in the order of about 5 %. It is also important that the models are localized for a specific area which is defined firmly by given boundary conditions. Outside these limits, the accuracy of these models is significantly lower.

3.7.4 Interpolation of Values

The method of value interpolation is used to predict the monthly average values of the global amount of incident solar energy. It relates to the interpolation of values from a certain quantity of known values. For example, when using the values from the database described in Sect. 3.6.6, which contains data for a specific area, it is possible to interpolate values for the global solar radiation between two points of the area with a different value of the observed parameter. The inaccuracy of this method also varies in the order of percent, usually about 7 %, and is higher than in the methods mentioned above.

3.7.5 Satellite Images

In addition to the prediction methods using measurements of terrestrial weather stations, there are prediction methods using the values of global solar radiation measured by meteorological satellites orbiting around the Earth.

The advantage of these methods is relatively high resolution, i.e., the area for which the value of global solar radiation is predicted has dimensions of about 10×10 km, which corresponds to 0.1° on the orbit. Except these images, the input data for the models using satellite images include data on altitude, atmospheric turbidity, amount of rainfall, the ozone layer, and snow cover.

3.7.6 The Methods of Existing Systems

Given the fact that the prediction of values of incident global solar energy is complicated, the current commercial predictive systems are based on a combination of two or more of the mentioned methods. Absolute minimum is a combination of a database of measured values and satellite images.

3.7.7 Variability of Solar Energy Sources

Year-on-Year Variability
Analyses carried out on the basis of comparing the measured amounts of solar energy with satellite images showed variations in the annual volume of solar radiation. These variations occurred in the range of 4–6 %; in areas with dry climates, they were lower than in mountainous and coastal areas.
A similar monitoring relates to the year-on-year energy variability for each month. These observations show that the highest deviations occur in winter (in December, up to 20 % or even up to 35 % in some regions). In contrast, the summer months (June) show deviations only around 12 %.

Long-Term Variability
Solar radiation energy is the subject of 10-day and other long-term trends, although these changes are very small and vary about 0.05 $kW \cdot h/m^2$/day during one 10-day period. Compared to other inaccuracies in these predictions, we can neglect the effects of long-term trends. Likewise, it is possible to neglect changes in the energy of solar radiation due to volcanic eruptions.

3.7.8 Inaccuracies Due to the Use of Transposition Model

The transposition model is used for converting the global solar radiation incident on the horizontal surface into solar energy that reaches the surface of the photovoltaic panel which is installed at a certain angle depending on the position of the respective photovoltaic power plant. Currently, there are several transposition models that are used for these conversions. The input data used by individual models are different according to models. Regarding the input data, some models utilize the monthly average values of solar radiation while other models are more exacting and require hourly or even shorter intervals of the average values of solar radiation.

There are models that need the division of average values of solar radiation into individual components, i.e., direct and diffuse radiation. Some of them are able to perform this decomposition automatically.

When using the transposition models, an average error varies in the order of several percent, about 4–8 % in cases where the model does not decompose the radiation into individual components. If the model also performs the mentioned decomposition into direct and diffuse radiation, the achieved errors are higher.

Generally, it can be stated that there is no single “best” model which would show the highest long-term accuracy in predicting the total amount of solar radiation incident on the horizontal surface; the results of the predictions are dependent on the model selected or a combination of more models, which is currently commonly used.

3.7.9 Inaccuracies Due to the Operation of Photovoltaic Power Plants

Operating states of any photovoltaic plant are characterized by the so-called performance ratio; the meaning of this parameter was introduced in the chapter. The final value of the performance ratio is particularly influenced by the efficiency of photovoltaic panels, the presence of snow and panel aging.

Performance Ratio
Extensive long-term studies suggest that the system efficiency, the so-called performance ratio, varies between 66 and 82 %, as evidenced, for example, by the stud entitled "performance analysis of various system configurations on grid-connected residential PV systems." The studies also found relatively large differences in the performance of individual photovoltaic panels from various manufacturers; these were caused by overestimated label values of these panels. Currently, there are no extensive studies regarding the efficiency of systems for photovoltaic power plants with installed capacity in orders of units of MWp. It is believed, however, that the efficiency of these systems will move at the upper limit of the above-mentioned range.

Deviations from the Rated Power
It is quite common that photovoltaic panels are unable to supply the power indicated by their manufacturers. The failure to achieve rated powers is one of the main causes of the reduction in the resulting performance ratio. Various foreign studies show that these deviations can reach up to 20 % of the performance declared by the manufacturer.

These significant deviations from the rated values should prevent by standard IEC 61646 [13] and IEC 61215:2016 [14] standards. The use of overestimated label values negatively affects the accuracy of the prediction of the amount of incident solar energy.

Aging of Photovoltaic Panels
Aging of photovoltaic cells is generally divided into two groups:

- Primary (early) aging, a very rapid decrease in efficiency during the first few years of operation.
- Long-term reduction in efficiency during each year of operation.

The primary reduction in the efficiency of photovoltaic panels made out of crystalline silicon is estimated at 2–4 %. Absolutely typical value normally considered in the predictions is 3 %.

It is more or less impossible to determine a single value of the percentage reduction in efficiency during each year of the photovoltaic panel operation. Foreign research and tests of various types of photovoltaic panels show that the average decline in efficiency is around 1 % (but rather below this value) depending on the

position of the respective photovoltaic power plant. PPPs in desert regions showed greater decreases in efficiency than PPPs installed in colder areas.

Service Availability of the System

In general, due to the components of which the photovoltaic plants are composed, the fault rate of PPPs is relatively low. Compared to other types of power plants, this is mainly due to the absence of rotating machines and less maintenance requirements. Nominally, the service availability of photovoltaic power plants achieves high values, highly above 90 %; the majority of them reach almost 99 %.

The photovoltaic power plants also do not show any major maintenance downtimes, since the vast majority of maintenance work can be performed when PPPs do not supply electricity. Shutdowns of PPPs occur rather for reasons of faults (unfavorable weather conditions) on the lines to which they are connected.

In PPPs, the most common causes of operation failures include the faults of the control system, faults of inverters, malfunctions in switchboards, faults of photovoltaic panels or faults on the AC side. Likewise, it is possible to consider failures caused by lightning, the high resistance of switch contacts on the AC side, malfunctions of blocking diodes or problems with insects or rodents.

The causes for shutdowns of photovoltaic power plants are predominantly associated with faults of inverters.

The Presence of Snow

The presence of snow is considered one of the leading causes for the reduction in power supplied from photovoltaic power plants during the winter season. The snow also causes the high deviation between the predicted and actual performance of PPP systems.

The importance of snow cover is directly related to the position of the respective photovoltaic plant; it is entirely clear that this influence is different in desert areas and in the Nordic countries. Differences between the degree of influence in lowland and mountain areas are equally noticeable.

The elimination of this negative effect is possible only on the basis of good monitoring aimed at the state of the photovoltaic power plant and short response times of the maintenance crew of the PPP operator.

Regarding the variants of snow covers, there are more important parameters, such as the type of snow cover, snow age, temperature, the angle of inclination of photovoltaic panels, the type of supporting structure, the distance between the panels or the distance between the panels and the ground.

Due to the large variability of these parameters, it is difficult to generalize the influence of snow cover on the PPP power and performance prediction.

Pollution of Photovoltaic Panels

It is very difficult to accurately estimate the accumulation of pollution and its effect on the performance of photovoltaic cells, since it depends on dustiness as well as intensity, quantity, and frequency of rainfall in the given site. Usually, the losses caused by pollution of the surface of photovoltaic panels are considered around 7 %.

Especially in urban areas, it is appropriate to consider the pollution caused by birds, which can lead to losses in percentage units (approximately 3 %).

Shading and Inclination

In photovoltaic power plants where the panels are arranged in individual rows, it is possible that one row of photovoltaic panels shades the other row. This shading can be reduced only by changing the arrangement of the rows of photovoltaic panels; therefore, this factor must be considered already when designing the PPP layout.

Predicting the PPP power output in partial and simultaneously variable shading is still quite difficult (Figs. 3.22, 3.23 and 3.24).

Other Possible Losses of the Photovoltaic System

Other potential losses, to be considered when predicting the production of photovoltaic power plants, include thermal losses, spectral losses, losses due to lower performance in low light conditions, losses due to reflections on the upper layer of photovoltaic panels, wiring losses, losses due to bad connection and losses in converting DC voltage into AC voltage. The total amount of these additional losses is estimated at 3–5 %.

Likewise, it is necessary to count with a certain uncertainty which arises in the modeling of individual types of losses mentioned in the previous chapters. Usually, 3–5 % inaccuracy is considered.

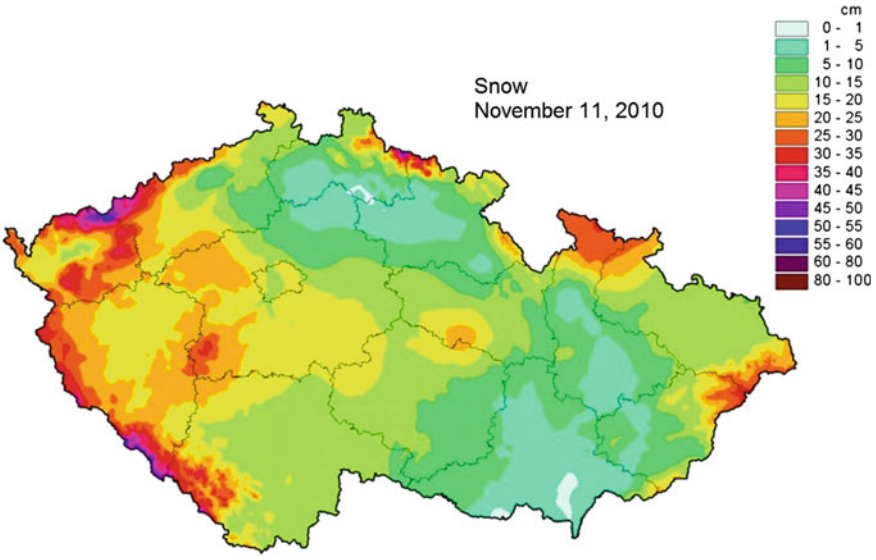

Fig. 3.22 Snow cover height in the territory of the Czech Republic

Fig. 3.23 Pollution of the surface of photovoltaic panels [15]

3.8 Assessing the Possibility to Increase the Available Power Output of PPPs

Availability of the power output of a PPP relates to the attainability of power output during a defined period. As the source of energy in photovoltaic power plants is solar energy, the availability of power output of PPPs is limited already due to their principle. Figure 3.25 shows that a PPP with installed peak capacity of 1100 kWp reaches average highs just over half of its installed capacity during summer months. During winter months, the average highs reach about a quarter of the installed peak capacity.

This principle, on which PPPs are based, enables only limited options to increase the availability of their power output. The following chapters describe the various possibilities of increasing the availability of power produced by PPPs purely from a technical point of view; economic and legislative conditions of these options are not

Fig. 3.24 Properly designed spacing between individual rows of panels

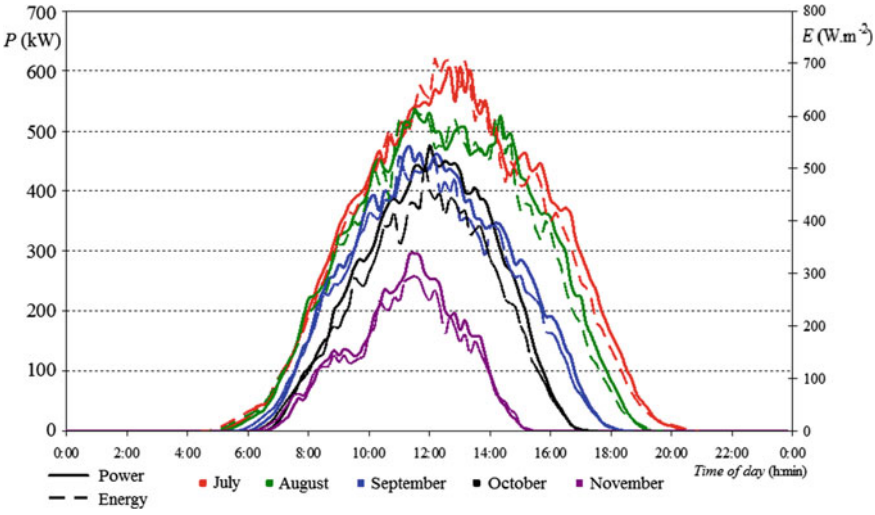

Fig. 3.25 Average output of a PPP for the selected months

considered. Individual options can then be divided into several categories according to the ways of increasing the availability of power from PPPs:

- Tilting systems
- MPPT
- Concentrators
- Efficiency of photovoltaic panels.

3.8.1 Tilting Systems

The operating principle of photovoltaic cells indicates that the cell power output depends on the angle of incidence of solar radiation. Photovoltaic cells deliver the highest power when the solar radiation strikes upon them perpendicularly. This can be achieved, for example, by tilting the photovoltaic panels in the direction of the Sun.

Practical solutions to the panel tilting system can be implemented in several variants:

- autotraction in one axis with a fixed optimum inclination of the panels;
- autotraction in one axis with the possibility to abruptly change the inclination of the panels according to the season;
- continuous autotraction in two axes.

To compare the yield of power output in installations with fixed panels and installations with continuous autotraction in two axes, a simple calculation for both variants is given below.

The Earth rotates around its axis with a period of 24 h which causes the alternation of day and night. The Earth's axis of rotation and the orbit plane make an angle of approximately 23°. During winter in the northern hemisphere, the maximum height of the Sun above the horizon is only about 16°—see Fig. 3.26.

In summer, the maximum height of the Sun is about 63°, implying the need to tilt the panels, so that they are always positioned perpendicularly to the Sun throughout the year.

The results of our long-term measurements of the energy of solar radiation indicate that the values of solar energy in our conditions do not significantly exceed the value of 1000 $W \cdot m^{-2}$, and further, assume 12 h as the time during which the solar radiation is incident. The calculation will be made for a unit area. Energy calculation is given by the following relationship:

$$W = \int_{t_1}^{t_2} P \mathrm{d}t = \int_{t_1}^{t_2} GS \mathrm{d}t, \tag{3.7}$$

where P (W) is the power of the incident radiation, S (m^2) is the surface projection at oblique incidence, and G ($W \cdot m^{-2}$) is the energy of solar radiation.

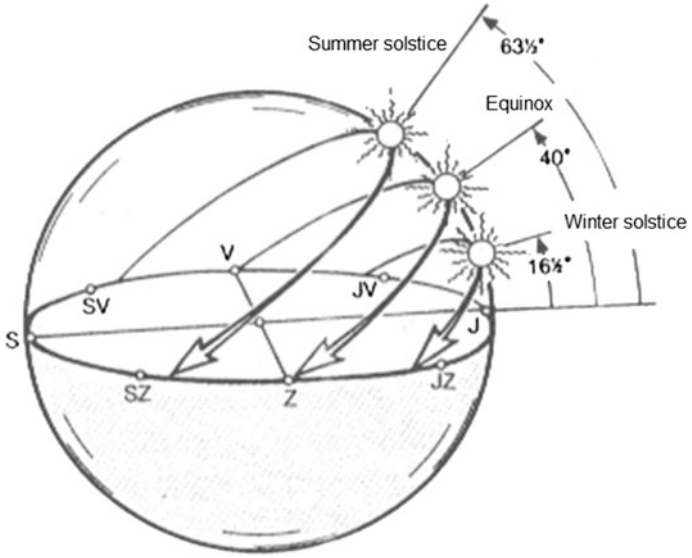

Fig. 3.26 The path of the Sun across the sky

3.8.2 Photovoltaic System Without Traction

In photovoltaic systems without traction, the angle of incidence of sunrays changes during the day in the range from −90° to 90°. An example of the course of power output in a system with fixed installation of panels is shown in Fig. 3.27.

The angular velocity of the Sun is given by the Eq. (3.8):

$$\omega = \frac{2 \cdot \pi}{T} = 7.27 \cdot 10^{-5}\,\mathrm{s}^{-1}. \tag{3.8}$$

When not considering the influence of the atmosphere, the calculation of energy incident on a unit area is as follows:

$$\begin{aligned} W &= \int_{t_1}^{t_2} GS\mathrm{d}t = \int_{t_1}^{t_2} GS_0 \cos\omega \mathrm{d}t = G \cdot S_0 \cdot \int_{t_1}^{t_2} \cos\omega \mathrm{d}t \\ &= G \cdot S_0 \cdot \left[\frac{\sin\omega}{\omega}\right]_{t_1}^{t_2} = \frac{2 \cdot G \cdot S_0}{\omega} \\ &= \frac{2 \cdot 1000 \cdot 1}{7.27 \cdot 10^{-5}} \cong 2.75 \times 10^7\,\mathrm{W} \Rightarrow \frac{2.75 \cdot 10^7\,\mathrm{W\,s}}{1000 \cdot 60 \cdot 60} = 7.64\,\mathrm{kW \cdot h} \end{aligned} \tag{3.9}$$

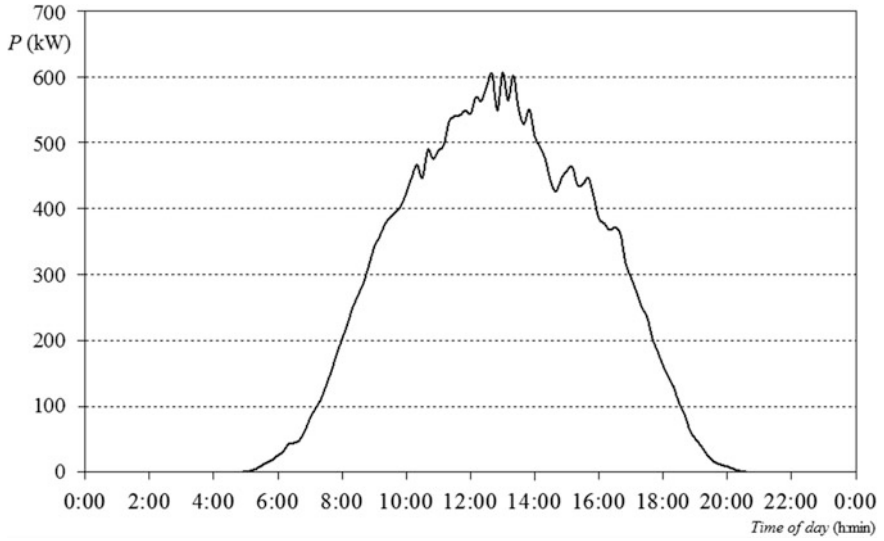

Fig. 3.27 The course of power output in a photovoltaic system with fixed installation of panels

3.8.3 Photovoltaic System with Autotraction

Systems with autotraction in both axes represent the optimum in tracking the trajectory of the Sun across the sky during the day. The energy of autotraction systems is given as:

$$\begin{aligned} W &= P \cdot t = G \cdot S_0 \cdot t \\ &= 1000 \cdot 1 \cdot 60 \cdot 60 \cdot 24/2 \cong 4.32 \cdot 10^7 \,\mathrm{W \cdot s} \\ &\Rightarrow \frac{4.32 \cdot 10^7 \,\mathrm{W \cdot s}}{1000 \cdot 60 \cdot 60} = 12 \,\mathrm{kW \cdot h} \end{aligned} \tag{3.10}$$

3.8.4 Comparison of Both Systems

When comparing the generated electric power for systems with fixed installation of panels and systems with a full two-axis autotraction, we obtain the following relationship:

$$\frac{W_{\text{two axes}}}{W_{\text{Fised installation}}} = \frac{12}{7.64} = 1.57 \tag{3.11}$$

The above ratio of energies shows that the use of autotraction devices can result in obtaining up to 57 % more energy than in the case of systems with fixed installation of photovoltaic panels. However, the above calculation is true only for the ideal case where, among other things, we also neglect the influence of the atmosphere and consider a constant energy of solar radiation throughout the period of PV system operation.

In fact, the tilting system is able to convert by about 15–40 % more power than the system with fixed installation (Fig. 3.28).

3.8.5 Maximum Power Point Tracking (MPPT)

Due to the shape of the voltage–current characteristic of photovoltaic cells (see Fig. 3.29), the maximum power output of the photovoltaic cell requires that the cell is continuously working in the so-called maximum power point. During operation of PPPs, it is, therefore, necessary to use methods and procedures that enable maximum power point tracking. Currently, the MPPT functions are implemented in

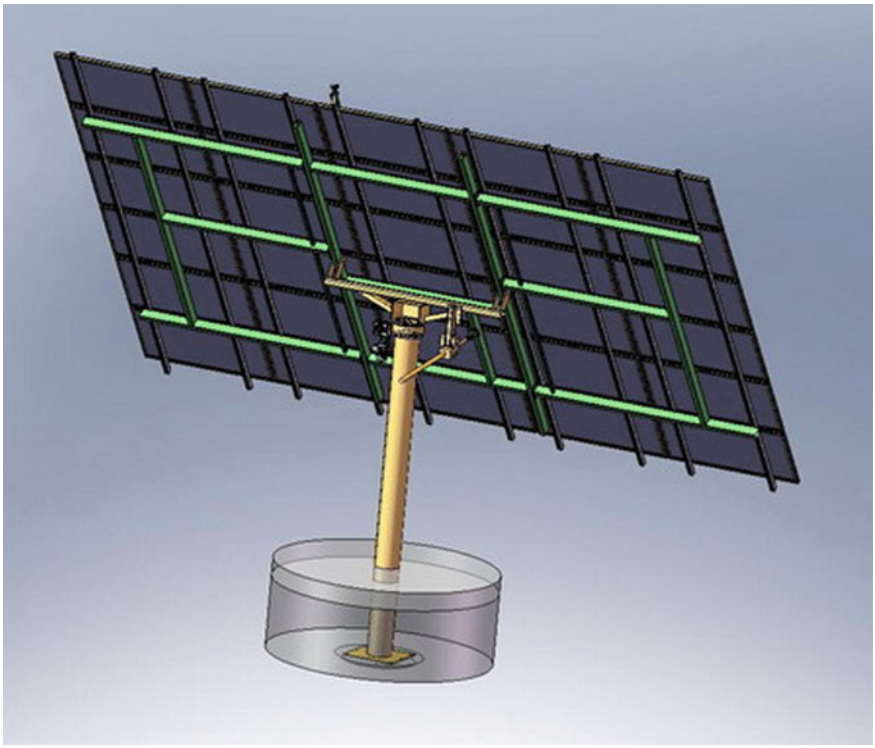

Fig. 3.28 Two-axis tilting system

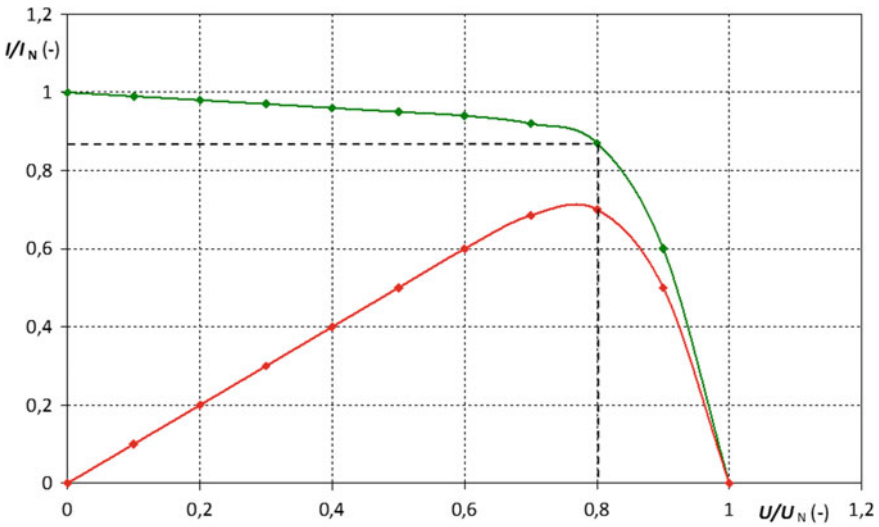

Fig. 3.29 Voltage–current characteristic of a photovoltaic cell. In *red*—power output of the cell; in *green*—voltage–current characteristic

inverters. The question is how good is the control algorithm that ensures maximum power point tracking. The ideal case is when each DC string connected to an inverter has its own MPPT regulation which provides the possibility to achieve maximum power output.

As mentioned above, the objective of MPPT techniques is to search such values of U_{MPP} or I_{MPP} at which the photovoltaic panel is capable of supplying the maximum power PMPP at a particular temperature and incident solar energy. It should be mentioned that the voltage–current characteristic can have multiple local maxima in cases where the panel (chain or the whole plant) is partially shaded; in general, however, the maximum power point is always only one. The methods mostly respond to changes in both attributes (temperature and energy of solar radiation), but some of them are more applicable in cases where the temperature is approximately constant, which is in most cases. Usually, the techniques also automatically respond to changes due to aging of panels; nevertheless, some methods require regular adjustment of parameters with regard to the age of the panels.

3.8.6 MPPT Techniques

The following text briefly describes the selected MPPT techniques.

Hill Climbing/P&O

These methods are based on creating a deviation and monitoring the system response to such a deviation. In practice, this means to create a change in voltage or

current, and subsequently monitor the increase or decrease in the power output. If the output decreases, an opposite deviation in voltage or current is induced and the change in the system output is pursued again. These deviations run in cycles, and this permanently maintains the operating state at the maximum power point—see Fig. 3.30.

The Ratio of Step Changes

Figure 3.30 shows the *P–U* characteristic of a PPP. If the system operating point is at the top of this characteristic (MPP), the slope of tangent (derivative) at this point of the output characteristic is zero; when the operating point is to the left of MPP, the slope is positive; when the operating point is to the right of MPP, it is negative. Mathematically, it can be written as follows:

$$\begin{cases} \mathrm{d}P/\mathrm{d}U = 0 & \text{MPP} \\ \mathrm{d}P/\mathrm{d}U > 0 & \text{To the left of MPP} \\ \mathrm{d}P/\mathrm{d}V < 0 & \text{To the right of MPP} \end{cases} \tag{3.12}$$

The principle of this method is apparent from the above mathematical notation where the ratio between the change in power output and the change in voltage is monitored, and the system voltage is accordingly regulated, so that this ratio is constantly zero.

Other MPPT Methods

Currently, there are several other methods for tracking the maximum power point of PV systems. For example, it is possible to use the link between the panel no-load voltage and the voltage at the maximum power point which is linearly dependent.

Fig. 3.30 *P–U* characteristic of a PPP

Furthermore, it is also possible to use an almost linear dependence between the current at the maximum power point and the short-circuit current. Methods based on fuzzy logic, neural networks, and many others also have a wide utilization.

3.8.7 Concentrators

Concentrators are optical devices which are used to concentrate solar radiation from the surroundings of panels to their surface. The most common versions use mirrors or lenses (Fig. 3.31).

When designing concentrators, it is necessary to respect certain principles and limitations. An essential factor is the spatial arrangement (tilt) of concentrators so that they are able to concentrate also diffuse radiation. It is also necessary to choose the shape of concentrators, so as to prevent local heating of panels and the associated decrease in their performance. Concentrator should illuminate panels evenly and adequately; it is also appropriate to consider a natural cooling of panels with installed concentrators by air flow.

Fig. 3.31 Solar concentrators [16]

3.8.8 *Efficiency of Panels, the Use of Radiation Spectrum*

Another theoretical possibility of producing more electricity is the installation of new types of photovoltaic panels with higher efficiency. In the last two to three years, the efficiency of photovoltaic panels is gradually and slowly increasing up to the values approaching 20 %. Efficiency of panels installed two years ago was about 15 %.

When replacing the photovoltaic panels, the amount of produced electricity would be higher, but the distribution of production during the day would be the same. A way to increase the length of production of electric energy during the day is the use of panels of the third and higher generations (amorphous, microcrystalline silicon, thin film panels, etc.) which are able to absorb more parts of the spectrum of solar radiation. The actual use of these panels of the new generations, however, is blocked by high prices, remaining low efficiency as well as availability in the market.

References

1. Photovoltaic Geographical Information System—Interactive Maps (2016) http://re.jrc.ec.europa.eu/pvgis/apps4/pvest.php. Accessed 25 Feb 2016
2. System Operation Code of Czech Republic (2010)
3. Rubinova O (2012) Tepelně vlhkostní bilance budov. http://www.fce.vutbr.cz/TZB/rubinova.o/prednasky/A_VZT%2010_09.pdf. Accessed 8 Mar 2016
4. MeteoGroup (2016) http://www.meteomedia-energy.com/index.php?id=116&lang=1. Accessed 15 May 2016
5. ENFOR A/S (2016) Solarfor. http://www.enfor.dk/solar_power_prediction_solarfor.php. Accessed 4 Apr 2016
6. Institute for Energy and Transport (2016) Solar resources data and tools for an assessment of photovoltaic systems. http://re.jrc.ec.europa.eu/pvgis/solrad/index.htm#Approaches. Accessed 17 Mar 2016
7. HelioClim (2008) The HelioClim databases. http://www.helioclim.org/radiation/index.html. Accessed 30 Apr 2016
8. Satel-Light (2014) The European database of daylight and solar radiation. http://www.satellight.com/core.htm. Accessed 5 June 2016
9. Atmospheric Science Data Center (2016) Surface meteorology and Solar Energy. http://eosweb.larc.nasa.gov/sse/. Accessed 15 May 2016
10. DLR Institut für Technische Thermodynamik (2016) SOLEMI—solar energy mining. http://www.solemi.com/home.html. Accessed 5 May 2016
11. Meteotest (2016) Meteotest. http://www.meteotest.ch/index.php. Accessed 28 May 2016
12. Solargis (2016) Solargis forecast. http://geomodel.eu/index.php?d=products&f=solar-radiation. Accessed 8 June 2016
13. IEC 61646:2008 (2008) Thin-film terrestrial photovoltaic (PV) modules—design qualification and type approval

14. IEC 61215:2016 (2016) Terrestrial photovoltaic (PV) modules—design qualification and type approval
15. PV Education.org (2014) Birds. http://pvcdrom.pveducation.org/MODULE/Images/BIRDS.GIF. Accessed 15 May 2016
16. Photovoltaic Power Solar Systems (2016) Solar concentrators. http://www.solar-solar.com/Attachments/PI8CT21.JPG. Accessed 23 June 2016

Chapter 4
Hybrid Off-Grid Systems Using Renewable Energy Sources

Previous chapters describe the basic characteristic parameters and the results from the measuring of the fault and operational states of the wind power plants and photovoltaic power plants separately. The aim of this chapter is the introduction of the basic characteristic connection of these sources into the so-called hybrid off-grid system which is operated in the off-grid mode that means without dependency on the external power grid. This type of cooperation of mentioned sources is very specific due to combination of two sources with the stochastic character of their electric power production. Therefore, the basic specification of sources in the off-grid system presents the introduction part. The second part of this chapter introduces example of the off-grid system using for some application subsequently. And finally, the last part of this chapter presents results from the experimental measuring of the fault states in the off-grid system, and the functionality of some method of the relay protection method is shown too. The economic analysis of the off-grid system running is the part of the introduction part, and it was processed for the micro off-grid system.

4.1 General Description

Due to the reduction in redemption prices of electricity from photovoltaic power plants (PPP) and also with regard to a high tax burden, the investments in the construction of PPP are currently lowly profitable. Due to many legislative barriers, the same applies to the construction of WPPs (WPP) [1]. One alternative of utilizing these renewable energy sources (RES) is their use for operations in the off-grid mode, i.e., without their connection to the distribution network. According to the magnitude of the installed capacity of the respective PPPs and WPPs, the off-grid systems can be used to power small applications with outputs of hundreds of watts up to applications that are used to power family houses, buildings or even entire villages where the connected load has an output up to megawatts. Everything is

S. Misak and L. Prokop, *Operation Characteristics of Renewable Energy Sources*,
Green Energy and Technology, DOI 10.1007/978-3-319-43412-4_4

dependent on the installed capacity of individual sources, the type and capacity of the storage device, the control system, and devices to be powered by the off-grid system. Most commonly, however, we encounter systems that have to cover the electricity consumption in the order of several kilowatts [2, 3].

At present, the so-called hybrid renewable electricity sources are more and more popular. In most cases, this relates to a parallel collaboration between wind and PPPs, whereas the power output of individual sources is used for charging a storage device from which the power consumption in a separate voltage system, the so-called off-grid power system, is subsequently covered. The operation of hybrid power sources utilizes a different time dependence of the operation of each source. In practice, this means that storage device is charged by energy from the WPP during winter months when the predominant energy for the operation of the hybrid power source is that of wind flow. Conversely, during summer months when the number of days with optimal wind flow is minimal, the storage device is charged by energy from photovoltaic panels [4, 5].

Combining RES with different principles of electric energy conversion creates a uniform hybrid source which can supply isolated voltage systems; at the same time, the mentioned combination of operations of individual sources significantly increases and stabilizes the interval of electricity supply. Thus, formed hybrid systems can be used to power remote cottage settlements, family houses or buildings. Hybrid power systems can also be used to power street lighting, tunnels, meteorological stations, pumps used for pumping water, or in cases where the use of conventional distribution network is not appropriate:

- Connection to the distribution network is not possible because of high prices for establishing electrical connections (geographic location).
- Consumer decisions on the use of RES.
- Low operating costs, low environmental impact.
- Independence of the supply of electricity from the distribution system.

4.2 Specification of Sources for Off-Grid Systems

One of the ways to maximally utilize the potential of RES and minimize their negative impacts on the grid (distribution system, distribution network) is to use them for local consumption of electricity in the place of production. In this case, the off-grid systems are defined as objects independent of the electrical power supply from the external power grid. As the primary sources of electrical energy, they use RES of electricity together with the accumulation of electrical energy through storage devices.

Currently, there are several available topologies for off-grid systems. This topology of off-grid systems can be divided into AC and DC systems.

Topology of AC off-grid systems can be divided into one-phase and three-phase power systems. The one-phase power system can be used for energizing holiday

cottages and low-energy family houses with an installed capacity of 2–8 kW. If necessary, it is possible to parallel install up to three off-grid converters with a total power output up to 24 kW for one-phase power systems. The use of three-phase systems, whose connection is basically the same as for one-phase systems, is more appropriate for larger applications, e.g., for electricity supply to several family houses or office buildings. The installed capacity of these three-phase power units can be from 24 to 300 kW.

An essential element for off-grid systems is an off-grid converter. Off-grid converter creates a standard AC distribution network, is responsible for the stable operation of the off-grid network, and maintains the voltage and frequency of the AC network within specified limits. Currently, there are two possible ways of connecting the off-grid system.

The first connection option is based on the so-called by-pass concept. A simplified block diagram is shown in Fig. 4.1. One advantage of this type of power supply is that the respective WPP and PPP with their DC/AC converters are connected directly to the one-phase power system (main bus-bar of the off-grid converter—231 V, 50 Hz) created by the off-grid converter. The power output from the respective WPP and PPP can thus cover power consumption in the system without loading the off-grid converter and discharging the storage batteries. Excess power output is used for charging the storage batteries. The possibility of connecting the respective WPP and PPP directly into the one-phase power system allows the system to cover higher power input than that of the one-phase off-grid converter would be able to cover with its maximum power output. A disadvantage of this concept of power supply is represented by frequency fluctuations and the changing short-circuit power in the off-grid power system. This is primarily due to the changing value of the short-circuit power of individual power sources,

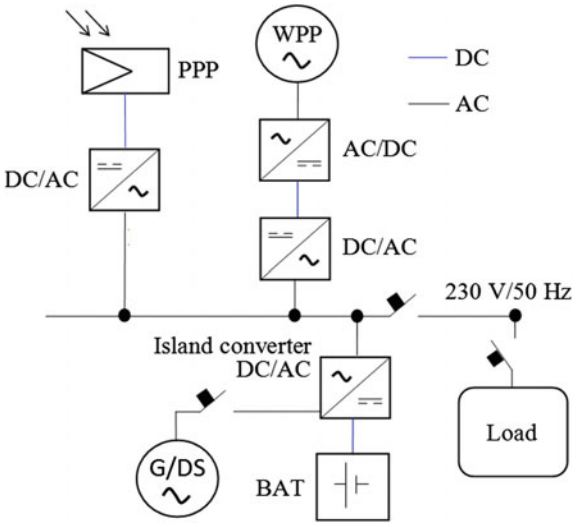

Fig. 4.1 A simplified block diagram of an off-grid system (the "by-pass" concept)

especially the WPP and limiting capacity of power electronics of individual conversion elements. The off-grid converters often use a frequency power control (FSPC). If WPP and PPP converters are connected to the one-phase off-grid network, the off-grid converter must be able to limit their power output in a situation where the storage batteries are fully charged and electric energy from the respective WPP and PPP exceeds the required input of appliances. In this situation, the island converter changes the frequency at the AC output (50 Hz ± max. 5 Hz). WPP and PPP converters limit their power output according to changes in the frequency, which results in a short frequency fluctuation in the energy system.

Figure 4.1 shows a simplified block diagram of the by-pass concept. WPP output power is first rectified and the output voltage is adjusted to the optimum value of the voltage at the converter input. Subsequently, the WPP and PPP output power is brought through DC/AC converters to the one-phase AC power system created by the one-phase island converter. The island converter charges the storage batteries at electricity excess in the off-grid system; conversely, it covers the deficit needed to balance the power production at the lack of electricity. Under bad weather conditions and the lack of electricity from the installed electrical power sources, the off-grid converter allows the use of a backup fossil-fueled generator or connection to a classical distribution system.

The second option of connecting the off-grid system uses the concept with a charging controller. A simplified block diagram is shown in Fig. 4.2. Similarly, as for the by-pass concept, the off-grid converter creates the conditions defined for a standard AC one-phase network into which the individual electric appliances can be integrated. It is responsible for running the off-grid and maintains the voltage and frequency of the AC network constantly within permissible limits. Within this concept, the batteries are charged by the charging controller. WPP and PPP output power is brought into the charging controller which charges the batteries and powers the DC side of the off-grid converter. An advantage of this system is represented by lower acquisition costs and faster battery charging because of the charging controller. Another advantage, given by a different connection configuration in individual conversion elements, is the fact that no electrical sources (WPP

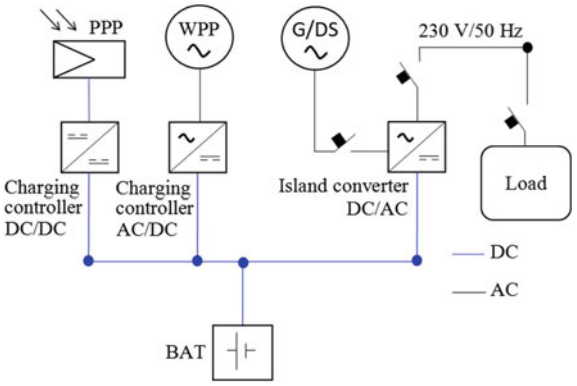

Fig. 4.2 A simplified block diagram of an off-grid system (the concept with a charging controller)

and PPP) are connected to the AC side of the off-grid network. There are no changes in the short-circuit power in the off-grid network caused by connecting or disconnecting other electrical sources. The disadvantage of this concept of connecting the off-grid system is that the WPP and PPP output power is brought into the DC side of power system components. This concept of connection cannot cover more power consumption than the maximum power of the off-grid converter.

AC off-grid network due to connecting or disconnecting other electrical sources. The disadvantage of this concept of connecting the off-grid system is that the WPP and PPP output power is brought to the DC side of the power part of the system. This connection concept cannot cover higher power consumption than that corresponding to the maximum power output of the off-grid converter.

DC off-grid topology is suitable for applications with low installed capacities. The advantage of this system of connection is its simplicity and lower constructional costs due to short distances and a relatively low system output. These systems are operated at the levels of 12, 24, and 48 V DC. However, main disadvantages of the low-voltage systems include higher operating currents and the need to select larger cable cross sections to minimize losses. Another significant disadvantage is the limited availability of DC commercial appliances. Optimal battery charging and discharging are ensured by the charging controller. The off-grid system can be utilized for connecting appliances powered by direct current. These systems are used, for instance, as power sources for small cottages, caravans, traffic signaling, telecommunication equipment or monitoring devices in the field.

4.3 Micro Off-Grid System

Figure 4.3 shows an example of a micro grid hybrid off-grid system implemented in the premises of the VŠB-TUO. As power sources, it uses classic small wind power station with a horizontal axis of rotation and polycrystalline photovoltaic panel. The second hybrid system is designed similarly; in addition to a monocrystalline photovoltaic panel, unlike the first hybrid system, it includes a small wind turbine with vertical axis of rotation. Between the two hybrid systems, there is a common distributor with NiCd storage batteries which are used to accumulate electric energy from both hybrid off-grid systems. Furthermore, the distributor contains controllers for recharging batteries and an inverter feeding light sources. All breakers and measuring elements are also located in the distributor [6].

The hybrid power off-grid system consists of two PPPs and two WPPs which together charge storage batteries with a nominal voltage of 12 V. The batteries are used to power two lamps of public lighting. Capacity of the storage battery was dimensioned for a 3-day consumption without charging input power from individual power plants. Battery charging from both PPPs is controlled by the charging controller (RN). The same controller protects the storage batteries from discharging by appliances. The WPP1 has a built-in charging controller; therefore, it is connected directly to the storage batteries. The WPP2 contains a three-phase

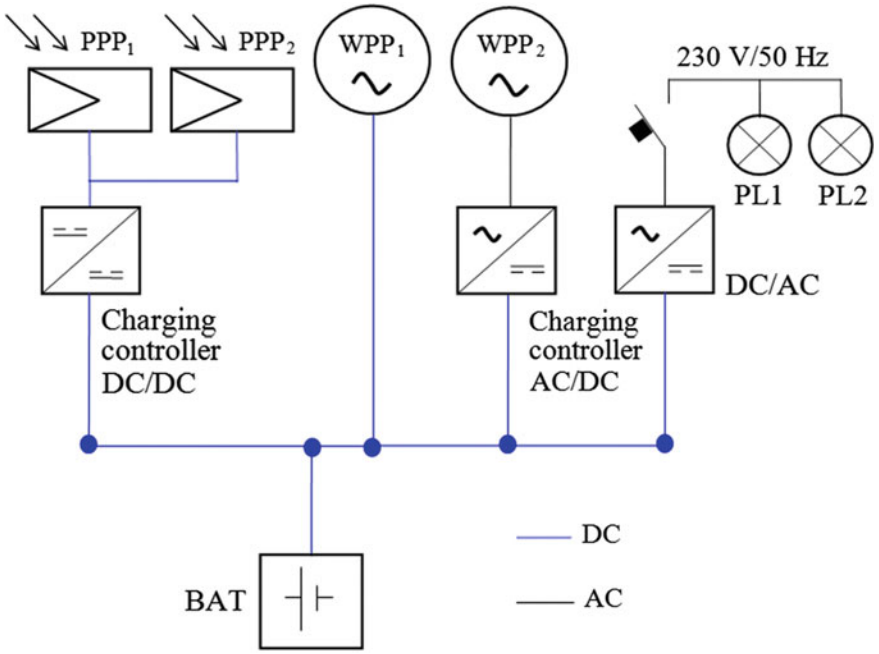

Fig. 4.3 A simplified block diagram of the island hybrid system intended to supply public lighting

synchronous generator with permanent magnets. The output of the generator is connected to a rectifier. Rectified electricity from the WPP2 charges the battery via the charging controller. Appliances in the system are two lamps of public lighting (PL1 and PL2). Both lamps are working at voltage of 230 V AC which is provided by a DC/AC converter. The hybrid system for powering the public lighting is shown in Fig. 4.4.

If expressing the share of individual sources in the overall power output of the island hybrid system, we obtain an idea of what type of sources dominates or stagnates in the given season. In addition to information about the flows of energy and time courses of required quantities in various components of the hybrid system, the measuring system also provides information about the status of the storage device, i.e., storage batteries, in our case. Results of the analysis of the capacity of this storage device within long-term measurements are shown in Fig. 4.5.

Measured voltage and current signals are used to evaluate operating states of the island hybrid power system. A proper operation of the system requires enough electricity stored in batteries as the installed power sources first charge these storage batteries which then power connected appliances. Figure 4.5 shows that the capacity of storage batteries is around 90 % in the evening which means that the power sources are able to recharge the batteries during the day. A substantial part of recharging takes place during the day; the load is connected at night hours when the

Fig. 4.4 Photos of the off-grid power system built in the premises of the VŠB-TUO; the usage of two hybrid power sources

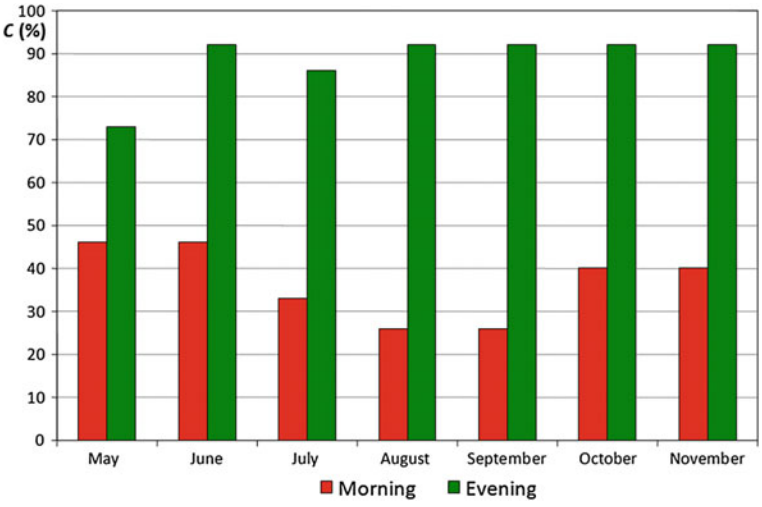

Fig. 4.5 Capacity of storage batteries within long-term measurements

stored electrical energy is consumed and photovoltaic panels do not operate. Given the dimensioned capacity of storage batteries, the off-grid hybrid power system can operate for some time even without recharging the batteries. The length of this time

depends on several criteria; an example can be the outside temperature. In winter, the requirements for the operation of storage batteries are much higher than during summer months; it can therefore be assumed that the operation time without recharging in winter will be shorter than in summer.

Despite this negative effect of some factors, the expected operation time of the system without recharging the storage batteries is about 3 days; this time should be enough for restoring the operation of sources, i.e., recharging the storage batteries. Likewise, it is important to keep in mind that the discharging of storage batteries below a certain level is undesirable and adversely affects the number of charging cycles, i.e., also the life of batteries.

A key criterion for assessing the operation and verifying the correct design of sources is the analysis of the energy balance of the entire island hybrid power system. Figure 4.6 shows the system energy balance, i.e., the average daily production, consumption and excess of energy, in each of the monitored months; it can be seen that the output power of all the sources used is sufficient to cover the consumption of the load, and that even an excess of electrical energy is generated in some months.

The amount of electricity consumed can be controlled by adjusting the regulator in several modes which allows the operator to flexibly react to the availability of individual sources; this is an important feature of the regulator, because the sources used are RES with irregular electricity supply. Availability of various sources of electrical energy depends on meteorological conditions of the respective location as well as daytime. Speed and direction of wind are decisive for WPPs, while the intensity of solar radiation and temperature is crucial for photovoltaic panels.

Figure 4.7 shows the shares of individual sources in the total electricity production of the island hybrid power system. When analyzing in detail the month of

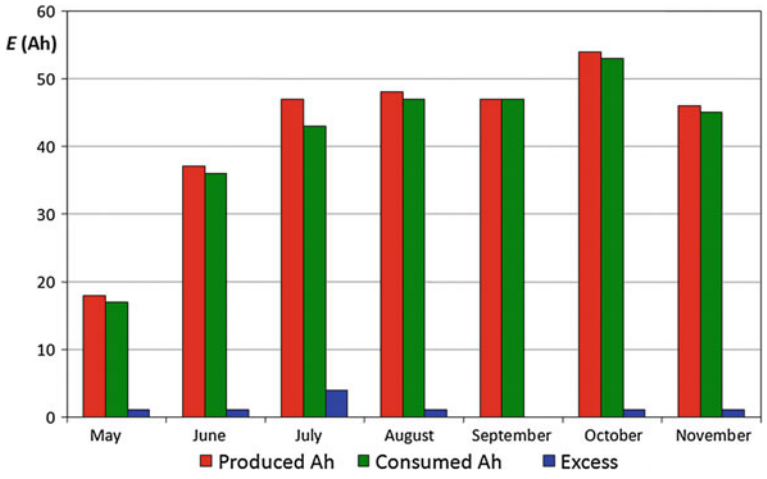

Fig. 4.6 System energy balance for each month of the operation

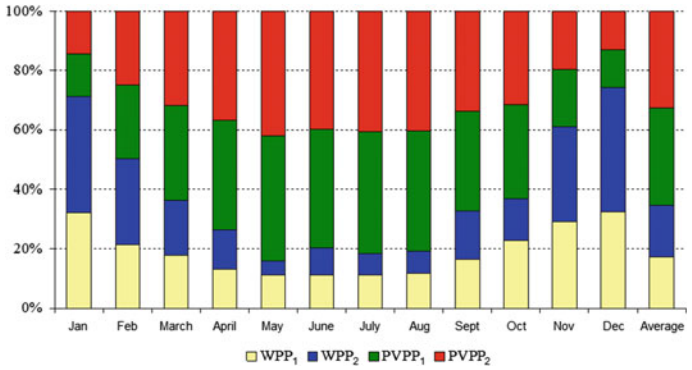

Fig. 4.7 Shares of individual sources in the total electricity production by the hybrid power system

May, i.e., the month with the largest coverage of electricity from photovoltaic panels, we find that more than 80 % of the electric energy is produced by photovoltaic panels. Less than 20 % is then produced by WPPs. In the same way as for the month with the largest contribution of photovoltaic panels to the overall produced electricity, we can also display the month of December when the situation is reversed and the supply from WPPs is maximal. In this month, the WPPs supply 41 and 33 % of the total electricity produced, while photovoltaic panels supply only 26 % [6–8].

The combination of wind and solar power plants to power the off-grid system has proved to be particularly appropriate due to the possibility of reducing the installed capacity of individual sources; both of these sources suitably complement each other at the time when one of them has a lower availability.

4.3.1 Simplified Economic Analysis of Micro Off-Grid System

The economic analysis compares the construction of micro off-grid systems with the construction of a classic network connection for supplying the public lighting mentioned and described earlier in the book in terms of investment returns.

To calculate the respective investment returns, it is necessary to adopt certain assumptions and simplifications, so that the calculation is feasible. An absolutely essential condition is that the source part of the off-grid system, consisting of a wind power plant and photovoltaic panel, will be able to produce enough electricity to power the lamps throughout the lifetime of the off-grid system, even assuming that the efficiency of the photovoltaic panel during its service life decreases by about 0.8 % per year.

The total cost of the hybrid systems was calculated as the sum of partial relevant costs. These costs mainly include material cost, labor cost, and operating cost. The first two items of costs are fixed and no longer increase after the implementation of the off-grid system. Operating cost is variable and grows linearly with the length of the equipment operation.

Mathematical expression of the total cost of the off-grid system is then as follows:

$$C_{\text{OFF-GRID}} = C_{\text{CON}} + C_{\text{LAB}} + C_{\text{OP}}, \tag{4.1}$$

where $C_{\text{OFF-GRID}}$ is the total cost of the off-grid system, C_{CON} is the cost of materials for the off-grid system, C_{LAB} is the cost of labor for the off-grid system, and C_{OP} is the cost of operation for the off-grid system.

The labor cost in the construction of hybrid systems is calculated as the product of the price for skilled manual work set at CZK 400 per hour of work and the number of hours worked. For the off-grid system, the number of hours worked was 75 h, and the labor cost then was CZK 30,000. The cost of operating the hybrid systems include the cost of maintenance and monitoring of the photovoltaic panel, batteries, and lamps. The respective price is estimated at about CZK 3000 per year for the entire system. This price consists of the costs of forklift platform, labor itself, the liquid to batteries, etc. Maintenance is expected to be performed once a year. Selected batteries have extended interval of water replenishment and need only one electrolyte content during their entire lifetime. Battery life stated by the manufacturer is longer than 20 years. The total investment cost of the construction of the hybrid system built in the premises of the VŠB-TUO amounted to CZK 218,000.

The cost of connection to the network is predominantly represented by the cost of the network connection construction, the lamppost, lamps, and the cost of electricity consumption. Price for excavation work and the supply cable was set at about CZK 700 per 1 m of the route. The price includes machine trench sinking, finishing, cable laying, filling with sand, safety foil placement, trench backfill, compaction, and cable CYKY 3 × 2.5. This price was determined for the undeveloped terrain, without the necessity to push through communications (roads), with rock type IV along the whole route. Furthermore, the total budget must include the price for the construction of a meter board cabinet, assuming the respective cost of about CZK 25,000. Consumption of electricity from the grid is determined by the time of operation, i.e., 8 h a day. With the lamp power output of 45 W, the total annual consumption makes 131.4 kW·h. Further calculation uses Standard D01d electricity rate. In the following calculations, the changes in electricity prices are not considered, and all the calculations are made at prices valid for 2016.

The total cost of the construction and operation of the public lighting powered from the distribution system is then expressed as:

$$C_{\text{NET}} = C_{\text{CON}} + C_{\text{CAB}} + C_{\text{EL}} + C_{\text{MAIN}}, \tag{4.2}$$

where C_{NET} is the total cost of connection to the network, C_{CON} is the cost of constructing the connection, C_{CAB} is the cost of the meter board cabinet, C_{EL} is the

cost of energy consumption, and C_{MAIN} is the cost of the public lighting maintenance.

After substituting for individual items in Eq. (4.2), we obtain the final expression for the cost of the system powered from the distribution network.

Equation (4.2) contains two parameters that affect the overall cost of the system connected to the distribution network (grid), i.e., the system operation time uptime and the length of the cable connection to the grid. Regarding the economic assessment, there are two possibilities: to set a fixed length of the connection, while the system operation time would be variable, or determine the system lifetime and change the resulting cost of this method of supply by changing the length of the connection, so as to allow comparison with the above-described hybrid island systems.

To assess the second variant, the lifetime of all the systems is defined as 30 years. For this lifetime, we calculated the cost of the hybrid systems and the system powered from the grid. The total cost of the system connected to the grid is modified by changing the length of the connection. At present, the cost of electricity connection is paid by the property owner (the length over 50 m). The price depends on the length of the connection, whereas the lowest price is CZK 700 per m^2 (soil type IV). For better clarity, Fig. 4.8 shows only the variant with connection length of 300 m.

Figure 4.8 shows that the off-grid system, since the initial investment, is economically preferable compared with the system connected to the grid. The results of this economic analysis implicate that there are situations where the construction of off-grid systems is more cost-effective than the construction of systems connected to the distribution network. Likewise, this analysis shows that every correct

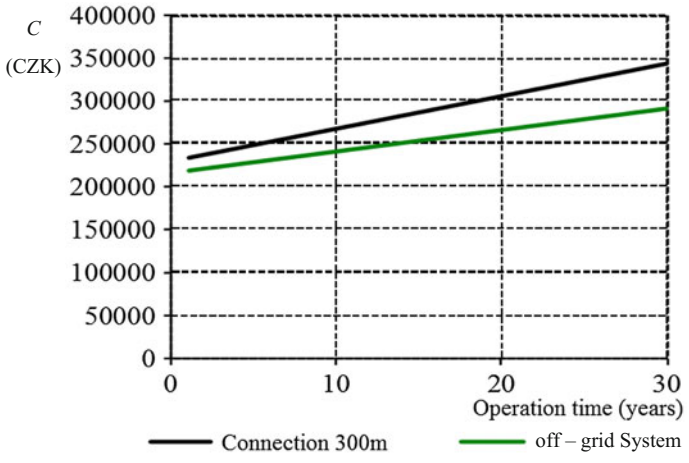

Fig. 4.8 Comparison of the cost of power systems; operation time: 20 years; length of the connection: 300 m; soil type IV

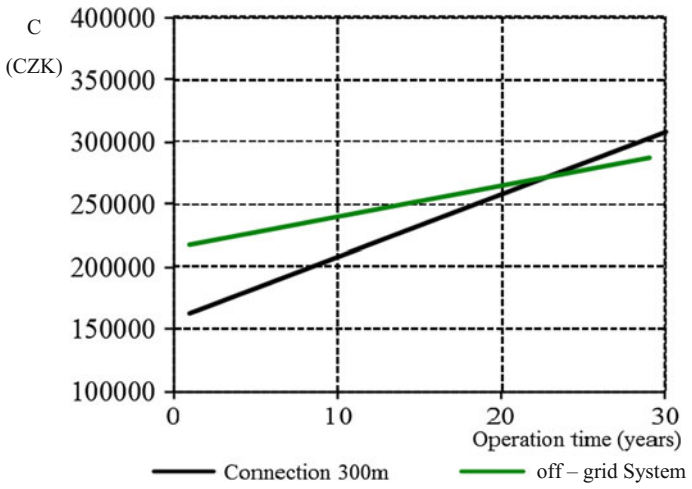

Fig. 4.9 Comparison of the cost of power systems; operation time: 20 years; length of the connection: 300 m; soil type I

decision-making process must respect the specific site conditions (soil type, length of the connection, and the life of storage batteries).

Figure 4.9 compares costs for the length of the connection of 300 m. The entire route of the connection leads in rock of type I. Price for excavation work and the supply cable was set at CZK 400 per 1 m of the route.

Regarding the analyzed variants, the graphs shown in Figs. 4.8 and 4.9 clearly illustrate that the usage of the system supplied from the distribution network is more advantageous for soil type I. However, this result is significantly affected by the simplifications and assumptions made in the beginning of this analysis. For example, any change in the assumed type of soil would increase the price per 1 m of the electrical connection, which would subsequently change the steepness of increase in the total cost of the system connected to the distribution network. In the hybrid power system, it is also important to consider the lifespan of batteries, which has a large influence on the investment cost.

4.4 Small Off-Grid System

4.4.1 Analysis of Consumption

A primary and important part in designing the off-grid system using hybrid electric power sources for supplying energy self-sufficient family houses or buildings in the island mode is the analysis of electricity consumption. It is also important to determine which appliances are to be supplied. There are many variants, but the

basic point is to determine whether it will be necessary to supply only ordinary appliances or also electric heating. This difference has a direct impact on the magnitude of the installed capacity of each power source as well as the capacity of the storage device.

As an example of the analysis of consumption, we selected a normal family house with a 5 + 1 spatial disposition and horizontal projection (ground plan) of a rectangle with dimensions 20 × 10 m, whose energy loss is calculated as 5 kW. The family living in the house has four members. Consumption of this classic house will then be compared with the consumption of newly built low-energy house with the same proportions. This low-energy house is inhabited by a two-member family. In both family houses, we do not suppose to cover energy for heating which is provided by other energy medium. Inhabitants of these family houses use common household appliances and appliances necessary to maintain the house and garden. A comprehensive list of appliances considered in the subsequent analysis is shown in Table 4.1, including their installed power [9].

Based on the measurements and monitoring of the operation of individual appliances as well as daily living habits of household members, it is possible to determine a consumption (load) diagram of the family house for each day of the week, when also considering the electricity consumption for the situations of repairs and routine maintenance in the house. The resulting daily load diagram is shown in Fig. 4.10. Figure 4.11 then shows a weekly course of the total power consumed. Measurements of power consumption should take place over several weeks, so as to minimize eventual anomalies in the normal house operation.

The exact determination of the electricity consumption of the house or building will have an impact on designing the power part of the system, ensuring the energy self-sufficiency in the long term as well as on the overall financial cost of the entire system.

Table 4.1 An overview of appliances

Appliance	Installed power (W)
Gas boiler	120
Washing machine	2100
Solar panels	80
Lighting circuits I, II, III	950
Refrigerator	70
Electric oven	2900
Microwave oven	2600
Vacuum cleaner	1200
Induction hotplate	2100
Dishwasher	2100
Hand mixer	300
LCD TV, notebook	150
Electric iron	700
Other appliances, garden, maintenance	2120
Total	17,490

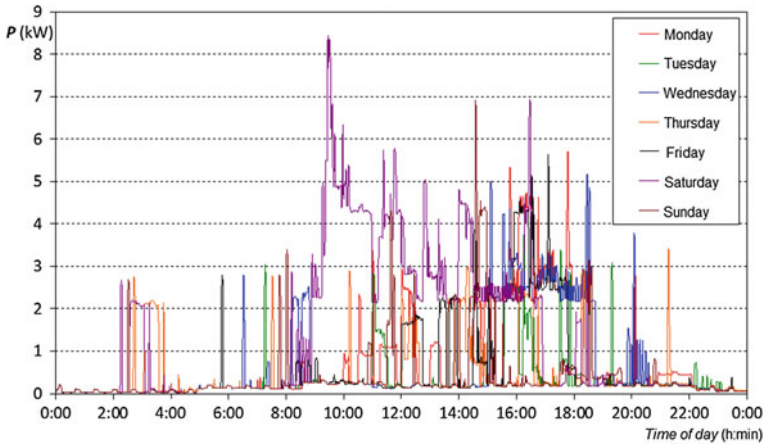

Fig. 4.10 Daily load diagrams for the weekly cycle of the family house

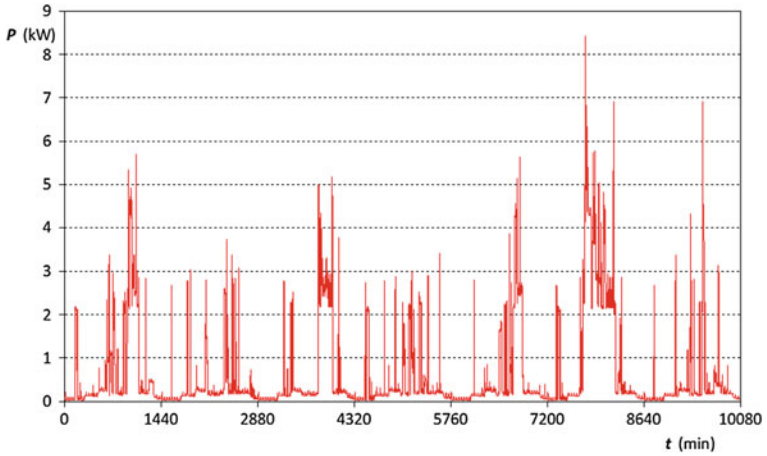

Fig. 4.11 The weekly course of the power output

Figures 4.10 and 4.11 show that the highest consumption of electricity is on Saturday morning when the activities associated with the house and garden maintenance as well as food preparation can be expected. Figures 4.10 and 4.11 further show that the situation of the highest daily demand takes place on Saturday morning and that the magnitude of consumed output power reaches peak values of more than 8 kW.

Table 4.2 shows the value of consumed electricity for each day of the weekly cycle.

Table 4.2 Electricity consumption

Day	Electricity consumption (kW·h)
Monday	17.33
Tuesday	7.89
Wednesday	14.83
Thursday	9.94
Friday	13.65
Saturday	32.04
Sunday	8.87
Total	104.55

Based on the above facts, it is subsequently possible to define conditions for designing the storage device, so as to fully cover the consumption of electricity for the needs of routine unlimited operation of the monitored house.

Figure 4.12 shows the course of load diagram of the monitored household for the selected day of the week, assuming that it is the day with maximum power consumption. Draft design of the accumulation and power sources should be made in accordance with these data.

Overall, the data for dimensioning the power system supplying this classic family house can be summarized as follows: daily power consumption is 32 kW·h (the day with maximum power consumption), weekly electricity consumption is about 100 kW·h, and the peak demand is >8 kW. The design of the entire energy concept should also be aimed at maintain an acceptable economic dimension; it is, therefore, appropriate to consider the possibility of reducing peak demands to reduce the initial conditions of the draft energy concept.

Figure 4.12 shows the course of load diagram of the monitored household of the low-energy house for the selected day of the week, assuming that it is the day with maximum power consumption. Data for dimensioning the energy system for

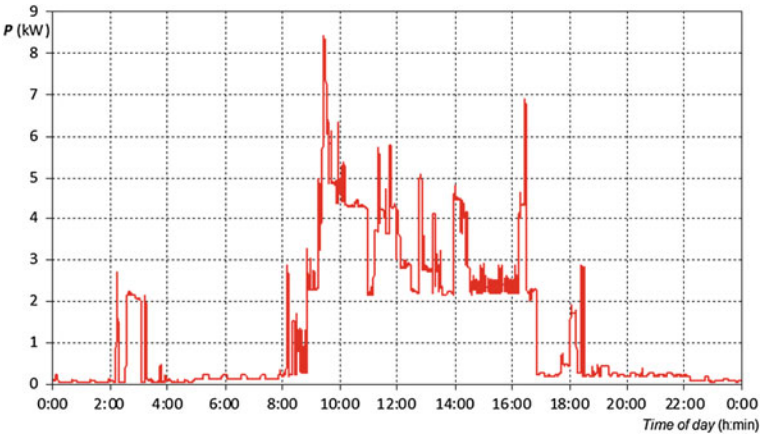

Fig. 4.12 Demand during the selected day

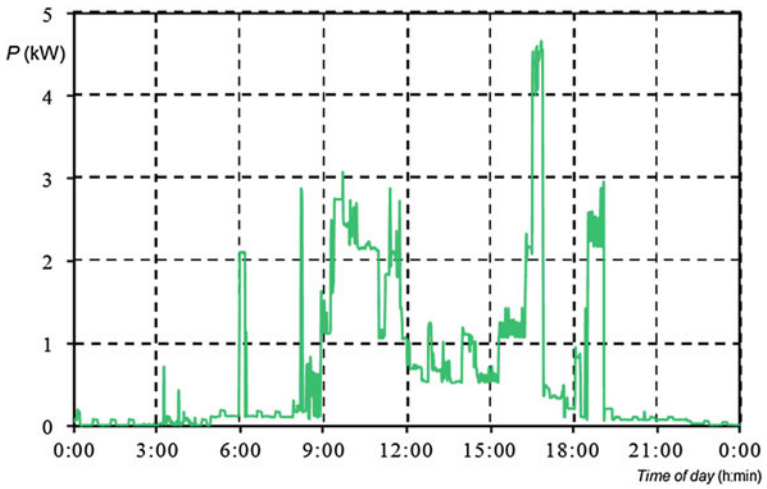

Fig. 4.13 Demand during the selected day

powering this low-energy house can then be summarized as follows: daily electricity consumption is 19 kW·h (the day with maximum power consumption), weekly power consumption is 60 kW·h, and the peak demand is >4.8 kW. Draft design of the accumulation and power sources should be made in accordance with these data. Since the low-energy house is inhabited only by two family members, the electricity consumption and maximum demand is nearly twice lower than in the family house occupied by the four-member family. This difference will have a big impact on the overall installed capacity of various power sources as well as the storage device (Fig. 4.13).

4.4.2 Design of the Storage System

Due to the nature of the hybrid power source using wind and solar power plants, the entire power system must include electric energy accumulation to ensure its island operation. A proper selection of the electric power accumulation system for the island operation will provide enough power to cover the consumption of the family house without losing electricity generated at the time when the production is higher than consumption of the house. The magnitude of the electricity consumption from the island system may be contrary to the magnitude of electricity supply from the photovoltaic and WPPs. The time of the highest power load of the family house does not always coincide with the availability of renewable electricity sources whose utilization, in this case, is a priority. The respective example is shown in Fig. 4.14, where the black line indicates the generated electric energy (wind + solar power plant for the selected day); the red curve corresponds to the actual

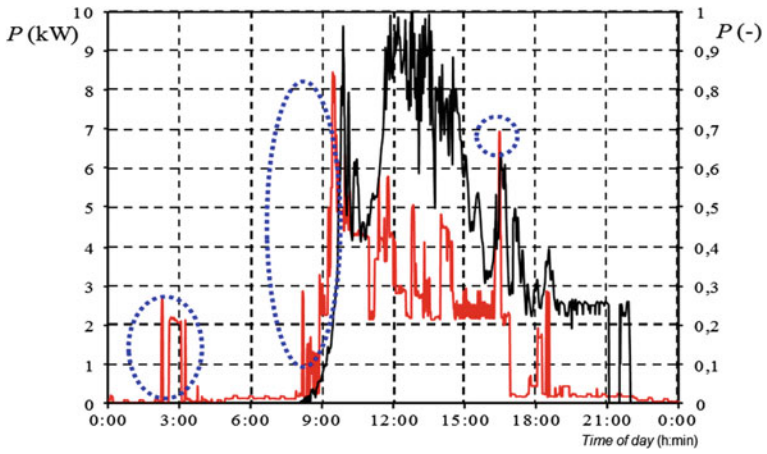

Fig. 4.14 Synchrony of the electricity production and consumption

consumption of the family house (the day with maximum consumption, see Fig. 4.12), and the blue ovals indicate the parts of electricity consumption that must be covered from the storage device fed by the off-grid inverter.

Because of the fluctuating output of the hybrid power sources, it is necessary to either adapt the power consumption or accumulate a part of the energy produced. The power output from the PPP and WPP is always given by the current climate conditions that cannot be controlled. There are many technologies for energy storage, but each has its limits and shortcomings due to which the individual technologies are usable only in certain applications or several types are combined. So far, no technology capable of storing energy has simultaneously enough capacity ($W \cdot kg^{-1}$) and power density ($W \cdot h \cdot kg^{-1}$). Therefore, the respective systems consist of different types of technologies that store energy.

According to the principle of conservation of energy, we can identify two groups.

Chemical principle of energy storage–storage batteries [10–12]:

- Lead–acid and alkaline batteries (Pb)
- Modern batteries operating on the following principles: lithium–ion (Li–ion), sodium–sulfur (Na–S), and nickel–cadmium (Ni–Cd)
- Supercapacitors
- Flow batteries.

The physical principle of energy storage [13, 14]:

- Flywheels.
- Pumped storage hydropower plant.
- Energy accumulation based on compressed air.

Regarding the first group, the energy is stored in chemical bonds of the electrode material, under conditions of reversible reactions between the electrode material and ions from the electrolyte. This group includes all the storage batteries as well as

Table 4.3 Comparison of technologies for storing electrical energy

Storage batteries	Advantages	Disadvantages
Pb	Price, energy density and energy output	Environmental performance, efficiency
Ni–Cd	Energy density and energy output	Environmental performance, efficiency
Na–S	Efficiency	High operating temperature
Li–ion	Energy density, capacity, efficiency	Price, safety
Flow batteries	High capacity, low cost	Low energy density
Supercapacitors	Energy output, efficiency, lifetime	Low energy density, self-discharge, price

supercapacitors which allow a short-term coverage of power consumption in appliances with very sharp rise in the current load. Advantages and disadvantages of each type of storage batteries are shown in Table 4.3. The second group uses transformation of potential and kinetic energy.

Currently, the most appropriate way of accumulating electricity for the off-grid systems seems to be the use of storage batteries. Figure 4.15 shows the efficiency and lifetime of individual types of storage batteries.

For charging of the storage batteries, the majority of types of island converters as well as charging controllers use the characteristic of IUoU Active Inverter Technology. This charging consists of three phases. In the first phase, the storage device is charged with high but limited current of a constant value, over 100 A. In the second phase, it is charged with constant voltage. In the third phase, after achieving a sufficient level of charge, the voltage is reduced to a maintenance value, usually compensated by temperature of the charged storage batteries as well as temperature compensation against the surrounding environment. This method of charging allows recharging of the storage batteries to full capacity in the shortest

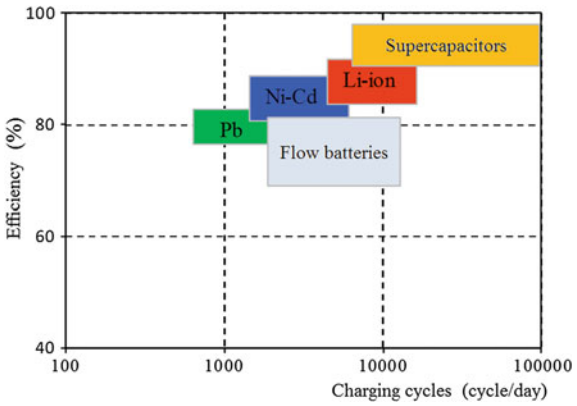

Fig. 4.15 Efficiency and lifetime of individual types of storage batteries

time. This charging characteristic is ideal for charging from hybrid power sources, such as the combination of WPPs and PPPs.

In the first phase of charging, the charging current remains at a constant level until a certain voltage of the storage battery is achieved to ensure the fastest possible charging. At the end of this phase, the storage battery is charged to 80 % of its maximum capacity. After exceeding this value of charging, the charging current declines. In this second phase, the battery is charged to 100 % of its capacity. The charging characteristic then changes into the mode of maintenance charging. The purpose of this maintenance charging is to eliminate the risk of spontaneous discharge during long periods of inactivity and preserve 100 % charge status of the storage batteries.

Based on the results from the analysis of power consumption for the given house or building, it is possible to design a system of storage batteries and calculate the magnitude of their capacity to ensure a sufficient amount of accumulated electric energy. A proper selection of the storage batteries for the off-grid system will ensure enough power to cover the consumption of the house without losses of electricity generated at the time when its production is higher than its consumption. The selected magnitude of the capacity should be such that the storage system is able to power appliances without charging, i.e., in cases where the meteorological conditions in the site with installed off-grid system are unfavorable. The magnitude of the capacity also has a big impact on the highest possible current that can be delivered by the storage system to the off-grid inverter (Fig. 4.16).

In today's market, there are three main types of storage batteries suitable for use in the off-grid system: lead–acid, nickel–cadmium, and lithium–ion batteries. The advantage of nickel–cadmium and lithium–ion storage batteries is higher specific energy compared with lead–acid batteries, and shorter charging time. The disadvantage is a higher purchase price.

Currently, several methods can be used for determining the capacity of the storage device. The most commonly used methods include those described in detail in [15]. The design of the battery capacity was based on the procedure in [4], which is presented by the following relationship:

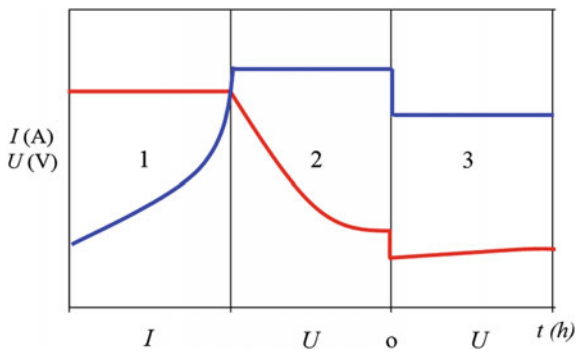

Fig. 4.16 Charging characteristic IUoU Active Inverter Technology

$$C_B = \frac{(E_Z \cdot n)}{(V_B \cdot \mathrm{DOD}_{MAX} \cdot T_{CF} \cdot \eta_B)}, \tag{4.3}$$

where C_B is the battery capacity, E_Z is the energy consumed by the load, n is the number of days without charging, V_B is the battery voltage, DOD_{MAX} is the depth of the battery discharge, T_{CF} is a temperature correction factor, and η_B is the battery efficiency.

For the proposed system, it is necessary to choose the right values of the quantities listed in relationship (4.3).

- E_z—to be selected for the day with maximum power consumption.
- n—the number of days; the period during which the storage system must be able to power appliances through the island converter without charging, i.e., when the weather conditions in the area of installation are unfavorable. The length of the period with low wind velocities and cloudy sky, i.e., with a low intensity of solar radiation, varies in dependence on the installation site and season.
- V_B—voltage of storage batteries; this value is selected according to the input DC voltage of the island converter. The most frequent values, achieved through series–parallel connection of storage batteries, are 12, 24 and 48 V.
- DOD_{MAX}—depth of the battery discharge; this value ranges from 20 to 80 % of the battery charge level and is determined by the type of batteries used.
- T_{CF}—temperature correction factor; its value depends on the battery placement. Temperature correction factor for locating the batteries in cellars without significant temperature changes is equal to 1.
- η_B—battery efficiency; this value depends on the type of storage batteries and ranges from 50 to 90 %—see Fig. 4.15.

In the phase of dimensioning the magnitude of the capacity of storage batteries, it is necessary to consider the amount of investment and space requirements for placing the storage batteries. It is, therefore, necessary to consider a reduction in demands on the amount of electricity supplied by the island application as well as the possibility of reducing the number of days during which the system must be capable of powering appliances without any charging due to adverse meteorological conditions.

Table 4.4 shows a calculation of the storage system capacity according to relation (4.3) for different variants of the length of powering the house without charging the storage batteries. The calculation of the magnitude of the battery capacity is done for the day with maximum power consumption of 32 kW·h and average weekly consumption of 15 kW·h. Battery voltage was chosen at the level of 48 V, and the maximum depth of battery discharge without effects on durability is indicated as 0.9. The selected average battery efficiency for this model calculation was 85 %.

Table 4.4 clearly shows that the cost of investments in the storage system is not returnable during the period of the system operation when respecting the battery effective life. Lifetime of storage batteries is determined by the type of batteries

Table 4.4 Capacity of storage batteries

Number of days without charging	Capacity (A·h)	
	Maximum consumption	Average consumption
12	10,500	4900
10	8730	4080
8	6980	3260
6	5240	2450
4	3490	1630
2	1740	816

used (approx. 10–20 years, depending on the type) and is also affected by cycling (charging/discharging). It is, therefore, necessary to consider a reduction in demands on the amount of electricity supplied by the off-grid application as well as the possibility of reducing the number of days during which the off-grid system must be capable of powering appliances without any charging due to adverse meteorological conditions.

Maximum power consumption, for which the primary calculation of the capacity requirement was performed, occurs just in 1 day of the year. The amount of electricity consumed on this day significantly differs from the amounts of electricity consumed during other days of the year. When considering this diversity and admitting that the day with maximum power consumption is partly covered from other energy sources, we can calculate the required capacity of storage batteries based on the weekly average electricity consumption.

Another option to reduce the required capacity of storage batteries and thus allow for a return on investments shorter than the effective life of batteries is to use a control system for regulating the flows of electricity in the off-grid system. Using the control system, the consumption of the family house can be optimized, so that the appliances, in which it is possible, are switched on within a longer time period. In this way, it is possible to reduce the amount of electricity needed in the off-grid system and, thus, the required magnitude of the storage device capacity.

4.4.3 Design of the Source Part

Nowadays, there are several modeling software tools for analyzing and designing the hybrid power systems. In this case, the term “hybrid power system” indicates a cooperation of more power sources, most commonly the cooperation between photovoltaic and WPPs together with accumulation. These software tools, such as HOMER ENERGY [16], Solar Off-Grid Calculator [17], and Solar Off-Grid Configurator [17], are available on various websites and allow us to configure an entire power supply unit. Using these software tools, it is possible to assemble the power part of the off-grid system, from sources, through converters up to a defined

load. Their advantage is that they work with meteorological data to refine the overall energy balance and efficiency of the system, determine the magnitude of the storage device, and enable the basic economic evaluation. This software provides considerable comfort for dimensioning the individual components in the off-grid system.

One of the software tools available on the web is the above-mentioned Solar Off-Grid Calculator. This simple software takes into account only the available electrical energy from PPPs (as the name implies). In its menu, the users can choose from several predefined loads or add their own loads using the definition of input power/number of appliances and hours of their use per day. After completing the list of loads, they can choose the number of days of autonomous operation, voltage levels on storage batteries, or even the depth of battery discharge and their effectiveness. Furthermore, the users can determine the percentage of consumption to be covered by the PPP, the energy yield, and overall system efficiency. The result provided by this Solar Off-Grid Calculator is a simple message that contains the basic configuration of the system and load combination.

Off-Grid Configurator is another software tool available on the web. This system combines a selection of options—whether to use only a PPP or also a generator. Using this software, it is possible to gradually configure the entire off-grid system of photovoltaic panels, via inverters and storage batteries up to the economic evaluation of the project. However, this software does not offer the possibility of implementing WPPs. Simple applications, as the mentioned Solar Off-Grid Calculator and Off-Grid Configurator, just demonstrate that it is possible to create a simple program highlighting the possibility of using RES even without the support of multinational companies. Nevertheless, programs of this type are too simple and lack any application benefits for the users.

Modern modeling software tools include the software called HOMER. This simulation tool is intended for the design and analysis of hybrid power systems that contain a mixture of conventional energy sources, combined sources for the production of heat and electricity, wind and PPPs, storage batteries, fuel cells, small hydro power plants, biomass, and other inputs. With this software tool, it is possible to model on-grid and off-grid systems using the mentioned power units. The user environment is shown in Fig. 4.17. The application HOMER also comprises an optimization algorithm for the analysis which enables the user to perform economic evaluations of the project.

Application HOMER, created with the support of the US government, requires a large amount of input information from the user. HOMER performs the optimization process to determine the best configuration of hybrid energy from the selected RES. Based on the selected electricity consumption of the given building and the meteorological conditions in the respective area, it suggests the ideal combination of the hybrid power source, capacity of the storage batteries, and the magnitude of the power output for DC–AC converters. A detailed specification and usage of this software is described in [16].

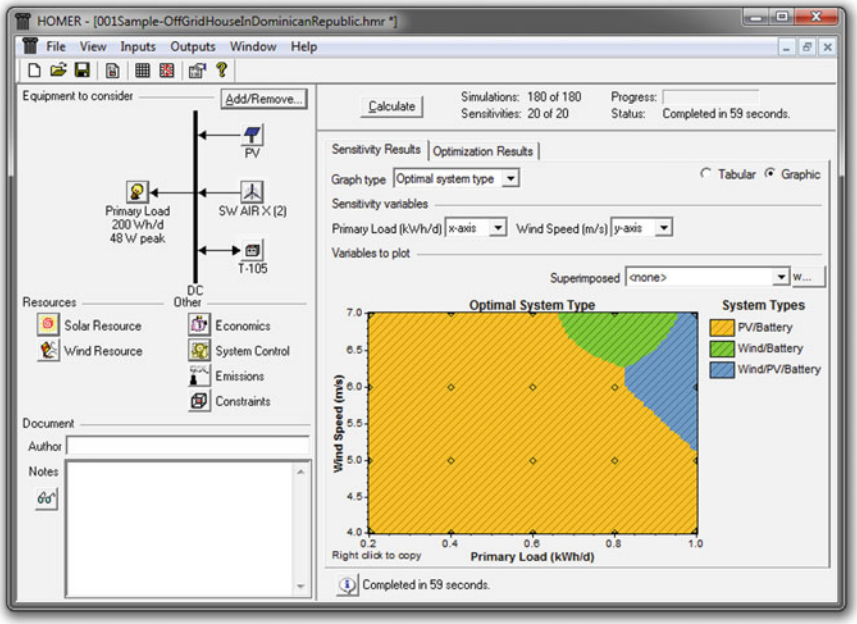

Fig. 4.17 User environment in the application HOMER [16]

4.4.4 Design of the Control System

Since the described off-grid systems utilize power sources with unstable electricity supply, there are high demands on controlling the entire island system operation. The respective control system must ensure the accumulation of sufficient amounts of electrical energy to cover the expected consumption with maximum possible efficiency; however, it must also be able to control the power consumption based on pre-defined priorities when dividing the consumption into several categories according to the possibilities of the time shift. The first category includes appliances whose operation is permanent and which consume electricity throughout the day. The second category includes appliances (e.g., washing machine and dishwasher) whose operation can be postponed to a later time when it is possible to expect good conditions for the production of electricity from hybrid power sources. The third group includes appliances whose operation is dependent on the will of the operator, such as TV sets or computers.

The control of power flows between various components connected to the off-grid system can be implemented through an appropriate control system. The utilization of an active control system for ensuring economical operation and controlling the flows of electricity in the off-grid system will optimize the connection of individual appliances in the family house. Based on the information about the predicted value of electricity from the solar and WPPs, pre-defined

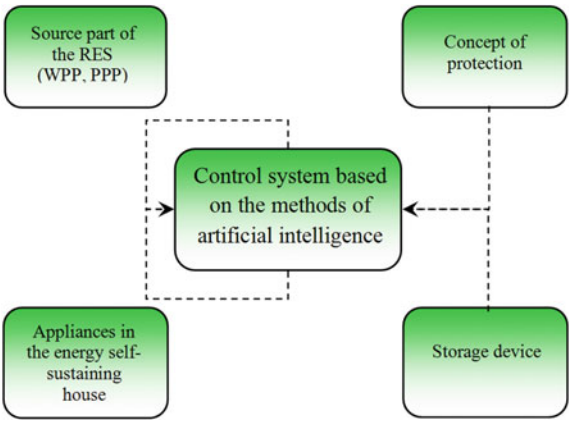

Fig. 4.18 The basic structure of the control system for supplying family houses operated in the off-grid mode

priorities for connection of individual appliances and actual capacity values of storage devices, the active control system will provide safe power supply for the off-grid system throughout the year.

The input data for decisions of the control system are taken from meteorological models (prediction of production); on their basis, the control system predicts the expected available power and prepares a plan of operation for the individual appliances, so that the requirements for running the household are always met, including the optimally selected energy reserve to cover unforeseen needs of electricity. The basic structure of the control system for ensuring economical operation and controlling the flows of electricity is shown in Fig. 4.18.

It is well known that the issue of the operation of RES is very timely, whether with positive or negative response from professionals and the amateur public. Operation of renewable power sources in the off-grid mode together with the control system eliminates the negative arguments against RES. Example of micro off-grid system used to power public lighting was built in the premises of the VŠB-TU Ostrava several years ago, within the research of renewable power sources. Experience gained in the construction and operation of this system was used in building the small off-grid system with substantially higher installed capacity, which serves as a physical model of powering family houses. Construction of the off-grid system, which should simulate the house supply, was based on an analysis of consumption of an ordinary family house. This analysis was subsequently used to design the storage system with respect to performance requirements but also with respect to the amount of the initial investment and payback period regarding the entire energy unit. Hybrid electric power source was chosen with regard to supplying a model family house.

The off-grid system, i.e., island system, built in the premises of the VŠB-TUO is composed of three basic parts. The first part, i.e., source part—see Fig. 4.19, uses a WPP and two versions of photovoltaic systems as the hybrid power source. The first PPP is located on a positioning unit and uses monocrystalline panels. The second PPP is located on a fixed roof structure and uses polycrystalline panels. The second

Fig. 4.19 A photo of the WPP together with an adjustable swivel unit of the PPP

part was made for the transfer of energy, and the third part defines the accumulation and power (consumption) management using the active control system.

The whole energy concept was designed, so that it can cover electricity consumption of a standard family house in the off-grid operation, i.e., independently of the external power system. More detailed information about the dimensioning of the hybrid power source for the source part of the off-grid system together with accumulation is published in [18–20].

The physical model of the off-grid system was complemented by a measurement system for measuring values on the individual system components. A scheme of the monitoring chain is shown in Fig. 4.20. Basically, this detailed displacement of sensors allows us to continuously monitor partial efficiencies of the whole system. Through such a monitoring system, it is possible to determine the overall efficiency of the system with high accuracy, to define the share of individual sources within a long period of time and, thus, specify the usability of the designed energy concept for any weather and energy conditions, not only in the place of the built test platform of the off-grid system.

An important part of the monitoring system is evaluation of meteorological conditions. The weather station provides a sufficient number of measured values for the density of global solar radiation as well as wind speed and direction.

Using the G language (environment LabView—Laboratory Virtual Instrument Engineering Workbench), all the measured values are then processed and evaluated,

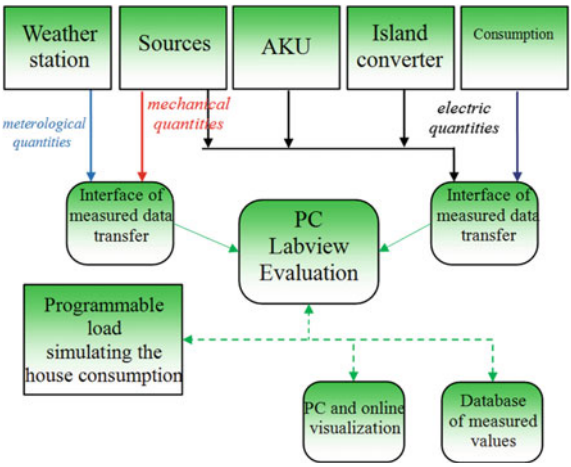

Fig. 4.20 A scheme of the monitoring chain

and subsequently also visualized. All the results from the monitoring system are stored for subsequent postprocessing in a database of long-term measured values in 1-min intervals and published through a web interface on the Internet domain which has been created for the test platform of the off-grid system. Using this database of measured values, it is possible to optimize and evaluate the chain of individual conversions of electrical energy, power flows and operating states in the off-grid system.

The main objective of the monitoring system is to provide the control system with sufficient information about the current weather conditions and predictions of relevant meteorological variables for the near future, as well as information about the charging state of storage batteries and expected consumption in the next time period. Consumption schedule is based on the database of operating states and the analysis of consumption referred to in this book earlier, when the ordinary conventions of the household are largely stereotypical and a certain portion of the stored electricity must be allocated to cover any incidental power consumptions.

The control system then automatically switches on individual appliances that could be included into the system of direct switching. From actual values of the individual measured quantities (variables), the control system is able to evaluate the condition of each source as well as the status of the storage system and, subsequently, inform the user. A simplified scheme of the active control system for controlling power flows in the off-grid system is shown in Fig. 4.21.

Supported by advanced IT technologies, the active control system recommends to the user a power consumption plan that is based on the database of operating states, the analysis of consumption, battery charge level, information provided by the monitoring system, predictions of relevant weather and meteorological variables, and predictions of production and consumption. According to the respective control algorithm, the control system recommends to switch on selected appliances or individual power supply circuits and informs the user about the status of each source as well as the entire system.

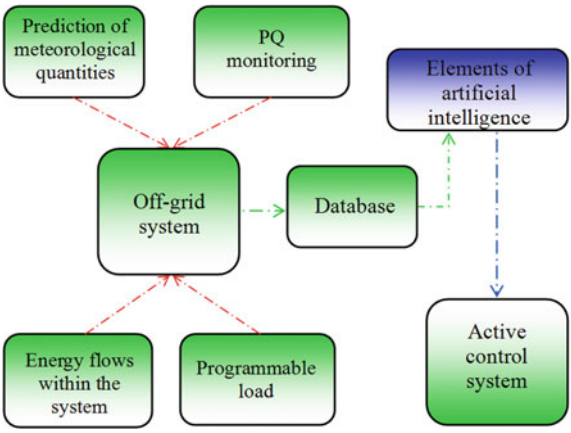

Fig. 4.21 A scheme of the active control system development

The development of the off-grid system built in the premises of the VŠB-TUO can be divided into three basic steps:

- Classification of energy flows.
- Creation of behavior scenarios.
- Testing of the created database.

The first stage consisted in long-term measurements on selected objects. These measurements, together with the measurements of relevant meteorological and geomorphological values, resulted in the creation of a standardized database with the classification of energy flows and standardized daily load diagram for the given household (family house). Thus, created standardized daily load diagram, along with experimental measurements of household appliances, serves as the basis for setting programmable loads and implementing these loads into the physical platform of the family house [21–23].

The second stage aimed at creating different scenarios of behavior of selected objects—energy flows within the system, which correspond to situations in everyday life. This was followed by optimization of the off-grid system operation with respect to specific requirements.

These requirements include:

- stand-alone (autonomous) operation;
- maximum utilization of RES;
- operational safety and reliability.

Information from the prediction model for the production of electricity from RES was used as supportive information to optimize power flows in the energy unit. Using the already built detailed monitoring system, every operator intervention is monitored in the form of an entry in a text file, including all relevant variables.

The third stage focused on creating a comprehensive database which was subsequently tested using elements of artificial intelligence with finding relationships

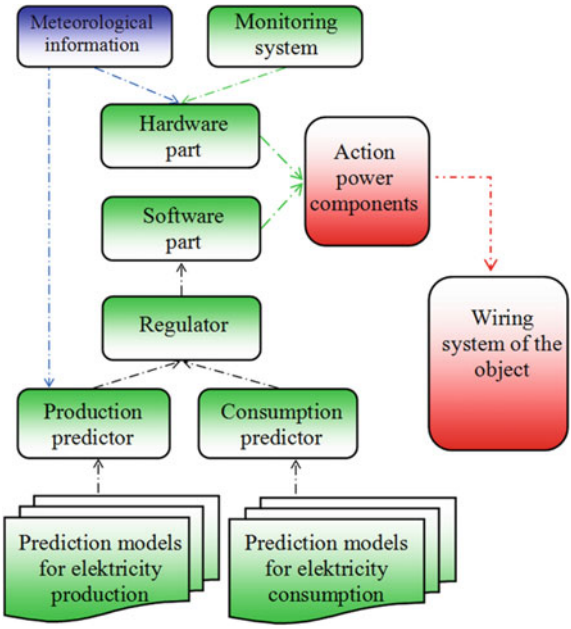

Fig. 4.22 Block diagram of active power unit of the off-grid system

between individual variables. The aim of the use of artificial intelligence is the application for managing energy flows with respect to the specific requirements listed above. The actual use of the methods of artificial intelligence was preceded by a trial operation to find any possible shortcomings.

The active control system with the support of artificial intelligence implements partial steps, whereas the operator evaluates the deviation of the reaction intervention of the control system from the desired value. Currently, the energy unit is tested using the active control system, and the achieved results are evaluated.

Figure 4.22 shows the connection of the active control system with the physical platform of the power unit. The source part can be supplemented by a gasoline/diesel/LPG aggregate, or micro-CHP (combined heat and power) unit for situations when there is not enough available energy from RES and storage batteries. The system will try to avoid such a state through setting priorities for individual appliances or their groups and timely disconnection of appliances with low priority. Based on current weather information, predictive models of production and consumption, and the actual values, the control system regulates energy flows within the system using active power components included in the object wiring. After adjusting communication technologies, this system can be installed, for example, into existing power circuits of the objects/buildings with minimal modifications.

Figure 4.23 shows the load diagram of the monitored household for the selected day of the week, assuming that this day has maximum power consumption. Based on long-term measurements of behavior of ordinary households in terms of switching individual appliances, the power load does not always coincide with the

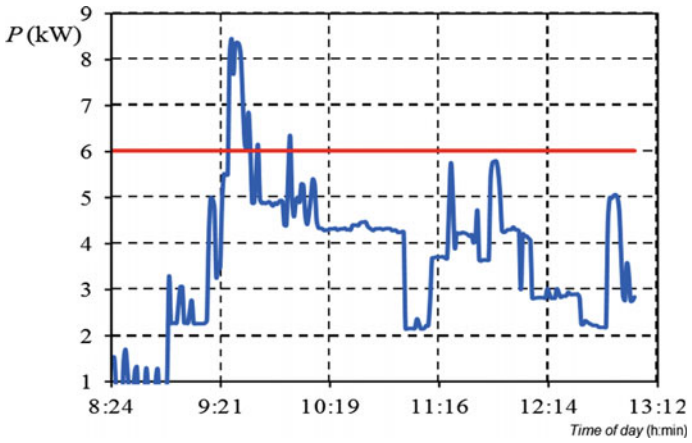

Fig. 4.23 Daily load diagram before using the active control system

availability of RES. In view of the volatility of electricity supply from RES, the island converter powered from the storage device must be able to cover the consumption of the family house without electricity from these RES. The respective example is shown in Fig. 4.23, where the red curve indicates the maximum power output of the island converter powered by storage batteries. The consumption of a standard family house exceeds the maximum possible power supplied from the off-grid converter after 9 o'clock in the morning, see Fig. 4.24. At this moment, several appliances are switched on at once; this results in exceeding the maximum power output of the off-grid inverter.

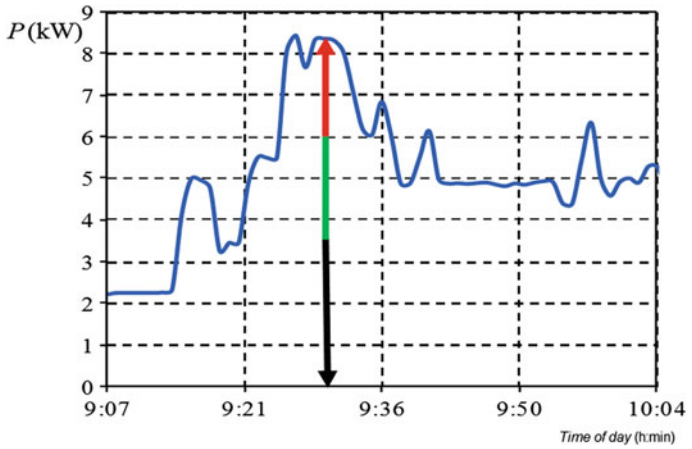

Fig. 4.24 Power peak in the daily load diagram

Using the active control system and according to predetermined priorities for switching of individual appliances, the daily load diagram and distribution of electric power consumption of a standardized family house is preset to less loaded period of time.

Figure 4.24 shows the power peak which cannot be covered by the off-grid converter. The peak power in the daily load diagram is caused by switching on several appliances at once. In our case, these appliances mainly include washing machine (in red), dishwasher (in blue), and other appliances that are marked in black.

Figure 4.25 shows a suppression of this power peak using the active control system of power consumption in the off-grid system. The consumption control system shifts the switch on of the washing machine and dishwasher to less loaded period of the daily load diagram which results in suppression of power peaks.

Figure 4.26 shows the energy balance of a 3-day operation of the off-grid system for powering a family house built in the premises of the VŠB-TUO. Blue columns indicate the electricity production by the hybrid source of the off-grid system. Red columns indicate the electricity consumption by the standardized family house. Green columns indicate the capacity of storage batteries at the end of the day.

Figure 4.26 shows that the power consumption during the second day of operation exceeds the power generated by the hybrid sources of the off-grid system. The off-grid converter must cover the consumption from storage batteries. The charge level of batteries used for electric energy accumulation in the off-grid system decreases to 52 % at the end of the day.

Figure 4.27 shows the energy balance for the same 3 days of operation of the off-grid system for powering the family house using the active control system which regulates its economy and electricity flows in the off-grid system. Through this control system, the electricity consumption is spread over a part of the day with

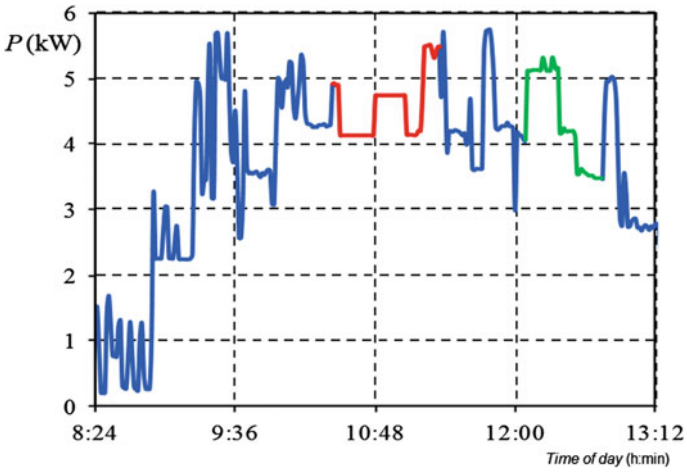

Fig. 4.25 Daily load diagram after using the active control system

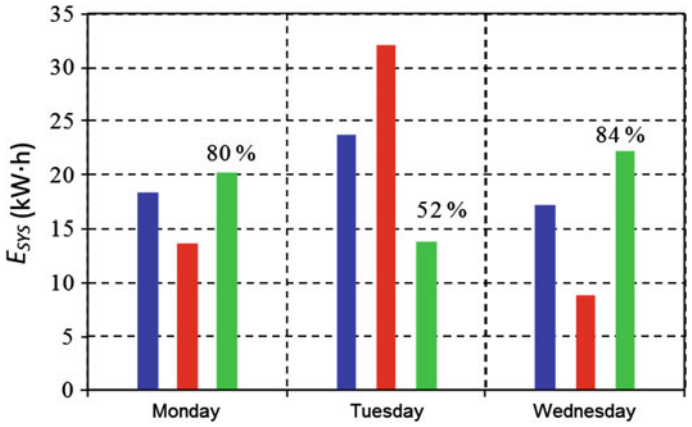

Fig. 4.26 Energy balance of a 3-day operation of the off-grid system without the active control system regulating the family house consumption

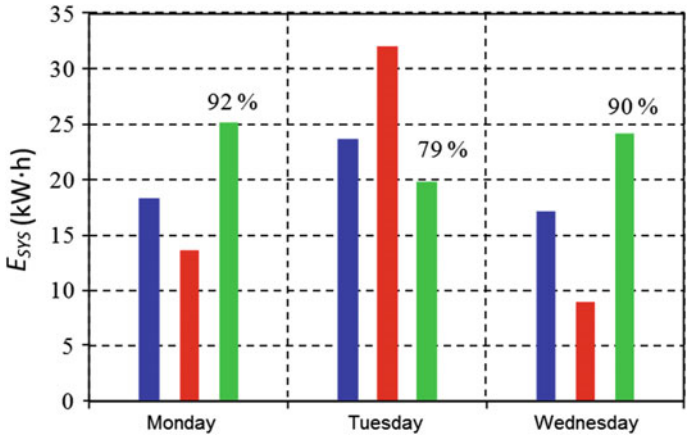

Fig. 4.27 Energy balance of a 3-day operation of the off-grid system with the active control system regulating the family house consumption

sufficient power production from the hybrid power source of the off-grid system. Storage batteries are not deeply discharged, and the off-grid system has enough energy reserve to cover unforeseen needs for electricity in the off-grid system.

4.4.5 Electric Power Quality

Consumers of electric power require the supply of electricity in the desired quantity and quality. The quantity is characterized by the supply of electrical work which is

represented by the current load of the electricity system in dependence on the consumers' connection points. The quality of electric power relates to maintaining the parameters of the supply of consumption amount in the appropriate value from the system providing this supply. Electricity produced in power plants in the prescribed quality is supplied to final consumers through the power system (PS), i.e., transmission systems (TS) and distribution systems (DS). During this path, the electric power is exposed to many external factors which may affect its final quality.

Power quality can be affected using RES such as wind and PPPs connected to the conventional electricity grid or used as hybrid sources for powering off-grid systems. This problem is caused by changing short-circuit power at the connection point of RES, stochastic supply of electricity from RES dependent on weather conditions in the given site, and voltage fluctuations related to variability of solar and wind energy. Mutual interference between the sources and the load can result in exceeding the parameters for electric power quality. Another significant problem is harmonic distortion, because both types of production facilities are usually connected both to the classical power network and off-grid system through chopper (pulse) converters.

The basic power quality parameters include limits for the system voltage, frequency, power factor, voltage harmonics, voltage unbalance, and long-term as well as short-term flicker. Observing the power quality parameters allows the electrical appliances to operate without significant losses in their performance and reductions in their lifespan.

Power quality for conventional electricity systems is processed and defined by several international technical and normalization organizations. The best known organizations include the IEC (International Electrotechnical Commission) and IEEE (Institute of Electrical and Electronics Engineers).

European standard IEC 61000-4-30 (methods of measuring the quality of energy) is part of the standards and regulations IEC 61000 (electromagnetic compatibility). This series of standards defines the methods of measuring and interpreting the results of power quality parameters in AC 50/60-Hz power systems. These standards describe measurement methods to obtain reliable results for the final analysis of the defined power quality parameters. The standard defines three classes of measurement—A, S, and B. Class A is used where accurate measurements are required, e.g., for contract applications or settlement of disputes. Requirements for measurement processing and accuracy for Class S are lower. Class B is outdated and least accurate. The standard also includes links to the other two standards: IEC 61000-4-7 for measuring the voltage of harmonics of higher orders, and IEC 61000-4-15 for measuring the flicker. Measuring devices, such as power quality analyzers with functions defined in IEC 61000, produce measurement data that must be processed statistically. European standard.

EN 50160 describes how the measured data should be processed for the resulting statistical evaluation of power quality.

Instructions for measuring and assessing the quality of electricity for photovoltaic systems are described in standards. Evaluation of power quality in off-grid systems has been published only in several publicly available sources [24, 25].

The analysis of electric power quality was based on the database of measured values which was created using the monitoring system in the off-grid system built in the premises of the VŠB-TUO—see Sect. 4.4.4. Sign convention corresponding to the appliance system (+ sign indicates electricity consumption, − sign indicates electricity supply) is applied to all quantities below. From the mentioned database, we selected a time window corresponding to the day with variable weather conditions. To compare the quality of electrical energy, the energy unit was connected to the conventional low-voltage network (off-grid–on-grid). For greater clarity and simplicity of the results, only PPP_1 and PPP_2 were in operation, while the WPP was shut down for a short term. The main selected system quantities characterizing the quality of electricity in the off-grid systems include:

- voltage;
- frequency;
- total harmonic distortion (THD) factor.

Under normal operating conditions, the network voltage must be in the permissible tolerance for rated voltage U_N (±10 %). The value of voltage drop, which can occur on the conductors, makes 3 % for light conductors and 5 % of the rated voltage. This value corresponds to the voltage drop between the feed point of the low-voltage network and the appliance. If the network voltage value is greater than the permissible value, the life of appliances will get shorter, and the insulation will deteriorate. Losses will be higher as well as the failure rate. If the voltage value is lower than the permissible value, the performance of electrical equipment will significantly decrease, and malfunctions of the equipment or its complete shutdown may occur.

Figure 4.28 shows the course of voltage in the off-grid system at various operating states. For the selected time window, the off-grid system energy unit is

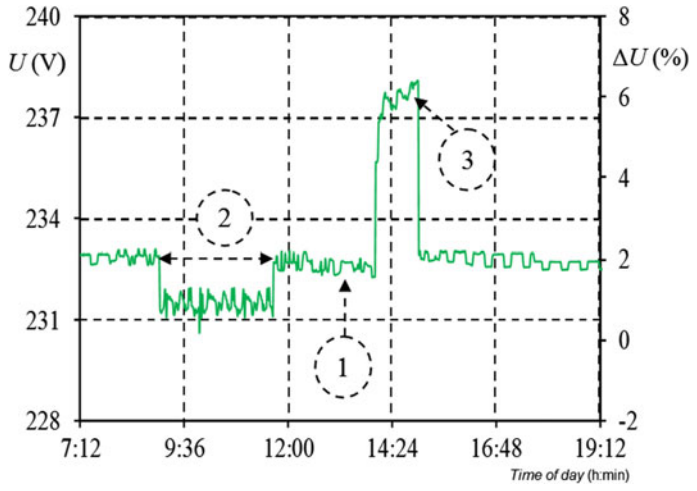

Fig. 4.28 The course of voltage in the off-grid system at various operating states (U_N = 230 V)

loaded with constant consumption of 2.3 kW. Point 1 shows the state when the island converter of the off-grid system is connected to the conventional low-voltage network. Voltage varies around the value of 233 V which is within the tolerance for rated voltage U_N (0.7 %). Point 2 shows the state in which the power consumption is covered by power from the PPP and the island converter charges the storage batteries. Voltage varies around the value of 231.5 V which is within the tolerance for rated voltage U_N (0.3 %). Point 3 shows the state when the network load is zero and storage batteries are charged to their maximum value. The off-grid system is loaded with consumption of power electronics and losses across the wiring. Voltage varies around the value of 238 V which is within the tolerance for rated voltage U_N (3 %). In all the three operating states of the off-grid system, the voltage value ranges within the permissible tolerance for rated voltage U_N (±10 %).

Figure 4.27 shows the course of active power in the off-grid system; measured values of active power are evaluated according to the European standard EN 50160. The selected time window can be divided into three operating modes. In the first mode (the time period from 0:00 till 8:00), the island converter of the off-grid system is connected to the conventional low-voltage network. From 8:00, the intensity of solar radiation G increases, and PPPs (PPP_1 and PPP_2) begin to supply the island network—this is the second mode. The load of the island network increases in line with the consumption of the classical family house. If the overall power output from PPP_1 and PPP_2 is sufficient to cover the actual load, the island converter uses excess electricity which is accumulated through storage batteries (P_{bat}^{+} = charging of storage batteries, P_{bat}^{-} = discharging of storage batteries). If the solar radiation begins to fluctuate and there is not enough electrical energy to power the actual load directly from PPP_1 and PPP_2, the island converter starts to cover the shortage of electricity in the off-grid network from storage batteries. After 16:00, the entire load is powered only from the off-grid converter with storage batteries—this is the third mode (Fig. 4.29).

Figure 4.30 shows the course of load P for the selected day together with frequency f and total harmonic distortion THD for voltage and current. For the power supply voltage, the standard EN 50160 sets rated frequency of 50 Hz. Frequency of the supply network depends on the interaction between the generator and the load. The variance range decreases with increasing ratio between the power output of generators and the load. Maintaining a constant value of the frequency requires sufficiently large production power output that adapts to the instantaneous total network load. However, since the production power output and consumption change discontinuously, there is a risk of mismatch which leads to a decrease or increase in the network frequency. This risk can be reduced in the conventional electricity grid by linking many networks into one large network. The power of such a network is then sufficiently large compared with possible network changes. This option does not exist in the off-grid system. Disruption of the active power balance caused by changes in the load and stochastic behavior of the hybrid source in the off-grid system leads to a change of frequency. The same applies to a disruption of the reactive power balance, which results in a change of the off-grid network voltage.

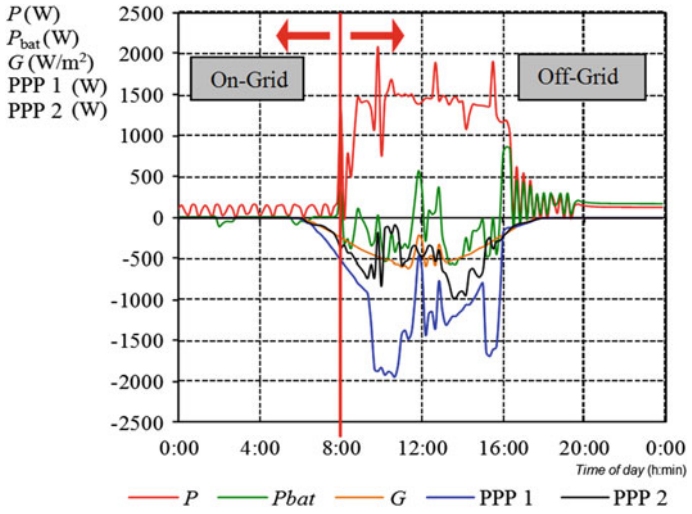

Fig. 4.29 Flows of active power during the selected day

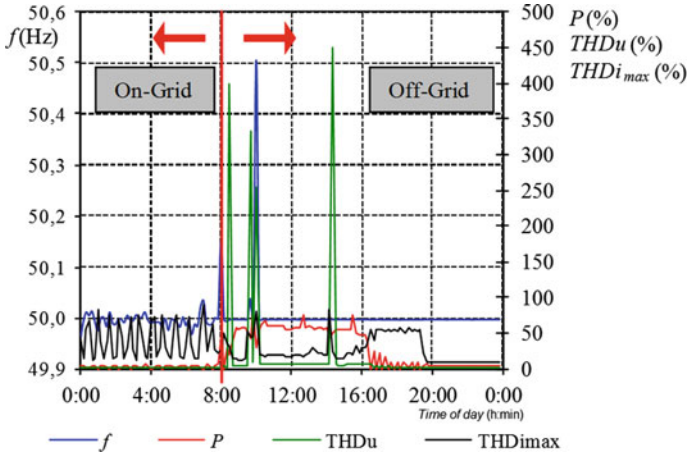

Fig. 4.30 The course of quantities characterizing the quality of electricity in the off-grid system

The parameter that characterizes the non-linearity (sine wave distortion) is called harmonic distortion factor of voltage and current, THDu and THDi. The abbreviation THD stands for "total harmonic distortion." It is defined as the ratio of the sum of the power of the first harmonic (50 Hz) and all components of the higher order harmonics to the fundamental harmonic power. The lower the THD, the lower the distortion of the resulting power. Appropriate compatible level for the total harmonic distortion THD is 8 %.

Figure 4.30 shows a slight frequency fluctuation in mode 1, which is caused by back affection of the external power supply system that covers the off-grid system consumption in the on-grid mode. Fluctuation of THD_{imax} is more pronounced; this corresponds to cyclic load changes (appliances in their STAND-BY mode: refrigerator, TV, etc.). THD_u parameter is within the desired limits due to the high short-circuit power of the external supply system. Short-circuit current and surge short-circuit power of the external low-voltage supply system vary around the values over 100 A and over 230 kV A, respectively.

In the second and third operating mode (the off-grid system is disconnected from the classical electric network), the power quality parameters are maintained within the required limits using the control system of the off-grid converter and are markedly dependent on the magnitude and nature of the load caused by individual appliances and the value of short-circuit power in the off-grid network. In the off-grid system, the value of short-circuit power, indicating the hardness of the network, is variable; it is dependent on the connected sources. In the operating mode, when the off-grid network is supplied only by the off-grid converter with storage batteries, the value of short-circuit current reaches several tens of amperes. This value is given by the short-circuit power of the used off-grid converter. Surge short-circuit power is around 10 kV A.

Figure 4.30 shows step changes in the consumed power, which corresponds to the changes in frequency and THDu outside the specified limit when the off-grid converter is unable to maintain frequency and THDu within the required limits due to actual short-circuit power in the off-grid network. After the power surge fades away, the off-grid converter is able to stabilize the frequency as well as THDu. THDi is a parameter corresponding to the load; therefore, significant changes in THDi and significant limit violations occur in the event of a cyclical connecting of the appliances containing semiconductor components (computers)—see Fig. 4.30, from 10:00 till 14:00.

From the results of the analysis of electric power quality, it is evident that the off-grid network in the off-grid system is more susceptible to changes in the values of system parameters representing the quality of electricity. This susceptibility is given by a variable and significantly lower short-circuit power than in the conventional low-voltage electrical network.

4.4.6 Active System of Power Consumption Management in the Off-Grid System

The trial operation of the active system of power consumption management for the built off-grid system was completed and started in 2013. This automated system is designed for management and control of flows of electricity in an off-grid network of family house or object within the power levels of family house. The active system of power consumption management with adaptive protection system represents an intelligent energy system intended for energy self-sufficient house or

building. The main goal of this smart energetic system is to ensure essential specific requirements intended for the off-grid system. These basic requirements include autonomous operation of the off-grid network without any dependence on electric energy from an external electricity grid, efficient, and maximum use of RES in feeding the off-grid network which contains electricity storage equipment, improvement and provision of the safety and reliability of the off-grid system operation.

Active management system uses information from the prediction model of electricity production from RES used in the off-grid system and optimizes the connection of various electrical appliances whose consumption forms DLD. Based on information on the predicted amount of electricity from solar and WPPs, and on pre-defined priorities regarding the connection of individual appliances and actual values of the capacity of batteries, the system regulates energy flows within the system using power actuators (contactors) implemented in the electrical distribution of the off-grid network. The application of active power consumption management system increases the benefits of off-grid system which is operated in the by-pass mode (ability to cover power consumption exceeding the capability of the off-grid converter). Flow diagram of the intelligent energy system is shown in Fig. 4.31.

A simplified description of the functions of the active system of power consumption management can be defined in the following points:

- The use and prediction of meteo (meteorological) values, prediction of values of global radiation and wind speed for the specified location using a weather

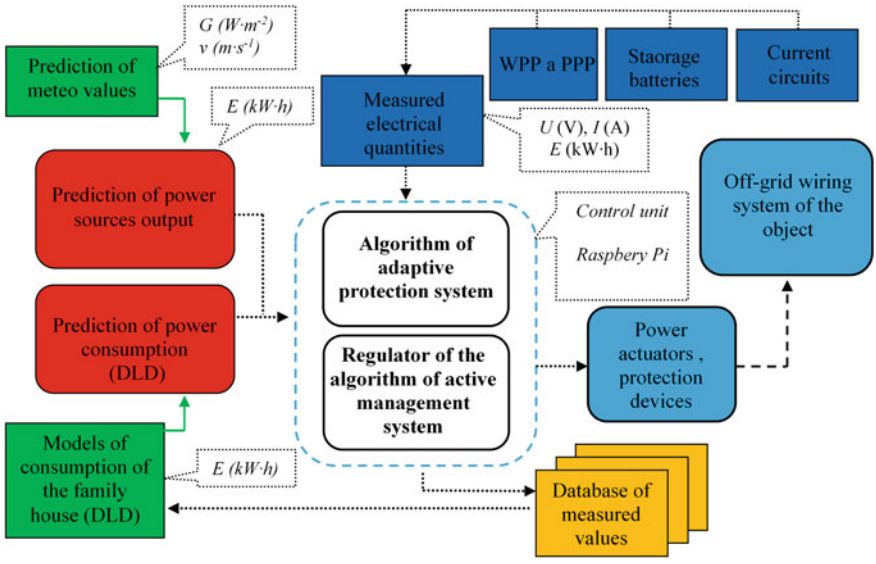

Fig. 4.31 Scheme of a smart energy system for the off-grid system

forecast agency—(data for three following days are sent via Ethernet); data acquired in this way are used to predict production of electricity for the PPP and WPP.

- Prediction of electrical energy consumption of the family house (DLD), the daily load diagram of the family house, may be different for working days, weekends or seasons. Therefore, a database of electric power consumption of a typical household was established, based on long-term measurements of electric power consumption of several family houses. This database allows predicting the expected scenario of the daily load diagram depending on the respective day, season, and behavior of consumers.
- The active power consumption management system receives both information inputs. According to the algorithm and measurement of electrical quantities, it evaluates usable electrical energy from the hybrid power source (PPP and WPP) and storage system. It determines whether the amount of electricity is sufficient to cover the expected energy consumption. In the event of a shortfall of electricity in the system, it regulates consumption (DLD) respecting the priorities in energizing individual appliances (appliances of the lowest priority—washing machine, dryer, air conditioning, and dishwasher). The daily load diagram is preset using the active management system and according to predetermined priorities for switching of individual appliances. The active power consumption management system moves and spreads the power consumption to less loaded period in the daily load diagram or moves operation of certain appliances (dishwasher, washing machine, and dryer) to a period in the daily load diagram with expected higher production of electric power from the hybrid power source—see Fig. 4.32. A more detailed description of the active system of power consumption management is presented in the following publications.

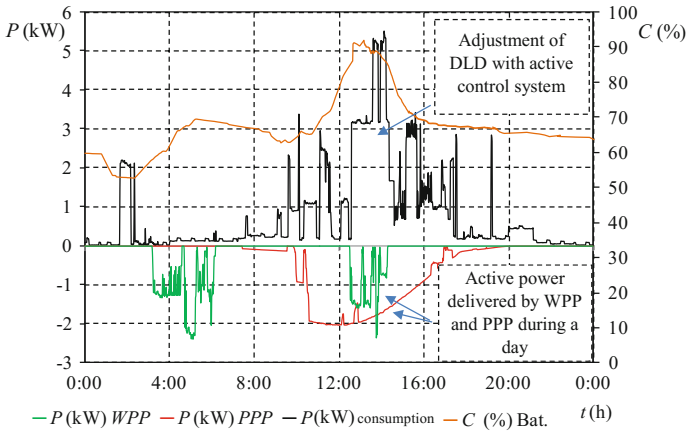

Fig. 4.32 DLD together with actual output from PPP and WPP and capacity of storage batteries during 1 day

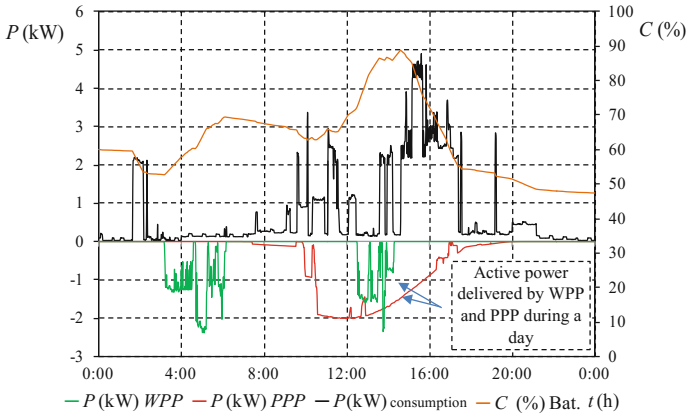

Fig. 4.33 A model example of the modification of DLD using the active power consumption management system

Figure 4.32 shows the course of DLD for a standardized family house together with the performance of the hybrid power source and capacity of storage batteries. From 12:00 to 15:40, the output of the hybrid power source is sufficient to cover the actual load; the off-grid converter charges storage batteries. From 16:00, power consumption increases and the actual output of the hybrid power source decreases. The off-grid converter must draw power from storage batteries to partially cover the electricity consumption of the standardized family house. At the end of the day, the capacity of storage batteries varies around the value of 48 %. Figure 4.33 shows a model modification of DLD through active power consumption management system. The active power consumption management system shifts power consumption to less loaded period in the daily load diagram with higher production of electricity from the hybrid power source. At the end of the day, the capacity of storage batteries varies around the value of 64 %.

4.5 Analysis of Fault Conditions in the Off-Grid System

The analysis focuses on abnormal and fault conditions in the single-phase testing of the off-grid system built within the premises of the VŠB-TUO. In terms of frequency of single-pole faults that can occur in the power distribution within the off-grid network supplied by the off-grid system, these include overload and single-phase fault. Simulation of a sudden single-phase fault will be shown for three operating states (modes) of the off-grid system—see Fig. 4.34.

- First operating state—the source of electricity for the off-grid system is only the off-grid converter powered from storage batteries.

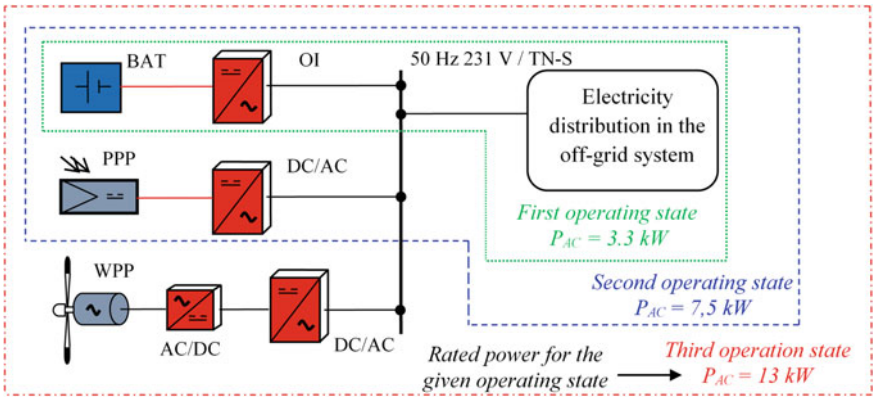

Fig. 4.34 Basic operating states of the off-grid system

- Second operating state—the source of electricity for the off-grid system is the off-grid inverter powered by storage batteries and PPP with power electronics.
- Third operating state—the source of electricity for the off-grid system is the off-grid inverter powered by storage batteries along with the hybrid power source—PPP and WPP with power electronics.

According to the manufacturer and according to EN 50178 and EN 610000-6-1, the off-grid inverter has its own protection against overheating and its output AC current monitored against short circuit and overload. In the case of short-term overload (motor starting current), the off-grid inverter of the testing energy platform can provide 50 A for 100 ms. After the elapse of the period specified for short-time overload and the detection of exceeding the maximum current consumption, which occurs in the case of single-phase fault and overload, the used off-grid inverter of the testing energy platform disconnects power supply from the AC side of the off-grid system. Using a power element (switch), which is controlled by the off-grid converter, it disconnects the main power circuit that feeds the secondary circuits and thus also individual appliances. The off-grid converter disconnects power supply from the AC side of the off-grid system after more than 6 s of the fault duration. This disconnection time is designed to protect the off-grid converter, but it does not correspond to the set time limit for automatic disconnection from the source in case of failures such as single-phase fault in low-voltage networks. For TN-S/231V networks, this time is determined by the standard EN 33, 200-4-41, ed. 2, as 0.4 s from the time of failure occurrence (electricity distribution in the off-grid system built within the premises of the VŠB-TUO is implemented in the form of single-phase TN-S network with grounded neutral point, protective conductor PE, and neutral conductor N, whereas both conductors are connected separately). Therefore, the system may produce a fault condition whose effects threaten people's health, safety and system reliability. For this reason, protection is applied in the event

of a fault when the basic protection fails (insulation failure, contact between the live part and conductive housing). In such a case, TN networks use protection measures consisting in automatic disconnection from the power source through overcurrent protection devices; within the standard concept of protection, these devices are fuses and circuit breakers. The automatic disconnection from the power source in the event of failure (single-phase fault and overload) takes place due to the passage of fault current which is detected by the protective device in the circuit in which the failure has occurred, whereas the device then disconnects the respective circuit from the power source.

4.5.1 Overload in the Testing Platform of the Off-Grid System

A random overload of the off-grid system (overload is a load of the off-grid system with currents which are higher than rated load currents; in the case of single-phase isolated off-grid system, it is a load higher than rated load of appliances) is illustrated for the first and second operating states of the off-grid system. Measured values of voltage and current in the circuit can be used to construct a graph showing the dependence of the terminal voltage on the consumed current, i.e., the so-called source load characteristic. The inclination of the load characteristic and the magnitude of the source internal impedance determine the hardness of the source—(i.e., the rate of terminal voltage drop due to increasing current consumption). According to the load characteristic, we distinguish hard and soft sources. Hard sources have low internal impedance, their terminal voltage drops slightly with increasing load, and short-circuit current can reach large values. Soft sources have greater internal impedance and their terminal voltage drops very quickly. With increasing load, the soft sources show higher drops of terminal voltage and short-circuit current reaches lower values.

Figure 4.35 shows load characteristics for a soft and hard power source. In our case, the hardness of the source is determined by the rated load of the off-grid converter together with the hybrid source and power electronics. Figure 4.35 shows the load characteristic of the off-grid system in the first and second operating states.

Figure 4.36 shows instantaneous values of current and voltage in the main current circuit measured with an oscilloscope when gradually loading the off-grid network from 1 to 5 kW in the first operating state. The off-grid system is loaded using a programmable and purely resistive load. Figure 4.37 then presents the calculated effective voltage values when gradually loading the off-grid system (the calculation is performed using FlexPro software). Immediate overload of the off-grid inverter used in the testing platform of the off-grid system in the first operating state occurs when the power consumption of appliances connected to the off-grid system exceeds 5 kW. According to technical parameters of the off-grid inverter, the inverter is able to cover the load of 4.8 kW for 1 min; overload occurs

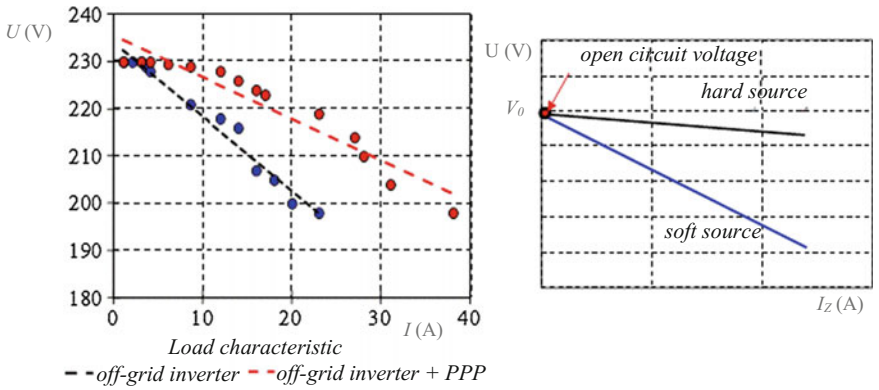

Fig. 4.35 Load characteristic of the off-grid converter (first operating state), load characteristic of the off-grid converter together with the FVE (second operating state)

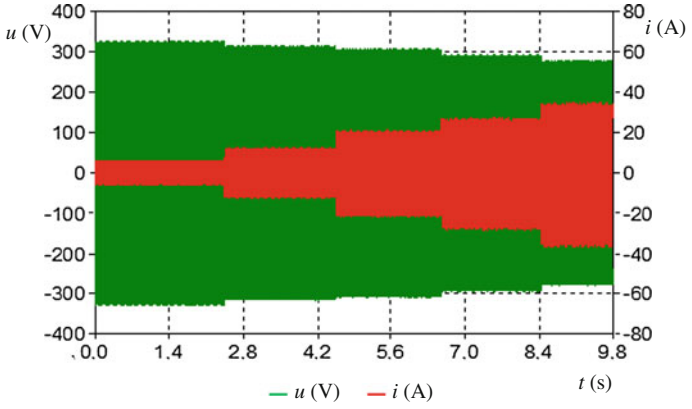

Fig. 4.36 Measured instantaneous values of voltage and current during gradual loading of the off-grid network in the first operational state

if this time is exceeded or if the load increases, and the off-grid system supply is subsequently interrupted. The off-grid inverter switches off and thus disconnects the supply of all current circuits within 6 s. This time of disconnection varies depending on the overload magnitude and the level of battery charge.

According to EN 60038 (330120), a change or drop in the voltage of low-voltage distribution networks (230/400 V, 50 Hz) is defined as +10 %/−10 % of rated voltage ($\geq$207 V; $\leq$253 V) for 95 % of measuring intervals. Larger voltage deviations from the rated voltage significantly affect the function of the appliance. Larger deviation then easily causes a malfunction of or damage to the appliance. Figure 4.37 shows drops in the effective voltage values during gradual loading of the off-grid inverter. When the load exceeds 4 kW, the effective voltage

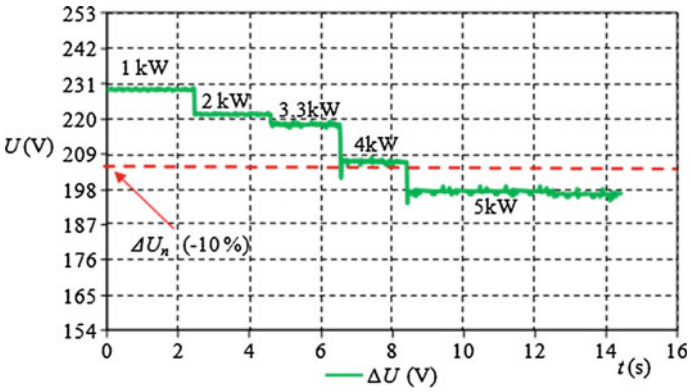

Fig. 4.37 Drops in the effective voltage value during gradual loading of the off-grid network in the first operational state

value in the off-grid system decreases below 207 V, which is the set limit of voltage drop in the grid. When the load is 5 kW, the effective voltage value is around 197 V.

Figure 4.38 shows the measured instantaneous values of current and voltage in the course of a sudden overload of the off-grid inverter in the testing platform of the off-grid system. Before the sudden overload, the off-grid system is in the second operating mode, and its actual load is at a value of 5.5 kW. Output of the PPP and off-grid inverter is sufficient to cover the actual load, whereas the effective voltage value reaches 225 V. The PPP output covers 70 % of the actual consumption; the PPP is disconnected after 30 s (worse weather conditions where PV panels are shaded with a cloud) and the off-grid system switches from the first to the second operating state, which causes the overload of the off-grid inverter. The WPP and

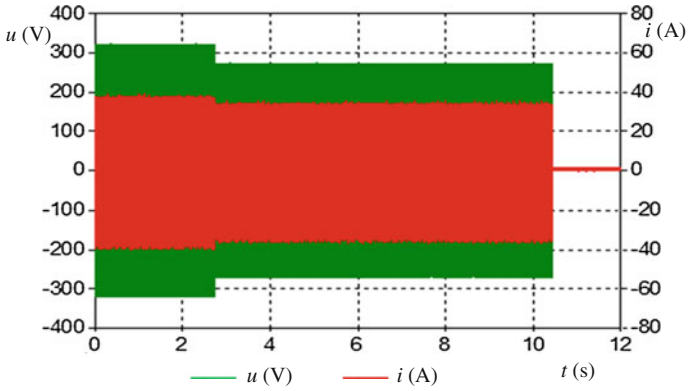

Fig. 4.38 Measured instantaneous values of voltage and current during a sudden overload of the off-grid inverter; transition from the first to the second operating state

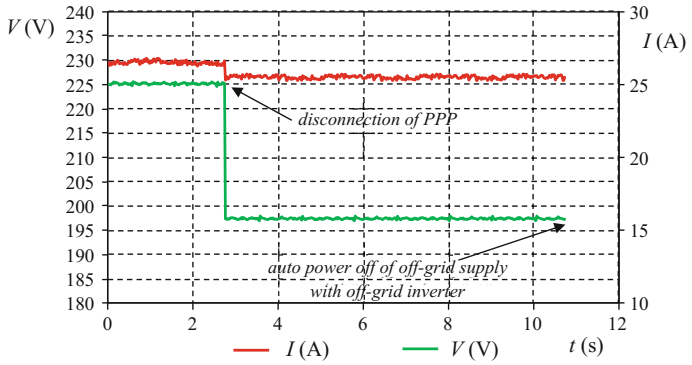

Fig. 4.39 Effective values of voltage and current during a sudden overload of the off-grid converter; transition from the first to the second operating state

PPP do not supply any power to the off-grid system. The off-grid inverter is powered only from the storage batteries charged to 91 % at the moment of overload. During this overload, the effective voltage in the off-grid system drops to 196 V—see Fig. 4.39. After 6 s of the overload duration, the off-grid inverter automatically disconnects power supply for the off-grid system. The off-grid inverter automatically restores power supply for the off-grid system only after the lapse of 10 min.

Figure 4.40 shows the measured instantaneous values of current and voltage in the main current circuit of the off-grid network during the second operating state. Electricity source for the off-grid system is the off-grid converter powered by storage batteries together with the PPP. Figure 4.41 shows drops in the effective voltage value when the off-grid network is gradually loaded. At the time of from 8 to 9.2 s, the off-grid network is loaded with a consumption of 6.8 kW; the PPP

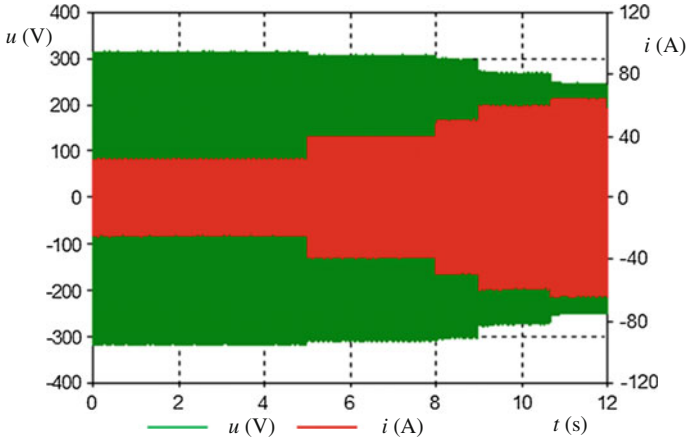

Fig. 4.40 Measured instantaneous values of voltage and current during gradual loading of the off-grid network in the second operating mode

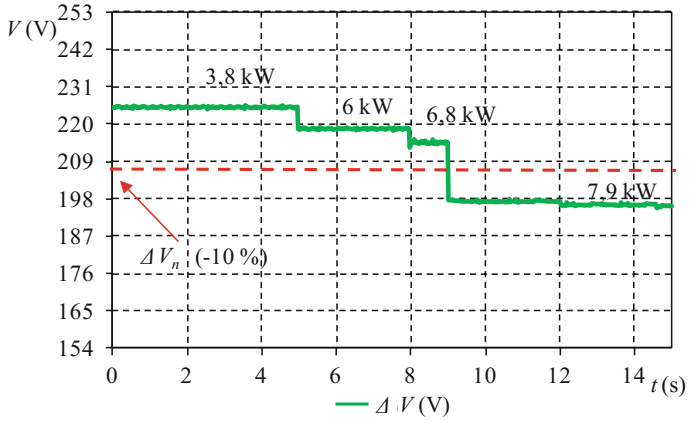

Fig. 4.41 Effective voltage values during gradual loading of the off-grid network in the second operating mode

covers 42 % and the off-grid converter covers 58 % of the actual load. Effective voltage value drops to 213 V. When the load increases to 7.9 kW, the effective voltage in the off-grid network decreases below 207 V. The actual output of the PPP covers 36 % of the load. The rest of the load must be covered by the off-grid converter (load >5 kW) which enters into a state of overload. After the lapse of 6 s, the off-grid converter automatically disconnects the power supply for the off-grid network due to this overload.

Overload protection consists in the automatic disconnection from the power source using protective devices which interrupt overload current flowing through the affected part of the circuit due to overloading; in the case of the off-grid system, this happens prior to the shutdown of the off-grid inverter, i.e., before interruption of the power supply for the entire off-grid system. The use of a classical protection elements for protecting the main supply current circuit L_1 (without limiting the maximum wattage of appliances, see Fig. 4.42), such as circuit breakers with characteristics B20, B16, does not ensure safe shutdown before disconnection of the off-grid inverter—normalized tripping characteristic of circuit breakers.

The analysis of data obtained from experimental measurements during the off-grid network overloading shows that the phase voltage effective value drops below 207 V when the off-grid converter is overloaded—see Table 4.5. This voltage drop in the off-grid system, caused by the overloaded off-grid inverter, can be used to ensure protection against overloading. One option is to use an under-voltage control relay—see Fig. 4.42. Undervoltage relays are designed to control the supply voltage (overvoltage/undervoltage) in phase conductors of electrical devices and circuits. The relay monitors the magnitude of phase voltage. When the adjustable lower voltage level is exceeded (140–200 V), the applied protective or power element (circuit breaker, contactor) is activated. This protective relay can be used for protection against undervoltage which arises in the off-grid network in the

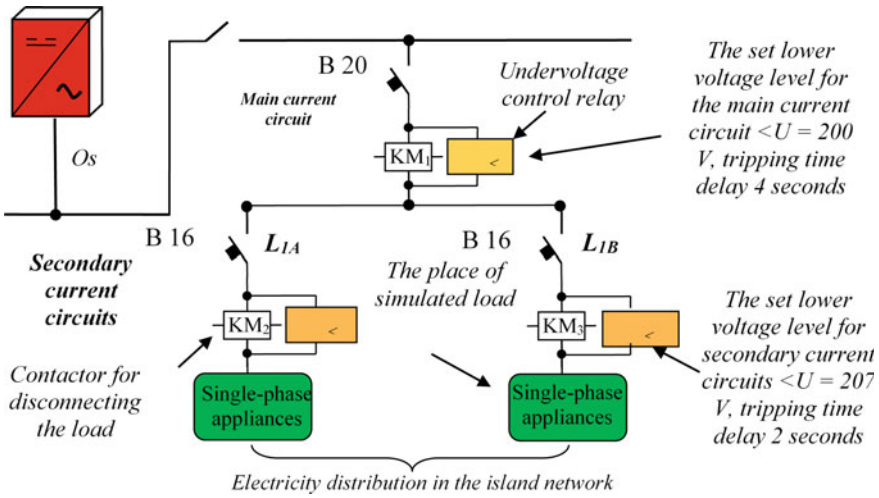

Fig. 4.42 The use of undervoltage control relay to ensure overload protection of the off-grid system (off-grid inverter)

Table 4.5 Effective voltage values during gradual loading of the off-grid system in the first and second operating modes

First operating state		Second operating state	
P^a (kW)	U (V)	P^a (kW)	U (V)
2	224	3.8	226
3.3	219	6	219
4	208	6.8	212
5	198	7.9	197

[a]Loading of the off-grid system using a programmable and purely resistive load

case of overloading. To avoid accidental tripping of the protective or power element in the case of short-term drops of phase voltage in the off-grid network (dynamic power consumption), the undervoltage control relay is equipped with the option of setting a tripping time delay. The delay time can be set from 1 to 16 s. This time delay with the option of setting the voltage level can be used to ensure selectivity—(the power supply is switched off only for the affected area in the electrical distribution of the off-grid system using a time or current protection stepping).

This method of protecting the off-grid system against overloading ensures that the main current circuit L_1 is not interrupted in case of overloading. However, the circuit breakers KM_1 and KM_2, designed for disconnecting the power supply for secondary current circuits, are activated (during the first operating state, the value of effective voltage in the secondary current circuits as well as in the main current circuit drops to 197 V). When protecting the off-grid system against overloading, the use of the undervoltage control relay does not provide protection selectivity in the case of the off-grid system overloading.

4.5.2 Short-Circuit Faults in the Off-Grid System

Short-circuit fault is an electromagnetic transient phenomena in the electric power system. It can be defined as an "accidental or intentional conductive connection of phases or one-phase with the earth in systems with directly grounded point." During this fault, short-circuit current flows through the circuit, and in the vicinity of the respective short-circuit place, it can be often several times larger than the operating currents. Magnitude of the short-circuit current and its waveform is determined by the voltage of the source (short-circuit power of sources), circuit impedance, and the time of emergence.

The main causes of short circuits include isolation failures due to mechanical damage to lines and cables, insulation aging, improper dimensioning of conductors, deterioration of insulation quality due to long-term overloading, various defects on electrical equipment, human factors (such as improper handling).

Effects of short-circuit currents are as follows. During the event, short-circuit currents flow through the electrical circuit to the short-circuit place; there is a risk of damage to electrical equipment and shock hazard to the operators. In the case of short-circuit event in the electrical circuit, the overall impedance of the electrical circuit decreases and voltage drops, especially in the place close to the short-circuit point. Voltage drops increase from sources to the short-circuit point, which is seen in varying degrees throughout the electrical circuit. Voltage drops due to short-circuit events have adverse impacts on the proper functioning of the electrical equipment and appliances. Electrodynamic (power) and thermal effects of the short-circuit current threaten all elements of the installation and electricity system through which it flows. Last but not least, the action of electrical protections during the short-circuit fault leads to interruption of supply routes and disconnection of sources of the short-circuit current, i.e., to the power disruption.

According to the basic classification, short-circuit faults can be divided into symmetrical and asymmetrical. Symmetrical short-circuit faults include three-phase (three-pole) short circuit, i.e., the connection of all the three phases. Short-circuit current often reaches the highest values. Asymmetrical short-circuit faults include one-phase (single-pole) connection of one-phase with the earth (phase-to-earth connection) in the network with grounded neutral point and two-phase (two-pole) connection of two phases. The course of the short-circuit current is a transient process that is influenced by many parameters. We monitor its beginning, intermediate part and steady part. There are two characteristic courses of the short-circuit current, symmetrical and asymmetrical. The moment of the short-circuit emergence determines whether the time course of the short-circuit current is symmetrical or asymmetrical.

Symmetrical short-circuit current: The short-circuit fault occurs when the sine wave of alternating (AC) voltage passes through its maximum. Short-circuit current then starts from its minimum value. Asymmetrical short-circuit current: The short-circuit fault occurs when the sine wave of alternating voltage passes through zero. Short-circuit current then starts from its maximum value. In addition to the

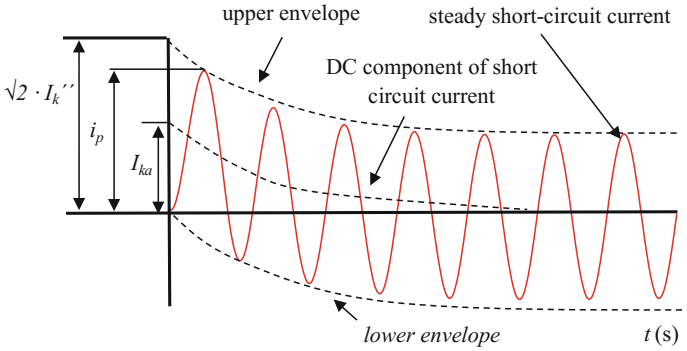

Fig. 4.43 The course of electrically remote short-circuit current with the largest DC component

alternating component of the short-circuit current, also a direct (DC) component is formed, which disappears in time—see Fig. 4.43.

It is a component of short-circuit current which appears if the short-circuit fault occurs when the voltage crosses zero (shifting the course of short-circuit current asymmetrically from the x axis). The size of this aperiodic component depends on the initial size of the AC short-circuit current, on the current flowing through the electric circuit before the short-circuit fault and the time of the short-circuit emergence with regard to the course of voltage in the place of the short-circuit fault. Furthermore, short-circuit faults can be divided into near-to-generator short circuits and remote short circuits. If the synchronous machines are not electrically sufficiently distant from the place of the short-circuit fault or if the contribution of asynchronous machines is not negligible, then we are talking about the near-to-generator short circuit. The course of the short-circuit current is more complex. It is possible to observe changes in the electrical parameters of the synchronous machine; reactance value is gradually changing from shock (subtransient), temporary (transient) to synchronous. Situation during the short-circuit fault can be found by measurements on an actual device or model, by simulation tests or calculations.

When determining the parameters of the short-circuit current, the short-circuit current is considered for the worst case but with operationally permissible connection. For proper dimensioning of electrical devices, we usually take values corresponding to the maximum short-circuit current; regarding correct design and operation of electrical protections and protective element, the values taken correspond to the minimum short-circuit current. If the protection of an electrical equipment against short-circuits faults is using fuses or circuit breakers limiting the short-circuit current, we first calculate or measure the initial short-circuit current without protective devices. This short-circuit current and limiting characteristics of fuses or circuit breakers lead to determining parameters of the limited short-circuit current which stresses the electrical equipment after the protective device. From the viewpoint of protection setting, it is not necessary to know a detailed interval of the

short-circuit current; we make do with characteristic values of short-circuit current described by relations (4.4–4.6).

- Initial short-circuit current $I_k^{''}$ (A)—it is an effective value of the alternating component of the short-circuit current at the time of short-circuit emergence, at a constant impedance. It is a transient AC current generated in the first moment of the short-circuit fault when the voltage still has its original value:

$$I_k'' = k \cdot \frac{c \cdot U_n}{\sqrt{3} \cdot |Z_k|} \text{ (A)}, \tag{4.4}$$

  where k is the coefficient for different types of short-circuit faults, as given by the standard, U_n is the voltage related to the short-circuit place (V), Z_k is the total impedance (Ω), and c is the voltage coefficient comprising an estimate of the internal voltage of sources, as given by the standard.
- Surge short-circuit current i_p (A)—it is the maximum possible instantaneous value of the prospective short-circuit current. The maximum possible instantaneous value of the surge short-circuit current can be achieved if the short-circuit fault occurs at a moment when the largest DC component of the short-circuit current is generated. This value is reached during the first half-wave of the short-circuit current in time of 0.01 s:

$$i_p = k \cdot \sqrt{2} \cdot I_k'' \text{ (A)}, \tag{4.5}$$

  where k is the coefficient for calculating the surge short-circuit current, as given by the standard, and $I_k^{''}$ is the initial surge short-circuit current (A).
- Equivalent heating current I_{th}—it is an efficient value of the current which has the same thermal effects and the same duration as the actual short-circuit current, which may include a DC component changes over time. It is important for the design of electrical installations in terms of thermal effects of short-circuit currents:

$$I_{\text{th}} = \sqrt{\frac{1}{t_k} \cdot \int_0^{t_k} i_k^2(t) \mathrm{d}t}, \quad I_{\text{th}} = k_{\text{e}} \cdot I_k'' \text{ (A)}, \tag{4.6}$$

  where k_{e} is the coefficient specified in the standard for different places of short-circuit faults and different times of their action, and $I_k^{''}$ is the initial surge short-circuit current (A).

Figure 4.44 shows a simplified diagram of the testing platform connection for the off-grid system, before using the active protection system and together with the connection of protective elements for automatic disconnection from the power source (circuit breaker, fuse) as a protection against single-phase short-circuit faults in the electricity distribution system of the off-grid system. Figure 4.44 shows the place of a sudden single-phase short-circuit fault on terminals of an appliance

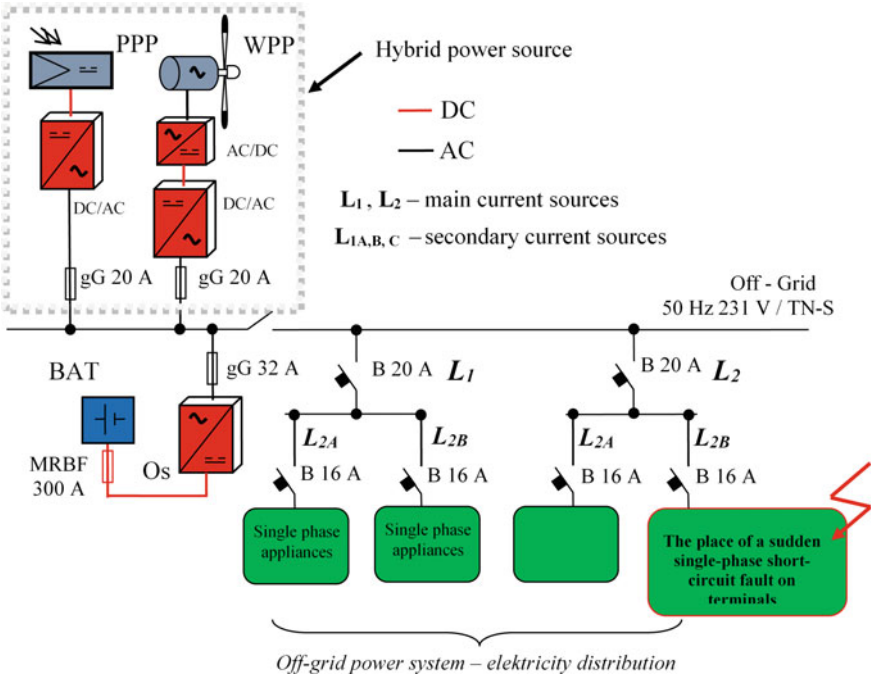

Fig. 4.44 A simplified block diagram of the testing platform connection for the off-grid system, together with the connection of protective elements and before using the active protection system

connected to the off-grid system. A shorting contactor (phase-neutral connection) is used to cause a sudden single-phase short-circuit fault in different operating states of the off-grid system; oscilloscope YOKOGAWA then records the voltage and current course before and after the single-phase short-circuit fault in different operating states of the off-grid system.

4.5.3 Single-Phase Short-Circuit Faults in the Off-Grid System—The First Operating State

Short-circuit power in the off-grid system is determined by the short-circuit power of the hybrid source, power electronics and off-grid inverter supplied from Ni–Cd storage batteries. To design a proper concept of protection for the testing platform of the off-grid system, it is necessary to know, measure, and calculate conditions during the single-phase short-circuit fault. Conditions during the single-phase short-circuit fault will be illustrated for the three basic operating states. Figure 4.45 shows a waveform of current and voltage during the single-phase short-circuit fault on terminals of an appliance (phase-neutral connection) supplied from the off-grid

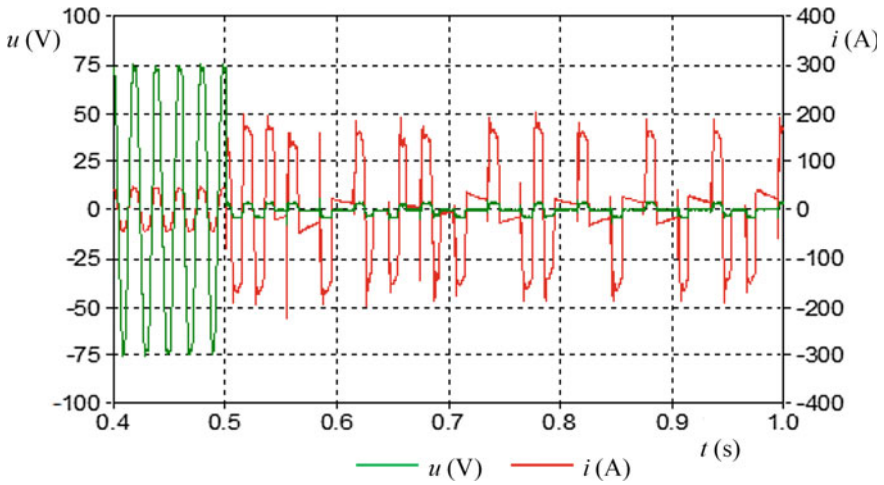

Fig. 4.45 The course of AC voltage (*green*) and current (*red*) in the place of the single-phase short-circuit fault in the off-grid electricity distribution system (Color figure online)

system in the first operating state. Before the sudden short-circuit fault, the off-grid inverter is loaded for 55 % of its rated load, and storage batteries are charged for 96 %. The effective voltage is 228 V, and the off-grid inverter supplies 8.2 A to the off-grid system. During the short-circuit fault and after stabilization of transients, the steady-state effective value of the short-circuit current is 34 A and effective voltage drops below 10 V. The short-circuit fault does not occur in the situation when the voltage crosses zero—(it contains only the AC component); the short-circuit current continuously follows the current flowing through the circuit before the short-circuit fault. The effective value of the initial surge short-circuit current I_k'' is around 36 A.

The off-grid inverter has its own protection against short-circuit faults on the AC output side. In the case of the single-phase short-circuit fault, it disconnects the power supply for the off-grid system, however, only after the lapse of 6 s from the fault emergence. This time of disconnection is intended for protecting the off-grid inverter, but it does not correspond to the specified time limit for the shutdown of failures, such as the single-phase short-circuit fault in low-voltage networks (0.4 s for TN networks).

A classic protective measure against the single-phase short-circuit fault is the protection based on automatic disconnection from the power source (circuit breaker, fuse) during the prescribed period of time. The protection ensures the automatic disconnection if the conditions according to Eqs. (4.7) and (4.8) are met. If this assumption is fulfilled, the respective faulty loop contains a short-circuit current (depending on the magnitude of the loop impedance) which is higher than the tripping current I_a of the protection ensuring the automatic disconnection from the power source. The protection is thus able to switch off the failure, as the single-phase short-circuit fault, within the required time limit (the prescribed tripping time is

0.4 s; this value has been specified for TN networks). When using a classic protection, such as a circuit breaker with characteristic B, I_n = 16 A, factor 5, the tripping current of the circuit breaker will be I_a = 80 A:

$$Z_{\text{sm}} \leq k \cdot \frac{U_0}{I_{\text{a}}} \ (\Omega), \tag{4.7}$$

$$Z_{\text{sm}} = 0.8 \leq \frac{2}{3} \cdot \frac{231}{80} = 1.93 \quad (\Omega), \tag{4.8}$$

where Z_{sm} is the measured impedance of the loop of faulty current, comprising the source, working conductor to the place of failure and protective conductor between the place of failure and the source, U_0 is the rated AC voltage, I_{a} is the current ensuring the automatic action of the disconnection protective element within the prescribed time limit, and k is the coefficient which takes into account the increase in resistance of the conductors as a result of their increased temperature due to the faults k = 2/3.

In the off-grid system, the loop impedance in the place of the sudden short-circuit fault is 0.8 Ω. The prerequisite for a safe automatic shutdown of the circuit is a low value of impedance Z_{sm}. The maximum allowed value of the fault loop impedance is given by relations (4.7) and (4.8). Values of impedance in the place of short-circuit fault were determined through measurements using multifunction devices EUROTEST 61557 for performing revisions according to the requirements of standards. During measuring the impedance of the shutdown loop, the off-grid system was not loaded. The connected load may cause voltage fluctuations in the off-grid system, which could affect measurement accuracy. The measuring instrument used for measuring the impedance measures voltage on the embedded measuring resistor before and during the flow of measuring current. Action of the measuring current I_m causes a voltage drop in the current loop. The difference of voltages before (U_0) and during the action of measuring current (U_m) can be used to determine the loop impedance Z_{sm} and short-circuit current I_{a} according to:

$$Z_{\text{sm}} = \frac{U_0 - U_m}{I_m} (\Omega), \quad I_{\text{a}} = \frac{U_0}{Z_{\text{sm}}} = \frac{231}{0.8} = 299 \quad (\text{A}). \tag{4.9}$$

When using a classic protection, such as a circuit breaker with characteristic B16, the tripping current of the circuit breaker will be 80 A. At the voltage of 231 V, the current flowing through the fault loop can be 299 A—see Eq. (4.7). This value is higher than the required tripping current of the circuit breaker, which is 80 A. Circuit breaker B16 should reliably shut down within the specified time limit according to tripping characteristics of circuit breakers. However, because it relates to protecting the off-grid system which is not connected to and supplied from a classic distribution system (see the low-voltage distribution connection 230/400 V AC 50 Hz which connects the supply point (consumer) to the distribution grid), the

protective element—designed for automatic disconnection from the power source in case of failure—is not activated in the event of short-circuit fault.

The above operational condition indicates that the use of the classical concept of electric protection (without limiting the maximum appliance input) used for the protection of low-voltage distribution does not provide a safe fault clearing such as the single-phase short circuit on the AC side of an off-grid system at the first operating condition within a specified time limit. The short-circuit current value is insufficient for furnishing security element such as a circuit breaker B16 and B10 (36 A < 80, 50 A) within a specified time limit, at the short-circuit place the limited short-circuit current that the standard protection concept is unable to interrupt flows through the off-grid inverter therefore causing in the off-grid system a fault condition, that through its effects threatens the people's health, safety, and system reliability.

Before a sudden short circuit, which is indicated in Fig. 4.45, the voltage at the storage batteries amounts to the value of 24.1 VDC, which corresponds to the charging level of 96 %. At a sudden single-phase short circuit on the AC side of the off-grid system, the off-grid inverter draws DC current that moves on the value of 300 A DC. The off-grid inverter at the single-phase short circuit disconnects the power supply of the off-grid system, but only after 6 s from the time of the short-circuit occurrence. This time off is dependent on the level of charging storage batteries, see Table 4.6.

Figure 4.46 indicates the waveform of current and voltage in the case of a sudden single-phase short circuit at the terminals of an appliance (connection of the phase conductor with the neutral one) powered by the off-grid invertor. The off-grid invertor works in the mode with the charge controller. The off-grid invertor is used for the storage of electrical energy of the lead–acid storage battery, rated voltage of 48 V DC, with a total capacity of 1000 A h. The rated power of the off-grid invertor is 8 kW, and for the period of 1 min, it is able to cover the consumption of 9.6 kW.

Before the sudden short circuit, the off-grid inverter is in the first operating mode and is loaded at 35 % of its maximum potential load. The effective voltage value is 228 V and the off-grid inverter supplies to the load 10 A. In the case of a sudden short circuit, the effective value of the initial surge short-circuit current I_k'' is about 51 A, whereas the root-mean-square value of voltage falls below 10 V. The off-grid

Table 4.6 Time of the power supply off of the off-grid system by the insular converter at the single-phase short circuit in the electrical distribution of an off-grid system at various levels of charging of accumulation batteries

The level of charging storage batteries used in the off-grid system (%)	Time of power off of the charge of the off-grid system through the island convertor at the single-phase short circuit t (s)
96	6
80	6
61	5.2
52	4.5

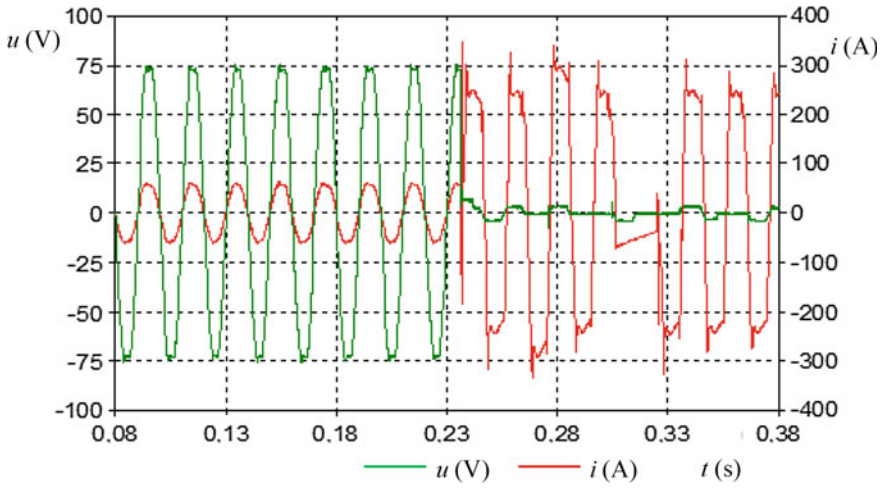

Fig. 4.46 Waveform of AC voltage (*green*) and current (*red*) at the place of the single-phase short circuit in the off-grid system (Color figure online)

invertor disconnects the current supply to the off-grid system at the time of 5.8 s. Data for designing Fig. 4.46 are obtained by measuring by YOKOGAWA oscilloscope. The above operational status indicates that using a protection element, such as the circuit breaker B20 and B16, does not ensure the safe fault clearing such as the single-phase short circuit on the AC side of the off-grid system within a specified time limit, without limitation of the maximum appliance power input.

4.5.4 Single-Phase Short Circuit of the Off-Grid System: The Second Operating Status

The second operating status in the off-grid system occurs when the source of electrical power for the off-grid grid is an off-grid invertor powered by storage batteries and photovoltaic plants with its invertor. As we mentioned in previous chapters, the hybrid source of the off-grid system is complemented by two photovoltaic plants (PPP_1 and PPP_2). The peak power of each PPP reaches about 2 kWp. PPP_1 uses polycrystalline panels connected in series, which are fixedly installed on the roof structure of the building. PPP_2 utilizes monocrystalline panels connected in series; they are placed on the two-axis tracking structure. The power of both PPP is led into the single-phase DC/AC inverter with the maximum performance 4.6 kW.

The maximum DC current that photovoltaic panels used in the test platform of the off-grid system are able to generate is I_{SC} (short-circuit current), which is directly proportional to the intensity of global radiation at the site location of

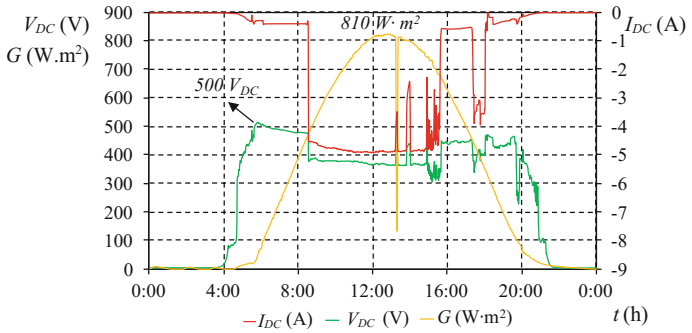

Fig. 4.47 Waveform of the DC voltage and current of polycrystallic PV panels (PPP_1) at changing intensity of the global radiation during 1 day

PPP. U_{OC} maximum voltage (off-load voltage) increases with the intensity of global solar radiation but the relationship is non-linear. Even at very low levels of global radiation (from about 50 W·m^2), DC voltage on PV panels is growing relatively quickly. At the values of the global radiation of 150 W·m^2, the voltage growth is minimal. Figure 4.47 shows changing DC voltage and current PPP_1 in 1 day.

The used PPP inverters contain two inputs (strings) to connect two strings of PV panels. For proper protection of DC side, it is necessary to know the short-circuit current I_{SC} of the two strings of PV panels connected to the invertor of solar panels. According to the parameters of the PV panels used in the test platform of the off-grid system, I_{SC} is with PPP_1 (polycrystalline panels) 5.32 A. For panels used in PPP_2 (monocrystalline panels), the value amounts approximately to 4.97 A. Both strings of PV panels are connected in series and connected to the two inputs of the PPP inverter. For the calculation of the maximum short-circuit current on the DC side of the inverter, it is necessary to multiply the nominal value of I_{SC} by the multifunction coefficient of 1.5, which considers the ambient temperature, increased global radiation values and the ability of the PV modules to produce more than the rated current values. The maximum value of the short-circuit current on the DC side of the PPP inverter is according to Eq. (4.9) 12.86 A DC. The PPP inverter used in the testing platform of the off-grid system includes an integrated DC switch with DC fuses (both inputs are protected against overload by two fuses g_{PV} I_{ng} = 8 A, U_{ng} = 1000 V DC). This continuous protection according to Eq. (4.8) shall ensure the safety of the operation of the PPP inverter and the used photovoltaic panels:

$$1.2 \cdot U_{0C} \leq U_{ng} \quad 1.5 \cdot I_{SC} \leq I_{ng}, \tag{4.10}$$

where I_{SC}—short-circuit current of PVP panels, U_{0C}—short-circuit voltage of PV panels, U_{ng}—nominal values of fuses, and I_{ng}—nominal current of fuses.

PPP inverters with its power electronics generally do not cause a great contribution to the short-circuit current to the off-grid system. The PPP inverters with their protective functions will contribute to the short-circuit current in AC electrical

distribution of the off-grid system in the maximum range of 1.1–1.5 times of the rated current of the inverter. This value is much lower than in rotating machines, which ranges from 4 to 10 times the rated current. There are two types of internal system of PPP inverter protection in the case of a short circuit on the AC side quick inverter disconnection—over several periods of the fault duration (disconnection of the inverter and the power supply interruption immediately at fault) or a short-term continuous operation (the time during which the convertor delivers the fault current can be adjustable). According to the technical specifications and after consultation with the manufacturer of the PPP inverter, the inverter used in the testing platform of the off-grid system should not contribute to the overall circuit current at the point of fault current >1.3 times the rated current. This means that the maximum current is defined as stated by the maximum current rating of the PPP inverter manufacturer. This information is disclosed to the manufacturer and requires no additional correcting coefficients. The system of instant protection and detecting undervoltage and overcurrent in the PPP inverter will cut off the inverter immediately upon detection of a fault. Figure 4.48 shows the waveform of current and voltage in the sudden single-phase short circuit at the terminals of an appliance at the second operating condition at the off-grid system. Before the sudden short circuit, the effective voltage network value in the off-grid system moves to the value of 226 V. The PPP power is sufficient to cover the current load in the off-grid system.

PPP with its invertor is before the short-circuit loaded at 60 % of its rated load and supplies to the off-grid system the current with a rms value of 10.5 A. At a sudden single-phase short circuit at the terminals of the appliance, the effective value of the initial surge short-circuit current is moving at a value of 48.5 A. PPP through its inverter contributes to the total initial surge short-circuit current of 13.5 A, which is roughly 1.3 times the PPP current of the inverter before short-circuiting. The instant inverter protection system (detecting undervoltage and overcurrent) of PPP begins the immediate disconnecting the inverter, and it automatically disconnects from the off-grid system in time <0.04 s. After disconnecting

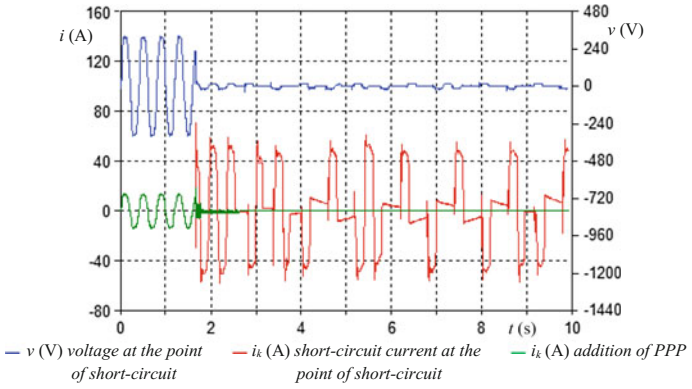

Fig. 4.48 The waveform of the AC voltage and current at the single-phase short circuit in the off-grid system, the second operation condition

Table 4.7 Contribution of the PPP inverter to the total initial surge short-circuit current at the place of the short circuit

Load of the PPP inverter before the sudden single-phase short circuit P (%)	Contribution of the PVP short circuit $I''_{k.PVP}$ (A)	Contribution of the short-circuit current of Os $I''_{k.Os}$ (A)	Surge short circuit at the short circuit at the short-circuit place I_k'' (A)
30	6.8	37.1	43.9
60	13.5	37	50.5
90	19.8	36	55.8

the PPP inverter, the short circuit only is powered by the off-grid inverter with the accumulation. The RMS value of the steady short-circuit current drops to 34 A. In the second operating condition in the off-grid system, the PPP inverter may, therefore, contribute to the overall short current at the point of the short-circuit point with 23.6 A, which is 1.3 times the rated current of the PPP invertor, see Table 4.7.

4.5.5 *Single-Phase Short Circuit in the Off-Grid System: The Third Operation Condition*

The third operating condition in the off-grid system occurs when the source of the electrical power for the off-grid system is the off-grid inverter powered by storage batteries together with PPP and WPP with power electronics. The hybrid source of the off-grid system is supplemented by WPPs with an installed output of 8 kW. WPP contains the three-phase 20-pole synchronous permanent magnet generator (PMG). WPP generator is connected to the off-grid system grid via a fully controlled electronics in the so-called "back-to-back" mode. For the proper draft concept of protection, it is necessary to know the parameters of the synchronous WPP generator shown in Eq. (4.9), which describes the behavior of the machine at a sudden short circuit. In the event that a short circuit is in the electrical vicinity of the synchronous generator, the waveform of the short-circuit current is more complicated, and the change of electrical parameters of the machine manifests during the short circuit, see Fig. 4.49. The reactance of the generator is gradually changing from the surge value to the transition and synchronous value. The maximum short-circuit current of the synchronous WPP generator is according to Eq. (4.11) in the case of the abrupt galvanic connection of input terminals at an idle state limited to the reactance of the machine, whereas the impact of the resistance is negligible:

$$I_{k_G(t)} = \left(\frac{U_0}{x_d}\right) + \left(\frac{U_0}{x'_d} - \frac{U_0}{x_d}\right) \cdot \mathrm{e}^{-\frac{t}{T'_d}} + \left(\frac{U_0}{x''_d} - \frac{U_0}{x'_d}\right) \cdot \mathrm{e}^{-\frac{t}{T''_d}} \text{ (A)}, \tag{4.11}$$

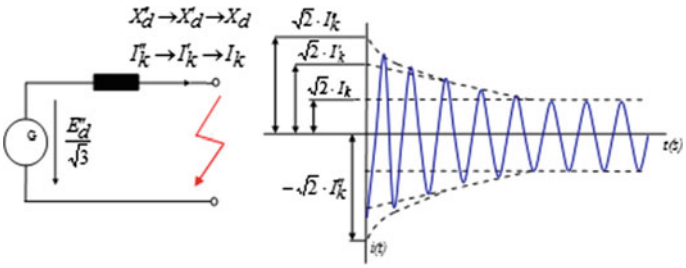

Fig. 4.49 The electric short-circuit close to the synchronous generator. I''_k—surge sub-transient short-circuit current, I_k'—transient short-circuit current, I_k—steady short-circuit current, and E''_d—surge (sub-transient) voltage of the synchronous generator, phase

where I_{kG} (t)—effective value of the short-circuit current, U_0—effective voltage value before the short circuit, X_d—synchronous reactance, X''_d—surge (sub-transient) reactance, X_d'—transient reactance, t—time period from the short-circuit occurrence, and T''_d and T_d'—surge and transient time constant.

Since some parameters of the synchronous generator, which represent the behavior of a synchronous generator at a sudden short circuit according to Eq. (4.11), were not specified on the label of the synchronous WPP generator, it was necessary to measure the synchronous generator at a sudden short circuit, which allows the subsequent calculation of machine parameters and represent the course of the short-circuit current with its sub-transient shorter component and transient longer component. For the determination and calculation of the initial and transient short-circuit current of the synchronous WPP generator, it is necessary to know the two basic aperiodic components represented by the transient (X_d') and sub-transient (X''_d) reactance of the synchronous generator, together with the time constants. These time constants express the time for the exponential drop in the current and represent the duration of these two aperiodic components. The standards and the literature [22, 23] describe in detail the issue of the manual oscillograph analysis and the practical calculation of the reactances of the generator from the measured values of the short-circuit current of the synchronous generator, by a sudden short-circuit method. The method of determining synchronous machine quantities from the test by a sudden three-phase short circuit based on the IEEE standard. If the waveform of voltage and current is at least partially similar to the sine wave, this method works with rms values of voltage and current. Covers connect individual peaks of the waveform of the short-circuit current of the generator, see Fig. 4.50. Figure 4.50 indicates plotting the cover curves (the upper cover red and lower cover blue). Performing readings of the size of the amplitudes from the expressed maximum—top cover to the minimum—lower cover curve will determine the size of the amplitude along with the relevant time. The equation for calculating sub-transient and transient reactance is described by Eq. (3.4).

During 2013, a repair of the swiveling WPP system took place, which allowed the transfer of the WPP generator to the lab of VŠB-TU Ostrava, allowing to

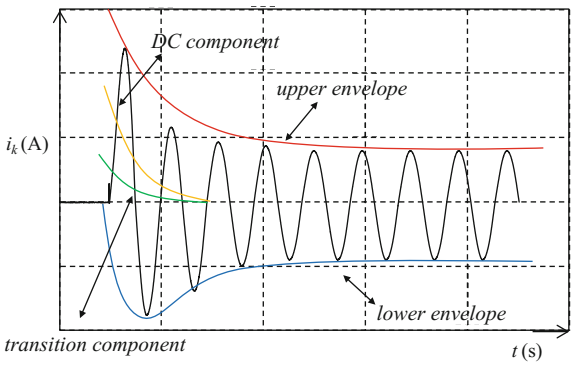

Fig. 4.50 The course of the short-circuit current of the single phase of the synchronous generator together with individual components of the current

measure the reactance of the synchronous generator by a sudden short-circuit method. The measurement procedure for determining the reactance of the WPP generator was as follows.

The WPP synchronous generator is rotated idle using the drive units (dynamometer) to the synchronous speed revolutions. During the test, the generator revolutions (or frequency) may differ from the nominal value, but should not fall below 0.2 times the nominal value. Using the short-circuit contactor, the galvanic connection of the output terminals (short circuit of all phases of the stator windings) of the WPP generator will occur, and the three-phase short circuit occurs. Using oscilloscope, the voltage and current waveform is recorded before and after the short circuit in all three phases, see Fig. 4.51. Switching short-circuit contactor occurred for a short time (<2 s) to avoid demagnetising PMG or change of the

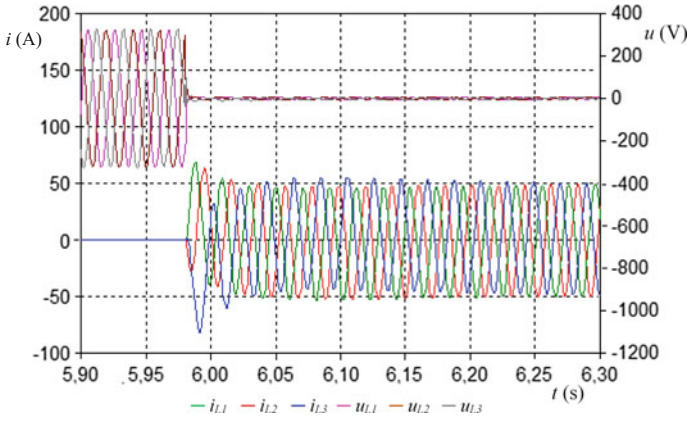

Fig. 4.51 Waveform of immediate values of voltage and current at the three-phase short circuit on WPP terminals (idle)

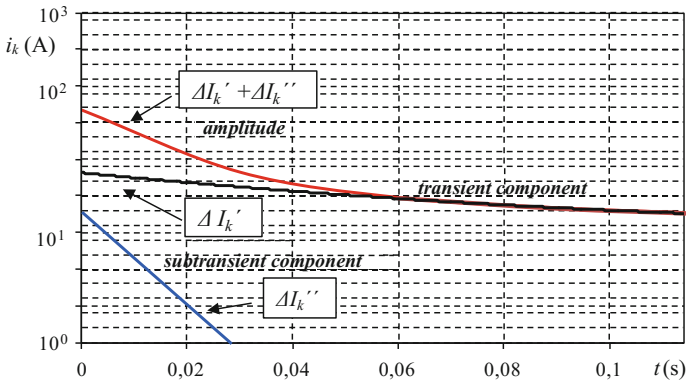

Fig. 4.52 Analysis of the AC component of the short-circuit current for one of three phases of the synchronous generator

magnetic properties of permanent magnets of the synchronous generator. The time change of the component of the current in each phase is determined from the oscillograph of the three-phase short circuit as the algebraic half sum and algebraic difference of ordinates of the upper and lower covers of the short-circuit current in the individual phases. For determining the transitional $\Delta i_k'$ and surge $\Delta i_k''$ component, the value of the short-circuit current is subtracted from the current curve. The remaining sum ($\Delta i_k' + \Delta i_k''$) is plotted in the diagram with semi-log coordinates of Fig. 4.52. The surge component of the current short circuit is defined as the difference between the curve ($\Delta i_k' + \Delta i_k''$) and the line representing the value $\Delta i_k'$. The time interval of the oscillography record should be at least $T_d' + 0.2$ s after a short circuit, where (T_d' and T_d'' are time constants, which represent the time required for the transient and surge component of the short-circuit current of the synchronous generator drops to the initial value).

The equation for calculating the parameters of the synchronous generator, which represent the behavior of the synchronous generator during sudden a short circuit according to Eq. (4.11) are as follows:

- Nominal impedance Z_N (Ω)

$$Z_N = \frac{\frac{U_N}{\sqrt{3}}}{I_N} = \frac{245}{14} = 17.5\ \Omega \tag{4.12}$$

- Synchronous reactance X_d (Ω)

$$X_d = X_1 = \frac{U_0}{I_{1fN}} = \frac{339}{14} = 24.2\ \Omega \Rightarrow \tag{4.13a}$$

$$\Rightarrow x_d = x_1 = \frac{X_d}{Z_N} = \frac{24.2}{17.5} = 1.38 \text{ p.j} \tag{4.13b}$$

To determine the surge and transient reactance, it is necessary to determine the surge $\Delta i_k''$ and the transient current component $\Delta i_k'$. For this determination, the stable value of the short-circuit current is subtracted from the periodic component of the current. The remaining sum $(\Delta i_k' + \Delta i_k'')$ is plotted in the chart with semi-logarithmic coordinates, see Fig. 4.52:

- Transient reactance X_d' (Ω)

$$X_d' = \frac{U_0}{\frac{I_k + \Delta I_k'}{\sqrt{2}}} = \frac{339}{\frac{46.5+20}{\sqrt{2}}} = \frac{339}{44.2} = 7.7\ \Omega \Rightarrow x_d' = \frac{X_d'}{Z_N} = 0.44 \text{ p.j} \tag{4.14}$$

- Surge reactance X_d'' (Ω), the surge reactance is determined as the ratio of the off-load voltage measured just before the short circuit to the initial value of the component of the short-circuit current derived from the oscillograph analysis.

$$X_d'' = \frac{U_0}{\frac{I_k + \Delta I_k' + \Delta I_k''}{\sqrt{2}}} = \frac{339}{\frac{46.5+20+17}{\sqrt{2}}} = \frac{339}{56.2} = 6.03\ \Omega \Rightarrow \tag{4.15a}$$

$$x_d' = \frac{X_d'}{Z_N} = 0.34 \text{ p.j} \tag{4.15b}$$

In Fig. 4.53, there are values of short-circuit current and open-circuit voltage of the WPP generator at various wind speeds, the WPP rotor revolutions. The permanent magnet generator cannot be controlled differently than by the change of rotations. The characteristics of the short-circuit current are thus plotted depending on the revolutions rather than on the excitation voltage U_b. Rotating inertial masses (moment of inertia of the wind turbine rotor and the synchronous generator) determine the mechanical and dynamic properties of the wind turbine (Fig. 4.54).

According to the measured and evaluated values, the maximum value of the initial surge short-circuit current at the 3*f* short circuit at the generator terminals at nominal voltage WPP 122 A, see Table 4.8. To protect synchronous WPP generator against a short circuit, blade fuses PHN 50 A 660 V are applied.

The WPP performance is led to the single-phase off-grid system through the three-phase rectifier and the single-phase inverter. According to the technical specifications and after consultation with the manufacturer of the WPP inverter used in the testing platform of the off-grid system, it should not contribute to the overall short-circuit current at the point of fault (sudden single-phase short circuit at the terminals of an appliance powered from an off-grid system) by the current >1.5–2 times rated current of the inverter. The WPP inverter includes the protection system

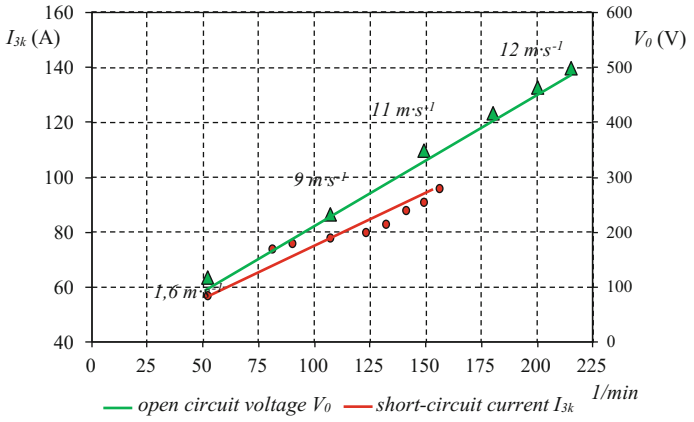

Fig. 4.53 Short-circuit current values and the off-load voltage value of the WPP generator at various values of the wind speed and WPP rotor revolutions

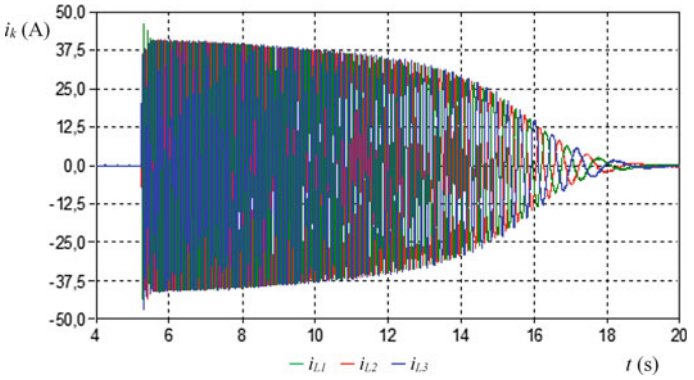

Fig. 4.54 Sample waveform of the current in the galvanic connection of the output terminals (short circuit of all three phases of the stator winding of the WPP generator) till WPP stop; WPP gets before short circuiting the output terminals of the generator spun using wind, whereas the wind turbine revolutions achieve 123 rpm

Table 4.8 Parameters of the synchronous generator WPP

Parameters	Values
Z_n—nominal impedance	17.5 Ω
X_d—synchronous reactance	24.2 Ω
X_d'—transient reactance	7.7 Ω
X_d''—(sub-transient) surge reactance	6 Ω
I_G''—surge (sub-transient) short-circuit VTE generator current	122 A
I_G'—transient short-circuit VTE generator current	95.6 A
I_G—stable short-circuit VTE generator current	30.5 A

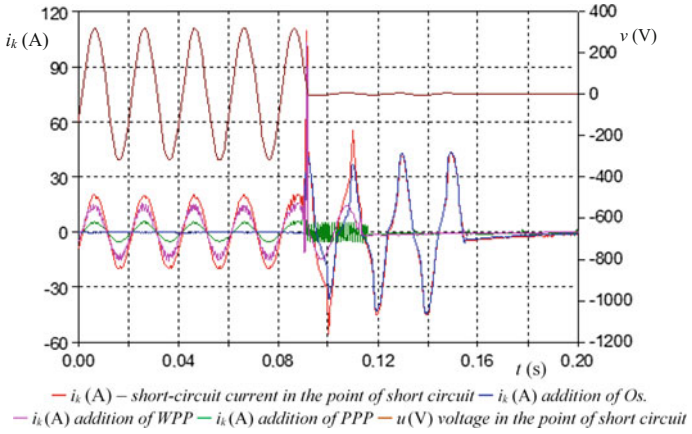

Fig. 4.55 Waveform of the AC voltage and current at the short-circuit in the off-grid system at the third operating state

for detecting undervoltage and overcurrent. After detecting the fault, the WPP convertor is immediately disconnected from the off-grid system. Figure 4.55 shows the waveform of current and voltage at a sudden single-phase short circuit at the terminals of the appliance at the third operating condition in the off-grid system.

Before the sudden shortcircuit, the power output of the WPP inverter is at 70 % and the power output of the PPP inverter is at 20 %. The power supplied from WPP and PPP is sufficient to cover the current off-grid system load. The off-grid inverter has enough power and charges the storage batteries. When a sudden 1*f* short circuit occurs at the appliance terminals powered by the off-grid system, the surge short-circuit current is created, which reaches an effective value of 86 A. After settling transients, the effective value of the steady short-circuit current is maintained at the value of 37.5 A. The voltage in the off-grid system drops below 10 V. Photovoltaic and WPP inverters will be automatically disconnected from the off-grid system for <0.04 s. After disconnecting the WPP and PPP inverters, the short circuit only is powered by the off-grid inverter with the storage devices. The effective value of short-circuit current drops to 34 A. For safety reasons (damage to the off-grid inverter), the power of the single-phase short circuit is off to 0.06 from the emergence of the single-phase short circuit using the undervoltage control relay. WPP together with the power electronics contributes to the overall surge short-circuit current at the point of short circuit 43 A, which is about two times the rated current of the WPP inverter before the short circuit, see Table 4.9. The PPP inverter contributes to the overall surge short-circuit current at the point of short circuit <5 A, the off-grid inverter 37 A. The value of the total initial surge short-circuit current at the point of short circuit is higher than the required actuating current of the circuit breaker, which is 80 A for circuit breakers with characteristic B16 and 50 A with the circuit breaker with the B10 characteristic. B16 breaker should switch off the fault reliably within a specified time limit.

Table 4.9 Contribution of the WPP invertor to the surge short-circuit current at the short-circuit place (WPP + off-grid inverter)

Loading of WPP invertor before the sudden single-phase short circuit P (%)	Contribution of the short-circuit current WPP I_k'' (A)	Contribution of the short-circuit current Os $I_{k.Os}''$ (A)	Surge short-circuit current at the place of the short circuit I_k'' (A)
30	13.7	36.2	50
55	24.9	36.5	61.5
80	37.4	36	74.4

The above operating conditions indicate that the use of the classical concept of electric protection (without limiting the maximum appliances power input) used for the protection of low-voltage distribution does not ensure a safe fault clearing on the AC side of the off-grid system within a specified time limit. Taking into account the changing value of the short-circuit power for various operating and fault conditions in the testing platform of the off-grid system, it is necessary to modify the standard concept of the protection of the used low-voltage power distribution. The change in the short-circuit power in the off-grid system is mainly given by the changing value of the short-circuit power of individual power sources connected to the off-grid system and limiting capacity of power electronics of individual conversion elements, see Fig. 4.56.

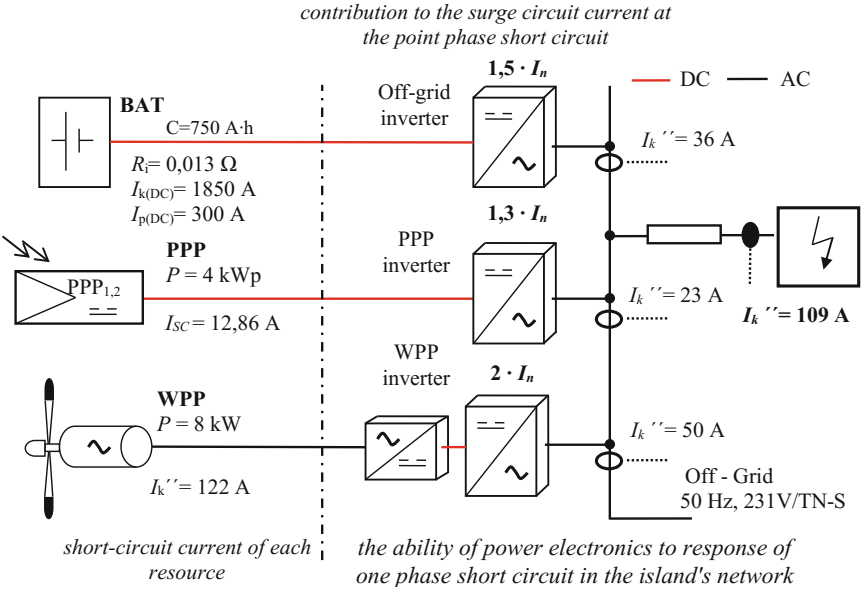

Fig. 4.56 Sources of short-circuit output in the off-grid system

4.5.6 Possibilities of Protection with the Use of the Existing Technology

The automatic disconnection from the power at failure such as the single-phase short circuit and overloading occurs due to the passage of a fault current, to which the protective circuit device responds, in which the failure has occurred, and this circuit is disconnected by the mentioned appliance from the power supply. In this case, the low-voltage power distribution applies protections by the automatic disconnection from the source using overcurrent protective devices, such as fuses and circuit breakers.

To maintain the benefits of the off-grid system connected in the by-pass mode (the ability to cover a larger power consumption than the off-grid inverter able to cover, in the case of the off-grid system built in the premises of VŠB-TUO it is 13 kW) must be for the protection of the main current circuit L_1 and L_2 applied circuit breaker of the tripping characteristic B, I_n = 20 A, factor 5, see Fig. 4.57. The tripping value of the short-circuit release of the circuit breaker will be I_a = 100 A. This value is higher than the short-circuit current in the first and second operating conditions.

Another possibility is the application of the fuse. This is the simplest protection device for the protection (automatic disconnection from the source) at a short circuit. They can respond quickly to fault currents with high *limiting capacity*—(the protection device trips before the short-circuit current reaches its peak value). The fuse of the functional class of PVA gG shall not trip the current of 1.5–1.6 times its rated value for a period of 1 h for fuses up to I_n = 63 A. If for the protection of the main circuit, gG 20 fuses are applied that the value of the short-circuit current for the equipment of the protection element is up to 0.4 with >90 A. This value is higher than the short-circuit current at the first and second operating states [18].

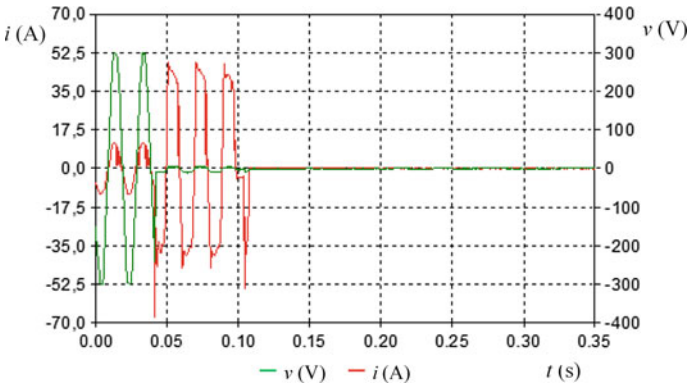

Fig. 4.57 Waveform of AC voltage and current at tripping the single-phase short circuit on appliance terminals using overcurrent digital protection [setting the impulse value $\gg I = I_n \cdot n$—to the value 1.5 (I_n = 20 A)]

Another option for the protection of the off-grid system is the use of modern digital overcurrent protections. In the commercial market, there are currently several digital protections designed for protection, measuring control and monitoring. These protections are normally used primarily for higher levels of voltage, i.e., the high-voltage level. With regard to the purchase price, it is rather a theoretical account for their use in the off-grid system. These digital overcurrent protections contain directional overcurrent protection with optional flash or inverse characteristic, and several possible sets of adjustable starting values of the short-circuit stage. Overcurrent stages can be blocked by external control signals from other protections. Furthermore, protections contain digital displays of measured and adjusted values and the values recorded at the moment of failure. These digital overcurrent protections can operate as a single-phase or three-phase. When exceeding the adjustable starting value of the short-circuit degree, the release is used to actuate the applied protection element, see Fig. 4.58, in our case B16 circuit breaker, see Fig. 4.44 applied for the protection of the adjacent power circuit L_{2B} with undervoltage release.

Another way to ensure protection against the short circuit in the electrical system of the off-grid system is to use an undervoltage relay. The undervoltage relay is designed to control the undervoltage in phase conductors of electrical equipment and circuits. The relay monitors the size of phase voltage. Exceeding the adjustable lower voltage levels (140–200 V) occurs via the release to actuate the applied protection element, in our case circuit breaker B16, see Fig. 4.57 applied for the protection of adjacent power circuit L_{2B} with undervoltage release, see Fig. 4.58. The protection relay can be used for protection against undervoltage, which arises in the grid in case of a short circuit. The undervoltage release is set at the level of the minimum rms voltage drop in the off-grid system at 200 V AC. The disadvantage of this protection concept consists in being prone to the equipment of

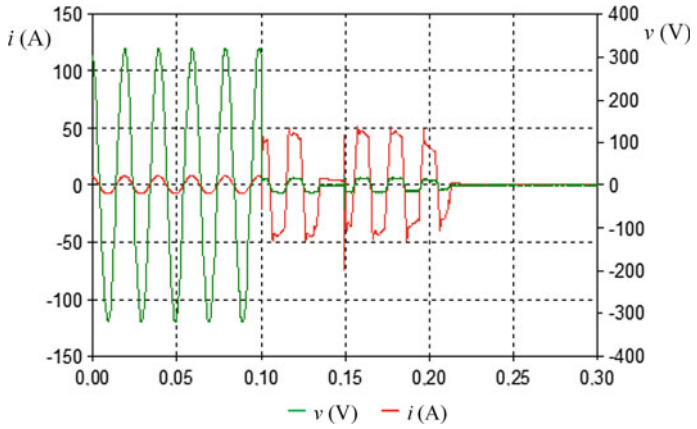

Fig. 4.58 Waveform of the AC voltage and current at switching off the single-phase short-circuit on appliance terminals, automatic switching off the fault using the undervoltage control relay and the circuit breaker B16

protection devices during short-time voltage drops in the off-grid system (by dynamic power consumption). This disadvantage can be avoided by adjusting the time delay of the tripping release. The undervoltage release with the delayed drop out is a combination of a separate delay unit and the respective release. It prevents circuit breaker switch off in the case of a brief power supply interruption. The delay time can be set from 1 to 16 s. However, the time required for the fault clearing increases.

Efforts to achieve greater use of RES have in recent years led to the development and design of new applications with the use of alternative energy sources based on the concept of intelligent grid, i.e., so-called micro grid intelligent distribution system. The presence of multiple diffuse sources can have a significant impact on the short-circuit power in the distribution system resulting in a change in the concept of protection. The latest protective equipment using automatic evaluation of a given situation and the ability to preset the threshold value of the impulse protecting article ensure the safety and reliability of the distribution system operations.

There are currently on the market several universally known multi-agent protective systems, digital overcurrent protections, and power circuit breakers of the third generation, which would be able to ensure with its function selective and one hundred percent protection against short circuits and overloads in the off-grid system. Using these protections in the newly designed systems, such as multi-agent (MAS), intelligent protection, monitoring, and control system leads to the ability to perform the electrical protection. The multi-agent system automatically evaluates the given situation, it is able to locate the fault point and preset threshold electric protections values in the grid, thus achieving higher sensitivity, and maintaining selectivity. Another feature of these multi-agent systems is the automatic resumption of operation and distribution grid power supply following the outage. However, these latest protection and control systems are proposed and designed for higher voltage and power levels than the low-voltage electrical distribution system in the off-grid testing platform of the system intended for supply to family houses or buildings (Fig. 4.59).

4.5.7 Adaptive System of Protection for the Off-Grid System

To ensure safe, selective protection against short circuit and overload in all operating modes of the off-grid system, it is necessary with regard to the changing value of the short-circuit current (hence, the short-circuit power in the off-grid system) to have a dynamically changing the value of the short-circuit release of the electrical protection for main current circuit, see Fig. 4.44.

In the first operating state (the source of the short-circuit current only is the warp invertor), the value of the surge short-circuit current only is 34 A. The impulse value of the short-circuit release must be set below this $I_n \cdot n < 34$ A. If this value of the short-circuit release also remains set for the second and, especially, the third operating condition, the concept of the by-pass system would limit the maximum

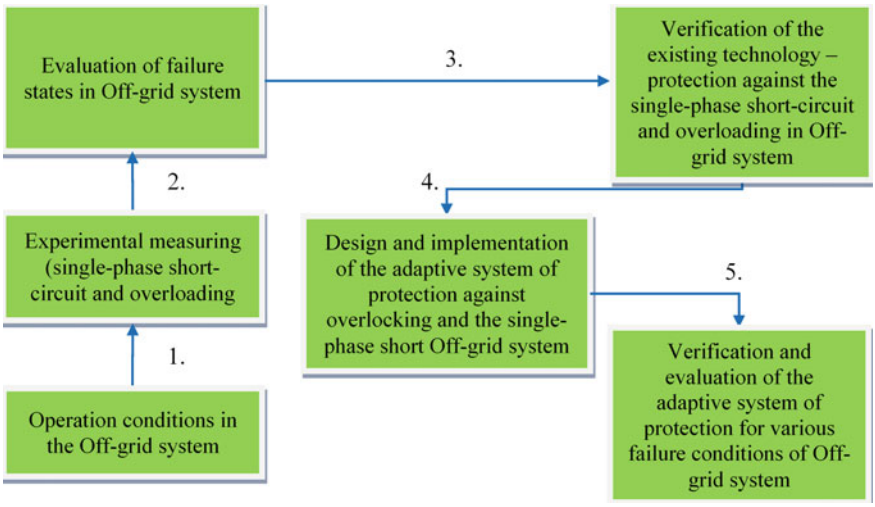

Fig. 4.59 Procedure at designing the adaptive protection system for the off-grid system

transmitted power achieved at the second operating condition (off-grid inverter and PPP) 38 A and the third operating condition (off-grid inverter together with photovoltaic and WPPs) to 60 A (maximum load, which the off-grid inverter together with the hybrid source is capable of covering, is 13.8 kW). The source with the highest performance and greatest contribution to the total short-circuit current in the off-grid system is WPP with its inverter. To avoid any undesirable activation of the short-circuit grade by exceeding the impulse value of the short-circuit release that would have been set for the first operating condition dynamic changes in this value must occur in real time based on the current performance of WPP together with PPP and their power electronics.

WPP is equipped with the internal evaluation and PLC Siemens LOGO 24 C control system (monitoring the voltage across the terminals of a synchronous generator and revolutions of the wind engine and monitoring of the temperature of the generator). Therefore, one option is to use the measured values of the rotation speed of the wind engine and values of global radiation (using a weather station) for the introduction of short-circuit release values. WPP parameters include the WPP startup wind speed of 2.8 $m \cdot s^{-1}$, which corresponds to 50 rpm of a wind turbine. The maximum wind speed is 12 $m \cdot s^{-1}$, which is an equivalent of 180 rpm. Figure 4.60 shows the WPP inverter output current depending on wind speed or wind motor revolutions. Figure 4.61 indicates the output current of the PPP inverter depending on the values of global radiation.

The adaptive protection system (hereinafter referred to as ARP—active relay protection) will therefore using the measured values of WPP rotor revolutions and global radiation values set up (increase/decrease) the impulse value of the short-circuit release for the main current circuit L_1, see Fig. 4.68. The impulse value of the short-circuit stage increases or decreases according to the current value of the

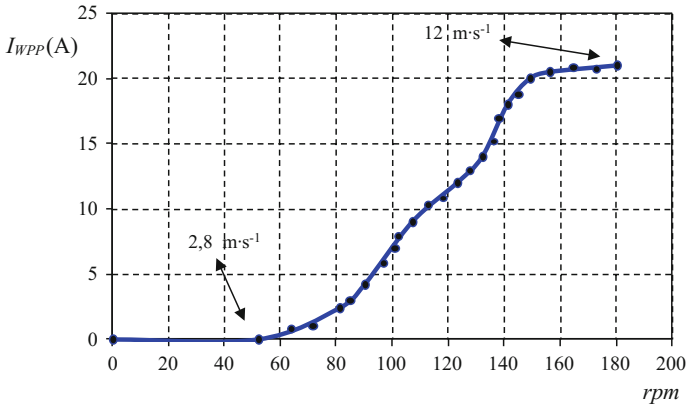

Fig. 4.60 Current values supplied by WPP through the single-phase inverter to the off-grid system at the normal operation condition at various wind engine revolutions (Color figure online)

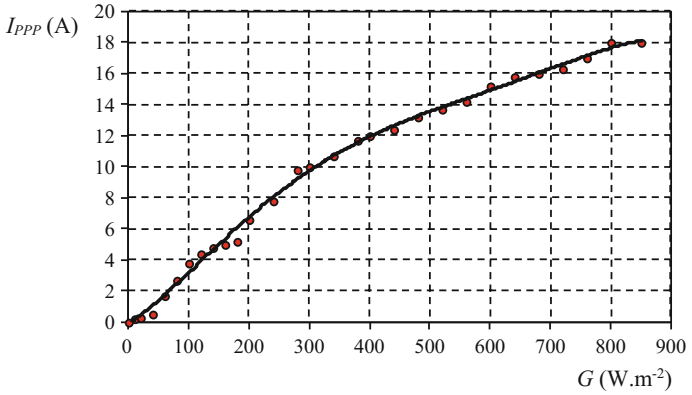

Fig. 4.61 Values of current supplied by $PPP_{1,2}$ through the single-phase inverter to the off-grid system at normal operating conditions at various values of the global radiation (Color figure online)

global radiation and the wind motor revolutions that are directly proportional to the wind speed. If the set impulse value of the short-circuit stage is exceeded the power of the respective release of the circuit breaker with the subsequent actuation of the circuit breaker trips. The undervoltage release contains a solenoid that at the voltage interruption triggers a tripping mechanism. The system is in the rest position when the release is permanently energized. Figures 4.62 and 4.63 show the setting of five impulse values of the short-circuit stage for various values of the global radiation and wind motor revolutions. The impulse value of the short-circuit release is set at I_n = 30 A (I_n = 20—the initial value given by the rated current of the off-grid inverter, n = 1.5, $I_n \cdot n$ = 30 A < 34 A—minimum value of the initial surge short-circuit current of the off-grid inverter see Fig. 4.45) (Fig. 4.64).

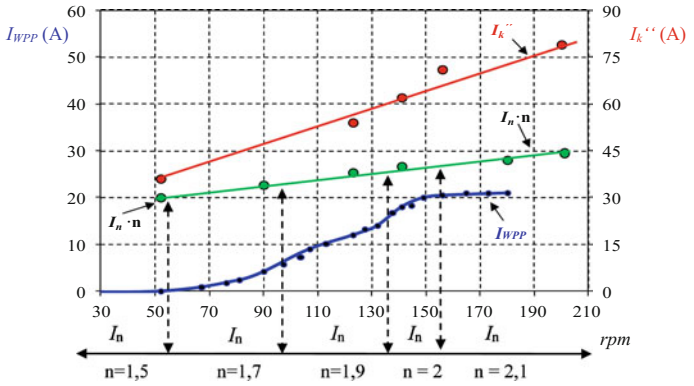

Fig. 4.62 Setting values ($I_n \cdot n$) of the impulse short-circuit level of the adaptive protection system—(off-grid inverter and WPP). I_k'' (*red*)—initial surge short-circuit current (contribution of the WPP inverter and the off-grid inverter), I_{VTE} (*blue*)—values of the current supplied by WPP through the single-phase inverter at normal operation condition at various wind engine revolutions

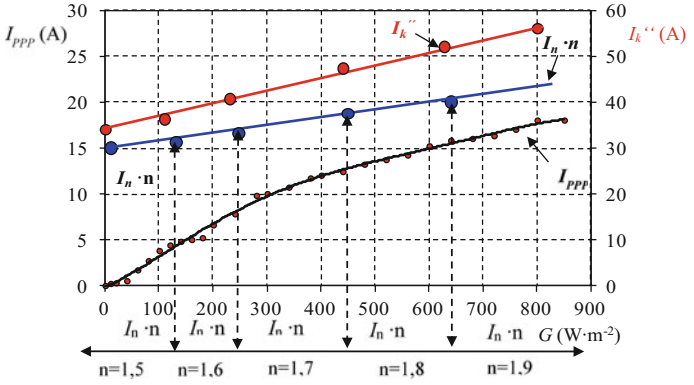

Fig. 4.63 Setting values ($I_n \cdot n$) of the impulse short-circuit level of the adaptive protection system—(off-grid invertor and PPP). I_k'' (*red*)—the surge short-circuit current (contribution of the PPP inverter and the off-grid inverter), I_{VTE} (*blue*)—values of current supplied by PPP through the single-phase inverter at normal operation condition at various values of global radiation

Figure 4.65 indicates the basic algorithm of the adaptive protection system. The impulse value of the non-delayed short-circuit release for the main current circuit is adjusted according to the current operating condition in the off-grid system. The changing impulse value of the short-circuit release for the main current circuit can be respected according to the pre-defined sets of parameters, see Tables 4.10, 4.11 and 4.12. To provide the current selectivity (difference in adjusted, non-delayed impulse release values, individual protective devices in the electrical island grid distribution), which ensures the ability only to turn off the affected adjacent current

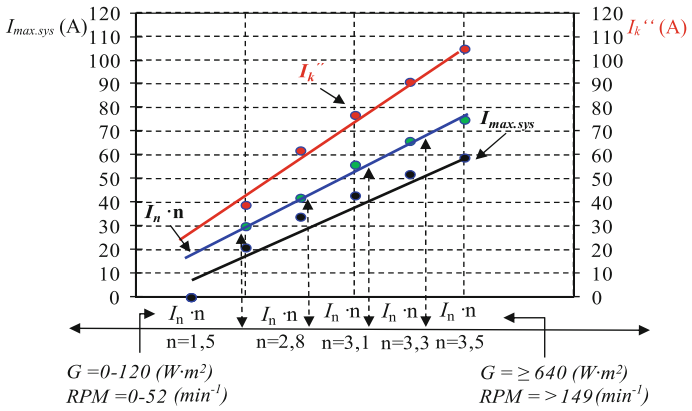

Fig. 4.64 Model situation, setting of values of the impulse short-circuit level of the adaptive protection system. I_k''—surge, short-circuit current (contribution of the WPP inverter, PPP and off-grid inverter)

circuit, the impulse value of the short-circuit release for the adjacent current circuits is fixed with the option of setting (given by appliances, nature of consumption and loading of individual adjacent current circuits). The algorithm of the adaptive protection system together with security features will increase the traffic safety of the off-grid system while allowing full use of the by-pass concept used for the testing platform for the off-grid system.

4.5.8 *Using SMC 144 for the Adaptive Protection System*

One way to use the proposed algorithm of the adaptive protection system is to use a circuit breaker of the third generation. These circuit breakers can in addition to a reliable protection against short circuits and overloads measure electrical values (voltage and current, frequency, power, and energy). Indisputable advantages include the fact that they do not need external current transformers. The system uses measuring transformers, which are inside the circuit breaker. A circuit breaker with this type of electronic unit allows you to replace analog measurement or network analyzer with external current measuring transformers. The third generation circuit breakers are equipped with a communication element (RS-485, Modbus or Ethernet protocol) with the superior control system. Circuit breakers are fitted with the advanced release with adjustable value of the impulse short-circuit stage. This can be understood as programmable relays with the possibility of adjusting the value of switching and disconnecting relays including time delays (at the protected circuit overload). However, the purchase price of these circuit breakers is considerable and amounts to about 5 % of the total costs of building the off-grid system. This is the reason why for the created algorithm of the adaptive protection system the multi-functional measuring instrument SMC 144 has been chosen. The multifunctional

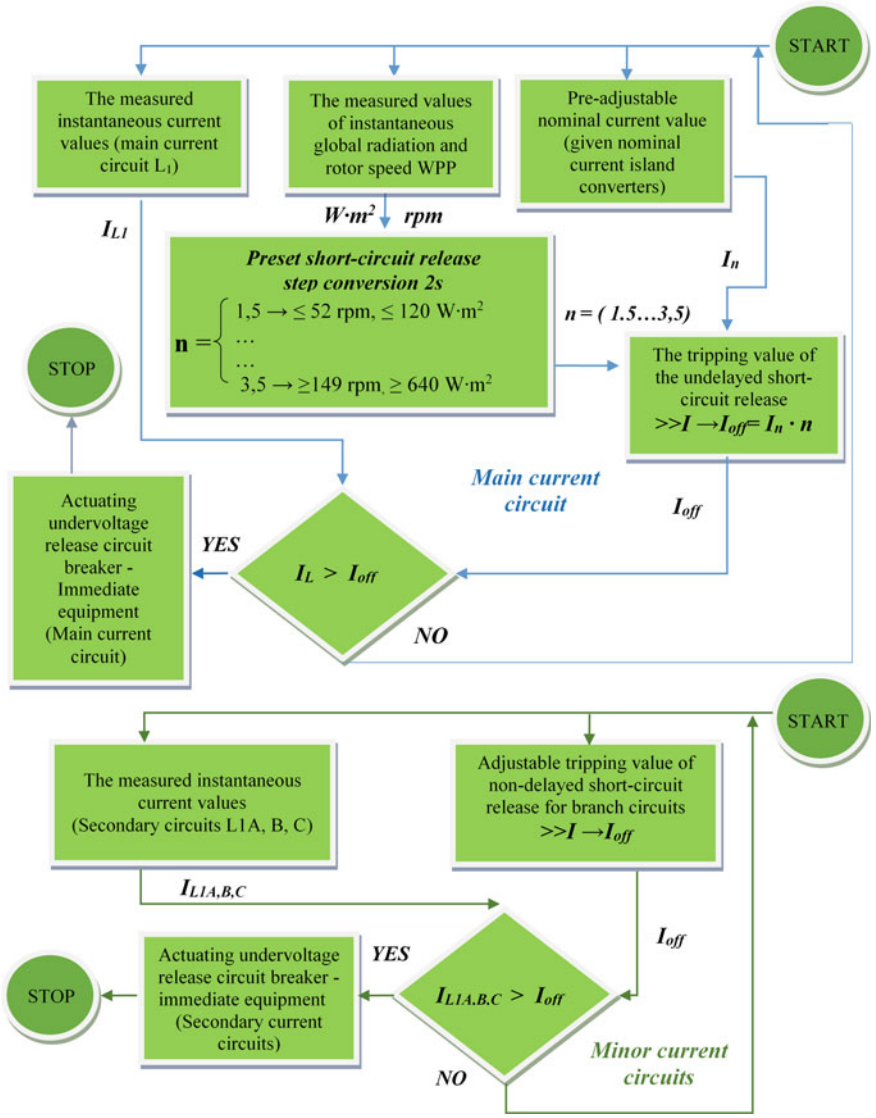

Fig. 4.65 Algorithm of the adaptive protection system—ARP. I_L—measured current value, main and adjacent current circuits, $I_n \cdot n$—adjustable value of the impulse short-circuit level, I_{VYP}—actuation value of the current of the short-circuit release, n—short-circuit release multiplier

network analyzer SMC 144 is designed for an accurate voltage and current measurements and power quality monitoring. This multifunctional measuring instrument is suitable for a wide range of applications in automation, load management, manufacturing processes, and remote monitoring over the infrastructure. This measuring device is equipped with four voltage inputs and four current inputs for

Table 4.10 Setting up the values of the impulse short-circuit level of the adaptive protection system (off-grid inverter and PPP)

RPM (to min^{-2})	n (−)	$I_n \cdot n = 20$ (A)	$I_{max.sys.}$ (A)[a]	I_k'' (A)
0–52	1.5	30	17.3	34
52–107	1.7	34	26.3	52
107–132	1.9	38	31	62
132–149	2	40	36	74
≥ 149	2.1	42	39	79

[a]$I_{max.sys.}$—maximum value of the power supply (given by the output of the 4 kW off-grid inverter and the WPP 5 kW inverter)

Table 4.11 Setting up values of the impulse short-circuit grade of the adaptive protection system (off-grid inverter and PPP)

G (W m^2)	n (−)	$I_n \cdot n = 20$ (A)	$I_{max.sys.}$ (A)[a]	I_k''(A)
0–120	1.5	30	21	38
120–240	1.6	32	25	43
240–440	1.7	34	29	49
440–640	1.8	36	33	52
≥ 640	1.9	38	35	56

[a]$I_{max.sys.}$—maximum value of the power supply current (given by the output of the 4 kW off-grid inverter and PPP 4.2 kW inverter)

Table 4.12 Model situation, setting up values of the impulse short-circuit level of the adaptive system of protection (off-grid invertor, PPP, WPP)

G (W·m^2)	RPM (to min^{-2})	n (−)	$I_n \cdot n = 20$ (A)	$I_{max.sys.}$ (A)[a]	I_k'' (A)
0–120	0–52	1.5	30	21	39
120–240	52–107	2.8	56	34	62
240–440	107–132	3.1	62	43	77
440–640	132–149	3.3	66	52	91
≥ 640	≥ 149	3.5	70	57	100

[a]$I_{max.sys.}$—maximum value of the supply power (given by the output of the 4 kW off-grid inverter, PPP 4.2 kW inverter and WPP 5 kW inverter)

external snap and die (split) measuring transformers for direct current measurement up to 600 A AC. The measuring voltage range (line voltage 5–500 V AC, phase 2–285 V AC) with a measurement accuracy of 0.1 %. Measuring current range (0.02–1.2 · I_{NOM}—measuring range of the transformer) measurement accuracy of 0.1 %. Maximum overload of the measuring device is 10 · I_{NOM}. Voltage and current signals are evaluated continuously without interruption. With the measuring device, the evaluation interval of rms voltage and current from 10 periods till one period can be set. All channels are sampled with 128 samples per period. RMS voltages and currents are evaluated from the sampled values for a measured period. The measurement device can be supplied at 75–510 V AC or 80–350 V DC.

For connection with the superior system or slave modules (multifunctional switching relays), SMC 144 is equipped with a communication line RS-485 or Ethernet. In this multifunctional measuring instrument, the function (on/off) can be set (programmed), which controls the outputs of slave modules (multifunctional switching relays). A complex condition may constitute up to 14 events or limits of exceeding preset limits of voltage and current values (four voltage inputs and four current inputs—for each input of the switch on/off function via the multifunctional switching relay when exceeding an adjustable voltage and current value for all measured areas). The diagram of APR connection together with using SMC 144 is shown in Figs. 4.66 and 4.67.

The SMC 144 measuring device measures by the direct measurement (measuring current transformers) currents in the individual current circuits (off-grid system, see Fig. 4.68). If the s set current value of the impulse short-circuit grade, SMC 144 is exceeded via the multifunction switching relay the power supply switches off the circuit breakers in question for affected current circuit and it leads to actuating the protective element to 0.32 s, see Fig. 4.71. To prevent accidental tripping of the protective element in the main circuit, SMC 144 using an algorithm of adaptive protection system adjusts (decreases/increases) the value of the impulse short-circuit stage. Using the Raspberry Pi microcomputer, which is used in the off-grid system used for active power management system, and which accepts via Ethernet every 2-s current values of the global radiation from a weather station and

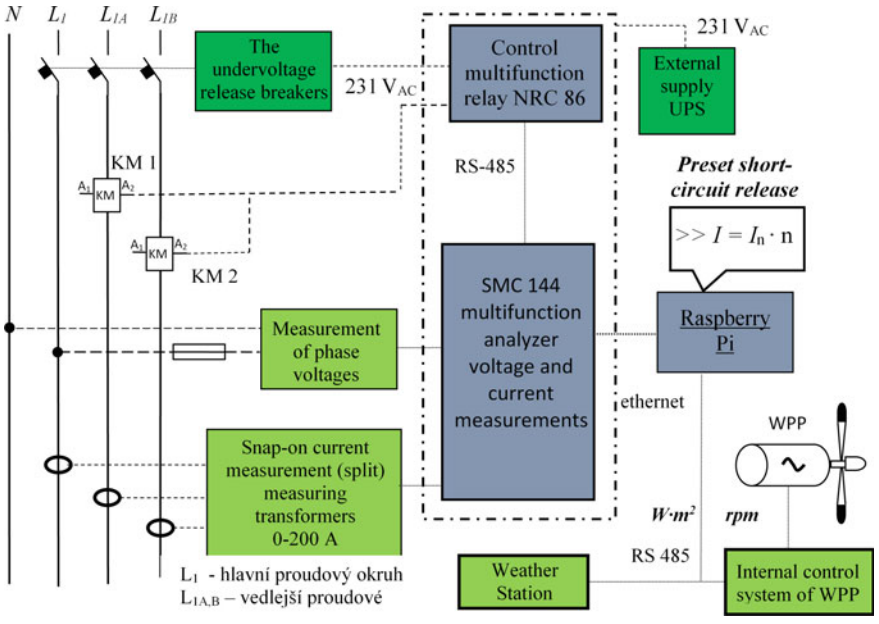

Fig. 4.66 Diagram of ARP connection in the *v* power distribution in the off-grid system using SMC 144

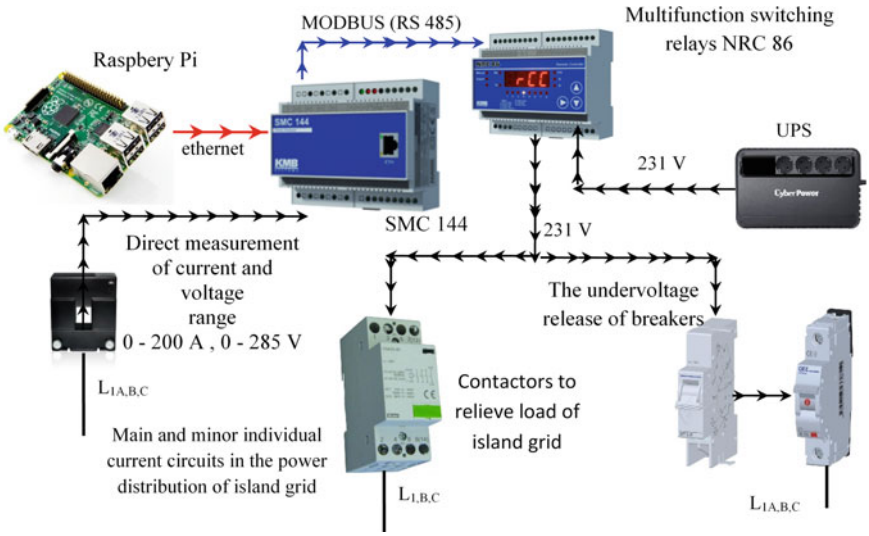

Fig. 4.67 Diagram of ARP connection using SMC 144 and conventional protection elements

the wind engine revolutions from the internal control system of WPP. Raspberry Pi according to the described algorithm, see Fig. 4.65, sets in SMC 144 the value of the impulse short-circuit grade for the main current circuit. The step of the conversion for setting the impulse value for the main circuit is 2 s. The speed of conversion is sufficient for dynamic changes (acceleration/deceleration of wind engine revolutions), at which the rotational inertia of the rotating masses is reflected.

For added protection against overloading of the off-grid inverter followed by powering off the entire off-grid system, it is possible to use contactors that are in the off-grid system applied to relieve the load of the off-grid system—(load management system, protection against deep discharge of storage batteries. When overloading of the off-grid inverter occurs the off-grid system experiences a decline of the phase voltage. SMC 144 monitors the phase voltage at the main electrical circuit of the off-grid system, see Fig. 4.65. If the off-grid inverter gets overloaded with a subsequent drop of the phase voltage in the off-grid system below 207 V, SMC 144 and the multi-functional switching relay is used to actuate KM_1 and KM_2 contactors. To prevent undesirable actuation of these contactors used for the protection against the deep discharge of storage batteries and relieving loading of off-grid system at overload, there is a time delay set with SMC 144, which prevents that during a brief voltage drop (dynamic current consumption) or the voltage drop due to the single-phase short circuit, the given contactor is switched off.

The analysis of the off-grid system overloading (or rather the off-grid inverter) results in switching off the off-grid inverter to 6 from the emergence of overloading. For this reason, the value of the time delay of actuating contactors KM_1 and KM_2 must be below this value. This time value of delay must be also longer than the

duration of actuating the protection element using APR at a single-phase short circuit in the off-grid system. (RMS voltage network at the off-grid system at the single-phase short circuit drops below 10 V). For these reasons, the time delay of actuating the contactor KM_1 is—3 s, the delay of actuating contactor KM_2 is—5 s. An algorithm to increase the protection against overload in the off-grid system is indicated in Fig. 4.68. Turning off the KM_1 contactor is to relieve the grid load, low priority load disconnecting (priority 1 appliances). If no increase of the phase

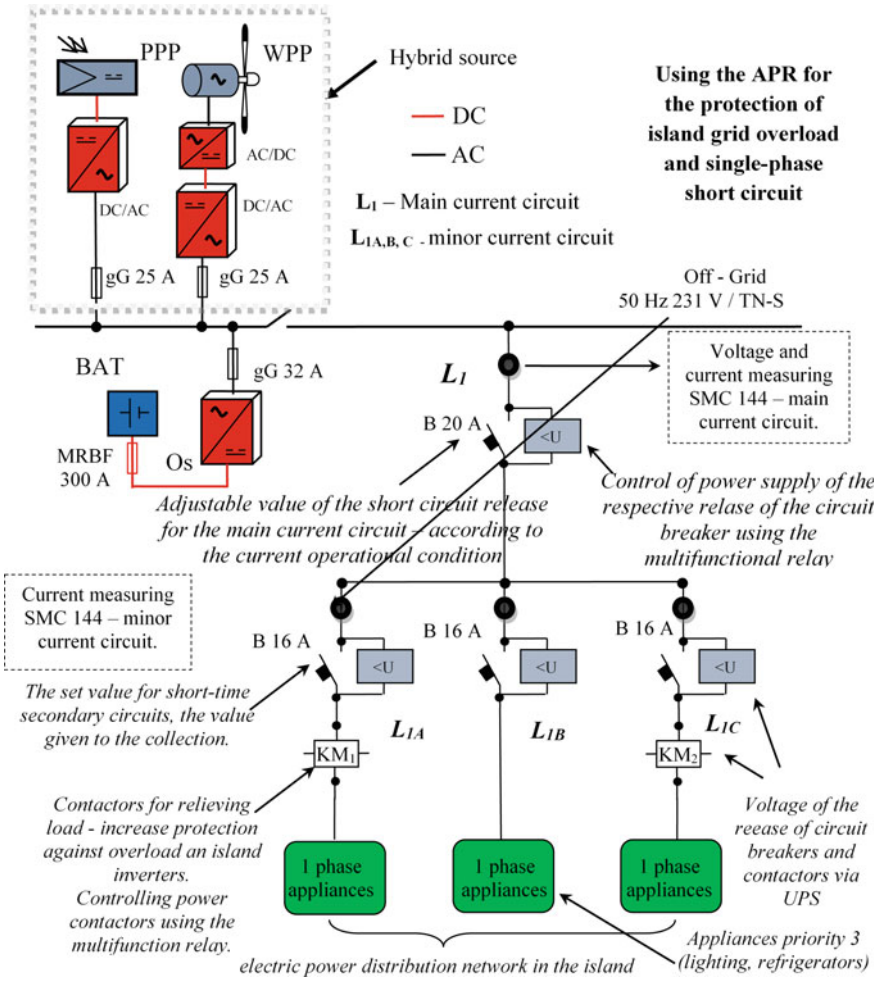

Fig. 4.68 The simplified block diagram of connecting the testing platform of the off-grid system built in the area of the VŠB—TUO together with connecting protection elements for the main current circuit L_1 and adjacent current circuits $L_{1A,b,C}$ using the adaptive protection system. On the adjacent L_{1B} current circuit no contactor is applied to relieve loading at overloading in the off-grid system due to the power supply to the highest priority appliances (lighting, fridge)

Table 4.13 Selected appliances for both levels of the load relieve, protection against the deep discharge of storage batteries and overloading the off-grid inverter

Level for load relieve	Chosen load
Level 1—priority one appliances (KM_1)	Hot supply water heating, microwave oven, air-conditioning
Level 2—priority two appliances (KM_2)	Kitchen stove, washing machine, dishwasher, drying machine
Priority three appliances	Lighting, fridge, freezer

voltage over the limit occurs, the contactor KM_2 is actuated, and lower priority appliances (priority 2 appliances) get disconnected. Table 4.13 indicates the model demonstration of selected appliances for both levels of the load relieve.

4.5.9 *Verification of the Adaptive System of the Off-Grid System Protection*

Figure 4.59 shows overloading the off-grid system. At the time to 1.68 s, the load of the off-grid system is about 5.8 kW (purely resistive load). PPP together with the off-grid inverter is able to cover the current consumption. At the time of 1.68 s, PPP gets disconnected (worsening weather conditions, shading of the PV modules by clouds) and overloading of the off-grid inverter occurs. APR monitors size of phase voltage on the main current circuit. At overloading the off-grid inverter, the effective value of the phase voltages drops to 193 V. APR according to the algorithm of the adaptive protection system for relieving the off-grid system, see Fig. 4.69,

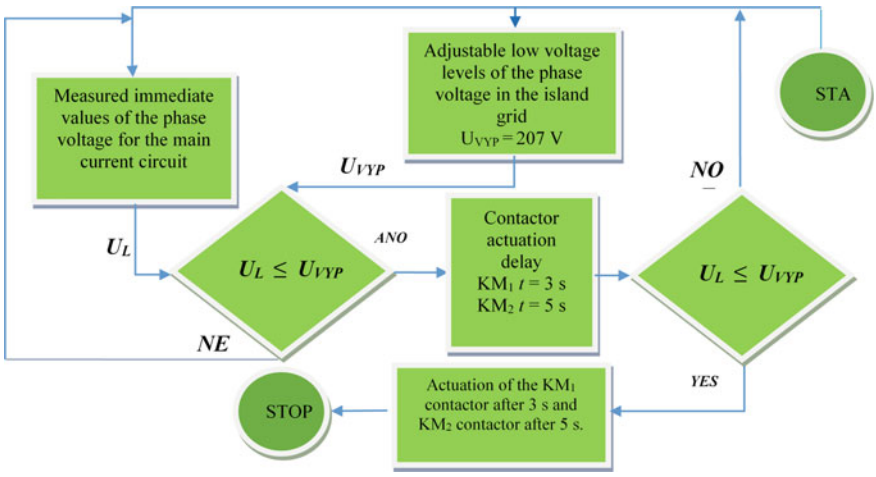

Fig. 4.69 Algorithm of adaptive protection system, relieving the island grid, overload protection

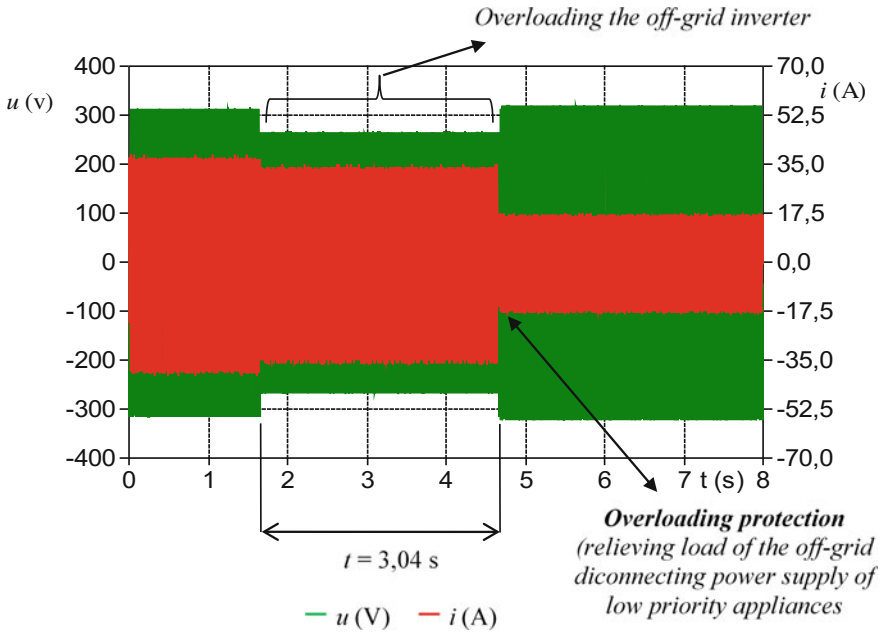

Fig. 4.70 Overloading protection, relieving the off-grid system using APR

disconnects the adjacent current circuit using the contactor KM_1 (Nizza priority appliances) at the time of 3.04 s. The load of the off-grid system falls to 2.7 kW. This load does not mean overloading for the off-grid convertor. To reconnect the contactor and to restore the power supply of disconnected appliances the manual activation button on the hand-held multifunction switching relay (switching on/off) is required to restore power control of the contactor coil (Fig. 4.70).

In Fig. 4.71, there is the voltage waveform before and after the single-phase short circuit on the main current circuit L_1 together with the current at the point of a sudden short circuit (current circuit L_{1C}—see Fig. 4.68, at this test, no circuit breaker is used for the protection of the adjacent power circuit L_{1C}). WPP inverter is loaded at 65 % (revolutions of the WPP wind engine are approximately 150 rpm) and the PPP inverter at 85 % (value of the global radiation is 630 W m^{-2}). According to the current values of the WPP rotor revolutions and values of the global radiation, the impulse value of the short-circuit release for the main circuit L_1 is set atto $I_n \cdot n = 66$ A. At the sudden short circuit in the electrical circuit L_{1C} at the time of 1 s, the effective value of the initial surge short-circuit current reaches 67.3 A. At the time up to 0.29 s after a fault occurs, the power is switched off using the circuit L_1 using APR and applied circuit breaker B 20 A.

Short-circuit currents can be dangerous for their thermal and electrodynamic effects. The protection device has to turn off the short-circuit current sufficiently quickly and reliably. In some cases, it is necessary to reduce through the limiting protective device the value of short-circuit current, and thereby reduce its

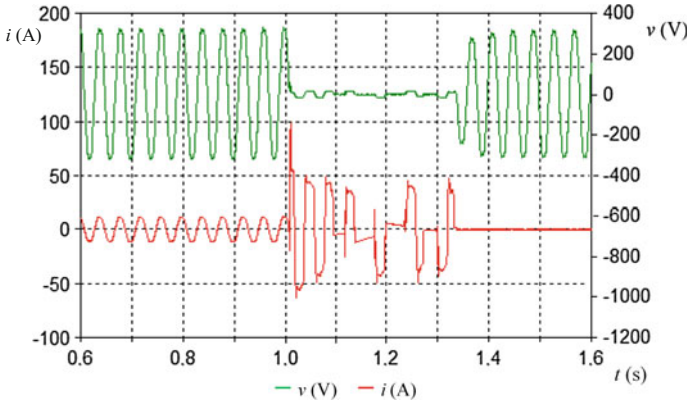

Fig. 4.71 Automatic disconnection from source at a single-phase short circuit in the off-grid system using the circuit breaker with the release in question using APR

electrodynamic effects to an acceptable level. If the protective device trips quickly enough, so to speak before the short-circuit current reaches its peak value, the value of short-circuit current, and hence, its thermal and electrodynamic effect are limited. The limited short-circuit current given with protection devices expresses the greatest instantaneous peak value of current that can occur with a limiting protective device under the most unfavorable conditions in the circuit, see Fig. 4.72. It is reported depending on the expected short-circuit current. The Joule integral according to Eq. (4.1) provided for protection devices characterizes the energy discharged by the protection device upon turning off short-circuit currents. This form of the integral is known as I^2t and referred to as a Joule integral, even though it lacks the R component and the resulting unit is a the current square for a given time interval (A^2 s) rather than the energy unit (J).

In some cases, I^2t is decisive for the proper selection of the protection device in terms of thermal and electrodynamic effects of short-circuit currents (Fig. 4.72):

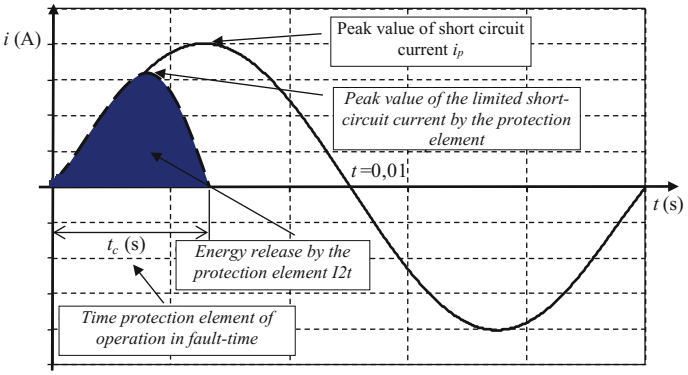

Fig. 4.72 Limiting the supposed short-circuit current by the protection element

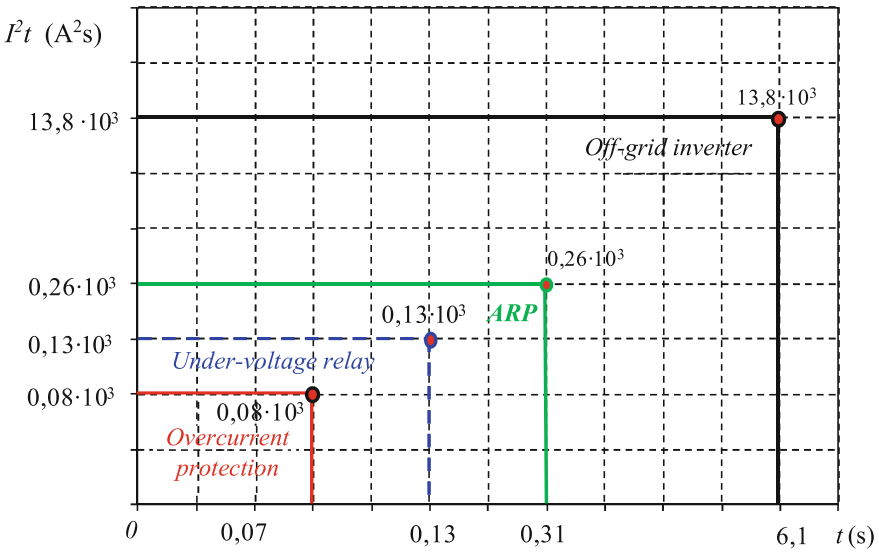

Fig. 4.73 Comparison of individual protective elements according to the released power by the protection element at the fault clearing (single-phase short circuit in the off-grid system) in the first operating condition in the off-grid system. *Subjective control relay—using the security element does not result in achieving selectivity when protecting the off-grid system against overload and the single-phase short circuit

$$W = \int_0^t R \cdot i^2 \cdot t\,, \quad I^2t = \int_0^t i^2 \mathrm{d}t\,. \tag{4.16}$$

Comparison of the effects of individual protection concepts applied in the off-grid system together with APR comparison is shown in Table 4.14. Data given in Table 4.14 were acquired by measuring using the YOKOGAWA oscilloscope. In Figs. 4.73 and 4.74, see a comparison of the various protection elements according to the released energy (I^2t), at the automatic disconnection from the source at single-phase short circuit, using a circuit breaker with the release in question applied for the protection of the main circuit L_1, see Fig. 4.68 (sudden single-phase short circuit occurs on the adjacent current circuit L_{1C}—at this measurement, no circuit breaker designed for protection of the adjacent power circuit L_{1C} is used). The results shown in Table 4.14 imply that during clearing a fault such as the single-phase short circuit in the island grid applied protective elements have not achieved limiting ability—(the protection device is switched off quickly enough, so to speak, before the short-circuit current reaches its peak value, thereby limiting the value of the short-circuit current, see Fig. 4.72). This capability could be achieved if for the adaptive protection system circuit breakers of the third generation would be applied. In addition to the reliable protection against the short circuit and

Table 4.14 Comparison of effects of individual types of protection elements for the automatic disconnection from the source at the single-phase short circuit in the off-grid system

Protection elements	Operating statuses	$\gg I = I_n \cdot n$ (A) $\ll U$ (V)	I_k'' (A)	i_p (A)	t_c (s)	I^2t (A^2•s)	Costs (%)[a]
Off-grid inverter	I.	–	36.3	51	6.1	13.8×10^3	–
	III.	–	68.2	98.6	5.9	14.9×10^3	
Over the current protection	I.	30	37.8	53.5	0.07	0.08×10^3	10
	III.	56	68.7	98.5	0.06	0.1×10^3	
Undervoltage relay	I.	150	36.6	50	0.13	0.13×10^3	0.5
	II.	150	48.8	68	0.12	0.14×10^3	
	III.	150	68.7	96	0.12	0.2×10^3	
APR	I.	30	37.3	52.4	0.31	0.26×10^3	2
	II.	38	54.4	63.7	0.3	0.28×10^3	
	III.	56	67.3	96	0.29	0.34×10^3	

[a]Costs for the purchase of protective elements used for the automatic disconnection from the source at failure—the costs are deducted from the total costs of building the off-grid system I_k''—surge short-circuit current at the point of short-circuit, t_c—time of protection operation during the fault clearing (single-phase short circuit), I^2t—official energy released by the protection device during the fault clearing such as the single-phase short circuit, $\gg I = I_n \cdot n$—the set value of the short-circuit release, $\ll U$—undervoltage relay—adjusted value of the minimum rms voltage drop, i_p—Surge short-circuit current at the single-phase short circuit, instantaneous value

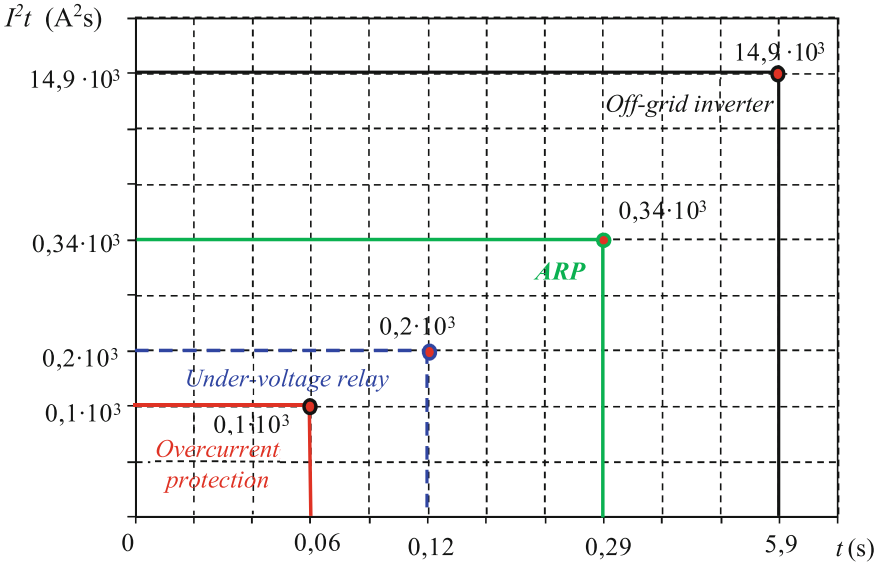

Fig. 4.74 Comparison of individual protective elements according to the energy released at fault clearing (single-phase short circuit in the distribution of the off-grid system) at the third operating condition. *Subjective control relay—using the security element does not result in achieving selectivity at protecting the off-grid system against the overload and the single-phase short circuit

overload, these power circuit breakers can measure electrical parameters (voltage and current, frequency, power, and energy). The indisputable advantage is that they do not need any external current measuring transformers. The system uses measuring transformers, which are inside the circuit breaker. The circuit breaker with this type of electronic unit would enable replacing the universal measuring instrument SMC 144 with external current measuring transformers and classic circuit breakers with undervoltage release. Circuit breakers of the third generation are equipped with the communication with superior control system, which would allow adjustment of the impulse value of the short-circuit grade using an algorithm of the adaptive protection system. The downside is the acquisition cost of these circuit breakers, which would increase the total investment costs of off-grid system.

The shortest time during the liquidation of failures has been reached by the overcurrent digital protection; the duration of action of this overcurrent protection is around 0.06. With regard to the cost of the overcurrent protection, which amounts approximately to 10 % of the total cost of the acquisition of the off-grid system, it is rather a theoretical idea for its use in the off-grid system.

References

1. ERU (2014) Energetický regulační úřad. www.eru.cz. Accessed 3 Apr 2014
2. Smart Grids (2014) Smart Grids Česká technologická platforma. http://www.smartgridcz.eu. Accessed 2 Feb 2014
3. Vramba J, Stuchly J, Kosmak J (2013) Family house off-grid conception. In: Proceedings of the 7th international scientific symposium on electrical power engineering: Elektroenergetika 2013, Stará Lesná, Slovak Republic, pp 196–199
4. Deshmukha MK, Deshmukh SS (2008) Modeling of hybrid renewable energy systems. Renew Sustain Ener Rev 12(1)
5. Off Grid Energy (2014) AC and DC system configuration: off-grid. http://www.offgridenergy.com.au/index.php/information/ac-or-dc-system-configuration.html. Accessed 2 Feb 2014
6. Misak S, Prokop L, Kacor P (2011) Results from hybrid off-grid power system operation analysis. In: 10th international conference on environment and electrical engineering. IEEE. doi:10.1109/EEEIC.2011.5874658
7. Misak S, Prokop L, Kacor P (2011) Results from hybrid off-grid power system operation analysis. In: 10th international conference on environment and electrical engineering. IEEE, 8–11 May 2011. doi:10.1109/EEEIC.2011.5874658
8. Bilik P, Kvapil J, Misak S (2011) Efficiency and internal power flow of renewable power supply system. In: 11th international conference on electrical power quality and utilisation. IEEE, 1–4, 2011. doi:10.1109/EPQU.2011.6128943
9. Misak S, Prokop L (2012) Energetická koncepce rodinného domu v ostrovním provozu. In: 13th international scientific conference electric power engineering, pp 753–758
10. Miller N, Zrebiec R, Delmerico R (1996) Battery energy storage systems for electric utility, industrial and commercial applications, In: Eleventh annual battery conference on applications and advances, pp 235–240
11. Lachs W, Sutanto D (1995) Application of battery energy storage in power systems. In: International conference on power electronics and drive systems, 21–24 Feb 1995, pp 700–705

12. FG-FORTE (2014) Lithiové baterie—LiFePO4. http://www.fg-forte.cz/cz/kategorie/241-lithiove-baterie–lifepo4.aspx. Accessed 2 Feb 2012
13. Anderson M, Carr D (1993) Battery energy storage technologies. Proc IEEE 81(3):475–479
14. Shahidehpour JM (2006) Battery energy storage systems in electric power systems. In: IEEE, pp 1–8
15. Hadjipaschalis I, Poullikkas A, Efthimiou V (2009) Overview of current and future energy storage technologies for electric power applications. Renew Sustain Energy Rev 13(6–7):1513–1522. doi:10.1016/j.rser.2008.09.028
16. Homer Energy (2014) Energy modeling software for hybrid renewable energy systems. http://www.homerenergy.com/. Accessed 11 Apr 2014
17. Kansara BU, Parekh BR (2011) Modelling and simulation of distributed generation system using HOMER software. In: International conference on recent advancements in electrical, electronics and control engineering. IEEE, pp 328–332. doi:10.1109/ICONRAEeCE.2011.6129804
18. Prased S, Lakshmi MVS, Sai Babu C (2012) Design of off-grid homes with RES. In: IET Chennai 3rd international conference on sustainable energy and intelligent system, pp 297–303. doi:10.1049/cp.2012.2229
19. Prymek M, Horak A, Prokop L, Mišák S (2013) Integrating RES using a smart household system. In: 13th international conference on environment and electrical engineering (EEEIC). IEEE, pp 68–73. doi:10.1109/EEEIC-2.2013.6737885
20. Prokop L, Mišák S et al (2013) Assessment of the energy balance of the PPP system on the basis of meteorological data. In: Proceedings of the 14th international conference on electric power engineering, pp 507–511
21. Prýmek M, Horák A, Mišák S (2013) Smart home modeling with real appliances. Adv Intell Syst Comput J 239:369–378. doi:10.1007/978-3-319-01854-6_38
22. Prokop L, Mišák S, Horák A, Prýmek M (2013) Řidicí systém pro malý ostrovní systém založený na agentním principu. In: Elektroenergetika 2013: proceedings of the 7th international scientific symposium on electrical power engineering: Stará Lesná, 18–20 Sept 2013, pp 500–503
23. Prokop L, Mišák S (2012) Smart home energy system—2012 issues. In: ELNET 2012, Ostrava, pp 57–62
24. Al-Haddad K (2010) Power quality issues under constant penetration rate of renewable energy into the electric network. In: Power electronics and motion control conference, 6–8 Sept 2010, pp S11–S39, S11–S49
25. Ortega MJ, Hernández JC, García OG (2013) Measurement and assessment of power quality characteristics for photovoltaic systems: harmonics, flicker, unbalance, and slow voltage variations. Electr Power Syst Res J 96:23–35. doi:10.1016/j.epsr.2012.11.003